



PHD

## Walking aids for stroke patients

Williams, J. R.

*Award date:*  
1997

*Awarding institution:*  
University of Bath

[Link to publication](#)

## Alternative formats

If you require this document in an alternative format, please contact:  
[openaccess@bath.ac.uk](mailto:openaccess@bath.ac.uk)

### General rights

Copyright and moral rights for the publications made accessible in the public portal are retained by the authors and/or other copyright owners and it is a condition of accessing publications that users recognise and abide by the legal requirements associated with these rights.

- Users may download and print one copy of any publication from the public portal for the purpose of private study or research.
- You may not further distribute the material or use it for any profit-making activity or commercial gain
- You may freely distribute the URL identifying the publication in the public portal ?

### Take down policy

If you believe that this document breaches copyright please contact us providing details, and we will remove access to the work immediately and investigate your claim.


# **Walking Aids For Stroke Patients**

*submitted by*  
**J.R. Williams B.Eng.**  
*For the degree of*  
Doctor of Philosophy  
of the  
University of Bath  
1997

## **Copyright**

Attention is drawn to the fact that copyright of this thesis rests with its author. This copy of the thesis has been supplied on condition that anyone who consults it is understood to recognise that its copyright rests with its author and that no quotation from the thesis and no information derived from it may be published without the prior written consent of the author.

This thesis may be made available for consultation within the University Library and may be photocopied or lent to other libraries for the purpose of consultation.



September 1997.

UMI Number: U116280

All rights reserved

INFORMATION TO ALL USERS

The quality of this reproduction is dependent upon the quality of the copy submitted.

In the unlikely event that the author did not send a complete manuscript and there are missing pages, these will be noted. Also, if material had to be removed, a note will indicate the deletion.



UMI U116280

Published by ProQuest LLC 2013. Copyright in the Dissertation held by the Author.  
Microform Edition © ProQuest LLC.

All rights reserved. This work is protected against  
unauthorized copying under Title 17, United States Code.



ProQuest LLC  
789 East Eisenhower Parkway  
P.O. Box 1346  
Ann Arbor, MI 48106-1346

UNIVERSITY OF BATH  
LIBRARY

To 10 MAY 1999



---

## CONTENTS

---

# CONTENTS.

<b>Synopsis</b> .....	ix
<b>Acknowledgements</b> .....	x
<b>Chapter 1 Introduction</b> .....	1
1.1 Requirement for walking aids .....	1
1.2 Introduction to the walking aids .....	4
1.2.1 Introduction to the balance aid concept .....	4
1.2.2 Balance aid aims and objectives.....	5
1.2.3 The balance aid system .....	5
1.2.4 Introduction to the intelligent stimulator concept.....	8
1.2.5 Intelligent stimulator aims and objectives.....	9
1.2.6 The intelligent stimulator .....	9
<b>Chapter 2 Background to stroke rehabilitation</b> .....	15
2.1 Introduction.....	15
2.2 The effects of a CVA .....	16
2.3 Anatomy of the lower limb.....	18
2.3.1 Introduction.....	18
2.3.2 Muscles of the lower leg.....	18
2.4 Physiology of locomotion .....	23
2.4.1 Muscle types .....	23
2.4.2 Muscle contraction .....	24
2.4.3 Neurone structure .....	29
2.4.4 Muscle fatigue .....	31
2.4.5 Strength - duration relationships .....	33

## **CONTENTS**

---

2.4.6 Spasticity.....	35
2.4.7 Human gait .....	37
2.4.7.1 Normal gait .....	38
2.4.7.2 Hemiplegic gait .....	42
2.4.7.2.1 Stance phase variations.....	42
2.4.7.2.2 Swing phase variations .....	42
2.4.8 Mechanisms of balance .....	43
2.5 Discussion .....	45
<b>Chapter 3 The balance re-training aid .....</b>	<b>47</b>
3.1 Introduction to balance re-training aids.....	47
3.2 Aims of the balance aid system in this PhD program.....	49
3.3 Prior research recommendations.....	50
3.4 System level description of balance aid.....	51
3.4.1 The balance aid components.....	51
3.4.2 Balance aid use.....	51
3.4.3 System level operation.....	52
3.5 Footpad hardware.....	53
3.5.1 Introduction to the footpad hardware.....	53
3.5.2 The foot position indication system.....	54
3.5.3 Pressure sensing hardware.....	58
3.5.3.1 Introduction to the pressure sensing subsystem.....	58
3.5.3.2 Differential air pressure sensing.....	59
3.5.3.3 Optical pressure sensing technique.....	61
3.5.3.4 Choice of the pressure sensing subsystem.....	71
3.6 The processing unit.....	71
3.6.1 The microcontroller.....	72

## **CONTENTS**

---

3.6.2 The liquid crystal display screen.....	72
3.6.3 The user interface.....	73
3.6.4 The power supply.....	74
3.7 Balance aid software.....	76
3.8 Balance aid construction.....	81
3.9 Balance aid testing.....	83
3.10 Discussion.....	87
<b>Chapter 4 The intelligent muscle stimulator .....</b>	<b>89</b>
4.1 Introduction to the intelligent muscle stimulator .....	89
4.2 Prior FES research.....	90
4.2.1 FES research .....	90
4.2.2 Stimulation waveform parameters .....	91
4.2.2 Chosen stimulator pulse train parameters.....	93
4.2.4 Alternative stimulation patterns.....	94
4.2.5 Stimulation pulse types.....	95
4.2.6 Electrode - skin connection.....	97
4.2.7 Deficiencies of existing stimulation systems.....	98
4.2.8 Methods of overcoming existing stimulator deficiencies .....	98
4.2.9 Intelligent stimulator aims.....	100
4.3 Initially considered stimulator configurations.....	101
4.4 Chosen stimulator system overview.....	102
4.5 Reference pulse synthesis.....	105
4.5.1 Pulse synthesis overview.....	105
4.5.2 Digital pulse synthesis description.....	105
4.5.3 Variable pulse edge generation.....	106
4.5.4 The complete reference pulse train synthesiser.....	107

## **CONTENTS**

---

4.5.5 Logic incorporation into a PLD.....	110
4.6 Slave microcontroller software.....	113
4.6.1 Requirement for master - slave operation.....	113
4.6.2 Slave software overview.....	114
4.7 The master microcontroller.....	116
4.7.1 Master microcontroller function.....	116
4.7.2 Master microcontroller circuit details.....	116
4.7.3 Master microcontroller software.....	118
4.7.4 Master microcontroller circuit layout.....	118
4.8 The power amplifier.....	119
4.8.1 Power amplifier requirements.....	119
4.8.2 Possible power amplifier configurations.....	119
4.8.3 Stimulator current requirements.....	121
4.8.4 Power amplifier circuit design.....	122
4.8.5 Feedback arrangement.....	128
4.9 The output transformer.....	128
4.9.1 Transformer requirements.....	128
4.9.2 Transformer design introduction.....	129
4.9.3 Pulse train harmonic analysis.....	130
4.9.4 Transformer design results.....	131
4.9.5 Transformer secondary winding loading arrangement.....	132
4.9.6 Transformer evaluation results.....	134
4.10 Transformer core flux reset function.....	138
4.11 Stimulator power supply.....	141
4.12 Mechanical layout of the stimulator.....	144
4.13 Stimulator performance.....	146

## **CONTENTS**

---

4.13.1 Stimulator output pulses.....	146
4.13.2 Stimulator power requirements.....	151
4.13.3 Movement produced by the stimulator.....	151
4.14 Intelligent stimulator discussion.....	153
4.14.1 Functionality of the stimulator.....	153
4.14.2 The performance of the stimulator.....	154
4.14.3 Suggested stimulator improvements.....	155
<b>Chapter 5 Control of the intelligent stimulator .....</b>	<b>157</b>
5.1 Introduction to control of the stimulator .....	157
5.2 Aims and objectives of chapter 5.....	157
5.3 Feedback generation methods.....	157
5.4 Chosen form of feedback.....	158
5.5 Underfoot pressure sensing.....	159
5.5.1 Floor mounted pressure sensing .....	159
5.5.2 Foot mounted pressure sensing.....	160
5.6 Pressure sensor placement.....	162
5.7 Possible methods of under-foot pressure sensing.....	164
5.8 The Hall effect pressure sensing system.....	164
5.9 Initial pressure mat testing.....	168
5.10 Pressure distribution data acquisition.....	170
5.11 Normal gait data observations.....	173
5.12 Stroke affected gait observations.....	184
5.13 Underfoot pressure trace analysis.....	192
5.13.1 Analysis introduction.....	192
5.13.2 Underfoot pressure transition relative timing.....	192
5.13.3 Underfoot rate of pressure change analysis.....	196

## **CONTENTS**

---

5.14 Data acquisition for the intelligent muscle stimulator.....	203
5.14.1 Introduction to the data acquisition subsystem.....	203
5.14.2 Data acquisition subsystem design.....	203
5.14.3 State machine operation.....	206
5.14.4 Data acquisition system construction.....	206
5.15 Master microcontroller decision making software.....	208
5.15.1 Software overview.....	208
5.15.2 Stimulation strategy overview.....	208
5.15.3 Stimulator operating cycles.....	209
5.15.4 Master microcontroller cycle.....	211
5.15.5 The gait tracking framework.....	212
5.15.6 The gait calculation cycle.....	218
5.15.6.1 Introduction to the gait calculation cycle.....	218
5.15.6.2 Underfoot pressure data pre-processing.....	218
5.15.6.3 Gait evaluation and stimulation parameter processing.....	219
5.16 Initial stimulator tests utilising the underfoot pressure feedback.....	222
5.17 Discussion.....	226
<b>Chapter 6 Conclusions and further work</b> .....	<b>228</b>
6.1 Balance aid conclusions .....	228
6.1.1 Balance aid philosophy.....	228
6.1.2 The balance aid system.....	229
6.1.3 Suggested balance aid improvements.....	230
6.1.4 Suggested further balance aid investigation.....	232
6.1.5 Balance aid summary.....	232
6.2 Intelligent stimulator conclusions.....	233
6.2.1 Intelligent stimulator philosophy.....	233

## **CONTENTS**

---

6.2.2 The intelligent stimulator.....	234
6.2.3 Suggested intelligent stimulator hardware modifications.....	236
6.2.4 Suggested intelligent stimulator further investigation.....	239
<b>Appendix A Beam calculations .....</b>	<b>241</b>
<b>Appendix B Balance aid software.....</b>	<b>252</b>
<b>Appendix C C. of G. calculation.....</b>	<b>262</b>
<b>Appendix D Pulse synthesis PLD code.....</b>	<b>263</b>
<b>Appendix E Stimulator parameter derivation.....</b>	<b>265</b>
<b>Appendix F Slave software routines.....</b>	<b>268</b>
<b>Appendix G Slave software listing.....</b>	<b>271</b>
<b>Appendix H Data transfer routines.....</b>	<b>274</b>
<b>Appendix I Transformer design.....</b>	<b>275</b>
<b>Appendix J Data acquisition software.....</b>	<b>279</b>
<b>Appendix K State machine operation.....</b>	<b>281</b>
<b>Appendix L Data acquisition PLD code.....</b>	<b>282</b>
<b>Appendix M Master software.....</b>	<b>283</b>
<b>Appendix N Conference paper.....</b>	<b>299</b>
<b>References .....</b>	<b>301</b>
<b>Bibliography.....</b>	<b>328</b>

# **Synopsis.**

The following report describes the development of a complete system for the rehabilitation of post cerebro-vascular accident (CVA) patients. The system is divided into two distinct components :-

(i) The first is a description of a portable, microcontroller based, automated aid for static and dynamic balance re-training of patients within their own homes. This research has resulted in the development of a unit that may be used by any stroke patient at their leisure for re-training of static balance and the dynamic weight shifts associated with the initiation of gait. The development of a novel, robust optical sensor permits accurate balance distributions to be sensed without undue movement occurring in the balance sensing pads. The 'take home' principle of this equipment provides a more intensive balance re-training course than would normally be available via contact time with a physiotherapist. The lightweight balance aid system may be easily transported by patients and is intended to be the first stage in the introduction of systems that bring a complete treatment and monitoring service to the patient within their own home.

(ii) The second is a description of an intelligent, modular and fully programmable functional electrical stimulation (FES) system for use in alleviating foot drop and effecting restoration of a smooth gait. This intelligent stimulator utilises arrays of novel dynamic pressure sensors to detect pressure changes under the feet of stroke patients during the gait cycle. This permits the point within the gait cycle to be detected and the required corrective stimulation to be ascertained. The system incorporates independent, real time modification of every parameter of the output pulse trains as necessitated by the under-foot pressure feedback from the patient. Decisions are made within the stimulator software on the quality of the patient gait and the required stimulation pulse trains are synthesised accordingly. This permits the intelligent stimulator to constantly provide correction for patient gait and physiological variation. This development is the first stage in the creation of a stimulation system that is able to correct foot drop without the requirement for a unique parameter setup to suit a particular patient. The modular system is expandable to  $n$  channels and the fully programmable design permits usage on any muscle grouping with appropriate software alterations, making it a useful, general purpose FES research tool.



---

## **ACKNOWLEDGEMENTS**

---

# **ACKNOWLEDGEMENTS.**

I would like to acknowledge the assistance provided by the following in the development of this thesis:-

Dr R.T. Lipczynski, University of Bath.

Dr R.F. Ormondroyd, University of Bath.

Mr J.D. Martin, University of Bath.

Mr R.J. Hill-Cottingham, University of Bath.

Dr I. Swain, Medical Physics Department, Odstock Hospital, Salisbury.

Mr P. Taylor, Medical Physics Department, Odstock Hospital, Salisbury.

Ms J. Burrige, Medical Physics Department, Odstock Hospital, Salisbury.

The University of Bath, for funding this research.

# **CHAPTER 1.**

## **INTRODUCTION.**

### **1. 1 Requirement for walking aids.**

Cerebro-vascular accidents (CVA) or strokes are the most common cause of neurological disability in the community [1,2]. Strokes arise as a result of the interruption of the circulation within the brain due to lesions or abnormal clotting. About three quarters of victims of stroke survive the initial event and of these survivors approximately one half to three quarters will recover functional independence [3]. Survival of the initial stroke is dependant on the site and size of the lesion. The extent to which the quality of life of a stroke victim is affected is subject to great variation and will be due to a combination of the following five stroke related syndromes, motor deficit, sensory deficit, hemianopia, higher cerebral dysfunction and brain stem deficit [3,4]. In many cases, the loss of partial or full voluntary limb locomotion as well as posture and balance difficulties are observed on the contralateral side of the body to the side of the brain affected by the interruption of blood circulation during the stroke [5]. This loss of function is a result of lesions within the upper motor neurones which do not have the ability to regenerate [6], resulting in only limited recovery of motor function [6]. Ambulatory function is usually recovered to some degree although gait defects are common in post stroke individuals [7] and if uncorrected can result in a high energy cost during locomotion [8].

This thesis details the development of equipment intended to provide the stroke patient with the means to overcome the balance and gait defects often observed as the result of such a CVA. This equipment takes the form of a balance aid suitable for high intensity 'at home' balance re-training and an intelligent muscle stimulator able to monitor the patient gait and apply the appropriate corrective stimulation.

The fact that the peripheral motor neurones are left intact and that the muscles are undamaged permits the use of a number of rehabilitation techniques including ice, infra-red heat, ultrasound and acupuncture [9]. Electrotherapy has been considered for various ailments since 50 A.D, when Scribonius Largus claimed success in the treatment of gout and headache using torpedo fish [10]. Artificial activation of the muscles by FES (functional electrical stimulation) has

## **CHAPTER 1 INTRODUCTION**

---

been investigated since 1759, when Benjamin Franklin attempted to restore voluntary movement to persons exhibiting paralysis [11]. This was followed in 1777 when The Abbe Bertholon used electrotherapy to relieve plantarflexor spasticity [12] and in 1792, when Galvani showed the effect of electricity on living tissue [13]. Modern uses of FES to restore locomotion began in 1961 with Liberson's alleviation of foot drop by the synchronisation of FES with the gait cycle [14]. FES utilises the application of voltage or current pulse trains [15] to either the motor neurone prior to the muscle or, using a higher magnitude pulse train, to the motor end plate of the muscle itself [16]. It has been successfully used to restore lost limb movements [17,18]. Muscle bulk wastes quickly with inactivity which may then affect lower motor neurone conduction velocity [19] making stimulation, whether artificial or natural, of the muscles vastly more difficult or impossible.

This leads to the conclusion that subsequent to a locomotion-affecting stroke, movement should be restored to the limb as quickly as possible to reduce the effects of tissue wastage. It is well known that the application of FES can halt or reverse this decline in muscle performance [20] This can initially be accomplished by the use of a stimulator to produce pre-programmed simple limb movement, purely for the purpose of muscle strengthening. The effectiveness of such a treatment is reported by Balogun [21] and Cozean et al. [2]. A general purpose programmable stimulator may be used in physiotherapy sessions to reduce or halt the otherwise inevitable tissue wastage by providing the required stimulation for muscle contraction. The gain in strength obtained through FES has been shown by Waters [22], Takebe et al. [23] and Delitto et al. [20] to 'carry over' and still be present after the cessation of periods of treatment.

It is believed that if the damage to the brain is not too widespread, then new neural pathways may be utilised to perform the functions previously assigned to the damaged areas [24,25,26,27,28,29]. Therefore, the restoration of locomotion as similar as possible to that exhibited before the stroke is of primary importance as "locomotor training represents a functional activity, potentially capable of forcing the use of unmasked pathways (in the brain) through intense sensorimotor stimuli" [30].

Movement restoration, such as that suggested above, is only possible using a multichannel stimulator that is able to operate with software that permits feedback from the body to be analysed and the output to the patient adjusted as required [31]. Stimulators featuring merely 'on-off' control cannot achieve the complex variation in stimulation parameters necessary to effect natural movements. It is likely that more than a single output channel will be required to effect smooth natural movement of affected limbs, though all channels used must be controlled

## **CHAPTER 1 INTRODUCTION**

---

from a single point to maintain synchronisation of the applied pulse trains. It was concluded by Malezic et al. [32] that different degrees of disability will require varying numbers of channels to effect the required movement and that the number of stimulation channels needs to be matched to the requirements of the patient. This leads to the requirement of a stimulator extendible to  $n$  channels, as well as possessing full programmability, to ensure complete versatility.

There is a problem, however, with the use of stimulators. In cases of loss of locomotion below the waist, the sense of balance previously enjoyed by the patient is lost or extensively modified. In the case of a large scale loss of locomotion, such as that caused by a spinal lesion, extremely complex multiple channel stimulator control, such as that employed by Malezic and Hesse [33], is required to restore gait and balance at the same time. This extent of control requires the design of sensors effective in monitoring balance during the periods of enforced locomotion.

The design of a new stimulator for the immediate application of such an extensive level of control is not presently practical due to the large number of muscle, and hence stimulation sites, required to effect whole body balance. Therefore, the design presented in this thesis will initially be employed to combat the condition known as foot drop, where the loss of locomotion due to the stroke is limited mainly to the ankle joint. Foot drop is not caused exclusively by CVA [34] but is a common outcome of the stroke [35]. This proves to be a great inconvenience to the patient, causing rapid fatigue and abnormal gait. The loss of balance involved in such cases is often recoverable with training and practice as the patient is able to adjust to the loss of sensory information which would normally be processed by the now damaged section of the nervous system. At present, physiotherapy under supervision is the method by which balance re-education is effected [36]. Naturally, the patient must be capable of maintaining balance whilst stationary before gait corrections may be effected [37] to avoid potentially injurious falls. In the case of foot drop being the only gait deficiency, the sense of balance is best gained by re-education rather than by any artificial means.

In order to facilitate the progression of patients exhibiting foot drop to a stage where the fitting of a stimulator is possible, an automated method of balance re-training utilising feedback is suggested. Basmajian et al. have reported the usefulness of audio-visual biofeedback in maintaining the motivation of the patient [38]. Ideally, this biofeedback would indicate visually to the patient the current state of their balance, permitting the patient to learn to alter their stance in a controlled manner, without the need for any specialist instruction or supervision. Such weight bearing activities are recommended by Dickstein et al. [39] prior to, and during, gait re-

---

## **CHAPTER 1 INTRODUCTION**

---

training. A stimulator may then be fitted when the patient is considered to have progressed to a suitable level of balance-maintaining ability.

Automated training procedures reduce loading on physiotherapy personnel, permitting the treatment of more patients in a given time. Biofeedback has been shown to accelerate patient recovery when compared to traditional physiotherapy techniques [39,40,41], so if equipment is developed that may be taken away and used by a patient at their convenience, then the possibility exists of greatly accelerated patient rehabilitation.

At present, it is necessary to adjust a stimulator to the needs of each individual using a number of different setup routines. This is because variables such as muscle atrophy, subcutaneous fat layer thickness, tissue conductivity and muscle output force cause each individual to require a unique stimulation pattern, which the universal control unit developed by Brandell sought to overcome [31]. In order to avoid such set up routines, which can be lengthy and frustrating for the patient, a stimulator might adjust the output produced to suit the needs of each individual by processing feedback from sensors located on the patient. The ability to perform constant self adaptation allows each stimulator produced to be identical and simply be fitted and left to 'learn' from the patient. As the patient regains strength and movement ability, so the stimulator might adapt its output to ensure that the gait is still as near to a normal gait as possible.

### **1. 2 Introduction to the walking aids.**

#### **1. 2. 1 Introduction to the balance aid concept.**

Balance and postural sway has been realised as an important factor in correct ambulation as far back as 1853, when Romberg's test was devised in order to quantify this parameter [42,43]. Standing balance has been defined as "the ability to stand and move in an upright position" by Hill et al. [44] and the ability to maintain and control the body over a small base is one of the fundamental skills involved in standing and walking [43,45]. One of the most frequently noted motor deficits of post stroke victims is hemiplegia where both stance, gait and balance are affected [46] and it is especially noted that such patients tend to favour their unaffected leg with an abnormally large percentage of their bodyweight [47,48,49]. The re-training of the ability to transfer this bodyweight to the hemiplegic leg is an essential precursor to a smooth entry into the swing phase of the gait cycle [50]. It has been reported by various authors that patient recovery begins immediately after the CVA but little further improvement is seen after three months of treatment [51,52]. This shows that to effect the maximum improvement in the condition of the patient, balance training should be undertaken as soon as possible after the CVA.

## **CHAPTER 1 INTRODUCTION**

---

In order to fulfil the requirement to provide immediate, intensive post stroke balance re-training and hence speed up the rehabilitation process of many stroke patients, the use is suggested of a system that can be operated by the patient without supervision or assistance from a physiotherapist. The removal of the necessity for physiotherapist contact time at each training session will dramatically increase the available training intensity, as the available time becomes the total time available to the patient and not the time that the physiotherapist is able to devote to that patient. Cozean [2] states, with respect to stroke patients, that “self administration of therapy represents a major advantage over therapy programs that require a practitioner in attendance.”

### **1. 2. 2 Balance aid aims and objectives.**

The requirement of a system able to provide the immediate, high intensity, unsupervised balance re-training described above, at a location convenient to the patient, led to the following objectives:-

- The development of a feedback utilising system that may be used by patients immediately post stroke, to begin the static and dynamic balance re-training procedure.
- The testing and evaluation of the balance aid unit.

### **1. 2. 3 The balance aid system.**

If the balance aid is to be used in the homes of the patients, it must be simple to operate and be easily transported by the patient. This rules out any complex PC based systems, such as the system used by Geurts and Mulder [53] or the Chattecx system used by Dickstein et al. [54], which require large cumbersome equipment, such as monitors to operate. To ensure portability, the balance aid will need to be disassembled for transit and reassembled by the patient when required for use. Therefore, assembly must be extremely simple and completely foolproof to ensure correct operation as well as the safety of the patient. Additionally, the balance aid must be usable by any size or weight of person as a custom build or set up for each patient would only further slow down the rehabilitation procedure, which can begin as early as 48 hours post stroke [37].

The simplest method of detecting the balance of a patient is to measure the weight distribution of that person in relation to the position of their feet; i.e. measure the centre of pressure (CP) of the patient. The position of the feet provides an ideal centre of balance position and the weight distribution across the soles of the feet provides a value relating to the actual centre of mass

## **CHAPTER 1 INTRODUCTION**

---

(CM) position. Wing et al. [55] have reported that the excursion of the CP is greater than that of the CM, therefore this method of assessment of balance will produce a more sensitive indication than a direct CM measurement. This method of detecting the balance position requires a form of platform that the feet may be placed upon so that the forces acting on the soles of the feet may be analysed.

It has been shown by various authors [58,59] that maintenance of balance is by means of pre-determined response patterns known as central sets [60] and open and closed loop control using as feedback: vision, proprioception, somatosensory, vestibular and stretch reflex cues. Authors such as Peterka and Black [57] and Diener and Dichigans [61] have utilised tilting platforms to ascertain the effects of disturbing the balance of hemiplegic patients. This effect is to be avoided in the re-training of patients within their own homes as the necessary safety harnesses to prevent falls will not be available. Therefore, the sensing arrangement used must not exhibit excessive movement or this will further degrade the balance of the patient. Hocherman et al. [62] reported that patients felt that static balance re-training helped to make them feel more stable and secure. The resulting loss of confidence that the movement of a balance platform would bring would then have the opposite effect to that desired and worsen the rate of recovery of the patient.

Prior research at Bath University by Ho et al. [63] found that the variety of stances exhibited by stroke patients could not be catered for in a single platform system, whilst maintaining this at a size consistent with high portability. Wing et al. [64] and Day et al. [65] have found that standing stability is very dependent on stance-width and that the degree of balance degradation of a patient will, to an extent, dictate their natural stance-width. The recommendation from the research of Ho et al. [63] was to use two separate platforms, one for each foot, that could be spaced apart as dictated by the stance of the patient. This platform configuration is used in the balance aid to ensure the convenient use of the device by as many patients as possible.

The balance information may be transmitted to the patient visually, in accordance with the biofeedback findings of De Weert et al. [50], as this will be an easy method by which the patient can interpret the balance data. A simple method of indicating balance information is by means of a cross displayed on a screen, with the position of the cross relating to the centre of balance position of the patient. It is possible to use on-screen arrows to indicate the direction in which the patient should adjust their balance, though this does not easily demonstrate when ideal balance is achieved and the degree of balance adjustment required. Coloured lights were employed in the Balance Performance Monitor, a two footpad IBM PC based system

## **CHAPTER 1 INTRODUCTION**

---

extensively used by Sackley and Baguley [47], to indicate the position of the patient centre of mass, though it is felt that such a system does not lend itself to the application of the stimulating games necessary to ensure patient motivation. Schmidt et al. [66] detail that these re-training activities should be varied to avoid the learning of a single mechanism by “blocked practice” where successive practice yields less and less benefit. Balance training games displayed on a screen and variable under software control will allow the necessary variation suggested by Schmidt et al. [66]. Schmidt et al. [66] also stress the need to ensure that the physiotherapist-taught actions can be repeated at leisure by the patient, “It makes little sense to be able to perform skills in the hospital if they cannot be performed when the patient returns to his home or job tomorrow.” A portable system for balance re-education fulfils these requirements.

It was decided that displaying a box on screen to show the ideal balance position as well as displaying the cross for actual balance position was the simplest method of data presentation for the patient to interpret. The method of attaining balance is simply to align the cross and the box. This approach provides data to the patient on both the required movement direction and the required amount of movement.

In order to permit visual feedback to be available to the patient and to ensure that the unit is portable, lightweight and robust, a liquid crystal display screen was the obvious choice. Light emitting diode arrays are available, although they do not permit the display of complex graphic characters as will be required to permit the implementation of stimulating training activities.

There is a certain amount of calculation and data interpretation required within a system that is monitoring balance sensing equipment and making decisions based on that data. There is also a need to ensure that the equipment produced is flexible enough to be upgraded when necessary with the minimum of effort. Upgrades are likely following trials of the unit and as the full potential of the device is realised. To maintain this degree of flexibility, it was decided to base the design around a microcontroller. Winstein [67] notes the importance of providing the patient with “knowledge of performance”, which is best evaluated and stored on a microcontroller based system. The program operated by this microcontroller can then be updated as required with no necessary hardware alterations.

The above decisions resulted in the concept of a balance aid system comprising three modules; two pads for foot placement and a combined microcontroller, LCD screen and power supply module, as shown in fig. 1.1.



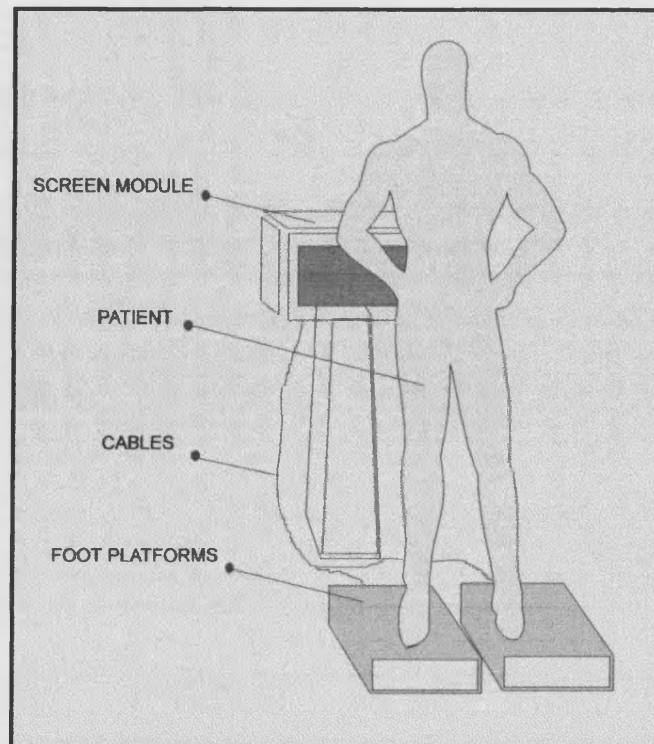


Fig. 1.1 Balance aid concept.

In fig. 1.1, the screen module is placed on a stand to permit convenient eye level viewing for the user. This module, which contains all of the processing circuitry, is linked to each of the foot platforms by data and power transmitting cabling. A balance aid in this format can be easily assembled with no specialist knowledge by attaching connectors to the appropriate sockets. The necessary operating instructions may then be displayed on the screen as required, so that the only required instruction is reduced to 'assemble and switch on'. Collen [43] and Sohlberg and Mateer [68] state that patients with neurological dysfunction may exhibit attention or learning deficits. This, therefore, is the level of complexity acceptable for use by stroke patients without supervision. Naturally, it is quite acceptable to consider that the first session in the use of the balance aid might be in the presence of a physiotherapist, to offer prompts to the user when necessary. Subsequent to this, though, the patient would be expected to be able to use the device unaided and would not be expected to remember complex setup procedures.

### 1. 2. 4 Introduction to the intelligent stimulator concept.

Since Liberson et al. synchronised electrical stimulation with the gait cycle in the 1960s [14], a number of researchers have investigated the application of FES to various muscle groups to alleviate a variety of conditions. These applications have included the restoration of locomotion

---

## **CHAPTER 1 INTRODUCTION**

---

to paraplegics [69,70,71], the restoration of hand function [72] and the alleviation of foot drop [72,73].

The application of constant cycles of stimulation have found only limited usefulness because of the variability of the responses of muscles [74], the effects of fatigue [75] and the variability in tissue conductance [76]. It has been realised by Franken et al. [69] that the stimulation patterns require constant updating to remain effective. An intelligent stimulator is considered to be a stimulator that is able to determine the required stimulation, provide such a stimulation to the chosen site, determine the effect of that stimulation and correct the applied stimulation as required. This requires the use of a closed loop system, utilising some form of feedback to provide information on the gait of the patient.

### **1. 2. 5 Intelligent stimulator aims and objectives.**

The rectification of post stroke gait defects by a device that is able to determine dynamically the necessary stimulation, requires the following objectives to be realised:-

- The design, construction and testing of an intelligent stimulator able to make gait related decisions and apply the necessary stimulation.
- The design, construction and testing of a feedback acquiring arrangement.
- The design and implementation of a stimulation procedure to effect control of the stimulation hardware.

### **1. 2. 6 The intelligent stimulator.**

If the stimulation system is to be able to analyse the patient gait and to alter its output to correct that gait at any instant, then it follows that the stimulator should be able to synthesise any desired pulse train output at any time as there will be no method of determining in advance the corrective action required for the next phase of gait. There has been much research into the mechanisms of gait and the phases of gait are well known [77], as are the likely variabilities in hemiplegic gait [78,79]. This knowledge alone does not allow gait correction to be effected, hence the requirement for patient gait feedback and the analysis of this information. The ability to analyse gait data and utilise the result to synthesise any desired stimulation pulse train led to the decision to base the intelligent stimulator around a microcontroller. The use of this device permits extensive decision making to be performed according to the rules set out in the program devised for the microcontroller, without the excessive bulk of computer controlled systems such as that used by Malezic et al. [32] and Meadows and McNeal [80].

## **CHAPTER 1 INTRODUCTION**

---

There are both single and multi-channel stimulation systems in operation today. The requirement for single, dual or multi-channel systems is dependant on a number of factors including the severity of the condition being treated and the permissible complexity of the stimulation system. As the number of output channels for a foot drop is a compromise between functionality and complexity [32], it was decided to design a system that permits simple expansion to any required number of output channels. This means that the system must be able to synthesise independent pulse trains simultaneously on any number of channels. Different stimulation patterns could be applied by the use of independent channels, as utilised by Brandell [31] and Malezic [32], so it is important that the output pulse parameters of each channel of the intelligent stimulator have no dependency on any other channels.

In order to guarantee a fast response to detected gait deficiencies and to be able to cope with any combination of circumstances, it was decided that the individual pulses of the output pulse trains should be individually synthesised and not generated as fixed-pulse trains. This permits a fast change of pulse parameters when required as there is no dependency on any previous or following pulses and hence no need to wait for a sequence of pre-defined pulses to finish before output alterations can be effected. This is the case with many current stimulation systems which imposes severe limits on their flexibility. In order to ensure that the intelligent stimulator stays as flexible and responsive as possible, it has been designed to allow independent variation of every parameter of the output pulse. This functionality of the stimulator permits its use in research into the effects of the combinations of different stimulation parameters, especially the effects of different pulse rise and fall times. These parameters may be of use in varying the intensity of the applied stimulation. The chosen parameter ranges and the reasoning behind these choices is discussed in chapter 3.

The necessity for independent pulse train synthesis led to the general stimulator structure shown in fig. 1.2, where the stimulator comprises a master and several slave units. The master module receives the gait related data and makes decisions based on this data such as the current position within the gait cycle and the required stimulation. The slave units then synthesise the output pulse trains according to the decisions taken by the master module. In this way, extra slave modules, or channels, may be added without any loss of system co-ordination as this is carried out by the single master module.

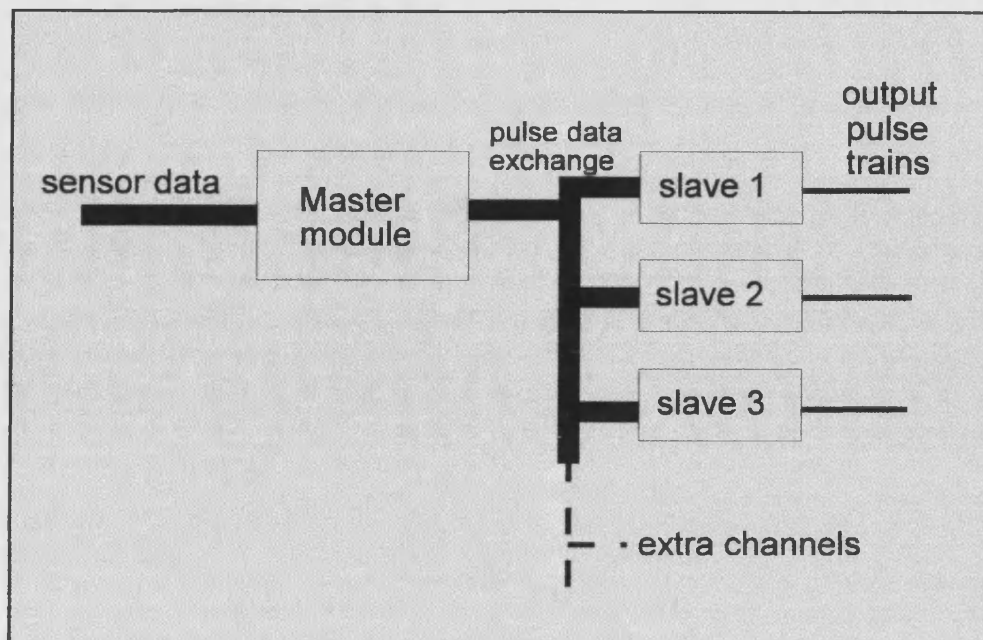


Fig. 1.2 Master - slave stimulator concept.

It is vitally important that a high quality gait monitoring system is developed to provide information to the decision making section of the intelligent stimulator. There can be no accurate gait correction without reliable and accurate information on the quality of the patient gait and the knowledge of exactly which point the patient has reached within the gait cycle. There are a number of research and commercially available gait monitoring systems available [81], which include force platforms [82], underfoot switches [83] and pressure sensitive treadmills [84]. These possess varying levels of suitability for use in a portable intelligent stimulation system and are discussed in chapter 5.

To achieve this level of gait analysis requires knowledge of both the actual patient gait and the desired 'ideal' gait. The 'ideal' gait model may be achieved by application of the sensing system to individuals with no gait deficiencies and by a study of literature published on the action of normal gait, such as that by Winter [77] and that by Mann et al. [85]. A study of normal individuals permits a core model of ideal patient gait to be obtained. There will always be small variations between individuals around this core model, as shown by Hill et al. [86] and as discussed by Wing [87], but the model gained should allow the correction of the gross gait deficiencies observed in foot drop patients.

It is extremely important that the patients are not handicapped further by bulky and cumbersome gait sensing systems as these are apt to alter the patient gait still further [88]. Foot switches

## CHAPTER 1 INTRODUCTION

---

mounted on insoles are commonly used in the current generation of stimulation systems as a trigger for fixed pulse train applications [89,72,73,90,86,91]. It was decided to develop this technique further to produce a pressure sensing insole that could generate sufficient information to permit the stimulator to operate in the manner suggested above. The use of under-foot pressure data appeared to be the method of feedback generation offering the greatest gait based information for the least amount of patient inconvenience.

The method of application of the pulse trains to the patient is to be by self-adhesive surface electrodes, which is the method currently used for many foot drop stimulation systems [73,32,92,93]. The electrodes are moistened and placed on the skin at the required stimulation site. The conductive gel composition of the electrode pads ensures a low resistance skin contact [73,93], which reduces the risk of contact burns from the current passed into the tissue by the stimulator. Other methods of stimulation application, such as percutaneous and subcutaneous electrodes require operations for system implantation [91,94,95,96]. This is not desirable for a system under development and does not lend itself to the rapid treatment of all foot drop patients with an identical, minimal setup time procedure. The intelligent stimulator is envisaged in the form shown in fig. 1.3, with the stimulator unit worn attached to a belt, the surface electrodes attached to the lower limb and these connected together by lightweight nylon reinforced cabling.

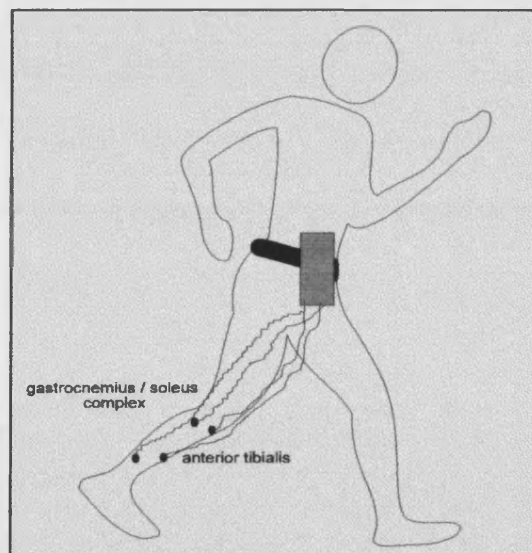


Fig. 1.3 Intelligent stimulator concept utilising two output channels.

The exact sites for electrode placement are subject to variation between individuals [73,94], although the general position of the electrodes for activation of any given muscle group is

## CHAPTER 1 INTRODUCTION

always similar and is well known [31,33,93]. It was decided to produce a two channel version of the intelligent stimulator in order to verify its performance without the complexity of a multi-channel system. Naturally, the system may be expanded to produce finer movement control when the general system performance has been assessed. The sites chosen for stimulation using the two channel system were the gastrocnemius / soleus complex, otherwise known as the calf muscles and the tibialis anterior muscle that runs along the outer edge of the shin. The general placement of electrodes for the stimulation of these two sites is shown in fig. 1.4. The exact electrode placement will be covered in more detail in chapter 2.

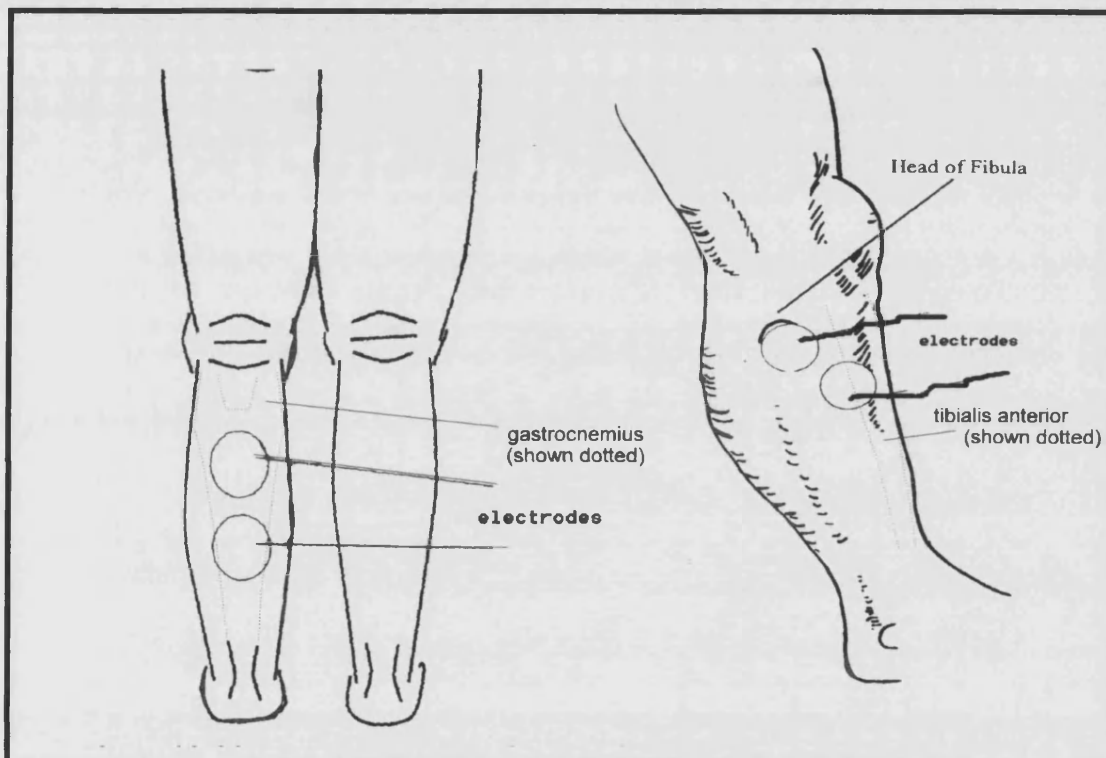


Fig. 1.4 Electrode positioning for stimulation of gastrocnemius and anterior tibialis [2].

The gastrocnemius / soleus complex and the tibialis anterior are an antagonistic muscle pair and cause the foot to push down and the toes to lift respectively. The push down or plantarflexion of the foot is essential for a good push off before the swing phase [79,97,98], in fact it is stated by Olney et al. [99] and Winter [100] that approximately half of the positive work associated with walking is provided by the plantarflexors. The toe lift or dorsiflexion is essential if the toes are to clear the ground during the swing phase [97,79], though this must reduce later in the cycle to reduce some of the shock of ground contact [79]. Stimulation of these two sites should be

---

## **CHAPTER 1 INTRODUCTION**

---

sufficient to determine the success of the intelligent stimulator in overcoming foot drop in stroke patients.

To summarise:- This thesis details the development of a portable balance re-training aid and an intelligent footdrop stimulator. The balance aid is intended to be used by a patient at home to provide a stimulating and challenging environment for static balance and weight shifting re-training. The intelligent stimulator is intended to provide a foot drop alleviating system that is able to analyse the patient gait via an underfoot pressure sensing system and adjust its output to suit the observed gait.

## **CHAPTER 2**

### **Background to stroke rehabilitation.**

#### **2. 1 Introduction.**

The development of novel walking aids requires an understanding of the following subject areas:-

- 1) The cerebro-vascular accident (CVA) , the possible results of and likely recovery from such an injury.
- 2) The anatomy of the lower limb.
- 3) The physiology of movement.
- 4) The mechanisms of balance.

The study of the occurrence and likely effects of a CVA permit an insight to be gained into the degree of disability likely to be experienced by patients. This also permits an indication of the possible recovery that may be observed with re-training and physiotherapy and the method by which this training should be applied. This permits equipment to be designed that will speed and extend this recovery.

A study of the anatomy of the area in which stimulation is to be applied gives an understanding of the best stimulation sites. The muscle insertion points, along with the direction of contraction of that muscle, permits an understanding to be gained of the movement that may be created by stimulation of that site. The range of possible movements that may be produced then requires comparison with the likely locomotion deficiencies of the patients. It is also important to realise that surface stimulation of any part of the body will affect more than one muscle. A study of the local anatomy provides an insight into the likely secondary effects of the stimulation.

It is essential to possess an understanding of the mechanisms that produce locomotion within the human body. These mechanisms illustrate the conditions that are suitable for treatment with FES and those conditions that are not suited to this form of treatment. A study of the physiology of muscle contraction serves to illustrate that each stimulation parameter has a



## **CHAPTER 2 BACKGROUND TO STROKE REHABILITATION**

limited range of usable values. This study also produces an insight into the effects of exceeding these ranges.

A study of the cycle of human gait, both in normal subjects and those exhibiting hemiplegic gait defects, permits an understanding to be gained on how best to apply FES for the correction of these gait deficiencies. Consideration of the various gait measuring techniques available will assist in the choice of a sub-system to provide the required feedback on gait quality to the FES system.

A study of the mechanisms by which the awareness and actuation of balance is achieved within the human body and the possible reasons for the loss of this ability after stroke will provide an understanding of how this skill might best be re-learned. A study of current re-training equipment and its associated deficiencies will permit the design of improved balance re-training systems.

### **2.2 The effects of a CVA.**

A CVA or stroke is the result of the disturbance of the circulatory system within the brain [5]. Following a CVA, it is known [101,6] that the damaged area of the brain does not regenerate significantly, however, improvements in patient motor skills are observed with applied physiotherapy [102, 36]. It is believed [101,6] that other areas of the brain may assume, to various extents, the functions of the damaged areas by a learning process that is initiated by the physiotherapy [26,27,28,29]. It must be stated though, that the mechanisms of this development are not understood in any detail [30]. Of those suffering an acute stroke, approximately three quarters survive [3], most of which will experience some degree of recovery [4]. The extent of recovery depends upon the size and site of the blood vessel damage or lesion [3] although there appears to be a reasonably fixed time over which this recovery occurs. Two to four weeks is often required for the patient to recover from the shock associated with the injury [103]. Duncan et al. found that most recovery occurs within 30 days and that little further recovery was observed after three months of therapy [4]. This result is also detailed by Wade et al. [52] although a figure of two months was found by Friedman [104] to be the upper time limit on recovery. Friedman also goes on to suggest that the application of rehabilitation techniques at an early stage after the stroke may be vital to subsequent gait recovery. It is also considered [4,79] that recovery is more pronounced in the lower limbs than in the upper extremities and that hand and finger movements are rarely regained [103]. Therefore, the application of walking and balance re-training systems soon after stroke may be the best way to ensure the maximum recovery of volitional movement [104].

## **CHAPTER 2 BACKGROUND TO STROKE REHABILITATION**

There are a variety of effects of the stroke which depend on the site of the lesion. It has been found that those patients with right hemisphere damage tend to experience more pronounced attention defects whereas those with left hemisphere damage tend to exhibit worse choice performance [105]. It is recognised that FES and balance re-training are recognised methods of producing the necessary movement and afferent responses to commence this functional learning in patients [102]. FES may also be used to trigger electrical activity within the body to make it appear to the central nervous system that the affected area of the body is functioning again [102]. It is also considered by Valencic et al. [106] that FES retards the atrophy of type I and type II muscle fibres in post CVA individuals. FES is also believed to promote terminal sprouting of ganglia [102, 106] in the peripheral nervous system and maintain the muscle output torque, even in denervated muscles, over a period of several months [106].

It is noted by Izzo and Aravabhumi [107] that subsequent to the CVA, muscular flaccidity occurs, only to be replaced by an increased muscle tone or spasticity, which is discussed further in section 2.4.6. This can lead to further gait complications other than the drop foot, such as equinus and varus. These conditions are a result of unbalanced muscle tone within antagonistic pairs of muscles in the lower leg [79,108]. Equinus is principally [107] the result of plantarflexor (gastrocnemius and soleus group) spasticity, whilst varus is essentially spasticity of the tibialis anterior muscle. These added complications, along with the discovery that the stimulation of antagonistic pairs of muscles together produces a more linear force response [109], has led to the development of multi-channel stimulators for the restoration of volitional movement [109]. These stimulators are further discussed in section 4.2.1.

Hemiplegia affects patient gait even when marked spasticity is not present [107] as balance may be affected and patients often adjust their weight to the unaffected side in an attempt to compensate for the weaker side as reported by Winstein et al. [110], Hocherman et al. [62] and Turnbull et al. [111]. Such behaviour must be rectified before a programme of FES assisted ambulation can commence. This fact is clearly stated by Izzo and Aravabhumi [107] ' *The ability to maintain standing balance independently is a prerequisite of ambulation training*', Winstein et al. who state that "*balance control is an essential component for the optimal functioning of any locomotor system*" [110] and further reinforced by Dettman et al. [112] and Hamrin et al. [113] whose studies detected a high correlation between static balance and locomotor function.. This highlights the requirement for balance re-training systems.

## **CHAPTER 2 BACKGROUND TO STROKE REHABILITATION**

### **2.3 Anatomy of the lower limb.**

#### **2.3.1 Introduction.**

The muscles and bones that comprise the lower leg may be seen in figs. 2.1 and fig 2.3, where an anterior and posterior view are shown. These diagrams provide a good indication of the relative position and attachments of the various muscles, throughout the lower leg. The correction of foot drop requires a knowledge of the limb from the knee joint downwards, so this section of the limb alone is considered. The innervation and function of each muscle is then discussed. The anterior and posterior innervation are then shown on separate diagrams in fig. 2.2 and fig. 2.4 to aid clarity and provide an indication of the required electrode positioning to effect dorsiflexion and plantarflexion of the ankle.

#### **2.3.2 Muscles of the lower leg.**

An anterior view of the muscles of the lower leg is shown in fig. 2.1.

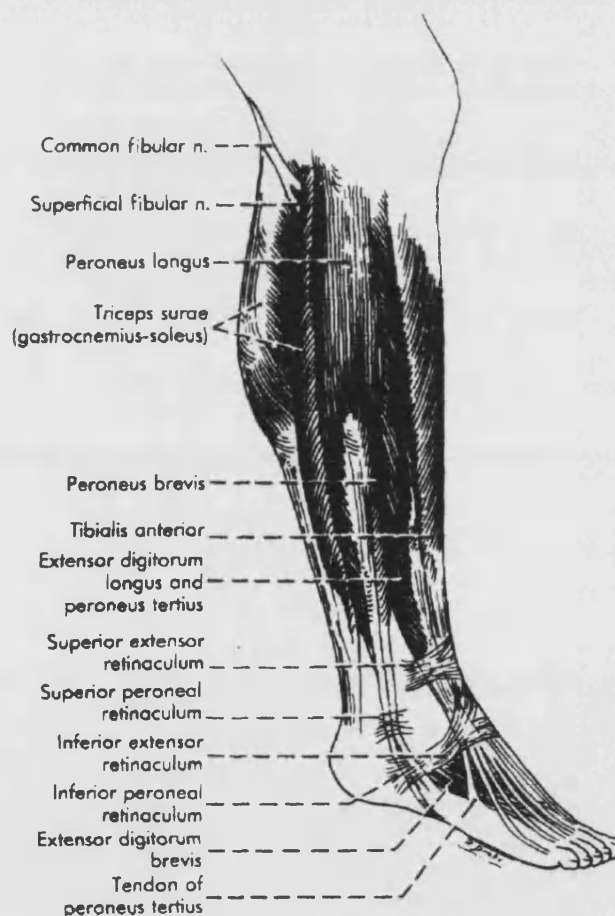


Fig. 2.1 Anterior view of the lower leg [114].

## CHAPTER 2 BACKGROUND TO STROKE REHABILITATION

The innervation of the leg muscles shown in fig. 2.1 is shown in diagrammatical form for clarity in fig 2.2.

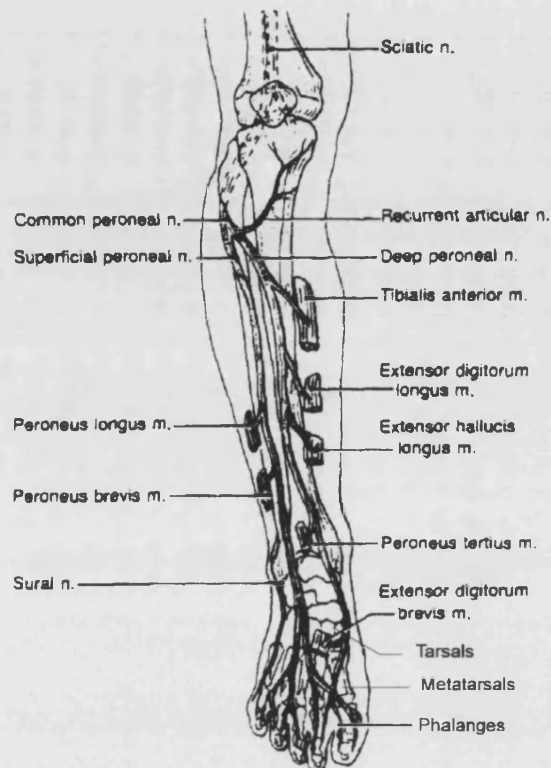


Fig 2.2 Innervation of the anterior leg muscles [115].

The function and innervation of each of the anterior muscles is as follows:-

**Tibialis Anterior:** This muscle, shown in fig. 2.1, has its origin on the tibia and produces dorsiflexion of the foot as well as the secondary effect of inversion of the foot. Inversion is the twisting of the ankle to permit the sole of the foot to be viewed from the medial side. Eversion is the twisting of the foot to permit viewing of the sole from the lateral side. The innervation of the tibialis anterior is by the deep peroneal nerve, a branch of the common peroneal nerve, shown in fig. 2.2 [116].

**Extensor Digitorum Longus:** This muscle, shown in fig. 2.1, runs from the lateral condyles of the tibia to the second through to the fifth phalanges. The extensor digitorum longus is innervated by the deep peroneal nerve, shown in fig. 2.2, and assists in the dorsiflexion of the foot as well as effecting extension of the toes.[117].

**Extensor hallucis longus:** The extensor hallucis, shown in fig. 2.1, lies alongside the tibialis anterior, has its origin on the fibula and is innervated by the deep peroneal nerve, shown in fig.

## CHAPTER 2 BACKGROUND TO STROKE REHABILITATION

2.2. It's function is to provide extension to the phalanges of the great toe and assist in the dorsiflexion of the ankle [117].

**Peroneus Tertius:** The peroneus tertius, shown in fig. 2.1, runs from the fibula to the dorsal surface of the fourth and fifth metatarsals. This muscle effects dorsiflexion and provides a means of everting of the foot. Peroneus tertius is innervated by the deep peroneal nerve, shown in fig. 2.2 [114, 115].

**Peroneus Longus:** The peroneus longus, shown in fig. 2.1, runs from the fibula to the lateral side of the foot and effects eversion of the foot. It is innervated by the superficial peroneal nerve, a branch of the common peroneal nerve, shown in fig. 2.2. It is suggested that the peroneus longus may act as a dorsiflexor of the ankle [118,117].

**Peroneus Brevis:** The peroneus brevis, shown in fig. 2.1, performs the same function as the peroneus longus and is also innervated by the superficial peroneal nerve, shown in fig. 2.2 [118].

The posterior view of the muscles of the lower leg is shown in fig. 2.3. The innervation of these muscles is shown separately in fig. 2.4.

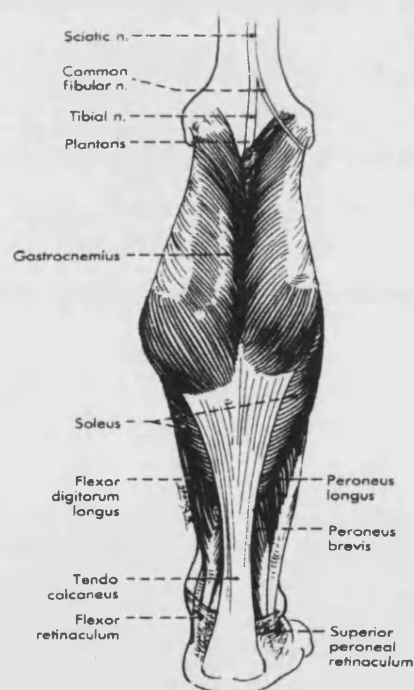


Fig. 2.3 Posterior view of the muscles of the lower leg [114].

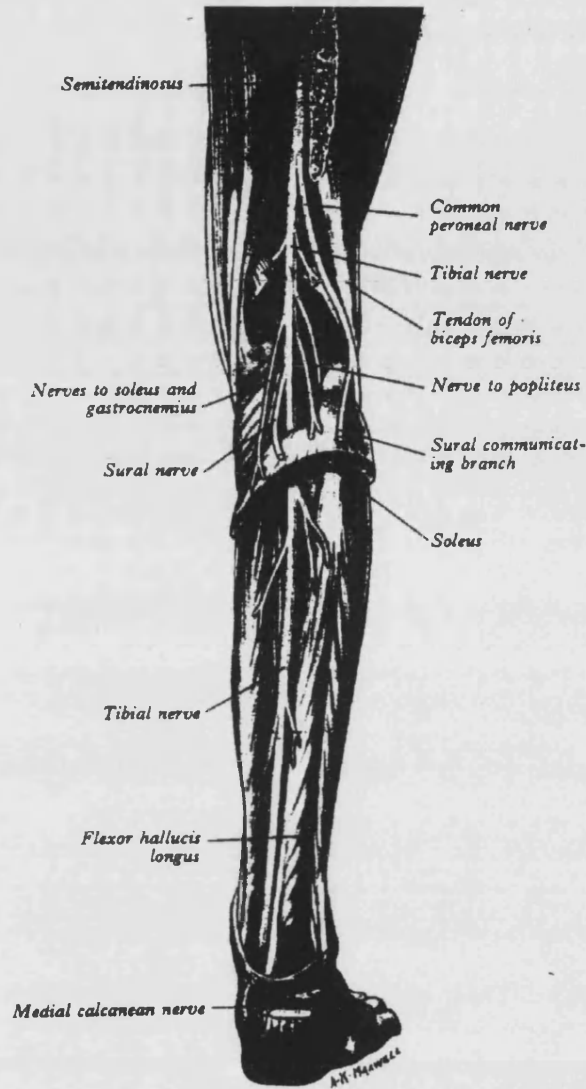


Fig. 2.4 Posterior view of the muscle innervation of the lower leg [117].

The innervation and function of the muscles shown in fig. 2.3 is as follows:-

**Gastrocnemius:** This large, powerful, double headed muscle shown in fig. 2.3, forms the 'belly' of the calf. It acts on both the knee and ankle joint. The larger medial head runs from the medial condyle of the femur and the smaller lateral head from the corresponding lateral condyle to the tendo calcaneus and the calcaneum. The gastrocnemius effects plantarflexion of the ankle joint, the bringing into line of the leg and the foot. The gastrocnemius, or calf muscle, is

---

## **CHAPTER 2 BACKGROUND TO STROKE REHABILITATION**

---

innervated by the tibial nerve, shown in fig. 2.4, and also causes some flexion of the knee depending upon the gait phase at the time of contraction [117].

**Soleus:** The soleus, shown in fig. 2.3, is located alongside the gastrocnemius and is innervated by the tibial nerve, shown in fig. 2.4. The soleus is also used to effect plantarflexion. The soleus is thought to play an important part in the stabilising of the ankle joint during standing because it is comprised of a high percentage of slow twitch fibres [116].

**Tibialis Posterior:** As the name suggests, this muscle, shown in fig. 2.3, is located to the rear of the tibialis anterior. Innervation is by the tibial nerve, shown in fig. 2.4, and the muscle serves to effect plantarflexion and inversion of the foot [119].

**Flexor Digitorum Longus and flexor hallucis longus:** The flexor digitorum longus, shown in fig. 2.3, has its origin at the tibia whilst the flexor hallucis longus, also shown in fig. 2.3, has its origin on the fibula. Both of these muscles are concerned with toe movements and providing support to the arches of the feet. These muscles are innervated by the tibial nerve, shown in fig. 2.4 [116].

The above descriptions of the lower leg muscle function outlines which of the muscles are required to effect dorsiflexion, plantarflexion, eversion and inversion of the ankle. It can be seen that the dorsiflexors are principally innervated by branches from the common peroneal nerve [115]. Similarly, it may be seen that the plantarflexor muscles are innervated by the tibial nerve [115]. Therefore, in general, FES applied to the common peroneal nerve will cause dorsiflexion of the ankle, for which the anterior tibialis is primarily responsible [120], and FES applied to the tibial nerve will effect plantarflexion of the ankle. The common peroneal nerve divides after circling the fibula into the deep peroneal and superficial peroneal nerves [118]. These are shown diagrammatically in fig. 2.5.

## CHAPTER 2 BACKGROUND TO STROKE REHABILITATION

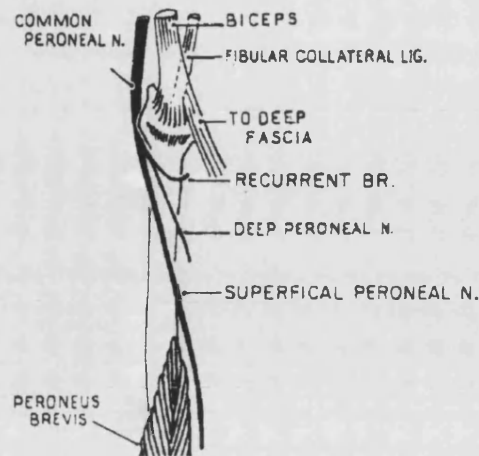


Fig. 2.5 Diagrammatic representation of the deep and superficial peroneal nerve [121].

The tibialis posterior is the principle inverter of the foot, though is substantially assisted by tibialis anterior [114]. The tibialis anterior is innervated by the deep peroneal branch of the common peroneal nerve [115], therefore FES applied to this branch will cause dorsiflexion with an associated inversion of the foot. The principle evertors of the foot are the peroneus longus and peroneus brevis [114], both of which are innervated by the superficial peroneal nerve [115]. Activation of the evertors causes ankle movement so that the sole of the foot may be viewed from the lateral side of that limb. Therefore FES applied to the superficial peroneal nerve will effect dorsiflexion of the ankle with an associated eversion of the foot. FES applied in the general area of these two nerves or to the common peroneal nerve will produce a combination of the two above effects.

### 2.4 Physiology of Locomotion.

#### 2.4.1 Muscle types.

It is well understood that a large variety of muscles are required to produce co-ordinated joint movement and effect balance and posture. Muscle may be broadly divided into three types skeletal (or striated) muscle, visceral (or smooth) muscle and cardiac muscle. Voluntary movement is accomplished using striated muscle, so only this muscle variety will be discussed.

Striated muscle is composed of a mixture of type I and type II fibres, which defines the contractile properties of that muscle [122,123]. Muscles with a predominance of type I fibres have “slow twitch” properties and those with a predominance of type II fibres have “fast twitch”



---

## **CHAPTER 2 BACKGROUND TO STROKE REHABILITATION**

---

properties [122,123]. Fast twitch, or white fibres as they are sometimes known [124], possess few mitochondria [125], the chief energy-producing sites within the muscle structure, and produce rapid movements [126]. The reduced number of mitochondria reduces the fatigue resistance of the fast twitch fibres [125]. In comparison, the slow twitch fibres possess an increased number of mitochondria [125], exhibit slow postural type movements [125,126] and exhibit a marked resistance to fatigue [125]. Muscles are composed of different proportions of fast and slow twitch fibres to produce muscles that exhibit different contractile properties [126]. These properties range from the very fast contractions observed of the extraocular (eye) muscles [124], which are composed mainly of fast twitch fibres to the very slow contractions of the latissimus dorsi (trunk), rectus abdominis (abdominal) and soleus (calf) [124] which are composed mainly of slow twitch fibres and are in place principally to maintain posture.

The properties of these fibres are not fixed, but are dependant on the activation and innervation of the muscle [127]. A typical rate of contraction for a fast twitch muscle is 10 - 40 msec from the onset of contraction to the occurrence of the maximum tension, whereas for a predominantly slow twitch muscle this figure is typically 60 - 120 msec [126]. These rates have been observed to change when muscle fibres have been innervated with nerve fibres that normally supply a muscle with a substantially different fibre composition [125,128,129]. It should be noted that the neurones innervating fast twitch muscle are typically of a larger diameter than those supplying slow twitch muscle and hence conduct more rapidly [130]. This conversion of muscle fibre also occurs when the muscle is stimulated with a wave form with a frequency different to that which would normally activate the muscle [130]. A number of researchers have noted the conversion of fast to slow twitch muscle fibre types within a single muscle under abnormal stimulation frequency [131,132,133].

This shows the importance of stimulation with a correct frequency wave form if the most effective contractions are to be elicited from each muscle with minimal muscle alteration occurring.

### **2. 4. 2 Muscle contraction.**

Striated muscle fibres appear striped on a macroscopic scale, whereas on a microscopic level, filaments within the muscle are seen to be formed from parallel groups of hexagonally packed, thick and thin myofilaments. The basic muscle fibre unit, the sarcomere, shown in fig. 2.6 is composed of these myofilaments [134].

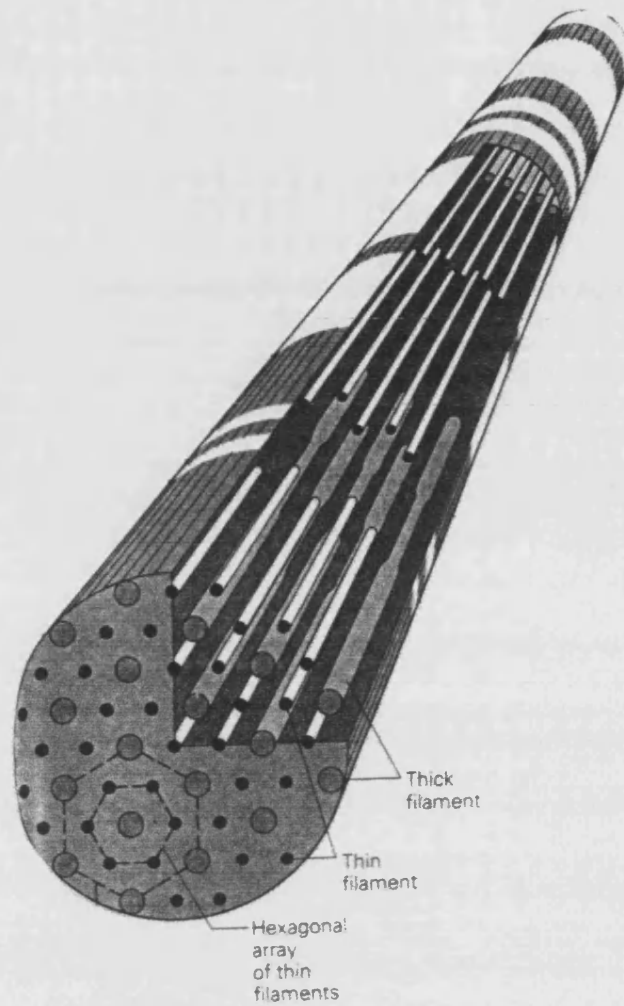


Fig. 2.6 Muscle Fibre Internal Structure [134].

The striping effect is caused by the overlapping of these thick and thin filaments. The various bands and zones that this produces are as shown in fig. 2.7.

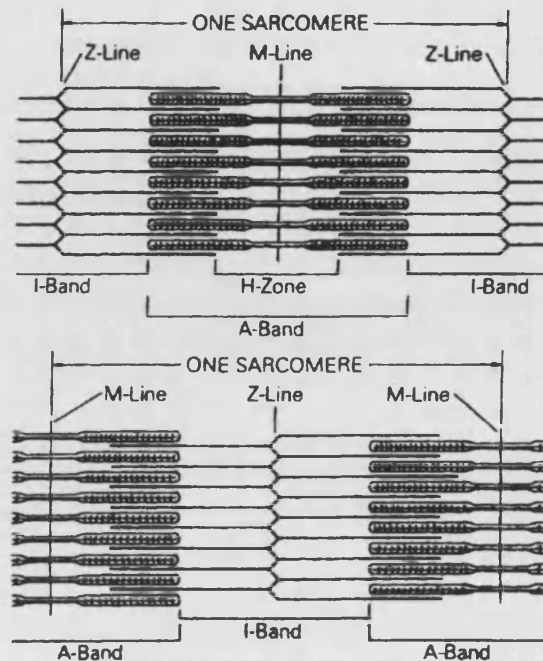


Fig. 2.7 Muscle fibre striation labelling [135].

It was first suggested by Huxley et al. in 1957 [136] and is further discussed by Keynes et al. [135] that contraction of the muscle fibre is by means of the filaments sliding across each other and that no individual components of the fibre changes its length. Many sarcomeres are joined end to end, see fig. 2.7, to form myofibrils and together these produce a usable variation in muscle length. The thick filaments are composed of a protein, myosin and the thin filaments of the protein actin. The myosin filaments exhibit radial projections that bind to sites on the helically structured actin filaments, producing the basis for the contractile mechanism. A muscle fibre consists of several bundles of actin and myosin filaments, surrounded by the sarcoplasmic reticulum and separated by mitochondria, which act as the main enzyme site. The fibre itself is surrounded by the sarcolemma and permeated by transverse tubules, passageways through the fibres that assist in the propagation of the contraction [130].

The sliding filament model of contraction, the most well established hypothesis [135, 136], suggests that the filaments described earlier slide past each other to facilitate the shortening of the muscle fibre.

Contraction is initiated by the excitation of the sarcoplasmic reticulum by an action potential. Calcium ions are released as the action potential propagates along the transverse tubular (T)

## CHAPTER 2 BACKGROUND TO STROKE REHABILITATION

system. These ions are released close to the actin and myosin filaments [126], suggesting an explanation for the rate of activation of even the largest muscles in the body. In fast twitch fibres, the faster contraction rate is partly explained by the greater volume of the sarcoplasmic reticulum and the T system [130].

There are crossbridges present between the actin and myosin filaments, consisting of a molecule of adenosine tri-phosphate (ATP) bound to the myosin projections. The calcium ions bond to a protein complex, troponin-C. This causes the bond angle of the crossbridges to alter from approximately 90 degrees to 45 degrees. This 'power stroke' pulls the filaments together and increases the protein overlap, as shown in fig. 2.8 [135,125].

The crossbridging cycle is responsible for both contraction and relaxation as the actin and myosin filaments must 'step' past each other to effect a muscle contraction and then 'step' back again to effect relaxation. The large number of these discrete steps occurring in each sarcomere appears on a macroscopic scale as a smooth, controlled movement and may be considered analogous to a form of linear stepper motor.

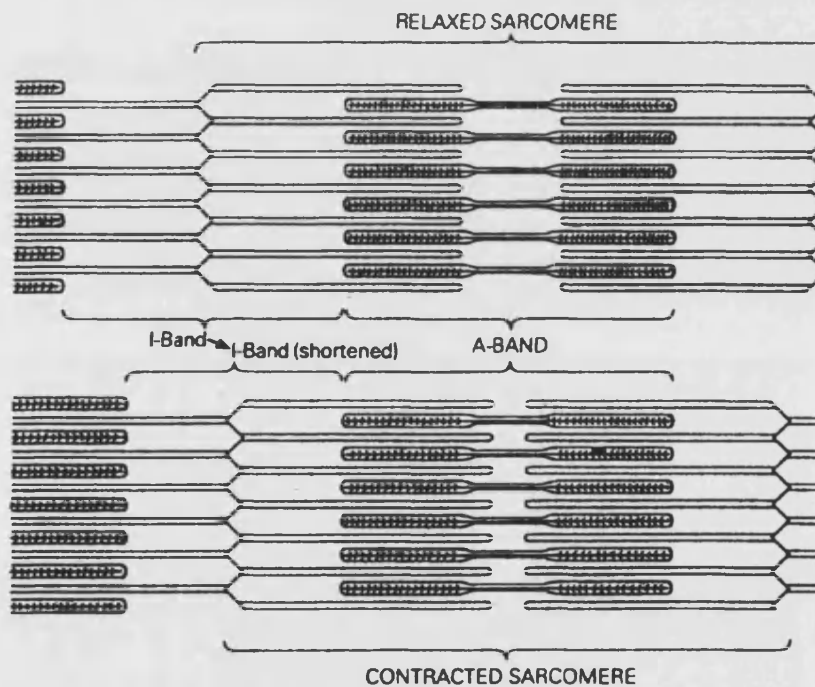


Fig. 2.8 Diagrammatic representation of muscle contraction [135].

Within any mode of contraction, the muscle may be observed to 'twitch' or maintain a tetanus or

## CHAPTER 2 BACKGROUND TO STROKE REHABILITATION

sustained contraction. In the first case, the twitch is in response to a single action potential [137, 124], where the calcium ion release is quickly followed by an ion uptake mechanism. The single stimulus does not permit sustained crossbridging cycles to occur and hence permit a force build up [127]. A tetanus, however, is effected by repeated action potentials that cause a repeated crossbridging cycle to occur. If the action potentials are widely spaced, a series of twitches will be observed, though if these closely follow each other, a process known as the Treppe phenomenon occurs and the twitches sum to produce a contraction [124]. This effect is shown in the diagram of fig. 2.9. A series of action potentials arriving at a frequency between that required to cause a twitch and a contraction will produce a series of twitches that will produce neither strength of contraction nor controlled movement. This demonstrates the need for the stimulator to produce the correct frequency of output pulse trains, if controlled limb movement is to be effected

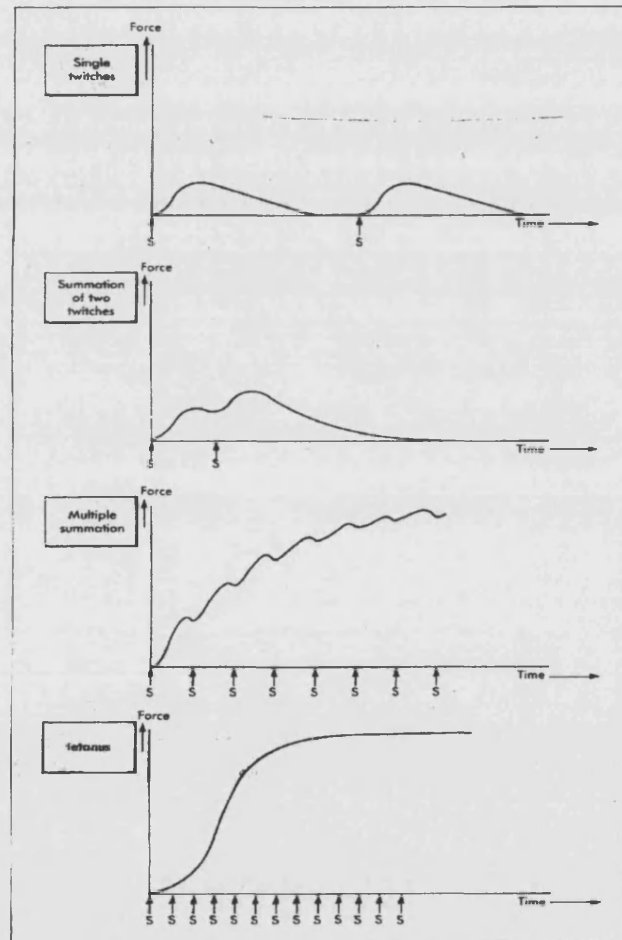


Fig. 2. 9 Summation of twitches to form a tetanus. [127]

## **CHAPTER 2 BACKGROUND TO STROKE REHABILITATION**

### **2.4.3 Neurone structure.**

The general structure of peripheral neurones is shown in fig. 2.4. These are the principle transmission element of the nervous system.

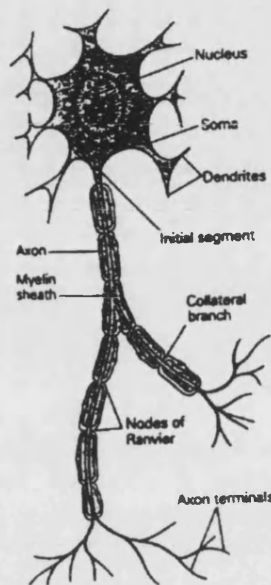


Fig. 2.10 Neurone structure.[138]

Neurones consist of four major sections, the soma, axon, axon terminals and dendrites [138]. The axon is the information transmission pathway, along which action potentials pass to muscles or other neurones [126]. The soma is the main metabolising centre of the nerve with dendrites branching away from this centre to effect contact with adjacent neurones [134]. Myelin, a fatty secretion, is present along the length of the axon to protect and insulate the axon. The gaps left between these myelin sheaths are known as the Nodes of Ranvier [127]. The axon contains a network of microtubules that permits the bi-directional transport of proteins and cell components along its length.

Ion channels are found within the membranes of all neurones and are used to effect changes in the cell ion balance and hence create action potentials [125].

Neurones are classified as either motor (efferent) or sensory (afferent). Motor neurones relay the instructions from the motor centres to the effector, the skeletal muscle. Sensory neurones transmit sensory information from a variety of sensors back to the spinal and cranial areas in

---

## **CHAPTER 2 BACKGROUND TO FES**

---

order to provide the feedback of a system which, when functioning correctly, operates under effective closed loop control [139]. Motor neurones join muscle fibres at the myoneural junction or motor end plate. Synaptic junctions are present along the length of both motor and sensory neurones and act as a form of gate to prevent overloading of the system by permitting only selected impulses to cross the synaptic cleft. Transmission across these junctions is by means of transmitter substances, such as acetylcholine, which is released from the pre-synaptic cells and received at the post-synaptic cells. This has the effect of slowing impulse transmission as a finite time is required for the migration of the transmitter substance [134].

Motor units consist of all the muscle fibres innervated by a single motor neurone [126]. Small units innervating few muscles are responsible for fine, precise movements, such as finger movements and large units are responsible for gross, powerful motions, such as that exhibited by the quadriceps [126]. Contraction either occurs in response to action potentials, which are all of similar size and duration at any given temperature [140, 141, 142], or it does not occur at all, so there are no 'weak' contractions [137]. In addition, an action potential conducted along an axon will activate all the muscle fibres innervated by this axon [142]. This similarity of all action potential trains means that the frequency of the action potentials controls the force produced by the muscle. This method is referred to as the frequency code of the nervous system [137]. In addition, the recruitment of further motor units, referred to as the population code of the nervous system, is also used to provide a degree of force control [137]. There are only a finite number of motor units per muscle and these are generally not utilised simultaneously, as the selective recruitment of these units reduces the onset of fatigue. Fatigue is further discussed in section 2.4.4. The size and shape of action potentials has been found by Bolton et al. [143] to alter with tissue temperature, but to stay constant at any given temperature. The amplitude and duration were found to reduce with an increase in temperature, whilst the conduction velocity of the neurone increased with temperature [143].

This possible alteration of action potential parameters with temperature is an example of the types of variation of physiological parameter that an intelligent stimulator would be able to overcome by correcting the applied stimulation on a stride by stride basis.

The action potential produced by a motor neurone is present for a fixed amount of time [140,143,141] and defines the limiting frequency of stimulation pulses that may be applied to muscle groups. The time in which no further depolarisation can occur is known as the absolute refractory period and lasts for about ten milliseconds, setting the absolute maximum frequency

## CHAPTER 2 BACKGROUND TO FES

to approximately 100Hz [144, 126]. Action potentials typically arrive at the motor end plate at the much lower frequency of 5Hz to 50 Hz [126]. A frequency of 20Hz or less is considered to result in an incomplete tetanus, whilst action potentials arriving at frequencies of between 20Hz and 60Hz are considered to produce a complete tetanus [139]. A further period, the relative refractory period, is present where the cell may be depolarised but possesses a much increased threshold value [144]. The components of the action potential, including the absolute and relative refractory periods are shown in the diagram of fig. 2.11.

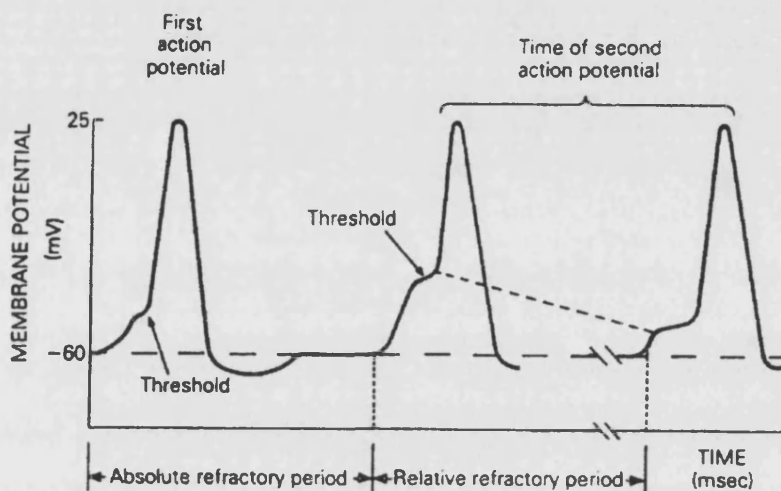


Fig. 2.11 Action potential and recovery period [144].

At the nodes of Ranvier the fibre membrane is exposed and many ion channels are present, permitting depolarisation to the threshold value. Full depolarisation of a node causes the adjacent node to depolarise to the threshold value and conduction of the impulse appears to occur. This process is known as saltatory conduction. The absolute refractory period of each Node of Ranvier ensures that conduction only takes place in the required direction [144,145,124].

FES creates a localised depolarisation of the neurone, such as the common peroneal nerve in the lower leg, and conduction continues to the motor end plate at the velocity supported by that type of axon.

### 2. 4. 4 Muscle fatigue.

The onset of muscle fatigue has been defined as 'any reduction in the force generating capacity



---

## **CHAPTER 2 BACKGROUND TO FES**

---

of the muscle' [145], and is measured by the maximal voluntary contraction force. It has been observed [145] that the fatigue resistance of muscles, especially the anterior tibialis, is often reduced after a stroke [145]. It is suggested [145] that this modification to the muscle behaviour is due to changes in the fibre composition of the muscles after the CVA, possibly due to a modified action potential pattern.

Fatigue affects the relaxation of muscles as well as the contractile properties. The sliding filament contraction model, analogous to a linear stepper motor, may exhibit a failure to contract or relax under extreme fatigue conditions and maintain its "under fatigue" length [126].

The exact mechanisms of muscle fatigue are not fully understood [146]. Fatigue is thought to be due to lactic acid, generated under anaerobic conditions, interfering with the contraction mechanism [127] in addition to a depletion of adenosine tri-phosphate (ATP) and creatine phosphate within the muscle [126]. Baldwin et al. [147] and Yan et al. [148] have shown that contractile activity produces an increased capacity for ATP production which leads to an improved resistance to fatigue, supporting the mechanism suggested above.

Whatever the actual mechanism of fatigue, the symptoms are a reduced muscle output force [145, 149] leading eventually to complete cessation of muscle activity [126]. Under normal activity, some motor units are recruited to assist in the contraction before others, possibly depending on their fast and slow twitch fibre composition [130]. This recruitment pattern increases the time to the onset of fatigue under exercise in normal individuals [130], but is very much reduced under applied FES, leading to a more rapid onset of fatigue [145]. If the stroke has caused damage to sensory areas, then the onset of this fatigue may not be adequately detected by the patient until the muscle ceases to provide the required contraction and relaxation cycles.

It has been shown [126] that repetitive high frequency (>100Hz) stimulation leads to the rapid failure of the contractile mechanism and that long periods of low frequency (approx. 10Hz) produce a reduced maximal voluntary contraction force [145]. It was also found that contractions in which the muscle length reduces caused a more rapid onset of fatigue [145].

As a summary, fatigue is a stimulation frequency dependant phenomenon, considered to be one of the limiting factors in applied FES [145]. Care should be taken to avoid excessively fatiguing muscles during applied FES, though a self compensating stimulator would be of use in providing altered stimulation patterns to reduce the effects of the reduced force which is a

## **CHAPTER 2 BACKGROUND TO FES**

---

consequence of the onset of fatigue and to generate fatigue minimising stimulation envelopes, as discussed in chapter 4. It has been observed that the EMG frequency spectra undergoes marked changes at the onset of fatigue, with a distinct rise in EMG amplitude [150,151], a distinct shift towards the lower end of the spectrum [152,153,154] and a decrease in axon conduction velocity [154]. It has been suggested by Lippold et al. [155] and Lloyd [156] that these changes may be due to the synchronisation of the activities of the motor units. Instrumentation has been developed to detect the onset of fatigue by EMG evaluation. Equipment such as that developed by Inbar et al. [154], Stulen and DeLuca [157], Shearn [158], Sime [159] and Carr [160] may be of use to determine when further FES application is no longer viable.

### **2. 4. 5 Strength - duration relationships.**

The strength-duration relationships for nerve and muscle fibre has been considered since the investigations of George Weiss in 1901 [161]. Strength-duration relationships provide an indication of the required FES pulse length and amplitude parameters and are also used to provide an indication of the condition of the peripheral nervous system [139].

The method used to determine these relationships is as follows [139, 162]:-

- 1) A stimulating electrode is placed over the required motor point.
- 2) A second electrode is placed on the skin.
- 3) Square voltage or current pulses of varying length are injected 0.01 - 100ms [163,139], 20 - 500us [163] and even up to 1s [164].
- 4) The minimum amplitude necessary to produce a contraction is noted for each pulse width.

Threshold tracking systems have been developed, such as that devised by Mogyoros et al. [165], to automate the process of acquiring the minimal stimulation values. This permits the pulse length and pulse amplitude relationship to be plotted, using either injected current or voltage for the pulse amplitude.

Both Weiss [161] and Lapicque [166] have fitted mathematical formulae to these relationships, an example of which are shown in fig 2. 12.

## CHAPTER 2 BACKGROUND TO FES

---

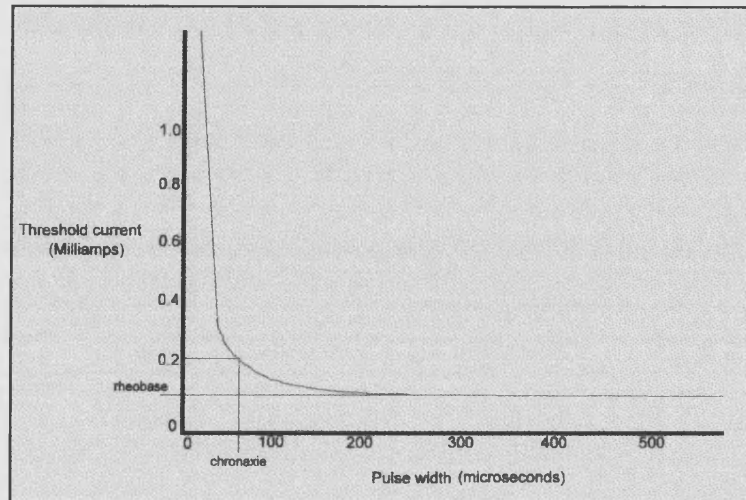


Fig. 2.12 Strength duration curve using pulse current amplitude [126].

In normal individuals, the axons are far more excitable than the muscles, hence the strength-duration curves refer to the performance of the motor neurones. In denervated muscles, the strength-duration relationships refer to the direct stimulation of the motor end plate, which is far less excitable than a healthy neurone [139]. Fig. 2.13 shows the effect of nerve damage on the strength-duration relationship. The chronaxie, or strength-duration time constant, of the curve [163] is shifted further to the right as neurone degradation increases.

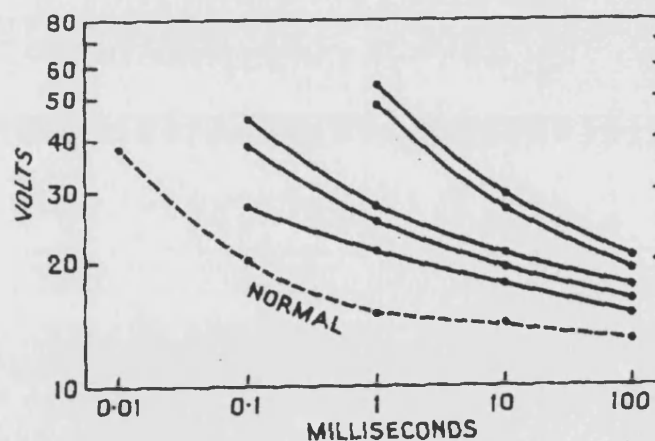


Fig.2.13 Strength-duration curve showing the chronaxie movement to the right with nerve dysfunction [139].

The curves are asymptotic as D.C. current is not able to elicit a contraction and will in fact cause

## CHAPTER 2 BACKGROUND TO FES

---

tissue damage by ion transport even when applied at low amplitudes [126]. The long pulse asymptote fixes the rheobase, the smallest amplitude that will elicit a contraction. This occurs at the longest pulses [126, 164]. Campbell et al [126] suggest that the shape of these graphs show that the total injected charge is the most important parameter, as this combines the pulse amplitude and length into a single variable. An example of a corresponding charge duration curve is shown in fig. 2.14.

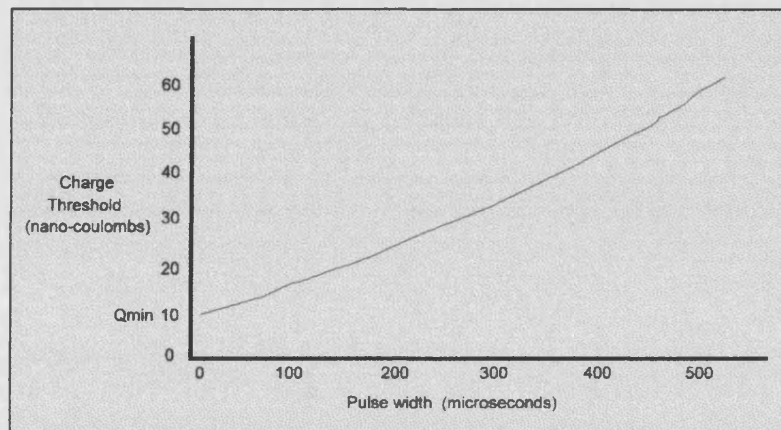


Fig. 2.14 Charge-duration relationship [126].

These relationships show the likely requirements for the parameter of pulse length in the applied FES. The possibility of effecting stimulation by keeping either the pulse magnitude or pulse length constant and increasing the other variable is also shown. The relationships show that stimulation may also be effected by commencing the pulse train with a low value of magnitude and pulse length and increasing both variables simultaneously.

### 2. 4. 6 Spasticity.

Spasticity is the term applied to certain types of abnormal striated muscle tone [167] and has been defined as “a motor disorder characterised by a velocity dependant increase in tonic stretch reflexes with exaggerated tendon jerks resulting from hyper-excitability of the stretch reflex” [168]. This effect results in a muscle tone increase upon the activation of a hyperexcitable stretch reflex. It is a motor disorder that can occur after lesions of various parts of the central nervous system [169], as well as by dysfunction of the peripheral nervous system [170] and spinal cord injury [171], the symptoms are exaggerated tendon reflexes, increased muscle tone, velocity dependant increases in the resistance to limb movement, muscle weakness and clonus [169]. Clonus is the repeated reflex contraction of an antagonist muscle, replacing the required

## **CHAPTER 2 BACKGROUND TO FES**

---

movement with an antagonist contraction [172]. The muscle belly is often seen to relax after a first contraction, the muscle spindle lengthens and the hyperactive stretch reflex causes another contraction. The cycle then continues, with the calf muscle being especially susceptible to this disorder [126].

Stroke patients are often seen to exhibit spasticity of the contralateral side to the central nervous system lesion [169]. The severity of the spasticity varies considerably between individuals [167,171] and can take the form of severe tonic spasticity that prevents all movement, or may cause sudden muscle spasms that disrupt the normally smooth locomotion of the patient [170].

Spasticity, when not causing rigidity that is constant throughout the range of movement, exhibits a phenomenon known as the 'clasp knife effect' [126]. This is where the peak resistance of the limb to a passive stretch is encountered at the beginning of the movement producing the impression of limb stiffness [172]. This then gives way suddenly allowing relative freedom of limb movement [171]. The increased muscle tone observed in the antagonist at the start of this passive movement often increases with the velocity of that movement [126].

Spasticity is often accompanied by muscle weakness, which is most pronounced in the lower limb flexors and upper limb extensors [171]. The increased tone in the lower limb extensors coupled with a weakness in the flexors can result in the extensor plantar reflex [126,103], where the ankle extensors cause excessive plantarflexion of the joint accompanied by splaying of the toes [171]. This overactivity of the extensors provides a major contribution to the spastic gait impairment [173].

There has been no evidence found to support the theory that the above effects are caused by increased muscle spindle sensitivity [169] and Thilmann et al. [169] suggest that the changes that have occurred are elsewhere within the reflex loop. Vodovnik et al. [174] and O'Dwyer et al. [175] suggest that fibre type changes within the muscle are responsible for much of the stiffness and spasticity, especially the disuse of white fibres and the remodelling of connective tissue around the muscle. In addition O'Dwyer et al. [175] suggest that muscle contracture following stroke, an adaptation to the stroke [175], causes the exaggerated stretch reflex. Corcos et al. [172] suggest that the main alteration occurring to produce the spasticity is the failure to suppress the stretch reflex in the antagonist muscle, which then goes on to invoke the clonus.

Whatever the causes of the spasticity, the gait of individuals is markedly affected by the

## **CHAPTER 2 BACKGROUND TO FES**

---

spasticity. Increased activity has been noted in the tibialis anterior EMG during the swing phase but with no resulting dorsiflexion [176]. Dietz [176] suggests that this may be due to opposing soleus activity and noted that in some cases sufficient plantarflexion was caused to cause the ball of the foot to contact the ground before the heel at the beginning of the stance phase. Corcos et al. [172] observed the inappropriate soleus activity which inhibits the dorsiflexion and noted that plantarflexion was in general achieved, though more slowly than in normals due to observed activity of the tibialis anterior and soleus.

Spasticity can be reduced by the use of certain drugs [167], alcohol ingestion [171] and electrical stimulation [174,177]. Warming of the affected limb has also been shown to reduce the apparent stiffness [176].

Applied FES has been shown to have an antispastic effect [177,178,12], as well as producing increased dorsiflexion [178]. Alfieri [177] found that stimulation of the weakened muscles produced a decrease in the spasticity of the antagonists. This initially lasted for about an hour and after some training a permanent improvement in the muscle spasticity was seen to occur. Vodovnik et al. [174] also noted some short term improvement in spasticity with antagonist stimulation, though could not conclude whether this was a more effective strategy than stimulation of the spastic muscle.

### **2.4.7 Human gait**

A number of methods have been used to measure the gait of both normal and stroke affected people. These have ranged from extremely simple systems, such as that used by Cerny [179], where pens were taped to the patients' feet to show where ground contact occurred, to complex versions such as the system employed by Tibarewala et al. [180] which utilises a pulley system and optical encoders to measure the walking speed of the patient. The methods for evaluating gait fall into one of several categories: walking speed, foot-ground contact measurement, video recording and analysis of limb movement and foot-ground pressure measurements.

Foot ground contact has been evaluated using a conductive rubber treadmill along with metallised shoe soles by Kauer et al. [181]. This produces foot ground contact data with respect to time as the patient moves on the treadmill. Similar systems have been used incorporating wire grids or conducting surfaces in association with conductive footwear [81, 182,183].

A more complete picture of the gait cycle of an individual is produced by use of the various photographic / cinematographic recording systems in use. Kirtley et al. [184] used the Vicon

## **CHAPTER 2 BACKGROUND TO FES**

---

multi television camera system which records the position of reflective markers attached to the patient. Intiso et al. [185] successfully utilised the Elite system which performs the same function of recording the movement of reflective markers attached to the patient. In addition Selspot [81,184], Expert Vision, Optotrak and Peak Performance are all systems permitting a similar visual analysis to be performed [186].

Foot ground pressure contact has also been used extensively to evaluate gait. Systems such as the Kistler force platform [184], the Footprint [84], the Pedobarograph [183] and the Foil Pedobarogram [81] have been used, as have other force platforms [187,78,85] embedded in walkways to produce detailed under-foot pressure information and hence determine the quality of the gait of the patient. In addition Morris [188] utilised a force platform in which the sensors were accelerometers to measure the impulses beneath the foot during gait.

It should be noted that many researchers have used more than one of the above methods of gait analysis at any time to provide additional information. EMG measurements have also been extensively utilised to indicate muscle activity during the gait cycle [189,185,186, 23,188,82].

These methods of gait analysis have permitted a model to be obtained of normal human gait and shown the deviations from this gait pattern that are likely to be found in stroke victims.

### **2. 4. 7. 1 Normal gait.**

Human gait is divide into two phases, the stance phase and the swing phase [79] with one cycle defined as heel strike to ipsilateral heel strike [186]. A diagram showing the stages throughout these two phases is shown in fig. 2.15.

## CHAPTER 2 BACKGROUND TO FES

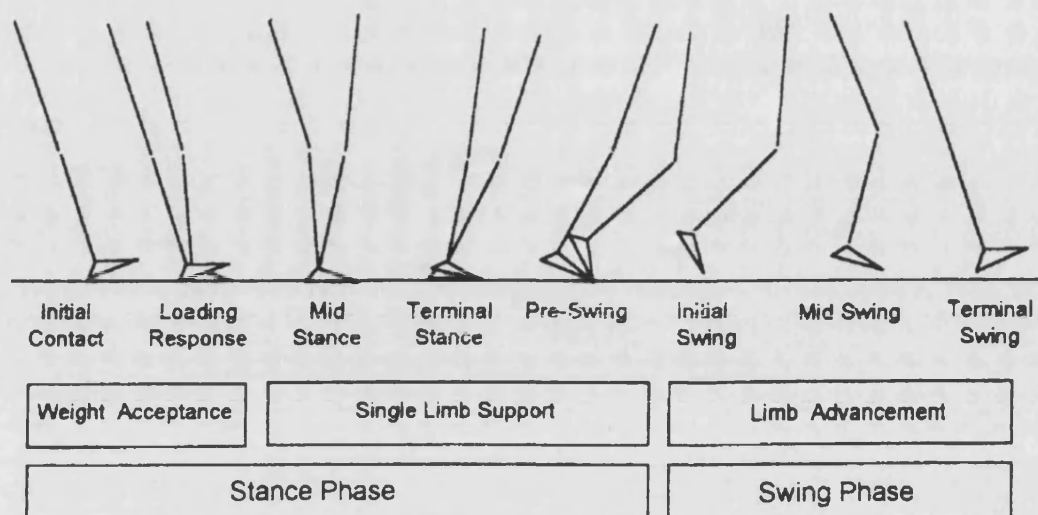


Fig 2.15 The stages of human gait [186].

At the beginning of the cycle, the heel strikes the ground, commencing the stance phase [79]. The body weight is progressively shifted forward over the stance limb until the stance limb is in the flat-foot state. The heel is then lifted and followed by a push off to impart forward momentum and finally the lifting of the toe [186]. This allows the gait cycle to be reduced to the four classic divisions of heel strike, flat foot, heel off, toe off. Any point within the gait cycle may be referred to by a percentage of the completion of the cycle. The percentage points of the major events is shown in fig 2.16.

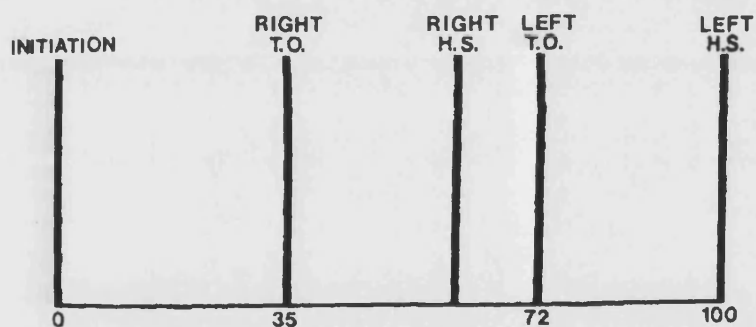


Fig. 2.16 Major points of the gait cycle [85].

The activity of walking is the control of an unstable system, which is often modelled as an



## CHAPTER 2 BACKGROUND TO FES

inverted pendulum with the centre of mass of the body remaining outside of the base area defined by the feet for most of the cycle [45]. The exception to this is during the period of double support when the bodyweight is borne by both limbs [184].

Initiation of gait is a complex task, which requires the body to act to destabilise the balance maintaining system [85]. It has been noted by Mann et al. [85] that gait is initiated as follows:-

The centre of pressure measured under the feet moves toward the swing limb and to the rear as the tibialis anterior causes the centre of pressure to move in a posterior direction. By the 20% point of the cycle, the centre of pressure starts to move in a medial-lateral direction towards the stance limb. This is accompanied by hip, knee and ankle flexion in the swing limb in anticipation of the toe off. Up until this point the stance limb exhibits little movement as it is supporting the body, though dorsiflexion of the stance limb ankle begins at the 22% point as the centre of mass of the body begins to move forward. Fig. 2.17 shows the movement of the centre of pressure in gait initiation, which is further confirmed by Winter [45]. The pressure movement is not uniform but starts slowly and accelerates in the posterior direction, slowing to change to a medial lateral direction and then accelerating forward to gait speed [85]. During this period, the stance limb anterior tibialis is active, initially to control the posterior movement and later to dorsiflex the ankle.

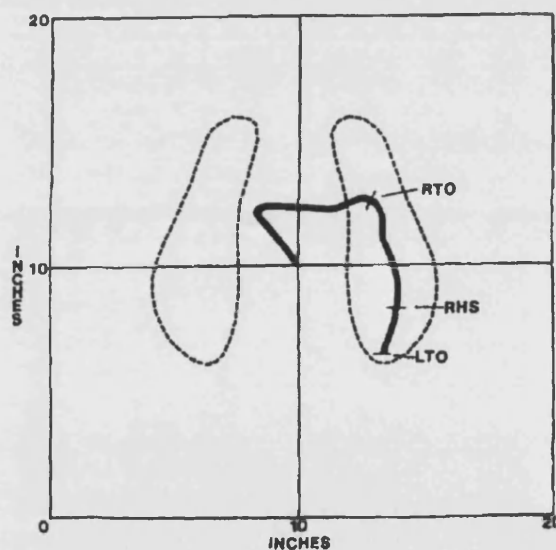


Fig. 2.17 Centre of pressure movement at gait initiation [85].

At the 35% point, the swing limb moves forward with flexion of the hip and knee. This flexion

## **CHAPTER 2 BACKGROUND TO FES**

is controlled to an extent by activity in the rectus femoris. Plantarflexion of the swing limb ankle provides the necessary forward propulsion by push off [85]. With toe off complete, the swing limb tibialis anterior shows rapid activity in order to dorsiflex the ankle joint and prevent toe-drag [190]. The stance limb now undergoes hip extension and progressive plantarflexion. Prior to heel strike, an increased vertical force is noted under the stance limb and an increased posterior shear force under the stance limb as the bodyweight falls forward.

The 60% to 72% is a period of double support. Prior to heel strike the foot is swinging forward and the strike rapidly halts this movement, forcing the foot into plantarflexion [79]. This effect is restrained by activity in the dorsiflexors [79], which show some activity prior to heel strike in preparation for the shock absorption required after heel strike [190]. Subsequent to heel strike, that limb undergoes hip extension, knee flexion and plantarflexion followed by dorsiflexion [85] to control the stance and to provide some shock absorption [79]. The limb that is moving out of the stance phase undergoes hip and knee flexion and plantarflexion prior to its swing phase. From 72% to 100% of the cycle, the limb functions are reversed, with the limb previously in the swing phase now dorsiflexed in the stance phase. The contralateral limb is now dorsiflexed and swung forward by knee flexion and hip extension. The dorsiflexion of the stance limb is then replaced by plantarflexion to thrust the body centre of mass forward to the end of the cycle [85]. The push off is effected by the peak plantarflexor activity of the gait cycle [190]. The push off is then accompanied by a rapid exchange of weight to the opposite limb [79] and will result in the next heel strike which prevents the body falling forward.

This describes the gait cycle and accompanying muscle activity. The evertors are also plantarflexors and the invertors are also dorsiflexors. The anterior / posterior and medial / lateral control of the centre of mass of the body depends on a balance of activity within these muscle groups [45]. The invertors and evertors cannot act independently in normal gait and correct operation requires collaboration between the plantarflexors and dorsiflexors of the same and the contralateral limb [45]. FES is of use in restoring the synchronisation of the operation of these muscle groups when this ability has been lost due to central nervous system damage.

It should be noted that walking patterns change significantly with age although no marked differences were noted by Kamayama et al. between the swing and stance phases of men and women [190]. Murray et al. [191] found that men over 65 years showed markedly different walking patterns to those in younger men, producing what is referred to by Fisher [192] as “over 65 gait”.

## **CHAPTER 2 BACKGROUND TO FES**

### **2. 4. 7. 2 Hemiplegic gait.**

It is generally agreed that hemiplegic gait occurs at a slower speed to normal gait [78,99,192] and its speed is further reduced with increased severity of the motor defect [193]. Hemiplegic gait also exhibits a pronounced asymmetry [182,194], with the restoration of symmetry being the ideal objective of rehabilitation [195].

Significant alterations to both the stance and swing phases of gait are often observed in hemiplegic patients [97]. There are also significant alterations seen at the transitions between these phases, largely due to the inability of the ankle to switch smoothly from plantarflexion to dorsiflexion and vice versa [185]. This leads to the inability to effectively shift the bodyweight in a smooth and controlled manner from one limb to the other [182].

#### **2. 4. 7. 2. 1 Stance phase variations.**

Hemiplegics tend to favour the unaffected side with more than the 50% of weight observed in normals and spend longer in the support of the unaffected side [182,78]. This effect also manifests itself as the patient rushing through the single support phase on the affected leg [182, 194]. Other stance phase deviations from normal include a decreased hip extension [194], altered knee extension [97], reduced or absent knee flexion [78,99] and a much reduced plantarflexor activity at the end of the stance phase [78,97]. An increased plantarflexor moment during the stance phase (which may be due to muscle shortening or spasticity) has been observed [23] and can prevent the dorsiflexion of the ankle, necessary to permit the stance leg to incline forwards [97,194]. This in turn can lead to a decreased hip extension in late stance [78,97]. The dorsiflexion during the stance phase is necessary to prepare the foot for the plantarflexor activity at push off [187]. A lack of mid stance dorsiflexion has been observed to lead to insufficient push off at the end of the stance phase [194]. Although technically a swing phase alteration, a lack of dorsiflexion, possibly due to weak dorsiflexors or a dorsiflexor / plantarflexor imbalance [194], during this phase has been seen [23] to cause a flat-footed entry into the stance phase. This then produces a reduced or absent heel strike [194]. In addition, a general lack of stability of the ankle joint is often observed due to disturbed muscle control [99].

#### **2. 4. 7. 2. 2 Swing phase variations.**

The swing phase is often characterised in hemiplegia by a stiff legged swing with a slightly bent knee throughout the swing [194]. The knee flexion range is often much reduced throughout this phase [23,78,99]. The favouring of the unaffected leg in the stance phase and the reluctance to

## **CHAPTER 2 BACKGROUND TO FES**

---

bear weight on the paretic limb leads to a shortening of the swing phase in the non-paretic limb [183] and an increase in the length of time taken for the swing phase of the paretic limb [99,182, 194]. A lack of dorsiflexion is often evident during the swing phase of the affected limb [78, 185], the condition known as foot drop, which can be caused by gastrocnemius and soleus spasticity [185]. This foot drop can cause the toes to drag on the ground [23] and the result is often observed to be a flat footed [194] or toe first entry into the stance phase [82]. Weak hip flexors will cause a reduction in the swing velocity [78] of the paretic limb, as will any toe drag leading to excessive late swing phase leg deceleration [78]. These characteristics may also be accompanied by inversion [23] of the foot and even the deformity equinus [82]. These impairments arise from a lack of plantarflexor / dorsiflexor balance.

These variations from normal gait lead to an increased effort requirement to maintain walking speed [192]. This is because the patient will often adopt a stance and gait that produces the greatest feeling of stability rather than the most economical movement [187]. As the gait of the patient improves, by FES or physiotherapy, the associated walking speed improves, hence walking speed is often used to evaluate patient gait [78,183,192,51].

### **2. 4. 8 Mechanisms of balance.**

Balance is the mechanism by which the centre of mass of the body is maintained vertically above its base [196,197]. During quiet standing, the body is observed to continually make small deviations away from ideal balance. It has been shown that these movements are random and that the movement as a whole can be described as chaotic swaying [198] or Brownian motion [199]. Chaotic movement of the centre of mass of the body can be detected in the centre of pressure of the body beneath the feet [200,199].

In healthy normals, this movement is not a problem as the excursions of the centre of mass remain too small to unbalance the body [65], in fact the movement of the centre of pressure is retained within a few tens of millimetres of the nominal position [201]. However, individuals with central nervous system damage may have difficulty in maintaining the required equilibrium because of excessive postural sway [65,202]. Much research has been conducted into the responses of the body to small perturbations in balance [203,204,205] and it has been observed [65,204] that small perturbations are arrested by ankle moment, larger disturbances require an additional hip moment and large movements of the centre of mass are arrested by foot movement.

## **CHAPTER 2 BACKGROUND TO FES**

There are a number of factors that contribute to the detection and maintenance of balance. These are the co-ordinated activity of the ankle, knee, hip and trunk muscles in response to detected balance perturbations [203]. Collins and DeLuca [199] suggest that the maintenance of balance is dependant on at least two separate control strategies. Specifically, these are an open loop system for short term control and a closed loop system for longer term balance maintenance. It is suggested [199] that this mixture of control strategies has developed to cope with the initiation to effect time delays.

It has been suggested that balance maintenance is effected by the activation of set patterns of muscle activation and co-ordination [204] and that these patterns are triggered by the various sensory inputs [204]. The central set mentioned above is one possible triggering input along with a number of sensory inputs. Moore et al. [205] and Diener et al. [204] postulate that the CNS receives the sensory inputs informing of a change of balance circumstances and analyse these in order to choose an appropriate patterned response.

Pressure sensed by the soles of the feet has been found by Hamalainen et al. [206] to play an important role in postural control by altering the threshold and strength reflexes in the musculature of the legs. An increase in postural sway has been noted [206] with an increase in mechanoreceptor impairment and Lord and Ward [207] state that peripheral sensation is the most important factor in postural stability. This has been shown by performing sway measurements with the patient standing on soft foam which removes the proprioception of the surface [208,209,210,211,207].

Vision is well known to play an important role in balance maintenance [65,212,213], especially visual contrast sensitivity [208,210]. Nashner and Berthoz [214] concluded that visual information produces a decrease in postural sway amplitude [65] although the response to induced sway is slower than the mechanoreception mentioned above.

Kerr et al. [215] found that maintenance of a difficult posture affected memory recall but not the performance of other physical tasks. The memory recall tasks were not found to affect the control of the posture.

Ankle proprioception, the detection of the moment applied to the ankle and the detection of its angle, have been found to be a significant sensory input [197,216,]. It was noted that postural sway was greatly increased when ankle proprioception was eliminated [197].

Touch has been found, when available, to be a great influence on postural stability [217,218].

## **CHAPTER 2 BACKGROUND TO FES**

Jeka et al. [219] found that postural sway may be greatly reduced by fingertip contact with a stationary object.

It is suggested by Lord et al. [210,211,207] that the vestibular system does not play any significant part in the reduction of postural sway. These authors found that deficiencies within the vestibular systems of patients did not elicit a significant increase in sway.

Another factor found to influence sway is age. The effects of ageing are varied but include an increased delay in muscle activation to balance perturbations [210,220], a decreased reliance on vision [207], decreased dorsiflexion strength [210] and a general decrease in lower leg sensation [210].

The reception of such incoming sensory information does not entirely control the various balance adjustments as the central set of the patient has much influence on the patterns of muscle activation necessary to maintain balance [204]. The central set is related to the expectation of the patient and its effect is increased by the response pattern programming that occurs during training [204].

These observations show that postural control is effected by a complex control system that can be affected by faults in a number of peripheral sensing subsystems or by faults in a central control pattern selecting CNS. It has also been stated that central set, the prediction of the required posture correcting patterns, has a significant effect on postural control. It was also stated that central set can be influenced by training. This produces a possible mechanism by which a balance re-training platform that permits a high intensity training regime may assist in the recovery of balance after a CVA. These observations have also shown the variety of sensing mechanisms involved in balance control. The design of balance equipment should take the requirements of these mechanisms and the likely effect of their disturbance into account.

It should be noted that distinct changes in balance ability occur with age. As stroke patients can be of any age, this suggests that any balance re-training aid should allow patients to train at a rate suited to the individual and even run separate training programs suited to the needs of the individual.

### **2.5 Discussion.**

This chapter has highlighted the limitations and possible results that may be obtained with the use of high quality rehabilitation equipment. It has been seen that a CVA is caused by a disturbance of the blood supply in the cranial cortex, leading to the death of the cranial cells in

## **CHAPTER 2 BACKGROUND TO FES**

the area of the trauma. The likely effects of the CVA on the balance and gait of the patient have also been described. The damaged cells cannot be regenerated, although adjacent areas may, with suitable training, 'learn' to implement some of the functions previously performed by the damaged areas. It is unlikely that full functionality will ever return after the CVA, so a rigorous re-training procedure followed by the use of a permanent walking aid is a likely requirement. The re-training undertaken by the patient should represent as closely as possible the actions to be re-learned. This means that training systems should either require the patient to perform the function which has been impaired, as is the case with the balance aid, or perform that function for the patient as is the case with stimulation systems. Muscle stimulation systems can induce recovery by duplicating the actions of the body, although little is known of the mechanism by which this recovery occurs. Re-training should commence as soon as possible after a CVA and be as intensive as possible to ensure the best results. Muscle stimulation prevents excessive muscle tissue atrophy, reduces spasticity and is useful in improving the gait quality of patients. The use of a balance re-training aid prevents a long term loss of patient confidence which can occur when a loss of balance is experienced. The need for a rapid response to the effects of a CVA suggests the use of portable equipment that the patient may 'take home' and use at their convenience. This philosophy of patient treatment requires a completely new generation of simple to use, portable rehabilitation equipment.

## **CHAPTER 3**

### **The balance re-training aid.**

#### **3.1 Introduction to balance re-training aids.**

Stance abnormalities in hemiplegics are well reported, with an unequal weight distribution over the feet a very common outcome of a stroke [47,62,111,221]. It has been shown by various authors [39] that balance re-training is a vital part of stroke rehabilitation and Goldie et al. [45], Collen [43] and Malouin et al. [37] state that the ability of the patient to control the body over a small base area is one of the fundamental tasks to be re-learned by a stroke patient. Hocherman et al. [62] state the improved confidence and stability reported by patients undertaking platform-based balance re-training. This report refers to the re-learning of static balance, which is mainly aimed at improving patient confidence and general stability. The importance of dynamic balance re-training is well reported. De Weerd et al. [50] state the importance of the re-training of weight transference, stating that “retraining of weight transference over the hemiplegic leg, during standing and walking, is essential in order to regain adequate balance and is a precondition to swinging the non-hemiplegic leg forwards when walking”. This is further emphasised by Winstein et al. [110] who state that “therapeutic retraining procedures that stress weight transfer to and weight bearing on the paretic limb might improve balance control”. Indeed, Dickstein et al. [54] state that one of the main objectives in the rehabilitation of hemiplegics is the ability to accept and bear bodyweight on the paretic side. In addition, Mann et al. [85] have shown the locus of weight transference necessary for the correct initiation of gait. Dettman et al. [112] suggest that the inability to perform this weight shift may underlie many of the observed hemiplegic gait defects.

These reports state the importance of balance retraining. There is some contention as to the value of static balance retraining in gait restoration, though this does appear to be of use in restoring patient confidence and improving stance stability [62]. It is generally agreed, though, that the ability to perform controlled weight shifts between the unaffected and the paretic limb is of primary importance in correct gait and rehabilitation [110].



### **CHAPTER 3 THE BALANCE RE-TRAINING AID**

There have been a number of procedures and systems devised to measure the degree of stance asymmetry of a patient, the degree of postural sway and also a number of systems devised to provide balance re-training.

At its most basic level, visual balance assessment has been used since the 1850s, when Romberg's test was developed [42, 43, 222, 223]. The patient is often observed performing a variety of tasks and their performance rated by the observer [224]. This method of assessment requires a trained observer to be in attendance, therefore is not a solution that can be taken home and used alone by a patient.

One very basic method used to assess postural sway by Lord et al. [207,208,210,211] consists of attaching a rod with a pen attachment to the back of a patient in order to trace out the locus of their movement on a fixed sheet of paper. Peterka and Benolken [56] and Peterka and Black [57,220] employed a similar method with the rod used to move a potentiometer wiper. This is obviously a very simple and easily implemented method of measuring the movement of the centre of mass of a patient, though does not allow the patient to observe these movements in real time, so cannot be used as a method of weight distribution and weight shift training by biofeedback.

A number of balance assessing platforms have been devised. These include the commercially available Chattecx system [54], the Kistler force platform [42,199,219, 225], the AMTI model OR6-5 [197], the Swayweigh system [196,222,226], the balance performance monitor [47], the standing feedback trainer [110], and the limb load monitor [50]. There are other examples of the use of custom built force platforms for balance assessment and re-training. These include platforms used by Katsarkas et al. [227], Hamalainen et al. [206], MacPherson et al. [228], Geurts and Mulder [53], Chodera and Lord [229] and the Double Video Forceplate used by Lord and Smith [43,201].

These systems have been employed to assess the balance of patients and in some cases to provide biofeedback oriented balance re-training. Some of these systems have been used in conjunction with tilting platforms and motorised actuators to discern the effects of balance perturbations upon the patient [43, 54, 64, 203].

The Chattecx system, Kistler force plate, AMTI , standing feedback trainer and the limb load monitor are all large, bulky systems requiring additional equipment such as monitors and computers for operation. The Chattecx system [54] requires an IBM PC for operation, whilst the limb load monitor requires a BBC Microcomputer and VDU for operation. The much used

---

## **CHAPTER 3 THE BALANCE RE-TRAINING AID**

---

Kistler platforms require an IBM PC, separate digitising unit and signal amplifier, whilst an external computer is required to sample the outputs from the AMTI forceplate. The Standing Feedback Trainer requires an additional feedback display console and system controller [110]. These systems are intended primarily to log balance data which will be used for patient balance evaluation subsequent to the tests and are therefore principally analysis tools.

The balance performance monitor [43,47] and the Swayweigh system, developed by Wing et al. [43,196,223,226] were designed to permit balance re-training. The Swayweigh system comprises a single plate and is developed from a set of bathroom scales. The visual output to the patient is by means of a single meter that indicates left or right movement of the centre of pressure beneath the feet of the patient. The Balance Performance Monitor is a portable system, utilising two separate footplates which indicates to the patient left to right and anterior to posterior centre of pressure movements. These are presented to the patient on a console by the activation of lights which show the position of the centre of pressure.

These two systems are portable and provide instant biofeedback to the patient, so fulfil part of the requirement for the balance re-training aid. Unfortunately, these systems only show the patient the position of their current centre of pressure, so are mainly concerned with static balance training [43]. Neither design permits the implementation of weight shifting training tasks, guided by on screen graphics. These tasks should take the form of loading and unloading the paretic limb and the movement of the centre of pressure through the locus that permits the initiation of gait, as discussed in chapter 2.

The ability to provide on-screen graphics that guide the patient through re-training exercises is considered to be essential if the correct training is to be undertaken and the training is to remain stimulating and maintain the continued attention of the patient.

### **3.2 Aims of the balance aid system in this PhD program.**

To design and construct a balance re-training system with the following features:-

- Sufficient portability to enable a patient to use the unit at home at their leisure.
- Foolproof assembly and disassembly.
- Simple operation.
- Full on screen instructions in usage of the unit to avoid instruction manuals.
- Visual centre of balance feedback to the patient occurring in real time.

---

## **CHAPTER 3 THE BALANCE RE-TRAINING AID**

---

- Graphical display to enable patient task guidance.
- The ability to provide the patients with, stimulating weight shifting tasks.
- The ability to determine patient performance and record this for future reference.
- The ability to provide skill levels to allow the patient to train at their own rate.
- The ability to store a measure of patient performance in a form that may be examined periodically by a physiotherapist.

### **3.3 Prior research recommendations.**

Day et al. [65] state that stance width often varies in stroke patients with the extent of the cerebral damage and that the stance is often widened to increase the feeling of patient stability. Prior research by Ho et al. [63] at Bath University has shown that the single platform could not easily cater for differences in patient stature and stance, whereas two footpads allow foot positions particular to each individual patient. In addition to these findings, Turnbull et al. [111] suggest that training with the feet placed in a diagonal arrangement may be useful as this simulates the position of the feet during gait. A two footpad system would permit balance re-training with this foot orientation to be undertaken.

Another system level recommendation of Ho et al. [63] was the use of a liquid crystal display (LCD) screen to ensure portability and a robust construction.

In order that the user does not ever require to observe his feet, a foot position indication system is required to show, and permit correction of, foot positioning. This system is required in addition to a pressure distribution monitoring system, which is necessary to determine the centre of pressure of the base of the patient with its relation to the centre of mass of the user [55]. If two separate foot placement devices are used in the design, then the foot position sensing need only be carried out in the front to rear direction, as the sideways location is defined by the location of the foot placement device.

Prior research into balance platform pressure transducers by Ho et al. [63] recommends the use of transducers other than strain gauges. These devices required skilled mounting using facilities including clean rooms and a baking chamber to cure the particular adhesive used in attaching these gauges to the section under stress. It was, therefore, decided to utilise a different, simpler method of balance measurement in order that all balance aid construction / repair might be performed without the need for these specialised facilities.

## CHAPTER 3 THE BALANCE RE-TRAINING AID

### 3.4 System level description of balance aid.

#### 3.4.1 The balance aid components.

The balance aid comprises three modules plus some interconnecting cabling, the relationship between which is shown in fig. 3.1.

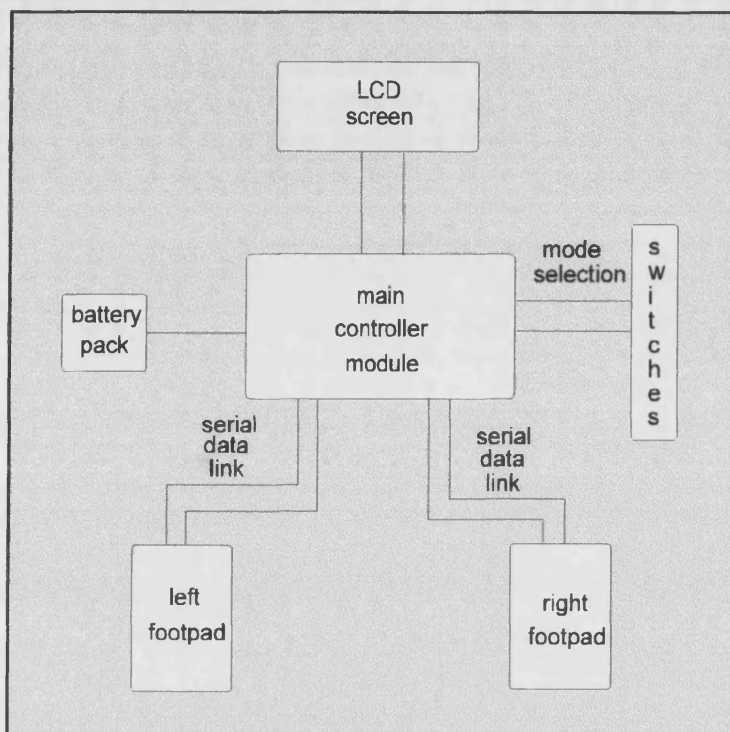


Fig. 3.1 System level diagram of the balance aid.

These modules are:-

- 1) The combined processing unit, display and power supply unit.
- 2) The left footpad, comprising platform, foot position indication system and pressure distribution indication system.
- 3) The right footpad, identical to the left footpad.

#### 3.4.2 Balance aid use.

Correct operation of the balance aid is by the positioning of the two footpads on the floor in a position suited to the stance of the user, who then places one foot centrally on each pad. The display screen and processing unit module is placed, using the integral stand, on a convenient bench in front of the user. The display then provides full sequential instructions for the use of

## **CHAPTER 3 THE BALANCE RE-TRAINING AID**

---

the balance aid, allowing the user to position his feet correctly, run test and calibration routines and practice balance skills. A watchdog routine constantly guards against errors in use and five skill levels are available to permit the user to build confidence at a pace suited to that individual.

When first powered up, an introductory page is displayed, welcoming the user to the balance aid. The system then performs a self calibration of all sensors and offers a test routine to the user, which may be used to check correct operation of all the sensors. The user is then asked to step onto the footpads and advised on the foot movements necessary to centralise his feet upon the pads. Once foot placement is correct, the user is offered the choice of static or dynamic balance training by an on-screen prompt. When undertaking static balance re-training, the user's centre of balance is indicated on the display by a cross and the ideal centre of balance position by a box. The user is ideally balanced when the cross is located within the box. When undertaking dynamic balance training, the user is instructed to adjust their balance to maintain the cross position within the moving on-screen box.

There are five skill levels available at all times to alter the sensitivity of the cross movements to changes in the patient centre of balance. When using the dynamic balance re-training option, the percentage of the time that the user has managed to keep the cross within the box is used to form a 'score' and stored in the battery backed memory. The score associated with each training session is stored in a separate memory location to provide a 'history' of training progress. The best session score to date is displayed on the screen.

### **3. 4. 3 System level operation.**

The balance data generated by the two footpads is transmitted to the main processing unit for interpretation. This information is gathered constantly by the subsystems within each footpad, as shown in fig 3.2.

Initially, the toe and heel extremity positions of the foot on each footpad is registered. This information is transmitted to the processing unit via a serial data link upon interrogation by that unit. The four pressure indicators mounted in the corners of each of the footpads produce an analogue signal proportional to the force placed upon them. These signals are continuously transmitted via separate lines to the processing unit where sample, hold and digitisation occurs under control of the microcontroller software. The microcontroller evaluates this data, taking into account skill levels and foot positions and calculates both the ideal and actual centres of balance. The result of this is balance information which is sent to the screen driver. The screen driver is a piece of dedicated hardware that translates binary codes from the microcontroller into

## CHAPTER 3 THE BALANCE RE-TRAINING AID

LCD screen driving signals, permitting microcontroller data to appear on the screen as a visually interpretable output.

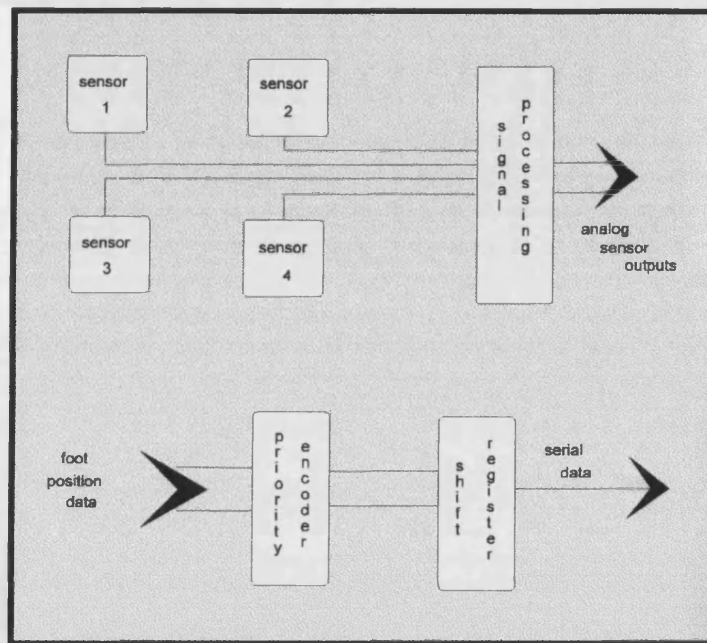


Fig. 3.2 Data gathering system level diagram.

Skill level changes, test routines and the option to quit the program are available to the user through four push buttons mounted alongside the LCD screen. Activation of these switches at permitted times results in the user's choice being accepted, whereas attempted activation at incorrect moments is ignored by the microcontroller.

### 3.5 Footpad hardware.

#### 3.5.1 Introduction to the footpad hardware.

The two footpads used are identical and therefore interchangeable. This removes the need for polarised connectors and simplifies the user assembly of the unit. The purpose of the footpads is to produce data on the location of the user's feet in relation to the footpads and produce data describing the distribution of the user's weight across each footpad. It was decided that it is only necessary to determine the front to back foot position. The left to right foot positioning is fixed by the initial placement of the footpads on the ground by the user. Any significant sideways movement of either foot when in use will result in a loss of contact with the footpad, which is flagged as an error to the user.

---

## **CHAPTER 3 THE BALANCE RE-TRAINING AID**

---

### **3. 5. 2 The foot position indication system.**

Thirty two equally spaced wire strips run across each footpad providing a resolution of 10mm in front to back foot placement. Each wire strip is separated from the neighbouring strip by a length of foam which stands proud of the wire strip.

The foam used was a high indentation load deflection (ILD),  $40 \text{ kg} / \text{m}^3$  CMHR 40 melamine free (flex) seat foam, selected for its compression properties. There are a number of properties associated with foams which describe their behaviour under load and with use over extended periods of time. These terms and the associated tests to quantify these terms are described by McFadyen and Stoner [230], whilst the procedures of compression testing alone of foamed materials is described by Campbell et al. [231]. A discussion of the structure and mechanisms of compression of foam is presented by Brown and Percy [232]. Should the long term mechanical properties of the foam used be found to be inappropriate, a variety of other materials with their associated properties are listed by Campbell et al. [231] and McFadyen and Stoner [230].

A conductive sheet is laid across the foam and wire. The sheet is permanently energised at +5V and is in turn insulated from the user by a rubber cover. All thirty two strips on each footpad have  $47\text{k}\Omega$  pull down resistors, so that with no pressure on the footpad the foam strips insulate the wire strips from the conductive sheet and each wire strip appears as a logic low. Pressure on the footpad causes the foam to compress locally, allowing the conductive sheet to contact and energise the strip below, presenting a logic high on that strip. This mechanism is shown in fig. 3.3.

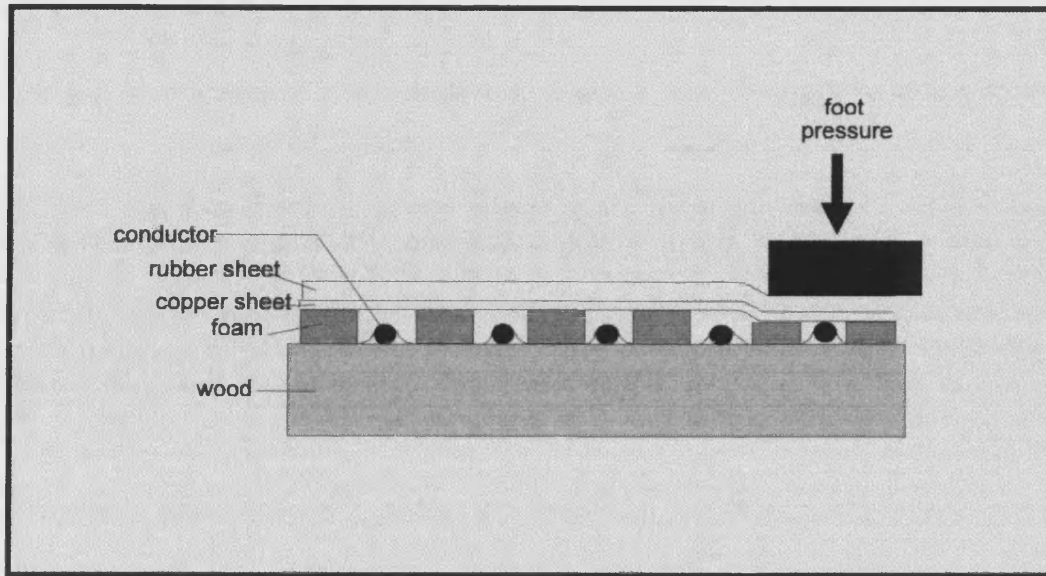


Fig. 3.3 The foot position detection system.

It is more efficient to transmit the position of the extreme toe and heel position of the foot than to transmit and store the position of every energised strip and then process this data to evaluate the foot position. This would be necessary in this case as 'spaces' such as those under the centre of the foot would need to be 'filled in'. These functions are instead carried out by the hardware situated within the footpad, shown in fig. 3.4. Each strip within a footpad is connected to the input of one of four CMOS 4000 series 4532 priority encoders, two of which take inputs from the front or toe end of the foot and two of which take inputs from the rear or heel end of the foot. The priority encoders produce a 4-bit binary code corresponding to the highest order active input. The 'enable in' and 'enable out' functions allow these devices to be cascaded, in this instance to refer to the highest order of sixteen inputs. In this way, the 4532 devices produce an 8-bit value corresponding to the strips activated by the toe and heel extremities, so that only the essential information of the positions of the two ends of the foot are recorded.



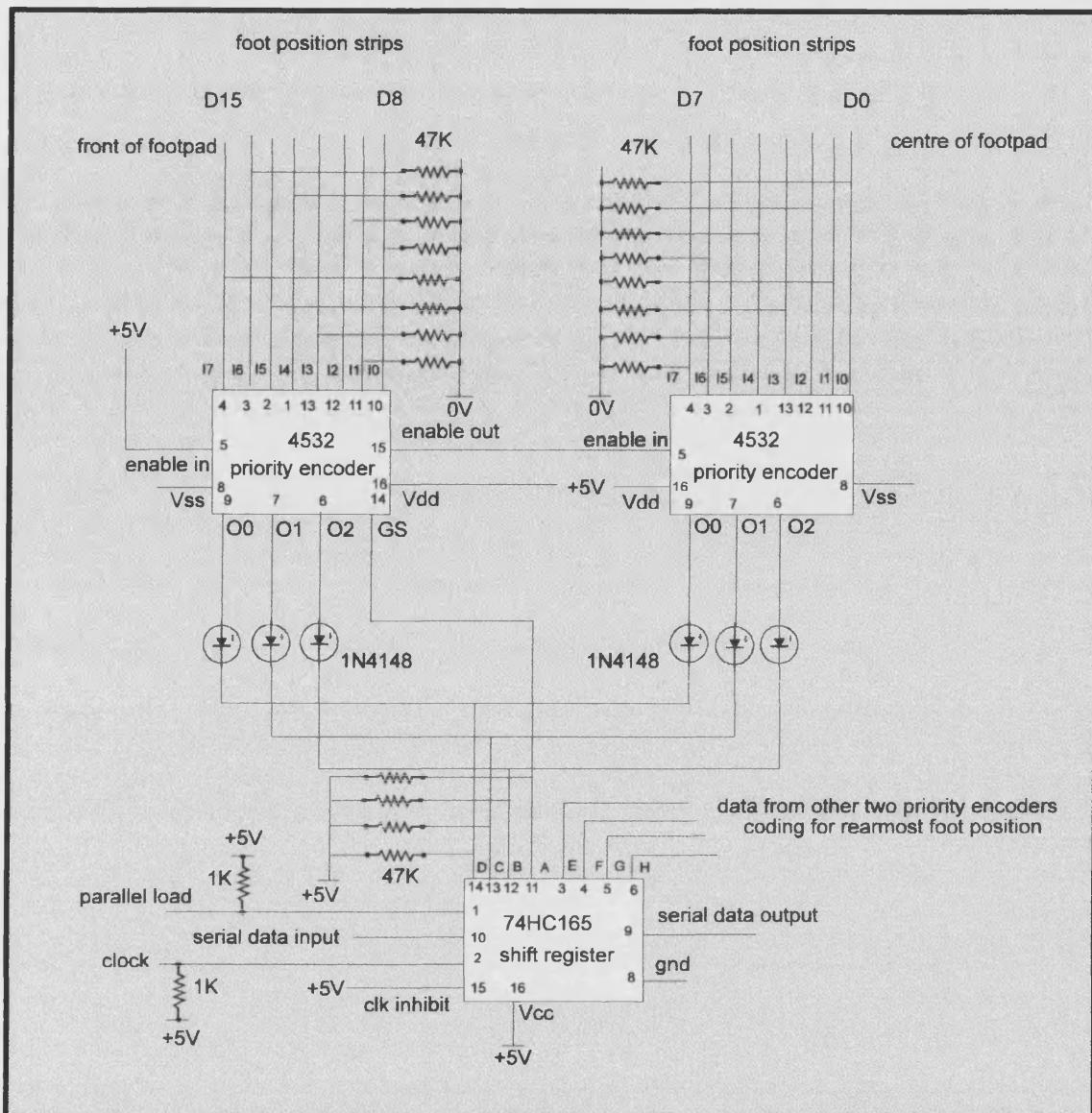


Fig. 3.4 The foot position encoding circuitry.

The two sets of four bit data outputs that make up the toe and heel extremity position of each foot are connected to the inputs of an eight bit shift register. An active low parallel load command from the processing unit causes all eight bits to be loaded into the shift register. A  $1k\Omega$  pull up resistor on this line ensures the reduction of spurious noise induced commands. Once a load has taken place, the first bit of data is available at the serial data output and will be succeeded by each bit in turn upon clock pulses arriving from the processing unit. In this way, the parallel data from the strips is converted to serial data. The serial data from the left footpad is transmitted to the processing unit but is then diverted to the serial data input on the right

### CHAPTER 3 THE BALANCE RE-TRAINING AID

footpad, so that the combined data of the two footpads becomes one serial data stream. The serial input to the left footpad shift register is grounded at the processing unit, so that the data stream is followed by a stream of zeroes. The serial data is always transmitted in the following order:-

- 1) Right footpad -- heel 4 bits
- 2) Right footpad -- toe 4 bits
- 3) Left footpad -- heel 4 bits
- 4) Left footpad -- toe 4 bits

A full 16-bit data stream is transmitted by the application of fifteen clock pulses from the processing unit. The foot position data for each foot extremity is tabulated in fig. 3.5.

MSB				LSB	
GS					
A	B	C	D	Strip Active	
0	0	0	0	D0	centre of foot
0	0	0	1	D1	
0	0	1	0	D2	
0	0	1	1	D3	
0	1	0	0	D4	
0	1	0	1	D5	
0	1	1	0	D6	
0	1	1	1	D7	extremity of foot
1	0	0	0	D8	
1	0	0	1	D9	
1	0	1	0	D10	
1	0	1	1	D11	
1	1	0	0	D12	
1	1	0	1	D13	
1	1	1	0	D14	
1	1	1	1	D15	

Fig. 3.5 Tabulated footpad data format.

## CHAPTER 3 THE BALANCE RE-TRAINING AID

### 3. 5. 3 Pressure sensing hardware.

#### 3. 5. 3. 1 Introduction to the pressure sensing subsystem.

The pressure sensing hardware is fundamental to the determination of the location of the centre of balance of the patient. Hospital trials of previous prototypes have demonstrated that the sensors must not allow appreciable movement under load, because movement of the platform has been found to be very disconcerting to the user, who is generally unsure of his balance even on a solid surface. Despite this requirement, the pressure sensors must provide an accurate measure of the pressure distribution over the footpad.

A test rig was constructed to permit a value to be obtained for the maximum allowable footpad movement. The rig was constructed from two footpad sized boards with a central pivot and adjustable movement limiting stops, as shown in fig. 3.6. This rig permitted a subjective feel to be gained for an allowable displacement of the corners of the footpad under load. The conclusion from this experimentation with normal volunteers was that a maximum progressive movement of 5mm is permissible before the user becomes aware of any instability. Previous attempts at a portable balance aid have suffered from excessive platform movement. These subjective tests show that this movement should be restricted to the 5mm maximum if the unit is to be used effectively by stroke affected persons.

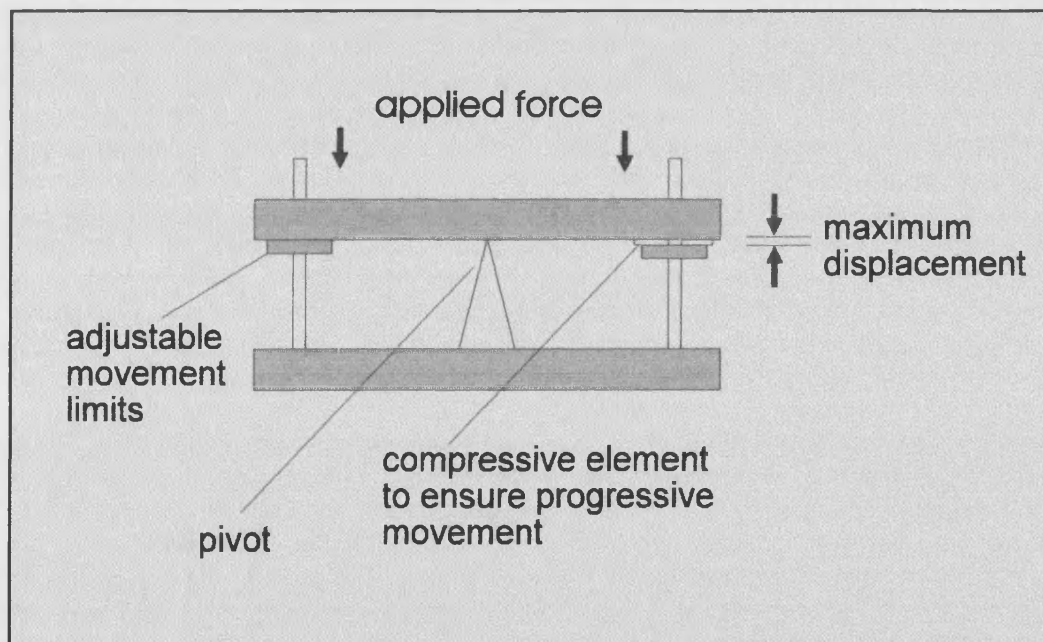


Fig. 3.6 Maximum footpad displacement test rig.

## CHAPTER 3 THE BALANCE RE-TRAINING AID

The imposed movement limit ruled out the use of traditional spring deflection sensors, sliding potentiometers and geared rotary potentiometers, so a novel sensor design was required. Two designs were investigated and these, along with their associated circuitry, are discussed separately.

### 3. 5. 3. 2 Differential air pressure sensing.

This technique uses a pressure sensing device, the SCC30DN, manufactured by Sensym, which produces a signal proportional to the difference in pressure applied to its two ports. To achieve an indication of the pressure placed on the footpads, a length of PVC tubing was attached to port 1, the high pressure port and sealed at the free end whilst port 2 was left open to the atmosphere. Plates were set to press down on the tube and raise the internal air pressure, increasing the differential pressure across the sensor.

The pressure sensor requires a constant current drive which must be temperature and time invariant to avoid drift between sensors. A value of 1mA is suggested by the sensor manufacturer for optimum sensor performance. The sensor produces a differential output which can then be converted to a single ended signal and conditioned to indicate the force acting upon the PVC tubing.

A time and temperature invariant, constant current source was devised, shown in fig. 3.7, employing five single substrate matched transistors.

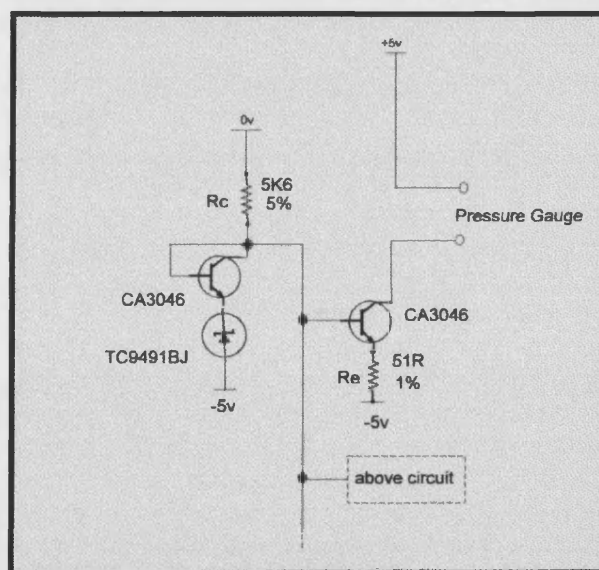


Fig. 3.7 Constant current source circuit.

### CHAPTER 3 THE BALANCE RE-TRAINING AID

A set of tests were carried out to test the viability of this sub-system, using the rig shown in fig. 3.8 and employing the current source to drive the pressure sensor, with the sensor output measured directly by a digital multimeter. A number of weights were applied to a plate above the tubing to simulate the user's foot pressure.

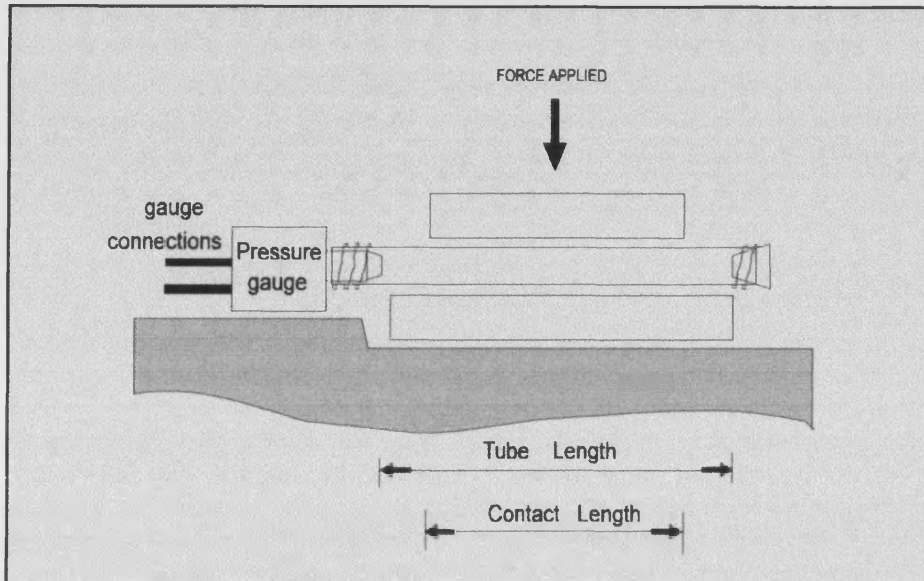


Fig. 3.8 Pressure sensor evaluation rig.

Two of the test results obtained using different tube and contact lengths are shown in fig. 3.9 and fig. 3.10.

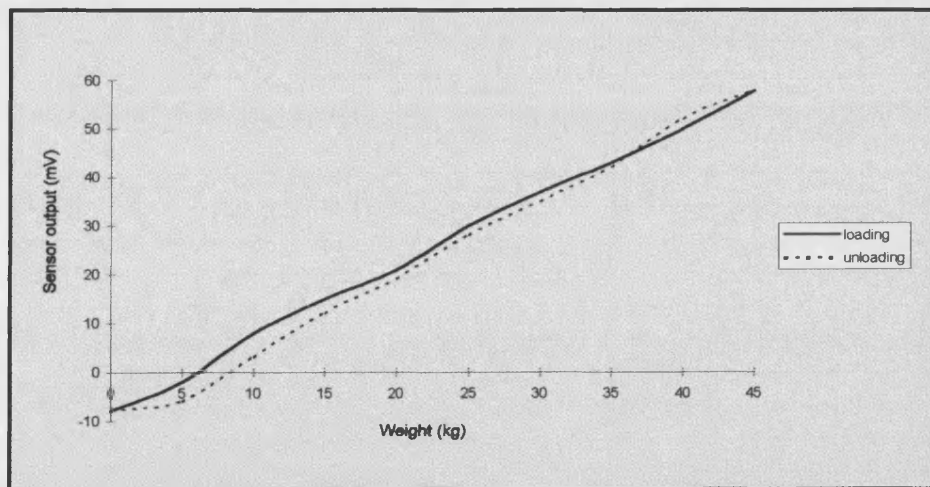


Fig. 3.9 Pressure sensor output with tube length = 110mm, contact length = 95mm.



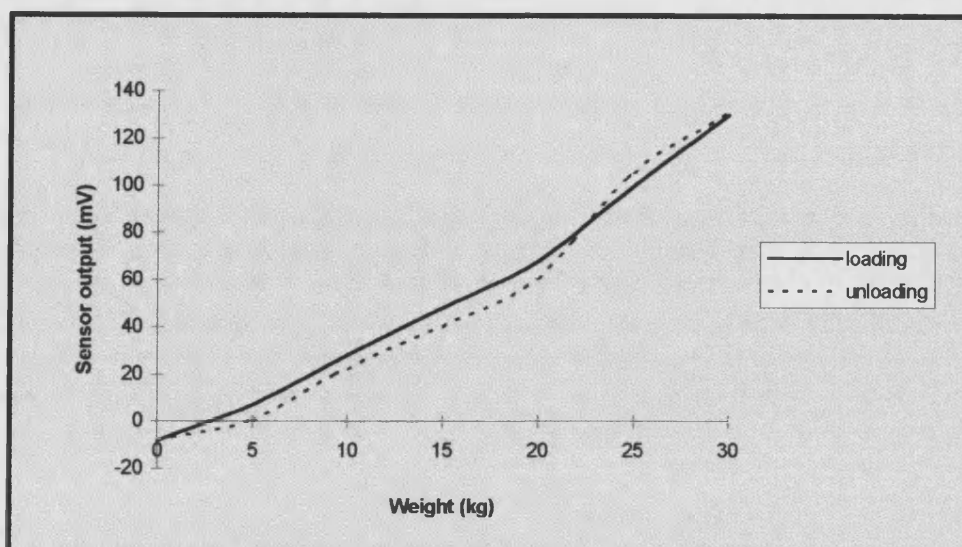


Fig. 3.10 Pressure sensor output with tube length = 60mm, contact length = 60mm.

Despite the good linearity of the loading curves shown in fig 3.9 and fig 3.10, difficulties were encountered with tube sealing during the tests and doubts arose over the long term reliability of the air pressure seal. Failure of any of the tube to sensor seals will cause the complete unit to fail to register correct balance information. In addition, the system exhibits significant hysteresis due to the energy storage within the PVC tube. For these reasons, the differential air pressure sensing solution was rejected.

### 3. 5. 3. 3 Optical pressure sensing technique.

This method of force indication employs a cantilever beam which deflects at the free end under load. This deflection is used to partially block a beam of infra-red light passing beneath the beam, changing the intensity of light incident on a sensor aligned with the light source. This method relies on excluding all ambient light from the sensor, so that only the internal light source can effect an output. In the stated environment within the footpad, ambient light is at a minimum, so is not expected to interfere with the light source or sensor. It is then only necessary to ensure that no sensor interferes with any other sensor, which can be achieved by careful screening and orientation of the devices.

An initial prototype sensor was constructed to test the linearity and repeatability of the optical section of the pressure sensor design only and to provide initial parameter indications.

The prototype test rig, shown in fig. 3.11, was set up using a matched infra red emitter and detector to assist in the reduction of ambient light interference. The beam on the test rig was

### CHAPTER 3 THE BALANCE RE-TRAINING AID

formed from thin aluminium, a material that permits easy deformation, enabling the stated beam deflections to be achieved with the application of small, convenient forces.

The emitter was driven by the constant current source shown in fig. 3.12, with the current set by the value of  $R_e$  according to:

$$I = 1.22 \text{ V} / R_e \quad (3.1)$$

A voltage of 1.22V is maintained across the TC9491BJ bandgap reference diode at all times.

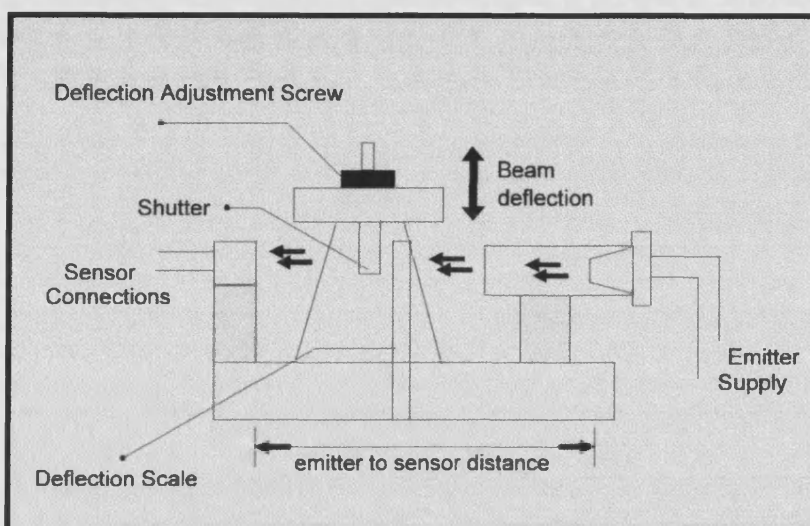


Fig. 3.11 Optical sensor evaluation rig.

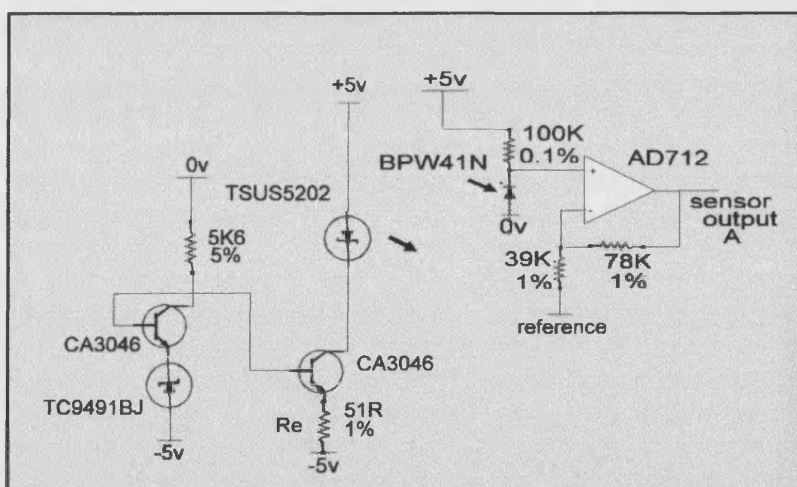


Fig. 3.12 Emitter and detector circuit for optical sensor.

### CHAPTER 3 THE BALANCE RE-TRAINING AID

Experimentation was performed by applying various beam end deflections by means of a clamp to determine the optimum values for the infra-red emitter current, the emitter to sensor distance and the maximum beam deflection. These parameters were varied during the tests to obtain the values necessary to produce a linear sensor output across the 0V to +5V range of the analogue to digital converter. The design of the mechanical aspects of the sensor may then be undertaken, using the parameter values determined by this experimentation.

Some of the results of these tests are shown in fig. 3.13 to fig. 3.16.

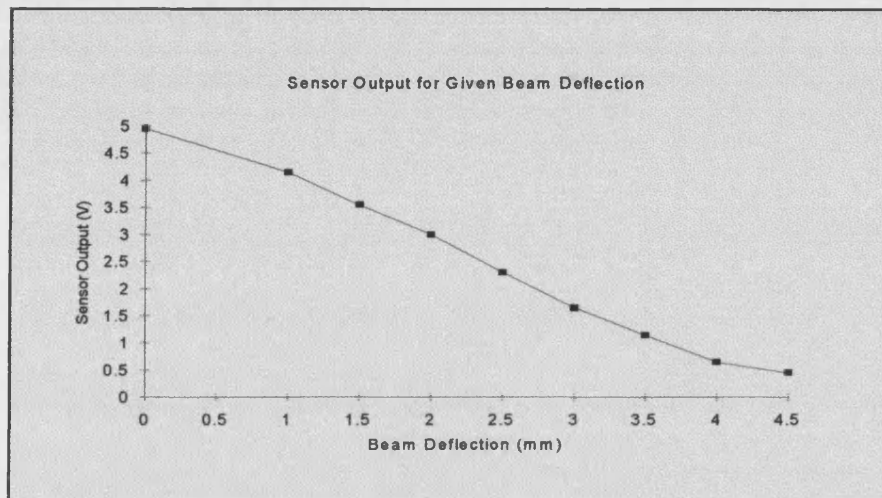


Fig. 3.13 Output for emitter current = 43mA, emitter - sensor distance = 31mm.

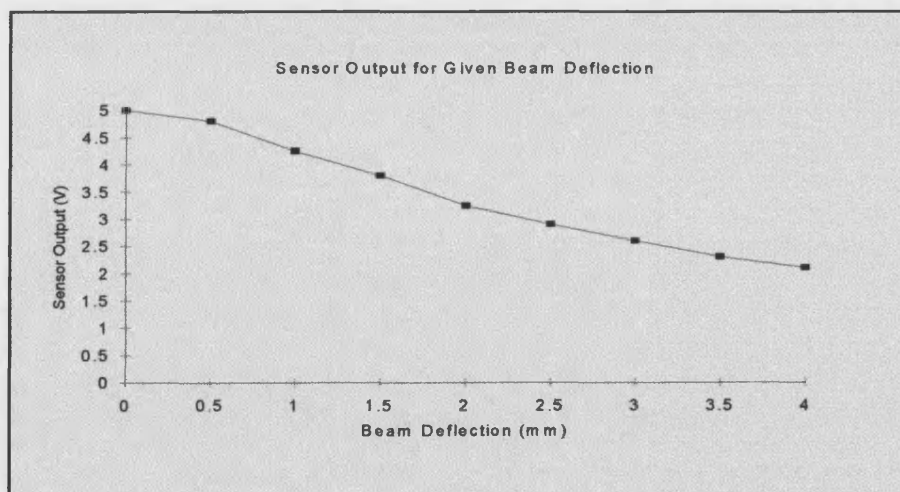


Fig. 3.14 Output for emitter current = 43mA, emitter - sensor distance = 38mm.



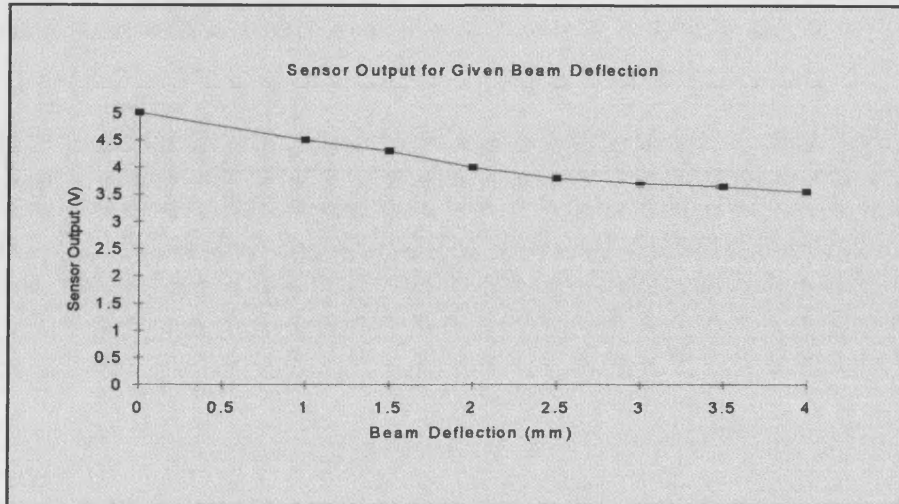


Fig. 3.15 Output for emitter current = 43mA, emitter - sensor distance = 40mm.

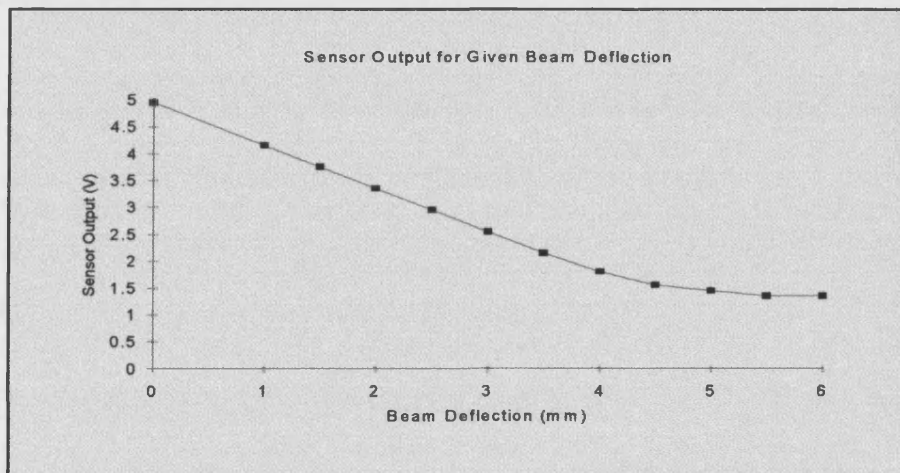


Fig. 3.16 Output for emitter current = 23mA, emitter - sensor distance = 24mm.

Fig 3.13 to fig 3.15 show the effect of altering the sensor to emitter distance whilst keeping the emitter current constant. The reduction of the separation distance has the effect of utilising more of the available output range, which produces an improved resolution when the sensor output is digitised. Fig. 3.16 shows the improvement in linearity obtained by reducing the emitter current to 23mA. The emitter - sensor separation was correspondingly reduced to 24mm to ensure a good sensor output resolution.

### **CHAPTER 3 THE BALANCE RE-TRAINING AID**

The conclusion from these tests was that the optimum parameters for the optical pressure sensor are as follows:-

Emitter current = 23mA

Emitter to sensor distance = 24mm

Maximum deflection = 3.0mm

The maximum permissible deflection of the cantilever beam requires accurate specification to allow endstops to be accurately positioned to prevent damage due to overloading. With this parameter specified, it becomes possible to begin an investigation into the physical characteristics of the cantilever beam.

Appendix A contains the derivation of the two equations used to determine the dimensions of the cantilever beam. Initially, the basic equations for beam bending were obtained from the texts stated in appendix A and then used to derive two separate expressions for the stored strain energy of the beam under load. This is not a known parameter, so these were equated to produce an expression for the maximum stress within the beam in terms of the load applied, the beam dimensions and the material properties. A separate expression for the deflection of the end of a cantilever beam under load was derived using the initial basic equations, thus providing a pair of simultaneous equations. Within these two equations are three unknowns, the length, width and thickness of the beam.

The deflection of the beam and maximum applied force were fixed values determined by patient weight and the earlier prototype performance. Initially, several different commonly available materials were considered. The use of each material fixes another two parameters, the Young's Modulus (E) and the maximum stress which is fixed at the material yield stress value. This leaves all three beam dimensions as unknowns. One of these was next chosen to be compatible with the footpad dimensions, leaving two unknowns and two equations which could be solved for the remaining two beam dimensions. This method was repeated with the material data for aluminium, mild steel, brass and nickel until a solution incorporating all three beam dimensions at a permissible value for the footpad application was obtained. Graphical representations of these equations allowed estimates of the suitability of each material to be made and provided guidelines within which to complete the numerical analysis of the dimensions, so reducing the time taken to find an ideal solution.

### **CHAPTER 3 THE BALANCE RE-TRAINING AID**

---

The results of such calculations for the different materials can be seen in appendix A. It was necessary to reduce the maximum beam deflection to 1.5mm in order to allow beam dimensions compatible with the footpad size to be calculated. This reduction in deflection only serves to improve the stability of the patient over the full range of the cantilever beam movement.

The optimum beam dimensions for the first fully workable prototype were calculated to be:

Beam material	-	brass
Beam deflection	=	1.5mm
Beam length	=	41mm
Beam width	=	14mm
Beam thickness	=	3.4mm

The beam was constructed from brass because of its high yield strength, low Young's modulus and low elongation value, which are listed in appendix A. These parameters satisfy the required beam dimensions and also give rise to a low hysteresis sensor as little energy is stored in brass under load cycles when compared to the other materials mentioned. The rest of the emitter and sensor holding structure were machined from aluminium of sufficient thickness to ensure that the brass beam is the only part of the structure to exhibit discernible flexion.

It was decided to connect the four infra red emitters within a single footpad in series, rather than creating four separate constant current circuits. This results in one drive of 23mA and ensures that each emitter in either footpad is driven by an identical current, producing an identical (within the device tolerances) luminous intensity. The circuit, shown in fig. 3.17, uses matched, monolithic transistors to minimise temperature related drift, with the final current value set by the 1% tolerance resistance.

To ensure that all the force sensing units within each footpad are as identical as possible, precision resistors are used where tolerances are critical. The  $100\text{k}\Omega$  sensor series resistor is most critical as these are separate for each sensor and of a high resistance value. For this reason 0.1% , 50ppm /  $^{\circ}\text{C}$  resistors are used here. The current set resistors are chosen at 1% tolerance as these only set the current to each emitter in the footpad and hence any inaccuracy will be common to the whole of the footpad. The buffer amplifier gain setting resistors are also chosen at 1% tolerance.

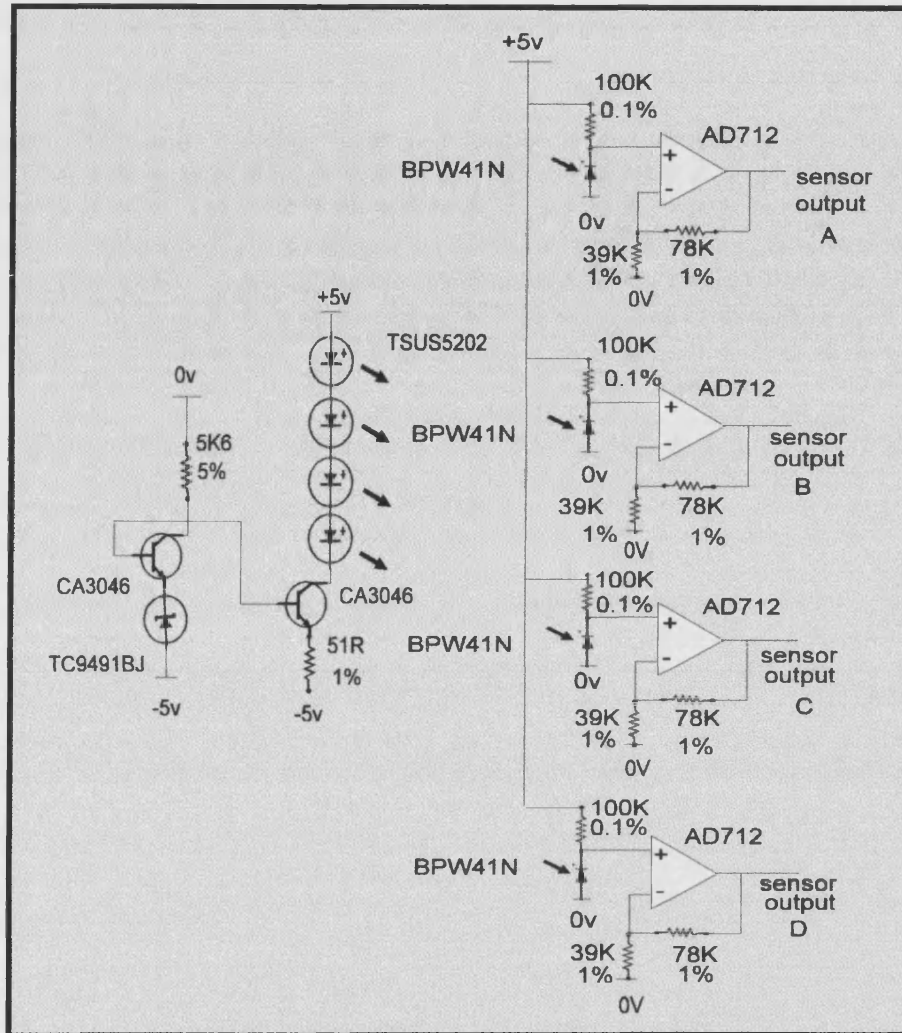


Fig. 3.17 Emitter and receiver circuits for the optical pressure sensing system.

The testing of an initial full specification prototype with a brass cantilever beam, shown in fig. 3.18, showed that there is an initial small permanent set in the beam that occurs after the first few operations under full load. Subsequent operations showed that no further set occurs. The small permanent sets in the beam are automatically removed by the auto zero function incorporated within the software. The prototype was seen to display the necessary deflection at the required loading and is robust enough to withstand all the user's weight on one sensor, thanks to the damage preventing end stops.

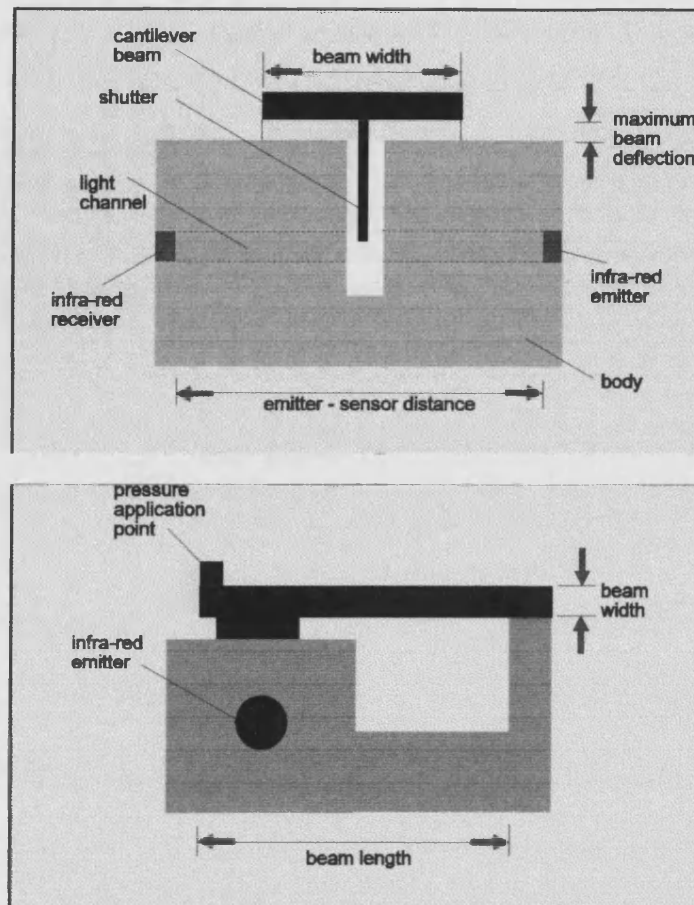


Fig. 3.18 Optical pressure sensor.

Electrical testing of the prototype showed that the signal received from the infra-red sensors could be buffered with a gain of 1.5 to produce a 0V to +4V output. The portion of the output characteristic used is determined by accurate trimming of the height of the shutter to give the required amount of light incident on the sensor under unloaded conditions. With the shutter length set to the optimum value, the need for offset correction within the buffer circuit is removed. The sensor output with the unit subject to loading and unloading and configured with the optimum shutter arrangement and size can be seen in fig. 3.19. With this arrangement, increased beam deflection causes a decrease in incident light on the sensor and an increase in the sensor output.

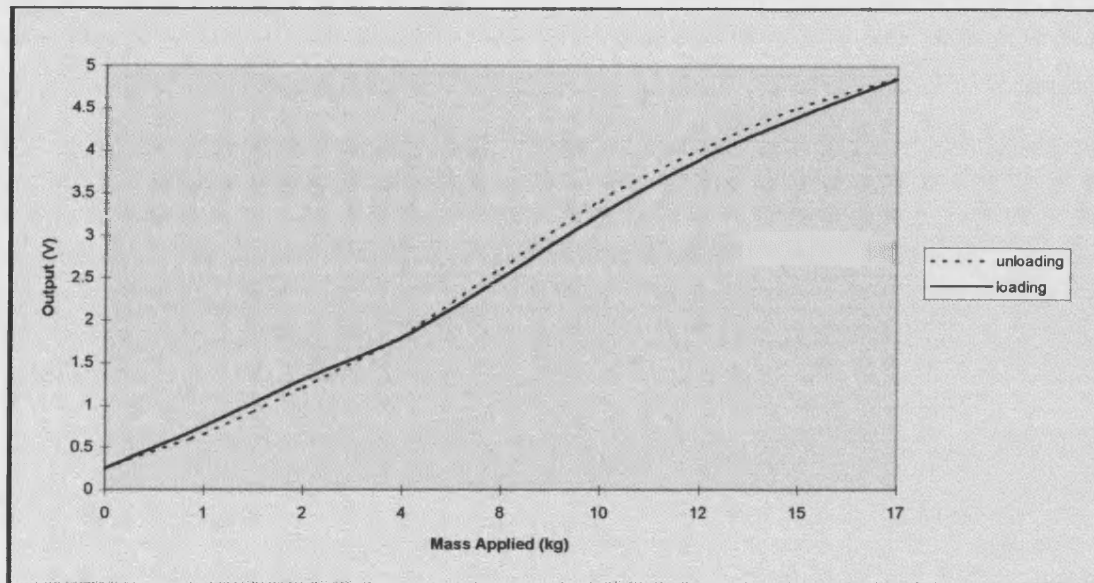


Fig. 3.19 Optical sensor output with correctly adjusted shutter.

The loading and unloading plot of the optical sensor shows that the hysteresis associated with this form of sensor is low (approximately 5% of the sensor output at the worst case load / unload deviation). This is due to the low energy storage associated with the brass beam and ensures that the indication of the deviation of the balance point from a nominal position will closely match the rate of return of that indication.

Fig. 3.20 shows the loading plot for four of the sensors and illustrates the close matching that may be obtained between the optical sensors. The close matching illustrated is important as the centre of balance is always determined by comparison of the various sensors rather than absolute values from each sensor. This degree of matching ensures that an accurate measure of the centre of balance is obtained.



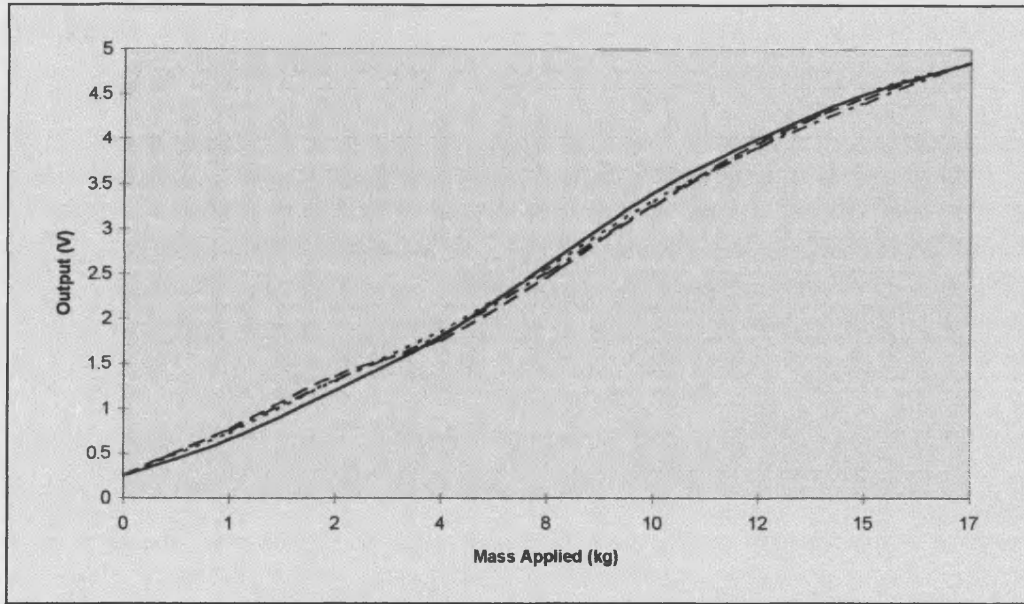


Fig. 3.20 Loading curve of 4 sensors to illustrate the sensor matching.

Fig. 3.21 shows the response speed available when using the optical pressure sensor. The output changes shown in fig. 3.21 were in response to a near instantaneous maximum deflection applied by a clamp to the free end of the cantilever beam. The full scale deflection response shown is approximately 20ms, which is considered to be adequate for detecting the shifts in the centre of pressure beneath the feet of a patient.

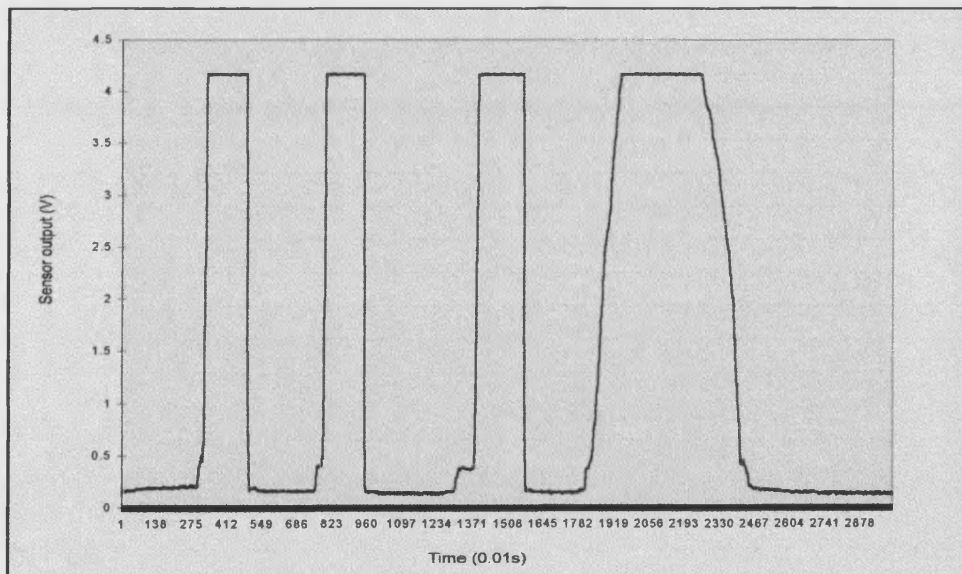


Fig. 3.21 Optical pressure sensor full scale response.

---

## **CHAPTER 3 THE BALANCE RE-TRAINING AID**

---

The final slower full scale deviation, shown in fig. 3.21, was performed to show that the output of the sensor to gradual pressure changes was not affected by the three previous fast full scale deflections.

The single module construction of this pressure sensor results in no specialised setting or aligning being required. The sensor needs only to be located inside the footpad and the electrical connections made. No calibration is required as this function is performed by the software.

### **3. 5. 3. 4 Choice of the pressure sensing subsystem.**

Both pressure sensing subsystems worked very well as prototypes, being simple to install, robust and exhibiting good repeatability and linearity. The cantilever beam was eventually chosen as the footpad pressure sensing system for three important reasons. When the cost of the two systems was compared, the cantilever beam components could be obtained for approximately one fifth of the cost of the pressure gauge system, primarily because of the high cost of the pressure gauges. Secondly, the movement associated with the cantilever beam system is approximately one third of that associated with the tube compression design, which will significantly add to the user's feeling of security. Thirdly, the possibility of pressure seal failures means that there is the likelihood of greater reliability when using the cantilever beam design.

### **3. 6 The processing unit.**

The processing / display unit is based around an 80C552 Phillips 8-bit microcontroller, featuring six input / output ports and an on board digital to analogue converter. The ports were allocated the following functions:-

- Port 0 - Low order address bus.
- Port 1 - General input / output port.
- Port 2 - High order address bus.
- Port 3 - Control lines for read / write and interrupts.
- Port 4 - Unused.
- Port 5 - Analogue inputs from pressure sensors.



---

## **CHAPTER 3 THE BALANCE RE-TRAINING AID**

---

### **3. 6. 1 The microcontroller.**

Although the microcontroller is of the 8-bit variety, provision is made for addressing a 16-bit address space. This is accomplished by publishing the low order address byte, latching it and then publishing the high order address byte. The timing for these operations i.e. the latch signal and the read and write enable signals are provided by the microcontroller via dedicated timing outputs. In this manner a 27C64 (8kByte) EPROM may be accessed, though for 8kBytes of ROM only thirteen of the possible sixteen address lines are required. The accessed data is placed onto the low order data / address bus and read into the microcontroller via port 0. It should be noted that all accessed data is 8 bits wide. The microcontroller has 256 bytes of accessible internal memory which is used for the storage of temporary variables and constants. In order that the microcontroller can store additional data, 32kBytes of SRAM is available and is accessed in an identical fashion to the ROM, the differentiation between these two data storage media being made by the control outputs of port 3. The dynamic balance scores achieved by the user are stored along with the associated skill level in this SRAM each time the balance aid is used. This permits the user to monitor his progress over time. The 80C552 is operated at the device maximum rated frequency of 12MHz and resets upon power up by means of an RC circuit employed to hold the reset pin in an active low state during power up. This forces the program counter to instruction number  $0000_{16}$ . The code then executes from this instruction. A reset switch is included in the circuit to permit a processor reset at any time after power-up. Naturally, this switch is located within the casing of the processing unit to prevent accidental user reset of the microcontroller. It is included for use in testing and diagnostic activities only.

### **3. 6. 2 The liquid crystal display screen.**

The LCD screen, a Seiko Epson G648D - 931E, measures 235 x 105 mm and has a resolution of 640 x 200 pixels. This is driven by a dedicated LCD screen driver, the SED 1330, which translates the binary codes from the microcontroller into screen commands for characters or text. The screen driver is accessed in the same way as the ROM and SRAM described earlier. The A0 address line is used to differentiate between screen commands and screen data. The SED 1330 operates at a clock frequency of 10 MHz and is allocated a separate 32kbytes of SRAM which is used for screen data storage. This device also incorporates a 'power-on reset' which is tied to the microcontroller reset, so a full system reset will occur upon power-up.

## CHAPTER 3 THE BALANCE RE-TRAINING AID

### 3.6.3 The user interface.

User selection of skill levels, the option to quit the program, the option to run a test program and general ready and turn page responses are effected by four push button switches mounted alongside the LCD screen. Activation of these buttons, labelled 'skill up', 'skill down', 'quit' and 'test', places a logic high on an input to a D-type latch. An RC circuit between the switches and the clock input ensures that the latch is clocked after the input pulse has arrived. The latch stores the switch pulse as a high level on the device outputs, the inverted outputs discharging the RC circuit and hence resetting the clock input. The device outputs are connected directly to port 1 of the 80C552 and read by the microcontroller at an instant determined by the software. After completion of a switch read cycle, the latch is reset by a low logic level applied to the latch master reset. This intermediate circuitry, shown in fig. 3.21, permits asynchronous switch and software operation, prevents single switch operations being construed as multiple operations and allows invalid switch operations to be ignored by using a master reset output without a read cycle.

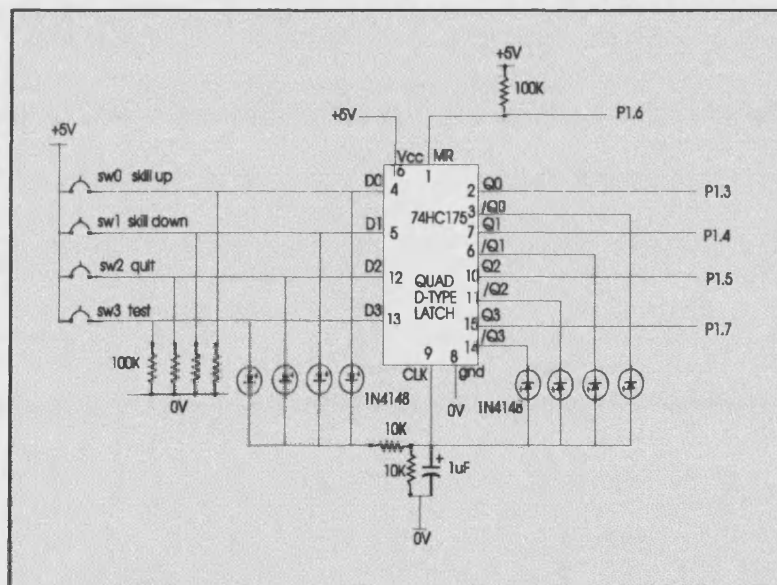


Fig. 3.21 Switch press detection circuitry.

The complete circuit diagram of the microcontroller, screen driver and user interface circuitry is shown in fig. 3.22.

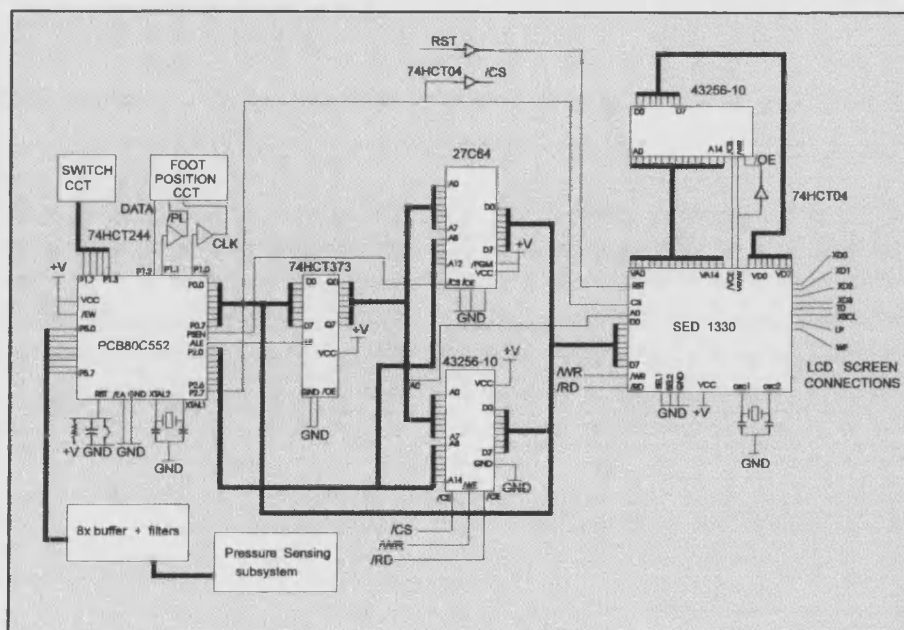


Fig. 3.22 Microcontroller and screen driver circuit.

### 3.6.4 The power supply.

It was decided that the balance aid should be capable of accepting power from either a mains outlet or from internal batteries. This permits convenient use of the unit at any point within the home.

When power is accepted from a mains outlet, this is utilised in two ways :

- 1) It is used to provide the power requirements of the system if this is in operation.
- 2) It is also used to charge the cells that supply power to Balance Aid when the unit is used remotely, away from a mains supply.

With the capability to operate and charge, the system may be operated, or merely left to re-charge the cells overnight.

It was decided that a battery life of greater than three hours was required. It has been observed, at Odstock Hospital, that patients require to rest after an average of about thirty minutes of rehabilitation training and that patient contact time with the physiotherapist is limited to around one hour. These two factors led to the decision that the balance aid should be able to operate from the internal cells for three hours between charges. Naturally, there is no limit on operating time when powered from the mains.

### CHAPTER 3 THE BALANCE RE-TRAINING AID

The available space within the unit and the required battery life led to the choice of six AA size nickel metal hydride (NiMH) cells, producing 7.2V. These cells have a rated capacity of 1.2Ah and require a trickle charge current of 120mA for 16 hours.

The required voltage rail is +5V, so allowing for a 1V drop across a blocking diode, six cells in series producing 7.2V was chosen to be the supply when the system is operated remotely. The current drawn by the system is 400mA at +5V (supply) and 120mA at +8V (charging). This produces a power requirement of 3W. The next commonly available transformer secondary above 7.2V is 9V rms. In practice, 12VA mains transformers are commonly available and of a size compatible with the box containing the processor board and screen. Having chosen these components, the rest of the power supply circuit was designed and is shown in fig. 3.23.

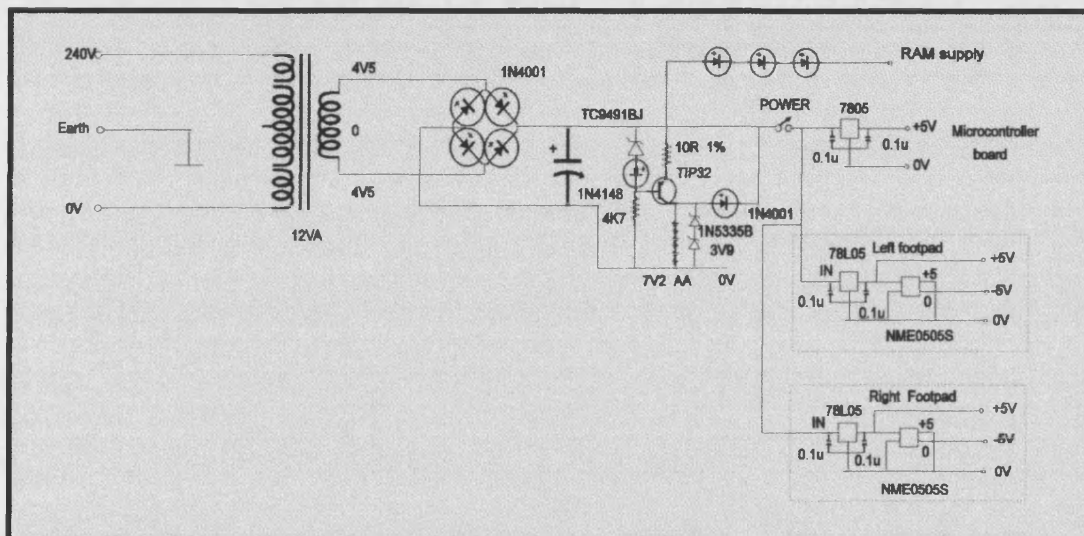


Fig. 3.23 Balance aid power supply unit.

The mains, 240V, 50Hz AC is transformed to 9V rms, rectified and a constant current source used to charge the NiMH cells with the 120mA stated. This occurs whenever the mains is connected. Current is either drawn from the rectifier or the cells to power the balance aid via a +5V regulator to provide the supply rail for the processor board. The supply to both the footpads is routed in unregulated form to alleviate the problem of voltage drop along the cable length. Within each footpad, the supply rails are produced by means of a +5V regulator and an isolated output +5V to +5V power converter. The arrangement shown in fig. 3.23 produces +5V and -5V supply rails at the footpads. Fig 3.23 also shows the RAM supply which is derived from the battery output. This ensures that the patient achievement information stored in the SRAM will be retained when the mains power is removed.

## **CHAPTER 3 THE BALANCE RE-TRAINING AID**

---

The two power zener diodes connected in parallel with the NiMH cells prevent over-charging of these cells by providing a current shunt path when the cell voltage rises sufficiently to bring these devices into conduction.

### **3.7 Balance aid software.**

The microcontroller software is written in 8051 assembly language utilising a BBC Microcomputer running the META assembler and the Portal EPROM emulator. The software code is contained within modules to enable this coding to be retained within the memory of the BBC Microcomputer. These modules, represented by bold text, are listed in fig. 3.24, along with the software routines, shown in italic text, contained within each module. The code within the modules may call other complete modules, routines within other modules or routines within itself. These all act as subroutines to the calling module. Fig. 3.24 shows which modules and routines are called by each module.

A general explanation of the function of the software follows, outlining the processes occurring and the interaction with the user. A full description of each software module is included in Appendix B.

Initially, upon power up, a welcome screen, shown in fig. 3.25, is displayed which introduces the balance aid to the user and prompts for a button press to continue to the next stage. The switches on the unit are monitored and upon detection of the correct switch press the welcome screen is replaced with a screen prompting the user to initiate the self calibration function. This removes any sensor offsets present with the platforms unloaded and counteracts any permanent set that may occur in the cantilever beam arrangement. On completion of this operation, a test procedure is offered to the user to ensure that each of the foot position detection strips and the pressure sensors are fully functional. This may be by-passed if desired by operation of the appropriate switches on the unit. All instructions are displayed on screen as required by the user. The test routine prints representations of the footpads upon the screen and adds a horizontal line for each functioning strip.

### CHAPTER 3 THE BALANCE RE-TRAINING AID

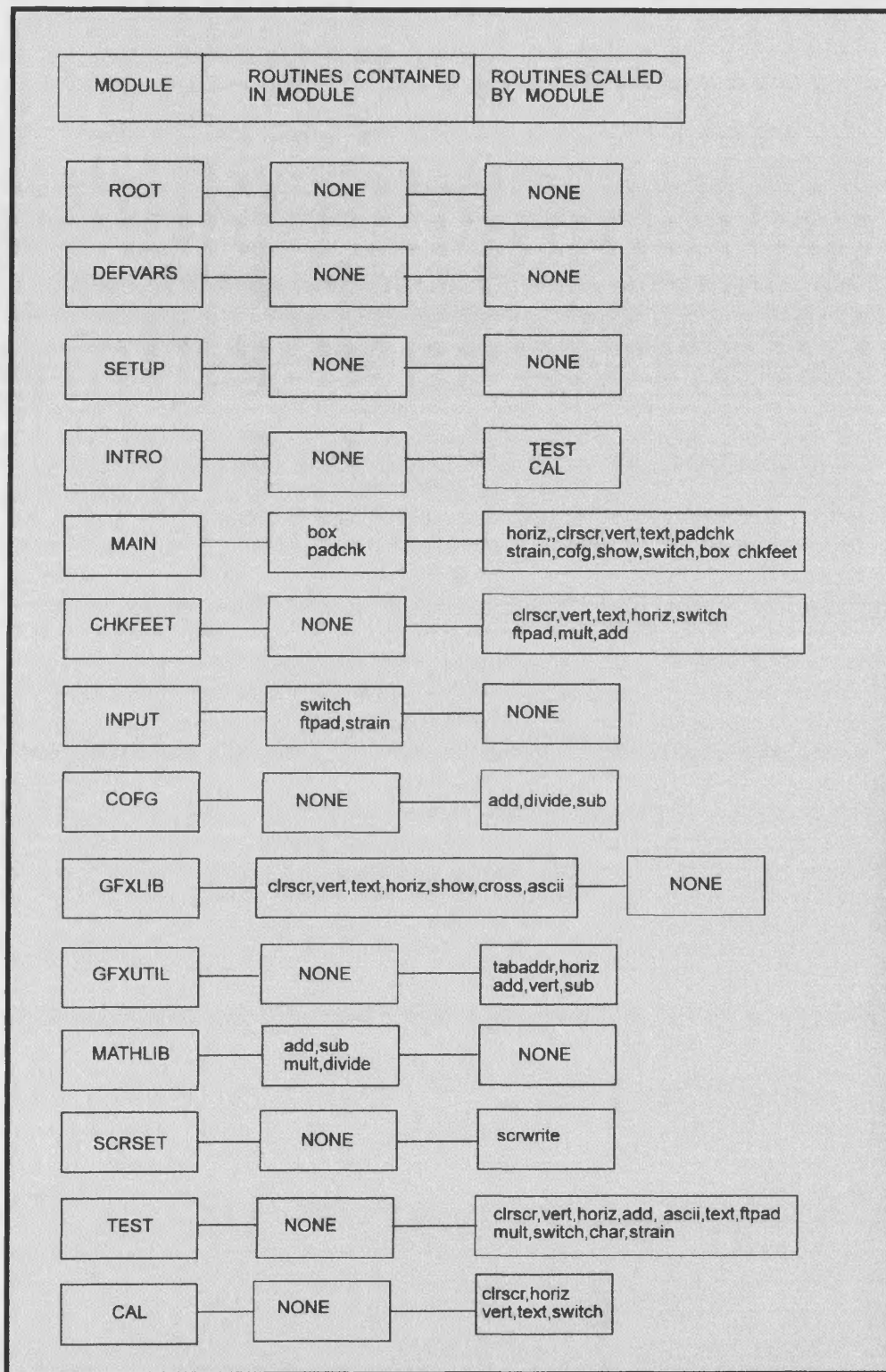


Fig. 3.24 Software module and routine organisation.



## CHAPTER 3 THE BALANCE RE-TRAINING AID

---

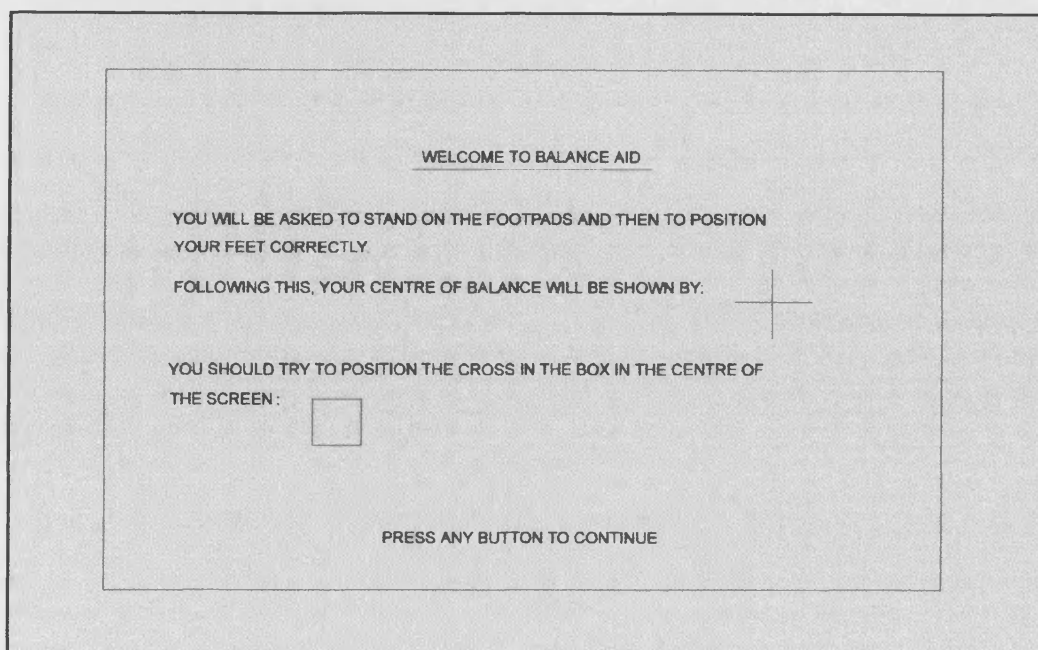


Fig. 3.25 Introductory screen page.

The maximum output of each sensor is also displayed in each corner of the footpad representation. This screen permits the user to quickly and easily determine the functionality of the unit.

As before, the user is prompted to exit this stage when satisfied that the tests are complete. When an appropriate button press has been detected the user is prompted to place both feet centrally upon the footpads. Two footpad outlines are drawn on the screen and the position of the foot on each pad is represented within these by rectangles of varying length and position. Once the foot positions have been drawn on the screen, checks are carried out to determine whether or not the foot placement is ideal. This is accomplished by comparing the distance from the toes to the front of the footpad with the distance between the heel and the rear of the footpad. If either is three or more times greater than the other, then that foot is deemed to be out of position and then the required error message is printed on the screen above the relevant footpad outline. Until the above criteria are met, the program will cycle through the foot position data acquisition and analysis, displaying the positions of the feet and any error messages required. When the feet are correctly positioned on the footpads, the user is informed by an on screen message and, when ready, may progress to the balance monitoring stage.

There are two possible balance options available to the user. The task in each case is for the user to alter their balance to keep the cross displayed within the on-screen box. In the static balance

### **CHAPTER 3 THE BALANCE RE-TRAINING AID**

---

option the box remains stationary at the centre of the screen, whilst in the dynamic balance option the box moves about the screen. Five user selectable skill levels are available which adjust the speed of the box movement when using the dynamic balance training option and the sensitivity of the cross movements to the movement of the user. In the case of the dynamic balance option the number of program cycles between updates of the box is obtained by dividing a scaling constant by the value of the skill level. The cross movement sensitivity is obtained by multiplying the difference in sensor averages calculated by the current skill level value. The result is then scaled to fit the screen using the same scaling constant regardless of the skill level employed, to preserve the different sensitivities required at each skill level.

The software calculates the position of the user's centre of balance by comparison of the pressure sensor outputs and adjusts the position of the cross accordingly. A detailed discussion of these calculations is shown in Appendix C.

Within each balance aid session, the number of cross re-draws inside and outside the box for each skill level are recorded and the best score to date displayed on the screen. The battery backed memory retains these values between training sessions to permit progress to be observed by the user and evaluations to be made by the physiotherapist.

A watchdog routine runs constantly throughout the balance monitoring stage to check for incorrectly placed feet. If this condition is detected, the software will revert back to the foot positioning function and once again prompt the user to stand correctly upon the footpads. Following such an occurrence, the user will be led back to the balance monitoring stage by further on screen instructions.

Two typical screen displays for the balance monitoring stage is shown in fig. 3.26. The upper diagram represents a typical screen displayed during static balance re-training. The lower diagram represents a typical screen display during dynamic balance training and shows the box movement and achieved score.



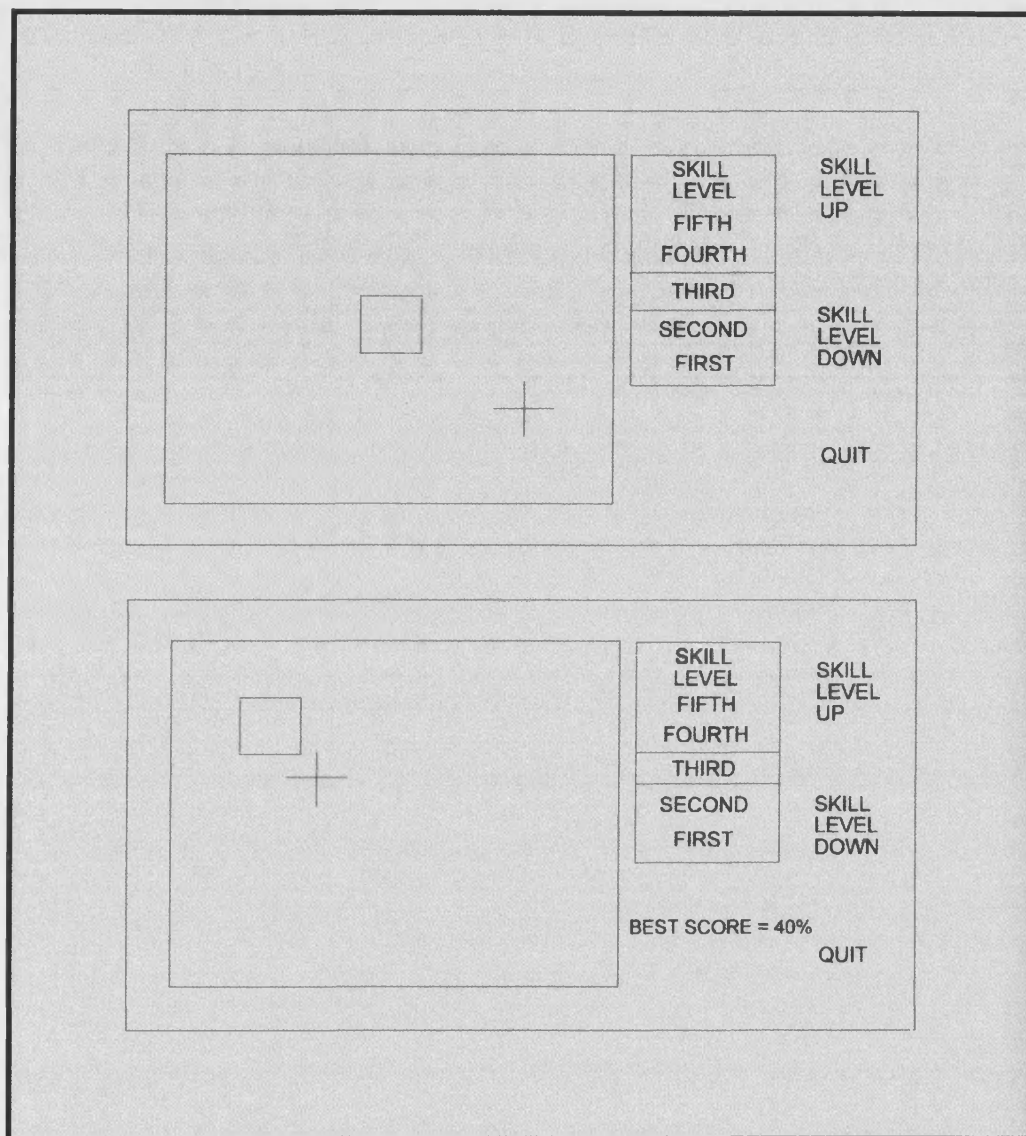


Fig. 3.26 Final screen display showing two possible states.

## **CHAPTER 3 THE BALANCE RE-TRAINING AID**

---

### **3.8 Balance aid construction.**

The balance aid processing unit is enclosed within a 'style 5' metal case of dimensions 431.8 x 177.8 x 65 mm. This casing renders the unit shock and splash resistant and incorporates a folding stand, to permit the unit to be placed on a surface at the user's eye level.

The microcontroller, screen driver and power supply circuitry are incorporated on one, double sided PCB, shown in fig. 3.27. This PCB is mounted behind the LCD screen, with all electrical connections made via PCB headers and cable shell assemblies. This permits easy removal of the board for repair.

The footpad components, shown in fig. 3.28, are enclosed within aluminium trays and utilise plywood bases to reduce flexion under load. The open tops of these trays are covered by rubber matting bonded to the aluminium trays with silicone sealant, to ensure resistance to moisture ingress. The pressure sensors located in each corner of the footpads are mounted upon aluminium plates to prevent damage to the plywood platform occurring under load.

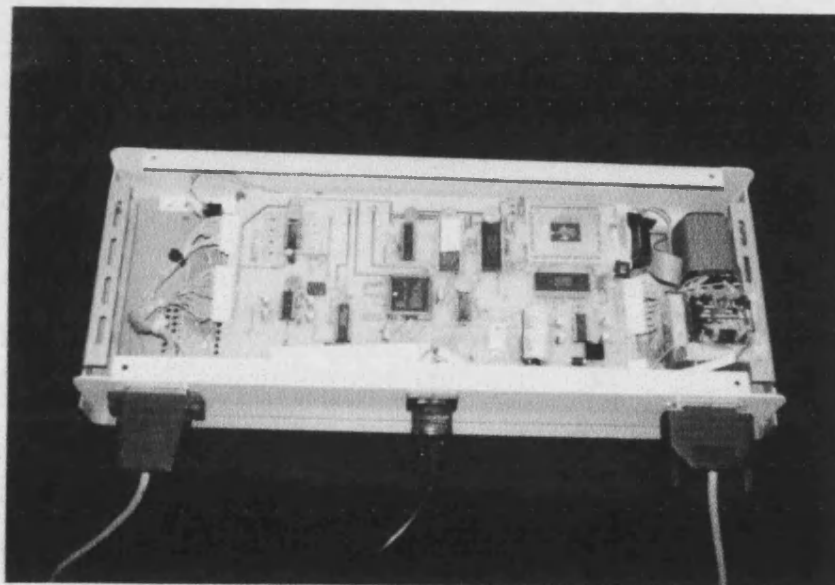


Fig. 3.27 A view inside balance aid main controller unit.

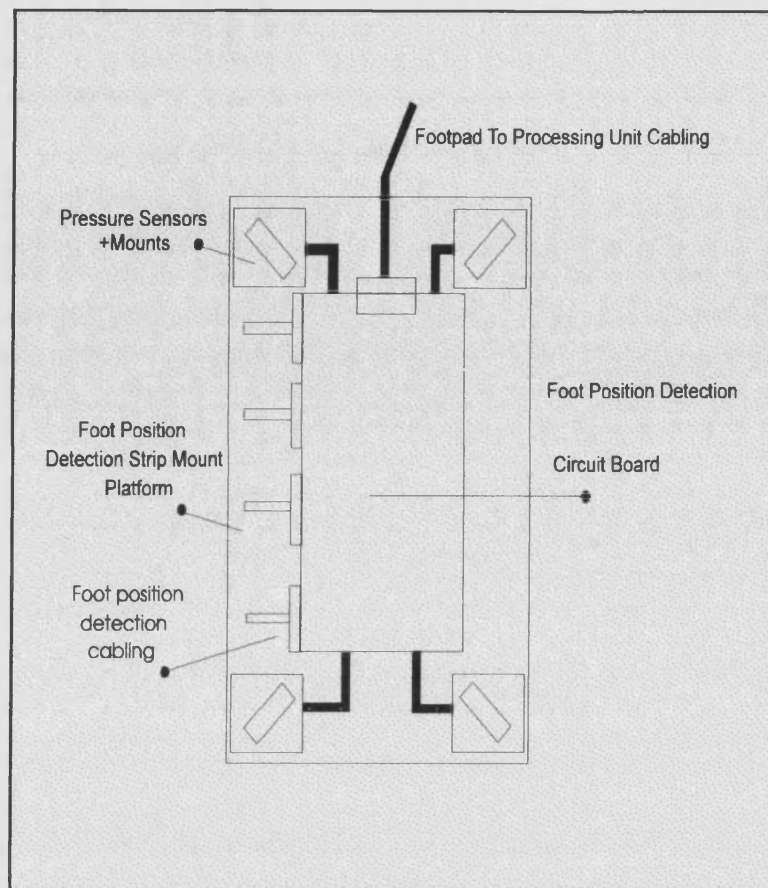


Fig. 3.28 Footpad internal layout, viewed from above.

Within each footpad, the pressure sensing circuitry and the foot position detection system circuitry are present on one, double sided PCB. In the footpads, as in the case of the main processing unit, all connections to the board are by PCB headers and cable shell assemblies. All modules are intended for interior use and so are only splash resistant. Full atmospheric sealing has been avoided to reduce costs and facilitate repair. The main interconnections, comprised of multi-strand screened data cable, between the processing unit and the footpads are used to carry the interrogation commands and data between these units. At either end, the data cables are attached to the modules by locking D-type connectors with strain relief. This provides a rugged method of interconnection, though still allows for easy dismantling, ensuring the portability of the system. Fig. 3.29 shows the balance aid in use in the laboratory.

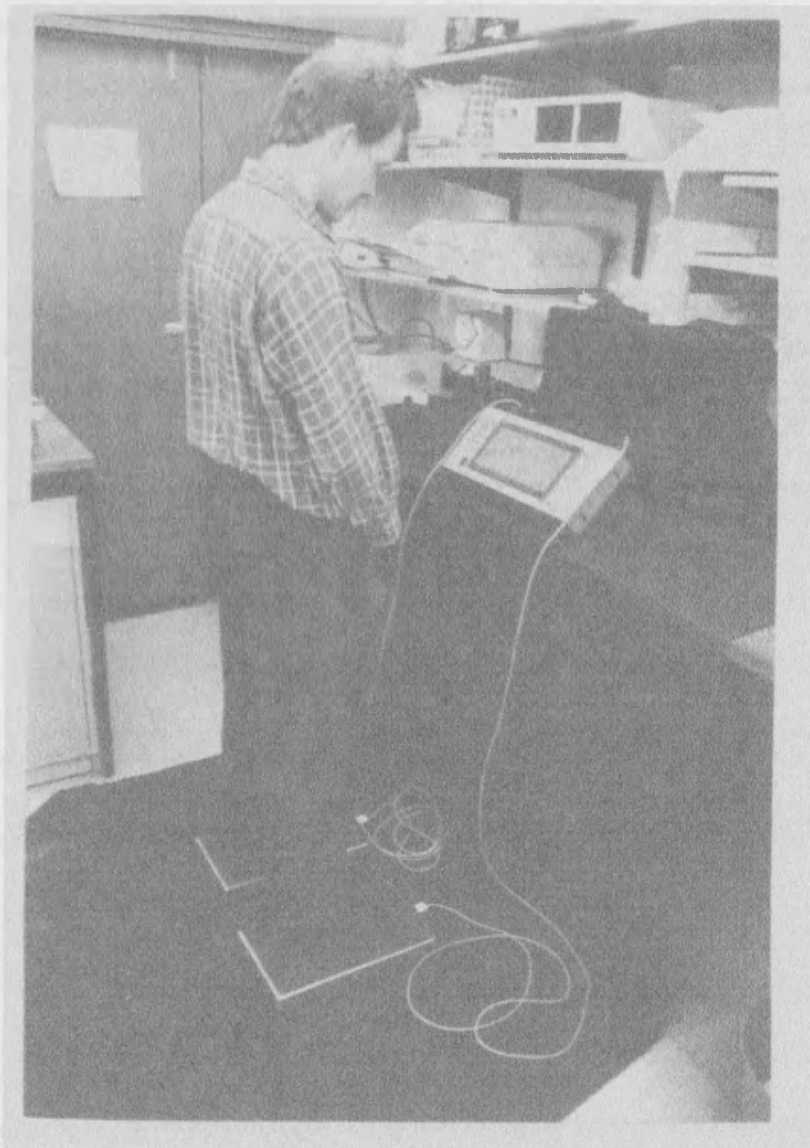


Fig. 3.29 Balance aid in use in the laboratory.

### **3.9 Balance aid testing.**

Initial testing of the balance aid involved applying forces to each of the footpads and observing the amount of deflection of the on-screen cross in response to different force combinations. The first set of tests show the response of the centre of balance indicating cross to lateral force differences. In these tests, the force combinations are applied centrally to each footpad and the horizontal deflection of the on-screen cross noted. In each case the direction of the cross deflection is marked. Subsequent to the lateral testing, a set of tests were performed to determine the effectiveness of the front to back weight distribution indication. In these tests,

### CHAPTER 3 THE BALANCE RE-TRAINING AID

equal forces were applied to the front of each footpad and to the rear of each footpad. In this case the front to back deflection of the on-screen cross was noted. The lateral deflection of the cross in response to the various applied forces is shown in fig. 3.30. The front / rear cross deflection in response to the various applied forces is shown in fig. 3.31. Once again, the direction of the cross deflection is marked on the table.

Equivalent mass applied (kg)		Deflection (mm)	Equivalent mass applied (kg)		Deflection (mm)
Left pad	Right pad	skill level 1	Left pad	Right pad	skill level 3
10	10	1 RT	10	10	1 RT
20	20	1 RT	20	20	1 RT
30	30	1 RT	30	30	1 RT
40	40	1 RT	40	40	1 RT
50	50	1 RT	50	50	1 RT
10	50	26 RT	10	50	55 RT
20	50	16 RT	20	50	43 RT
30	50	6 RT	30	50	24 RT
20	30	3 RT	20	30	18 RT
50	10	24 LT	50	10	55 LT
50	20	14 LT	50	20	41 LT
50	30	5 LT	50	30	22 LT
30	20	4 LT	30	20	17 LT
Left pad	Right pad	skill level 2	Left pad	Right pad	skill level 4
10	10	1 RT	10	10	20 RT
20	20	1 RT	20	20	20 RT
30	30	1 RT	30	30	20 RT
40	40	1 RT	40	40	20 RT
50	50	1 RT	50	50	10 RT
10	50	45 RT	10	50	55 RT
20	50	29 RT	20	50	50 RT
30	50	6 RT	30	50	35 RT
20	30	10 RT	20	30	30 RT
50	10	43 LT	50	10	55 LT
50	20	27 LT	50	20	48 LT
50	30	5 LT	50	30	33 LT
30	20	9 LT	30	20	28 LT
Left pad	Right pad	skill level 5			
10	10	3 RT			
20	20	3 RT			
30	30	3 RT			
40	40	3 RT			
50	50	3 RT			
10	50	55 RT			
20	50	55 RT			
30	50	50 RT			
20	30	45 RT			
50	10	55 LT			
50	20	55 LT			
50	30	48 LT			
30	20	44 LT			

Fig. 3. 30 Lateral weight distribution results.

**CHAPTER 3 THE BALANCE RE-TRAINING AID**

Equivalent mass applied (kg)		Deflection (mm)
Front	Back	skill level 1
20	20	0
30	15	10 F
30	10	15 F
15	25	10 R
10	30	15 R
Front	Back	skill level 2
20	20	0
25	15	10 F
30	15	25 R
15	25	10 R
15	30	25 R
Front	Back	skill level 3
20	20	0
25	20	10 F
30	20	20 F
15	25	15 R
15	30	25 R
Front	Back	skill level 4
20	20	0
25	15	15 F
30	15	35 F
20	25	20 R
15	30	35 R
Front	Back	skill level 5
20	20	0
20	15	20 F
25	15	40 F
15	20	25 R
15	25	40 R

Fig. 3. 31 Front / rear cross deflection.

It is possible to generate much larger lateral weight differences than front to rear weight differences as an excessive front to rear weight difference results in the lifting of a toe or heel



### **CHAPTER 3 THE BALANCE RE-TRAINING AID**

from the pad. This is flagged as an error and the user is returned to a setup screen to correctly place their feet. For this reason the greatest front to rear weight differences shown in fig. 3.30 are less than the corresponding lateral weight differences shown in fig. 3.31. Fig. 3.32 and fig. 3.33 show the balance aid screen displays during balance re-training sessions. Fig. 3.32 shows a screen display during a static balance training session and fig. 3.33 shows a screen display during a dynamic balance training session.

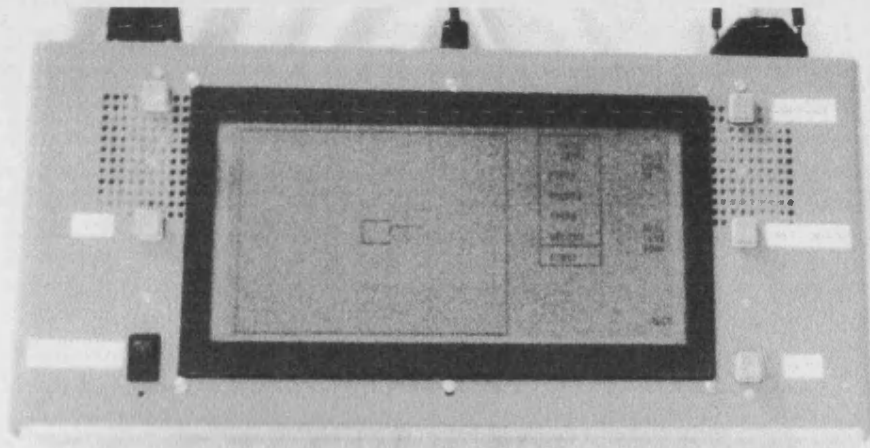


Fig. 3.32 Screen display during static balance training.

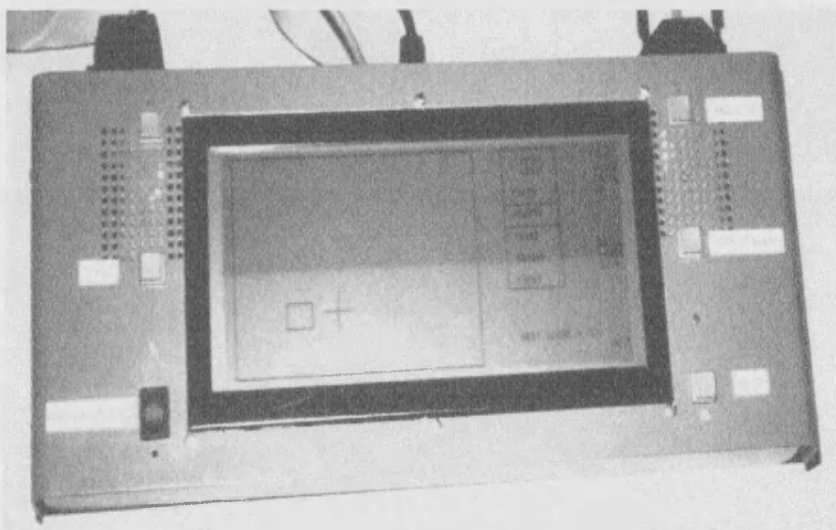


Fig. 3.33 Screen display during dynamic balance training.

## **CHAPTER 3 THE BALANCE RE-TRAINING AID**

---

### **3.10 Discussion.**

The balance aid has been developed to assist in the rehabilitation of stroke patients. This balance re-trainer is intended for use by patients that have very recently suffered a stroke and require to regain the skills of static and dynamic balance. This is an important first stage in the rehabilitation which may later require the use of a stimulator or mechanical prosthesis.

The unit is compact, lightweight and robust, so may be easily transported and used by the patient at home. Assembly of the unit is extremely simple, requiring no tools and no specialised knowledge. The unit is very simple to use and requires no additional literature as all instruction in its use is delivered to the user via the screen as required. This feature is especially important as the user may be easily confused following the stroke.

The balance re-training system is mains powered, though may be run from internal batteries for up to three hours between charges. This allows the user extra convenience in the usage of the unit, which may be placed in the optimum location for use within the home.

The novel, optical pressure sensor design permits the user's centre of balance to be ascertained with minimal platform movement. This is extremely important as it allows patients to use the balance aid without excessive platform movement causing further damage to their confidence.

The balance aid software runs direct from power-up instructing the user in its operation. Test routines are available to confirm that the unit is operating correctly. The position of the user's feet is monitored to ensure correct mounting of the footpads and to indicate when the feet are central to the footpads. The option of a static or dynamic balance training session is then offered. Within the static balance training routine the screen provides a visual indication of both the actual and ideal locations of the centre of balance of the user. The user then attempts to align these two centres of balance. This alignment indicates true balance to the user whilst preventing him from using external fixed points for visual feedback. The dynamic balance training routine causes the on-screen box to move about whilst the user attempts to maintain the alignment of the cross and box. Within the dynamic training routine, the percentage of time that the cross is maintained within the box is used to provide a 'score'. This provides progress feedback to the patient. These scores are stored in battery backed memory to provide the user and their physiotherapist with a session by session indication of training progress. It is considered that the association of the changing balance with a visual indication of the degree of balance change, begins the process of recruiting brain areas adjacent to those damaged by the stroke to perform the balance recognition functions.



### **CHAPTER 3 THE BALANCE RE-TRAINING AID**

---

The skill levels incorporated within the balance aid software permit patients to re-train at a convenient rate. This is an important feature as it allows the patient to control the degree of difficulty experienced and not feel dismayed at a lack of progress, or bored with too simple a challenge.

All of the above features allow unlimited re-training time by the patient at a time and a rate suited to that individual.

This provides an improvement upon the training time available with current physiotherapy, whether or not this is carried out with the aid of hospital based equipment. The current training time experienced by the patient is only during hospital appointments and therefore comprises only a small percentage of the total available training time. The presence of the training aid within their own home, permits use of the aid at any time convenient to the patient, greatly increasing the available re-training time. The convenience of having the re-training aid within their home, removes the stress imposed upon the patient by having to travel to hospital appointments for all of their treatment. The balance re-training undertaken by the patients also becomes more effective when travelling to a training session is no longer required. It has been observed that such travel has a pronounced tiring effect upon the patients, so it is expected that the removal of the need for such exertion prior to the training will produce a more efficient training session.

The system is easily upgradeable to permit new tasks to be implemented within the training regime as the patient recovery progresses. This should benefit the patient by maintaining a stimulating training environment.

The balance aid shows how rehabilitation equipment can be developed in such a manner as to provide the patient with unlimited access to the required training at their own convenience. This equipment provides the opportunity to provide a maximum patient re-training intensity whilst using minimal physiotherapy resources. It is suggested that the ability to provide patients with constant access to re-training facilities such as the balance aid will significantly reduce their time to recovery.

# **CHAPTER 4.**

## **The Intelligent Muscle Stimulator.**

### **4. 1 Introduction to the intelligent muscle stimulator.**

This chapter details the development of an intelligent stimulator that is able to analyse incoming data, make decisions regarding that data and synthesise output pulse trains in accordance with that data. In this way, it is suggested that the stimulator will be able to modify its output pulse-train parameters to maintain the required stimulation as the parameters associated with the patient change over time. It is also suggested that a self modifying stimulator will also be able to begin with a standard stimulation setting and modify the output pulse trains to suit the particular patient, reducing the required set-up time.

FES has been used, with varying degrees of success, for many years to correct lower limb movement deficiencies [10,11,12]. FES has been considered a viable option for rehabilitation since the 1960s, when Liberson et al. synchronised dorsiflexor stimulation with the gait cycle [14] and the scale of integration of electronic components allowed portable stimulators such as those by Halleck [233] and Hertzler and Kaminski [234] to be constructed. This research progressed throughout the 1970s when the advent of computers led to the introduction of more sophisticated stimulators [73,235,263], including programmable stimulation units [236].

Current stimulation systems in use in hospital departments are compact and portable [89] but extremely simple in operation, resulting in a very limited range of applications. Those in use for foot drop correction typically employ a force sensitive resistor (FSR) [89] or other switch [95,235,237,238,239], such as an air pressure switch [73] under the heel or ball of the foot. This detects foot lift and/or placement, sending a train of voltage or current pulses to the dorsiflexors or plantarflexors. The frequency and magnitude of the pulse train is generally adjustable to suit individual patients but fixed whilst in use. This mode of operation leads to the use of a fixed control strategy of the lower leg muscles, which cannot be modified whilst in use to compensate for physiological changes in the patient such as fatigue [126,127,145], temperature [143] and changes in the strength-duration relationships of the muscles due to exercise [139,163]. These

## **CHAPTER 4 INTELLIGENT STIMULATOR DESIGN**

---

parameter modifications are considered by Franken et al. [69] to be essential if the stimulation is to remain effective. Other factors, such as spasticity [167-171] and muscle strength [240], require unique stimulation parameters to be used for each patient. The recoveries noted in strength and spasticity with FES [12,177,178] are examples of the physiological changes for which a self adapting stimulator could provide compensation. These factors were discussed in detail in chapter 2.

One of the aims of the research described in this thesis was to design a stimulator that is able to receive patient gait data, interpret this data and synthesise a number of appropriate stimulation waveforms. Present stimulation systems apply fixed stimulation waveforms at the appropriate points of the gait cycle but are not able to alter this applied stimulation and require the fixed stimulation parameters to be carefully set. A stimulator that is able to interpret the patient gait data and synthesise appropriate stimulation waveforms, including specialised waveforms such as those claimed to reduce the spastic reflex, permits dynamic adaptation of the stimulation parameters to suit the patient and is likely to reduce the necessary setup time for a stimulation system.

When developing a stimulator that is able to make decisions based on gait related feedback and alter its output pattern respectively, it was decided to design the stimulator with the ability to alter every parameter of the output pulse train between pre-set limits. The new stimulator design would be able to perform these modifications at any time to cater for unexpected changes in the observed feedback data, for instance when a change of gradient is encountered or the patient begins to fatigue and allow the stimulator to synthesise any suggested stimulation envelope. This leads to a requirement to be able to synthesise a pulse train where each pulse may be independent of the previous or following pulse and is generated purely as a result of the decision making procedure. The requirement for this level of decision making ability suggests the use of a microprocessor or microcontroller-based system such as that used by Hoshimiya et al. [232]. Such a system permits the creation of software to implement the decision making procedure and effect the required gait correcting outputs.

### **4. 2 Prior FES research.**

#### **4. 2. 1 FES research.**

A considerable amount of research into FES for foot drop has been undertaken over the years, utilising single [95,101, 242, 243, 244], dual [245, 246] and multi-channel [109, 239, 241, 246, 247, 248, 249, 250] stimulation units. Multi-channel stimulation has been taken as far as 64

## **CHAPTER 4 INTELLIGENT STIMULATOR DESIGN**

---

channels by Handa et al. [109] and to 22 channels by Davis et al. in a device modified from an implantable hearing prosthesis [247]. Significantly, though, neither design incorporated the ability to perform self adjustment of any parameters. Multi-channel stimulation has arisen for a number of reasons although the multi-channel units have remained at the experimental stage for many years, due to the size and complexity of such devices [239] and also, in part, because of the sheer number of required electrodes [239,246]. Single channel units, though, are in everyday use in many hospitals and institutes around the world.

These systems utilise a simple heel switch to indicate the start of the stride and lift the toes of the affected limb by the application of voltage or current pulse trains. The stimulation systems developed to date utilise fixed pulse parameters during the stride and merely activate or deactivate the pulse train sequences. The parameters are pre-set during trials with the patient which it is suggested by Gracinin [244], should be of approximately one week duration and are not modified whilst the unit is active. The experimental multi-channel stimulators, such as the six channel programmable stimulator described by Brandell [237], are only manually programmable via switches on the unit and do not self-adjust or run a program that can in any way 'learn' from patient generated feedback.

Other methods of controlling stimulators include electromyogram (EMG) pattern recognition, respiration control and voice recognition. For example, Graupe and Kordylewski [250] postulate that upper body EMGs indicate a 'request' to move a lower limb and may be utilised to provide stimulator control. Their method relied on the patient to provide a 'punishment' input to the system to facilitate training of the neural network based controller. Consequently, this is not a totally automated system. Respiration control has been utilised by Hoshimiya et al. [241] to control the stimulation to the hand in tetraplegics, although it is not considered a valid method of control for foot drop. Voice recognition was attempted as a method of control by Handa et al. [109]. Control was achieved with some difficulty and not without the use of a PC plus plug in cards. It is considered that this solution to controlling a stimulator is best applied to those systems in use with tetraplegic patients.

### **4. 2. 2 Stimulation waveform parameters.**

The parameters of a pulse train are shown in fig. 4.1. These parameters may be summarised as: Pulse Width ( $t_p$ ), inter pulse interval time ( $t_s$ ), pulse magnitude (M), pulse rise time ( $t_r$ ) and pulse fall time ( $t_f$ ).

## CHAPTER 4 INTELLIGENT STIMULATOR DESIGN

Prior research into surface FES parameters has produced an outline requirement for the necessary stimulation parameters. The typical values of these parameters are generally agreed upon, though there has been much discussion into the usable limits of such ranges. Liberson et al. [14] used pulse lengths in the range  $20\mu\text{s}$  -  $250\mu\text{s}$  and pulse repetition rates of  $30\text{Hz}$  -  $100\text{Hz}$ .

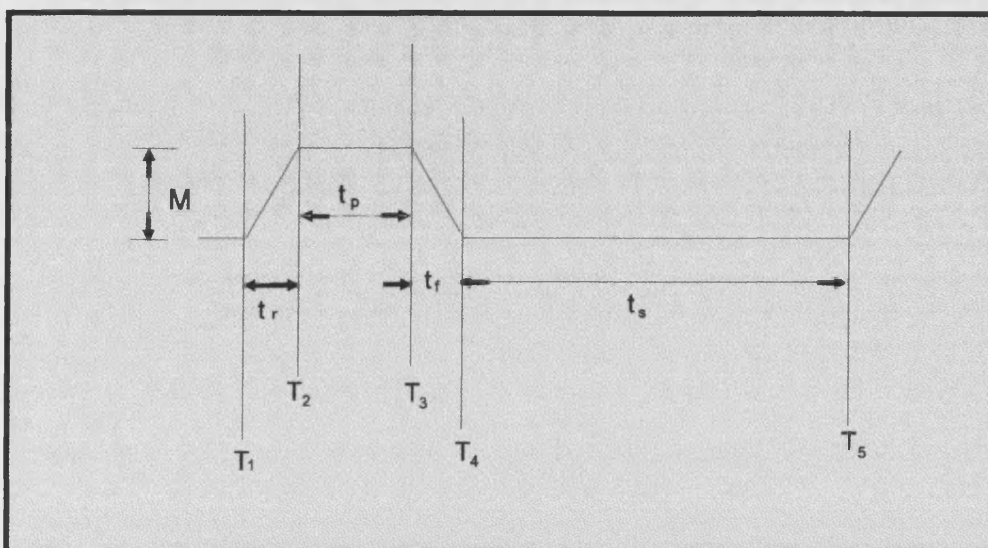


Fig. 4.1 Required pulse output waveform.

Malezic et al. [245] found the usable ranges for the pulse length to be  $50 - 500\mu\text{s}$ , with the pulse repetition frequencies in the range  $5 - 120 \text{ Hz}$ , although they stated that the mean frequency required by patients was  $30\text{Hz}$ . In a separate report, Malezic et al. [32] found that  $200\mu\text{s}$  pulse widths with pulse repetition rates of  $20\text{Hz}$  produced satisfactory results. The pulse repetition rate of  $20\text{Hz}$  is also suggested by Carroll et al [251] along with pulse widths of around  $150\mu\text{s}$ . Ranges approximating to those mentioned above have been found to be adequate for surface stimulation purposes by various authors [17,94,247, 252, 253, 254, 255]. Waters et al. [235] suggest that  $200\mu\text{s}$  pulse lengths and  $33\text{Hz}$  repetition rates are ideal values, whereas Handa et al [109] suggest that  $200\mu\text{s}$  pulses and  $20\text{Hz}$  repetition rates were found to produce the best results. A stimulator produced by Hertzler and Kaminski [234] operated over the pulse length range of  $50\mu\text{s}$  to  $80\text{ms}$ , with pulse repetition rates in the range  $0.1\text{Hz}$  to  $140\text{Hz}$ . Pulse lengths of  $200\mu\text{s}$  and a repetition rate of  $30\text{Hz}$  was successfully employed by Herbert and Bobechko [254] and Akazawa et al [248], re-enforcing the likely required nominal parameters of a general purpose muscle stimulator. Research into the isometric recruitment relationships of muscles by Durfee and Maclean [252] found that  $100\mu\text{s}$  pulses at a repetition rate of  $40\text{Hz}$  produced a useful torque / fatigue trade off. The digitally synthesised pulse trains of Hoshimiya et al. [241]

## **CHAPTER 4 INTELLIGENT STIMULATOR DESIGN**

---

employed a 200 $\mu$ s pulse width and 50Hz pulse repetition frequency for optimum results. Carroll et al. [251] state that peak torque was achieved by application of 150 $\mu$ s pulses with the pulse repetition frequency in the range 66Hz to 83Hz. This repetition frequency caused the mean torque to have dropped to 5% of the starting torque after thirty seconds stimulation, whilst a 50ms inter-pulse interval produced a drop to only 82% of initial torque after a similar length of time. It was also found by Carroll et al. [251] that pulse repetition frequencies of greater than 83Hz produced rapid high frequency fatigue. Therefore, it may be concluded that the pulse repetition frequency should not be greater than 66Hz, although it may be less than this value for lower torque and greater fatigue resistance.

The above discussion places the nominal pulse parameters at 200 $\mu$ s pulse width and 30ms inter-pulse interval, which produces a repetition rate of 30Hz. Koller et al. [256] found that this repetition rate did not cause any significant neural damage, though Agnew et al [255] found that constant stimulation at repetition rates of 50Hz and above caused irreversible demyelination and degeneration in cats. It should be noted that this was observed with epineural electrodes and there was some contention as to the mechanical effect of the presence of the electrodes.

Malezic et al. [17] successfully utilised pulse magnitudes in the range 20V to 80V, whilst Hertzler and Kaminski [234] found an upper magnitude limit of 67.5V to be adequate for surface stimulation. Bogataj et al [239] suggest the use of a slightly larger magnitude range of 0V - 120V which is further confirmed by Patterson et al. [93] who also suggest the use of 80mA - 120mA current pulse magnitudes, equivalent to the previous range when a 1k $\Omega$  body impedance is considered, and Takebe et al. [73] who produced a stimulator with a maximum pulse magnitude of 100V. Rohlicek [267] constructed a stimulator with a 2 $\mu$ sec rise time and fall time and Spencer [268] suggests that the ideal rise and fall time is in the range 5 $\mu$ sec to 10 $\mu$ sec.

### **4. 2. 3 Chosen stimulator pulse train parameters.**

The above stated value for both rise-time and fall-time parameters, equivalent to 1% of the nominal pulse length value, presents a fast rise-time and fall-time in comparison to the pulse length. This value was adopted as a minimum transition time value for use in the intelligent stimulator. The maximum value is set at the value of the expected nominal pulse width of 200 $\mu$ s. This range of rise and fall rates permits the effect of both slow-edged and fast-edged pulse trains to be compared. The nominal rise and fall rate is set to the minimum value as initial research will progress along the lines of previous work, using fast edged pulse trains.

## **CHAPTER 4 INTELLIGENT STIMULATOR DESIGN**

The variability of the pulse output parameters has been chosen to be about a nominal point, chosen through experience gained in prior research on the subject. The chosen nominal values for the pulse train output of the intelligent stimulator, along with the required variation ranges, are as follows:-

Pulse Magnitude	nominal 60V	min 20V max 150V
Pulse Length	nominal 200 $\mu$ s	min 100 $\mu$ s max 400 $\mu$ s
Pulse Frequency	nominal 30Hz	min 10Hz max 50Hz
Pulse Rise Time	nominal 2 $\mu$ s	min 2 $\mu$ s max 200 $\mu$ s.
Pulse Fall Time	nominal 2 $\mu$ s	min 2 $\mu$ s max 200 $\mu$ s.

### **4. 2. 4 Alternative stimulation patterns.**

Pulse trains with the parameters described in section 4.2.2 and shown in fig. 4.1 have been demonstrated by the various authors to be sufficient to provide the required muscle contraction. It has been suggested, though, that there may be stimulation strategies that will produce significantly better results than the application of repeated pulse trains with time invariant parameters.

It has been observed as long ago as 1948 by Denslow [259] that double discharges of single motor units, the muscle fibres innervated by a single motor neurone, often occur. These double discharges, or doublets, are characterised by a very short inter-spike interval which places the second activity spike within the refractory period following the initial activity spike [260]. Several authors including Partanen [261] and Roth [262] have suggested that this is due to abnormalities or malfunctions within the nervous system, though Bawa and Calancie [260] have observed voluntary control of doublet production in humans and strongly suggest that doublet production is a normal phenomenon.

A number of investigations have been undertaken into the stimulation of muscle using waveforms incorporating short inter-pulse intervals. Sandercock and Heckman [263] observed that the addition of doublets to trains of constant pulses produced a greater muscle output force

## **CHAPTER 4 INTELLIGENT STIMULATOR DESIGN**

than was the case when the stimulation pulse train did not contain doublets. They also noted [263] a greater rate of rise of muscle output force when doublets are included in the stimulation waveform. Sandercock and Heckman suggest that a value of 10ms for the short inter-pulse interval for doublets produced optimum results. This value is substantially agreed with by Eken and Gundersen [264] who suggest an inter-pulse interval of 5ms - 10ms and further confirmed by the observations of Bawa and Calancie [260].

This stimulation technique has been expanded upon by Karu et al. [265] by the use of N-let pulse trains where N varies from 1-6. They found the optimum value of N to be 2, i.e. the use of doublets, with an inter pulse period of 5ms and also suggest that the use of N-let pulse trains may alleviate many of the fast fatigue problems associated with FES.

An alternative method of fatigue reduction in FES has been proposed by Binder-Macleod and Barker [266]. They proposed the use of a variable frequency pulse train that begins with a high frequency and then reduces to a lower frequency to utilise a 'catchlike', or frequency threshold, property of skeletal muscle. Fatigue is dependant on the frequency of the applied stimulation and the number of applied pulses [267] and it has been noted that a given level of contraction may be sustained by a lower frequency than was required to initiate the contraction [268]. Binder-Macleod and Barker [266] observed a marked fatigue resistance when using a variable frequency pulse train commencing at 80Hz, then reducing quickly to 40Hz and then 20Hz, without loss of contractile force. This stimulation pattern is similar to the motor unit firing patterns observed by Bawa and Calancie where doublets increase the initial muscle activity frequency.

Stimulation amplitude modulation has been shown by Alfieri [177] to be useful in overcoming the hyperactive stretch reflexes associated with spasticity. It was found that using trains of pulses increasing exponentially in amplitude was successful in reducing the stretch reflex often elicited with constant amplitude pulse trains.

### **4. 2. 5 Stimulation pulse types.**

Monophasic stimulation requires the generation of unipolar pulses only and this is by far the simplest method of stimulation pulse train production. The currents associated with monophasic stimulation are unidirectional hence the charge is always injected into the tissue at a single electrode and not recovered by a following pulse of opposite polarity. This type of waveform, with the most unrecoverable charge, is most likely to cause tissue damage by ion transport [126, 269]. Biphasic waveforms, consisting of stimulation pulses followed by



## CHAPTER 4 INTELLIGENT STIMULATOR DESIGN

opposite polarity pulses, have been suggested by a number of authors as a safer method of stimulation because of the charge-balanced property of the waveform [126,269,270]. Rohlicek [257] states that capacitive coupling of the pulse train to the body to remove any d.c. component is not a suitable method of charge recovery and suggests that the use of alternating pulse polarities within the pulse train produces the best compensation for the ion transport of unipolar pulses. McCreery et al. [270] suggest that a further improvement on this system of alternating pulses is to replace the single pulses of the unipolar system with a positive pulse immediately followed by a negative pulse injecting an equal amount of charge with negligible inter-pulse delay.

Nilsson et al. [271] suggest that the immediate following opposite polarity pulse detailed by McCreery et al. [270] may follow the initial pulse at any time within the refractory period of the nerve under stimulation and in fact they achieved good results with a 200 $\mu$ sec delay between the positive and negative pulses. Nilsson et al. [271] and Spencer [258] detail the EMG stimulus artifact reduction observed when using a biphasic stimulation waveform. Fig. 4.2 shows the variety of possible stimulation pulses and the associated tissue damaging properties of each as ranked by Campbell et al. [126], where a greater number of marks represents a lower level of likely tissue damage.

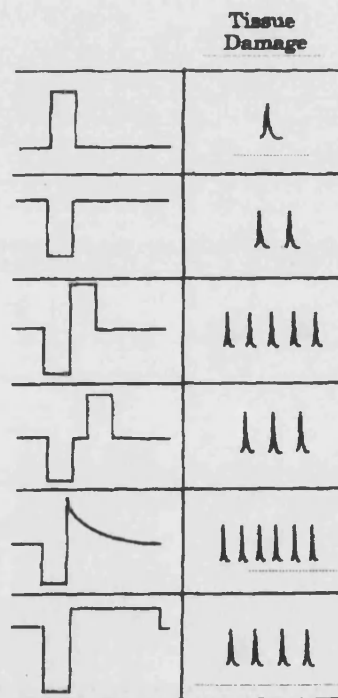


Fig. 4.2 Monophasic and biphasic pulse waveforms [126].

## CHAPTER 4 INTELLIGENT STIMULATOR DESIGN

### 4.2.6 Electrode - skin connection.

When designing FES systems, it is important to consider the load presented to the system by the body. Research by Stephens [272] found skin impedance to vary with applied waveform frequency. Stephens found that the skin impedance to surface electrodes could be modelled by a  $4\text{k}\Omega$  resistance shunted by a  $0.28\mu\text{F}$  constant capacitance. Mizrahi [273] found the resistive value to be  $500\Omega$ . Other authors [241, 274, 275] have utilised a  $1\text{k}\Omega$  resistance in parallel with a  $0.1\mu\text{F}$  capacitance as an approximation to the load presented by the human body. This assumes the use of surface electrodes in conjunction with a conductive gel to ensure a low impedance electrode-skin contact. It must be noted that the above values are considered to be typical values only and that variations will occur between individuals.

The electrode sites have been discussed in chapter 2, though electrode size is equally important. Alon et al. [276] found that the voltage required to produce a given strength of contraction reduced with increased electrode size, though the required current was increased. These researchers also found that the feeling of comfort was improved for any given contractile force as the electrode size was increased. It is obvious that the required accuracy of the electrode placement prevents the use of any size of electrode, so the size of electrode used is likely to be a compromise between stimulation site size and patient comfort. Bogotaj et al. [239] used a variety of electrode sizes for FES, including  $2.5\text{cm}$  electrodes for peroneal stimulation.

The cathode in each case should be placed over the nerve and the anode over the belly of the muscle [162]. The current from the anode will only reverse the neurone potential and cause an action potential when the injected current leaves the nerve which is under the cathode as shown in fig. 4.3.

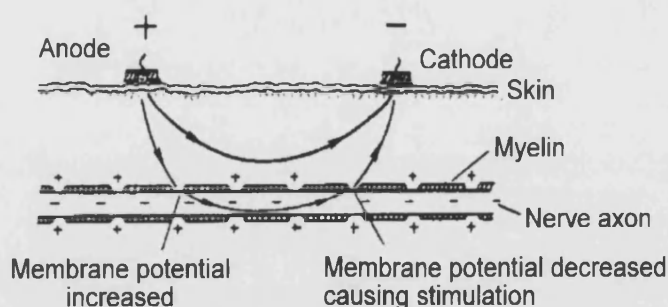


Fig. 4.3 Current path between surface electrodes [162].

---

## **CHAPTER 4 INTELLIGENT STIMULATOR DESIGN**

---

It should be noted that surface stimulation always requires the injection of more charge than the use of implanted electrodes [162]. This is due to the dispersion of the current in surface stimulation via the many possible pathways that it can take through the tissue. In this case only a small proportion of the current passes through the nerve, whereas in implanted systems the electrodes are placed in close proximity to the nerves and most of the supplied current passes into the nerve.

Each output channel must connect to the patient by a form of galvanic isolation, such as a transformer, to ensure that inter-channel currents cannot be induced, as currents as low as 20mA passing through the chest can cause ventricular fibrillation [277].

### **4. 2. 7 Deficiencies of existing stimulation systems.**

There are a number of deficiencies within existing stimulation systems, that it is considered may be overcome by the use of an intelligent stimulator of the type detailed in this PhD thesis. These deficiencies may be stated as follows:-

- The production of fixed pre-set stimulation envelopes.
- No ability to dynamically adjust the output waveform parameters to cater for physiological changes in the patient.
- No ability to perform an automatic stimulation parameter set-up procedure.
- No ability to interpret detailed gait data and make decisions based upon that data.
- No provision for easily expanding the stimulation system to  $n$  channels for instances where the control of further muscle groups is required.
- No ability to alter every parameter of the stimulation waveform to synthesise the outputs required by unique stimulation strategies.

### **4. 2. 8 Methods of overcoming existing stimulator deficiencies.**

Under-foot pressure sensing may be used as a method of supplying more information to the intelligent stimulator than is effected by the use of gait event detection switches.

Pressure sensing has been used by Malezic et al. [245] to produce objective measurements in gait improvement with some success, although this has not been applied as a source of detailed feedback to the stimulation unit. Pressure sensing shoes have been extensively utilised by Kirkwood [278] to provide a quantitative analysis of patient gait. Kljajic and Krajnik [279] developed a pressure sensing shoe utilising 9 steel strain gauges. The shoes were not found to

## **CHAPTER 4 INTELLIGENT STIMULATOR DESIGN**

significantly alter the pressure pattern of the foot, though problems were encountered due to twisting motion if excessive spasticity was present and due to the bulk presented by the strain gauges.

The use of such feedback rather than single gait events would produce a clearer picture of the required and actual gait and may permit a smoother, more natural gait to be effected, if this feedback is interpreted by the intelligent stimulator.

There are no instances of the use of the pressure distribution under the foot of both the affected and unaffected side being used to control a stimulation system. It is considered that this can provide a solution to the problem of controlling a stimulator. Control could be exerted by modifying the stimulator outputs to effect a match between the pressure distribution under the feet of the patient and a memory model of the pressure distribution expected under the feet of an unaffected person.

The effects of pulse repetition frequency, pulse magnitude and pulse length upon muscle contraction have been investigated in detail [106,241,247,248,249,251,252,253,254], although there is no evidence of research into the effects on muscle contraction of altering the individual pulse rise and fall rate. This may be significant, especially if there is a need to measure muscle group EMGs between pulses. It has been found by Whitlock [274] that these low level signals are easily swamped by the much larger voltage or current pulses associated with an FES procedure, especially by the fast discharge of the body capacitance at the trailing edge of the pulse. It is possible, therefore, that a fast leading edge and a slower trailing edge may lead to an improvement in measurement of the inter-pulse EMG.

The adjustment of the edges of individual pulses may also be used to control the amount of applied stimulation. Slow edged pulses with a greater d.c. component will produce less effective stimulation whilst faster edged pulses will produce a more effective stimulation and the modulation of this parameter may be useful in gradually applying the stimulation, especially where suppression of the hyperactive stretch reflex is required.

It is considered that the ability to alter every stimulation waveform parameter on a pulse-by-pulse basis will provide sufficient flexibility to enable unique stimulation strategies to be implemented. It is also considered that this ability provides the means by which to rapidly modify the applied stimulation in response to gait and physiological alterations during steady gait and when assessing the patient gait at the beginning of a walking session.

---

## **CHAPTER 4 INTELLIGENT STIMULATOR DESIGN**

---

The stimulators to date have always comprised a fixed number of channels and have not featured a modular design. The manual-only programming nature of these stimulators has required an individual set up for each channel, rather than each channel acting on parameter update instructions received from a decision making centre. This set up is then fixed until reset by manual means and does not alter as required by changes in the physiology or fatigue level of the patient.

It is considered that a bus structure such as that proposed by Brandell [237] could permit the co-ordinated use of a number of stimulation channels acting on different muscle groups. Such a stimulation system, with the associated ease with which it can be expanded, could prove invaluable in restoring co-ordinated movement to stroke patients.

### **4. 2. 9 Intelligent stimulator aims.**

One of the main aims of this research program was to design a stimulator with the following attributes:

- The ability to process analogue sensor feedback and use this to adapt generated pulse trains.
- The ability to generate pulse trains without waveform distortion into the impedance provided by the body to the surface electrodes.
- The ability to store data from sensors to provide a recent time history of patient gait.
- The ability to synthesise individual pulses within pulse trains.
- The ability to modify on a pulse by pulse basis every parameter of every pulse synthesised.
- A modular design permitting expansion to  $n$  channels.
- The galvanic isolation of every channel from the patient.
- The use of batteries as a power source.

To demonstrate the following:

- The ability of the stimulator to generate a variety of stimulation pulses and stimulation envelopes into the impedance provided by the body to the surface electrodes.
- To demonstrate the ankle joint movement produced by the stimulator.

## CHAPTER 4 INTELLIGENT STIMULATOR DESIGN

### 4.3 Initially considered stimulator configurations.

Three methods of achieving the above requirements were considered. The system diagram of one approach is shown in fig. 4.4. In this approach, a microcontroller is used to carry out any decision making and to synthesise an output consistent with that decision. This output is then used to control the generation of the pulse parameters. In this system, a switched mode converter generates the necessary power rails for the power amplifier, which produces an amplified version of a shaped reference pulse. The power rail of the amplifier is adjusted to a value slightly above that required for an undistorted output. This minimises the power dissipated within the output stage of the amplifier, by minimising the stand off voltage present across this section. Feedback taken from sensors attached to various parts of the body is fed into the stimulator system via continuously running A to D converters.

The complexity and likely size of this analogue system resulted in this possible stimulator configuration being rejected.

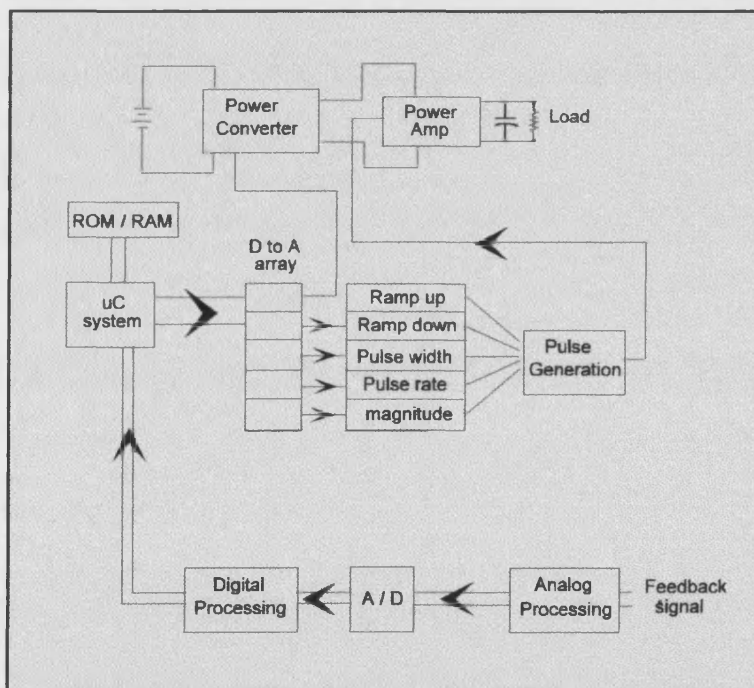


Fig. 4.4 An initially considered muscle stimulator system.

A second possible stimulator configuration is shown in fig. 4.5. This uses a pulse width modulation (PWM) controlled power amplifier in conjunction with a dynamic voltage clamp.

## CHAPTER 4 INTELLIGENT STIMULATOR DESIGN

In this configuration, a microprocessor section synthesises a reference pulse shape which is amplified using the switching amplifier. The fed-forward reference signal adjusts the clamp voltage to produce the required output. This smooths the switching amplifier output and removes overshoot and undershoot on the output waveform.

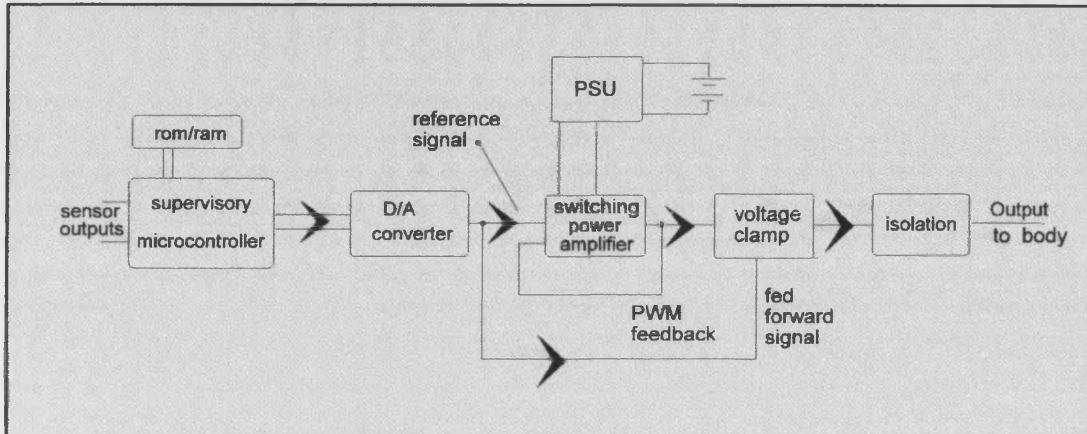


Fig. 4.5 Switching amplifier and voltage clamp arrangement.

This stimulator arrangement benefits from the increased efficiency inherent in switched mode operated systems. Unfortunately, the variable rise-time and fall-time requirement in the suggested range is not achievable with good linearity when using a switching amplifier. The power device turn-on and turn-off times prevent sufficient switching cycles to be performed to produce a good output representation of the reference pulse. For this reason the above stimulator configuration was rejected.

These two possible stimulator configurations were rejected in favour of a system utilising a digital pulse synthesis technique, linear power amplifier and a step-up isolation transformer. Digital pulse synthesis permits the generation of pulse trains with continuously varying parameters and the use of a low voltage amplifier plus step up transformer removes the need for high voltage power rail generation. This increases the efficiency and reduces the isolation requirements of the system as well as reducing the voltage requirements of many of the devices used in the system.

### 4. 4 Chosen stimulator system overview.

A system level diagram of the chosen stimulator design is shown in fig 4.6. The intelligent stimulator exhibits a modular form, permitting an expansion to  $n$  channels. The section inside the dotted line is duplicated for each additional channel.



## CHAPTER 4 INTELLIGENT STIMULATOR DESIGN

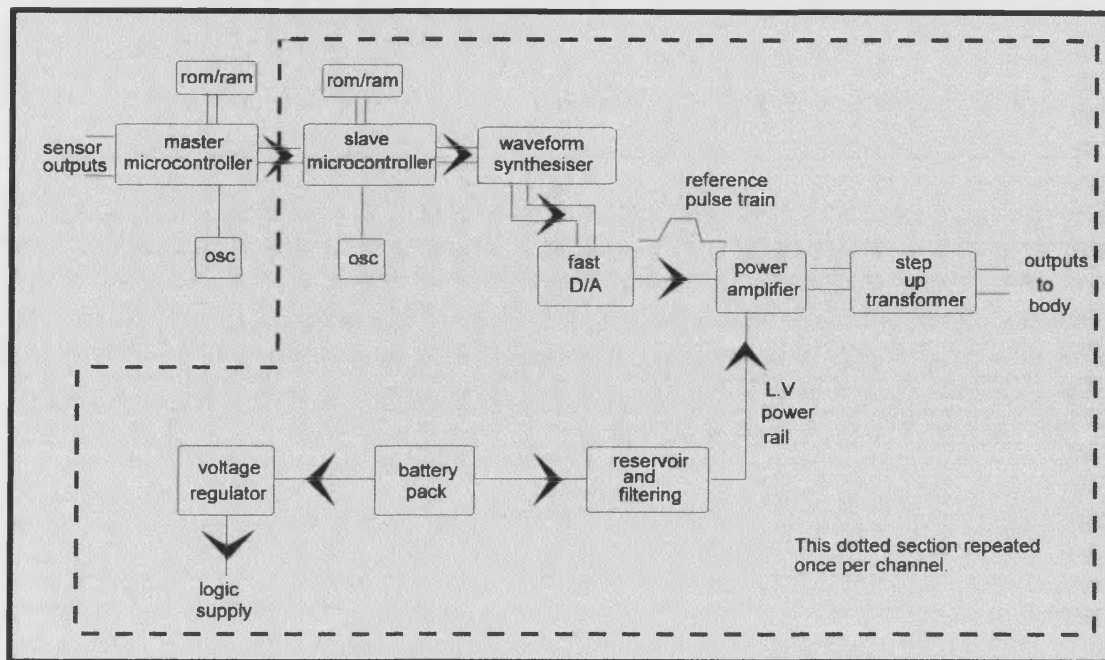


Fig. 4.6 Chosen stimulator system level diagram.

The master microcontroller receives data from the underfoot pressure sensing array described in chapter 5 and processes and interprets this data. An 8-bit bus is used to enable the master microcontroller to communicate with the attached slave modules. Pulse train parameter data is passed from the master to the slave microcontrollers to permit the slave microcontrollers to modify the reference pulse trains and hence the pulse trains output to the patient. A handshaking system is used in this data transfer to enable the slave microcontrollers to collect data made available on the data bus during the inter pulse interval, a time when these devices are not busy controlling the waveform synthesis. Data request and acknowledge signals permit data transfer at convenient times without the need to synchronise the cycles of the master and slave microcontrollers. Each channel is individually addressable from the data bus to allow any parameter value to be transferred to any channel, regardless of the number of channels connected to the data bus.

This stimulator configuration synthesises the output waveform digitally. This ensures total variability of the waveform under the control of the master microcontroller, keeping the stimulator as flexible as possible. A fast digital to analogue converter (DAC) is used to convert this digital representation of the output pulse train into an analogue waveform. This waveform is then used as the reference pulse train for the linear power amplifier. The power amplifier



## CHAPTER 4 INTELLIGENT STIMULATOR DESIGN

produces an amplified, current boosted version of the synthesised reference pulse train, which is then applied to the patient via a step up transformer. This transformer also acts as the galvanic isolation required on each channel, ensuring that currents are confined to flowing between the electrodes of one particular channel and may not 'leak' to other channel electrodes. The current leaving the positive side of the transformer secondary winding must return to the negative side of the same winding and does not flow to the negative side of any other channel secondary winding. This would be the case if no isolation transformers were used and the negative electrodes were all connected to a common ground. The use of isolation transformers is an important safety aspect of the design as it confines current flow to the stimulation site by ensuring that current flow occurs only between a specific pair of electrodes.

The slave microcontroller is used exclusively to control the stimulator reference waveform synthesiser and takes no part in the analysis of sensor data. The waveform synthesiser consists of counter-based digital logic that generates the digital reference waveform in the manner and at the instant specified by the slave microcontroller. This generation of the reference waveform occurs continuously and according to the flowchart of fig. 4.7.

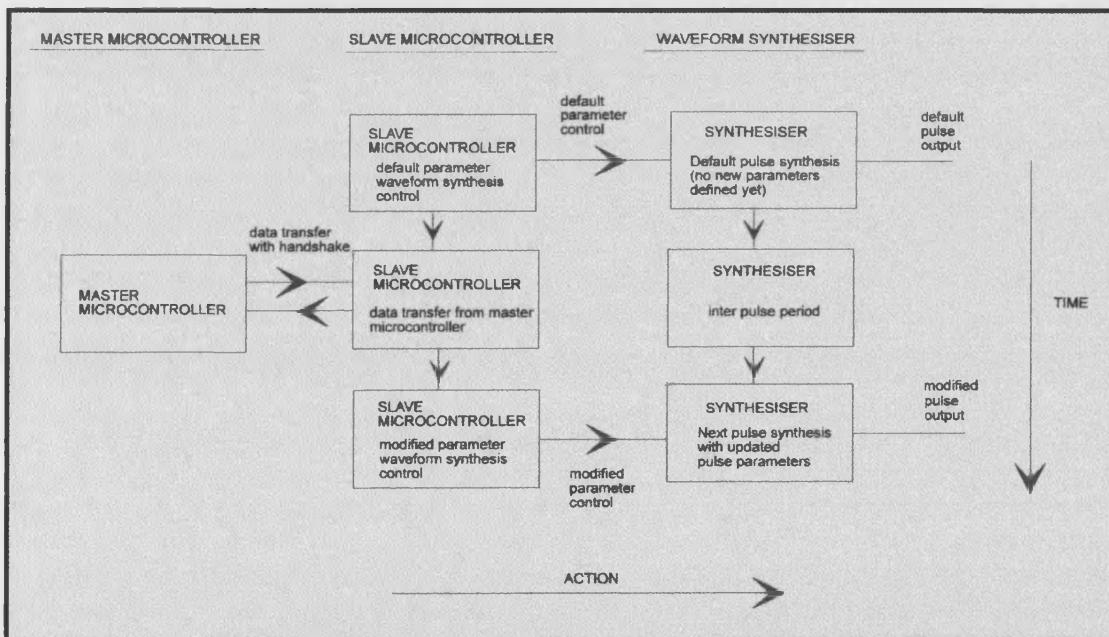


Fig. 4.7 Reference waveform generation.

It is necessary to use a waveform synthesiser in addition to the slave microcontroller in order to produce a high speed digital representation of the reference waveform. The slave microcontroller alone is not able to provide data at a rate consistent with the digital

---

## **CHAPTER 4 INTELLIGENT STIMULATOR DESIGN**

---

representation of a 2 $\mu$ s minimum rise and fall time. Instead, the slave microcontroller is used to receive parameter change data from the master microcontroller and to provide the necessary control over the waveform synthesiser.

### **4. 5 Reference pulse synthesis.**

#### **4. 5. 1 Pulse synthesis overview.**

Section 4.5 details the generation of the reference pulse train used as the input for the low voltage power amplifier. The synthesis circuit permits the generation of pulse trains under the control of the slave microcontroller. The slave microcontroller is provided with parameter updates, if required, during the inter pulse interval and uses this information to instruct the reference pulse train synthesiser to produce a modified reference pulse train. In this manner, the slave microcontroller is freed from the task of the pulse synthesis and permitted to receive the pulse parameter updates without delay when these are transmitted by the master microcontroller. This configuration also ensures that the parameters of a pulse do not depend on the respective parameters of the preceding pulse and ensures that any desired output pulse may be produced on any channel at any time.

#### **4. 5. 2 Digital pulse synthesis description.**

The circuit in fig. 4.8 performs the basic pulse generation function required for synthesising the reference pulse trains. The pulse edges are digitally generated by an 8-bit counter, counting up or down when clocked at regular intervals. The count direction is controlled by the slave microcontroller via the up / down control line. The magnitude of the pulse is set by the slave microcontroller applying the required magnitude value to one set of the comparator inputs. This value is latched at the moment a pulse edge is required as the change of value on the comparator input initiates a count. The output of the comparator is used to force the counter output up or down until the counter output is equal in magnitude to the demand value. The counter output, as well as being the circuit output, is fed back to the second set of comparator inputs so that when this equals the required magnitude, the count is halted. The trailing edge of a pulse is set by latching a magnitude value of zero which causes a count down to a zero value.

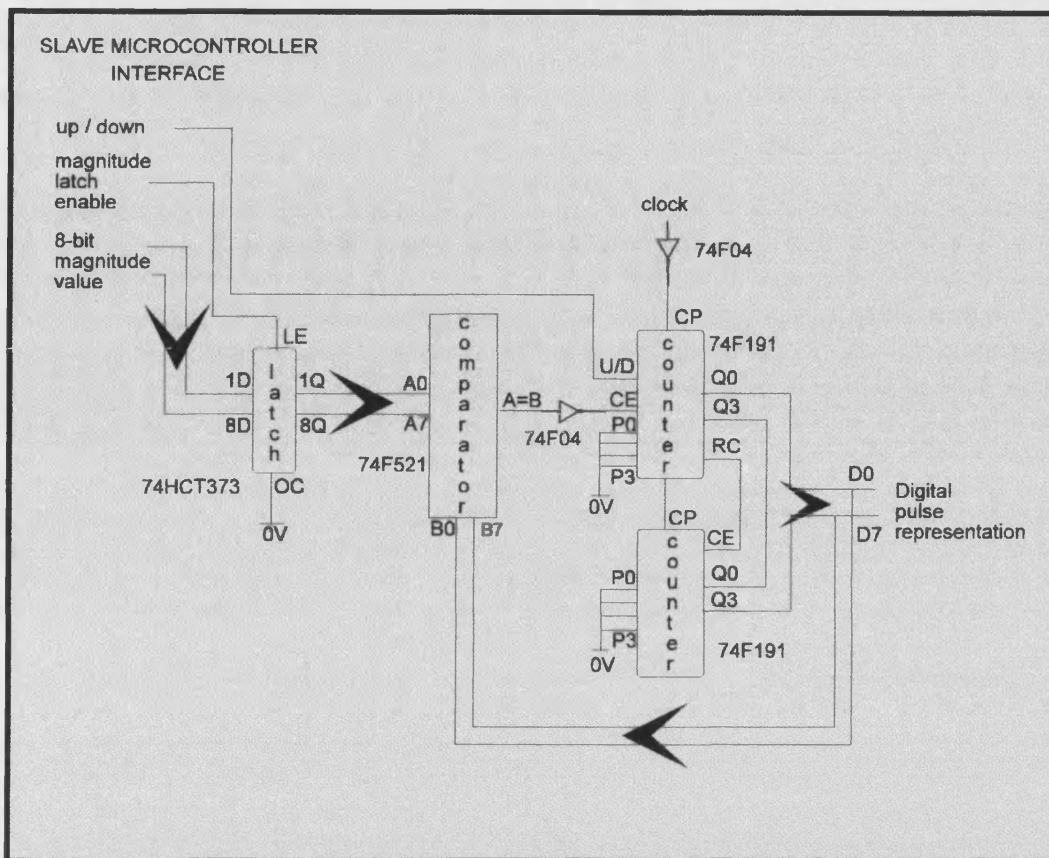


Fig. 4.8 Basic pulse synthesising counter circuit.

A 64 MHz TTL oscillator is used to generate the 8-bit counter clock. This is the fastest commonly available TTL oscillator and its use permits the greatest number of counts during the minimum specified pulse rise and fall times to be made. This permits the greatest pulse magnitude resolution to be obtained.

#### 4.5.3 Variable pulse edge generation.

If the pulse synthesiser counter is clocked at a constant rate, then the pulse edges will have a constant slope. Variation of the slope of these edges is achieved by the use of a programmable clock generator, shown in fig. 4.9.

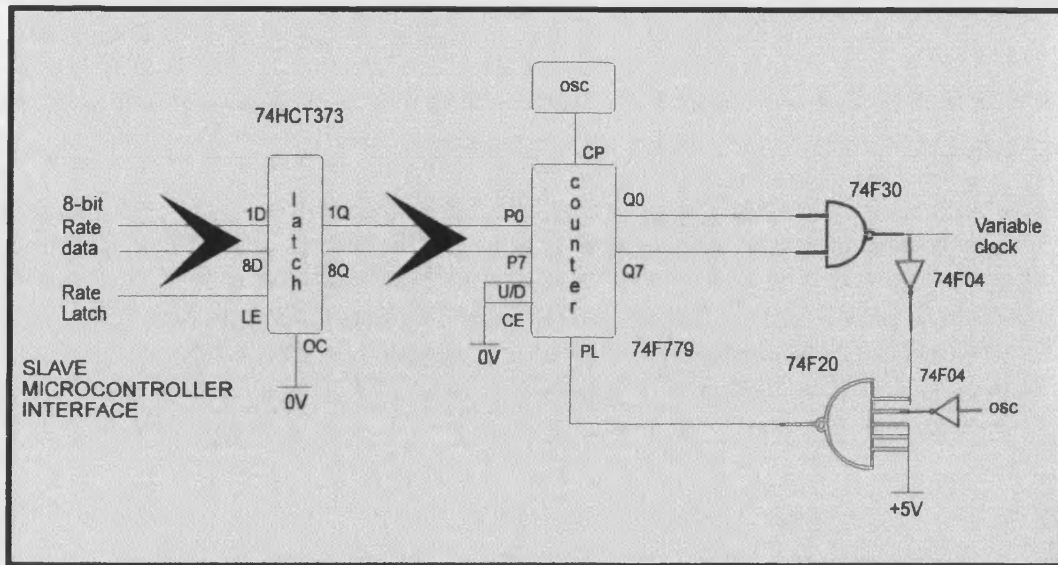


Fig. 4.9 Programmable clock generator circuit.

The programmable clock generator consists of a counter set to count up from a value placed on its inputs, when a 8-bit number from the slave microcontroller is latched to the counter inputs. Initially, the permanently enabled counter counts up from zero and upon reaching 255, sets the NAND gate output to zero. This NAND gate output is used as the active low variable clock to drive the pulse synthesiser counter. The extra inverters and NAND gate ensure that a parallel load only occurs upon the next negative transition of the clock. This prevents the counter outputs changing before the logic levels within the feedback loop have stabilised. A parallel load resets the variable clock output to a logic high, producing the rising edge needed to clock the main synthesiser counter. The parallel load of the latched rate number from the slave microcontroller is now used as the count starting point. The load of a new 8-bit number means that a different number of counts are now required to reach the value 255, at which point another parallel load occurs. In this way, the latching of different rate values produces a different time between successive clock rising edges. The lower the number loaded into the counter, the longer the period between clock edges and hence the lower the clock frequency. In this manner a free running clock is generated with a frequency that may be varied on the next count cycle by the load of a new rate value.

**4.5.4 The complete reference pulse train synthesiser.**

The complete, variable, analogue reference pulse train generator is formed by combining the digital pulse synthesiser with the programmable clock generator and adding a DAC. The

## CHAPTER 4 INTELLIGENT STIMULATOR DESIGN

complete pulse train synthesising circuit is shown in fig. 4.10. The system timing associated with this circuit is shown in fig. 4.11.

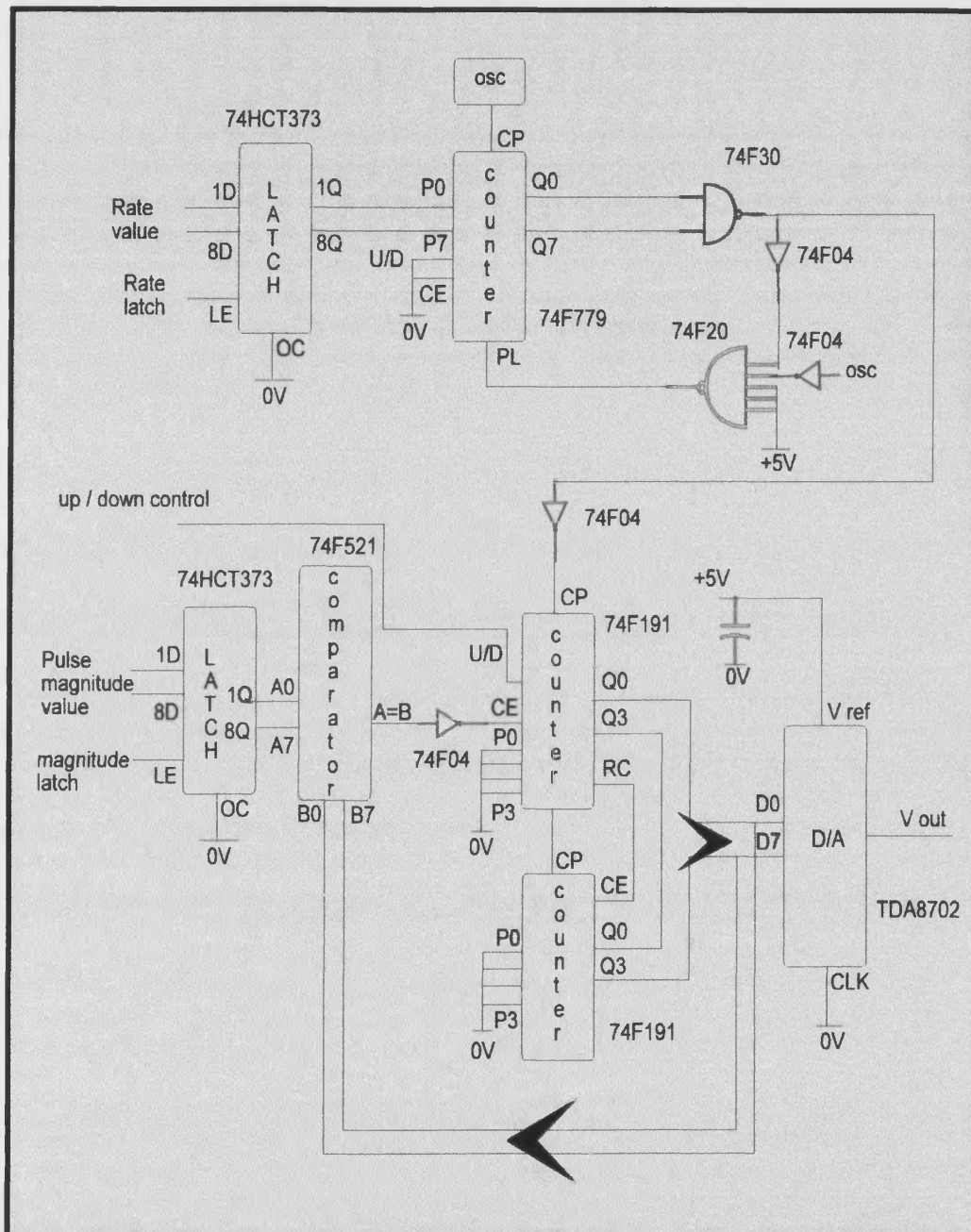


Fig. 4. 10 Pulse synthesiser circuit diagram.



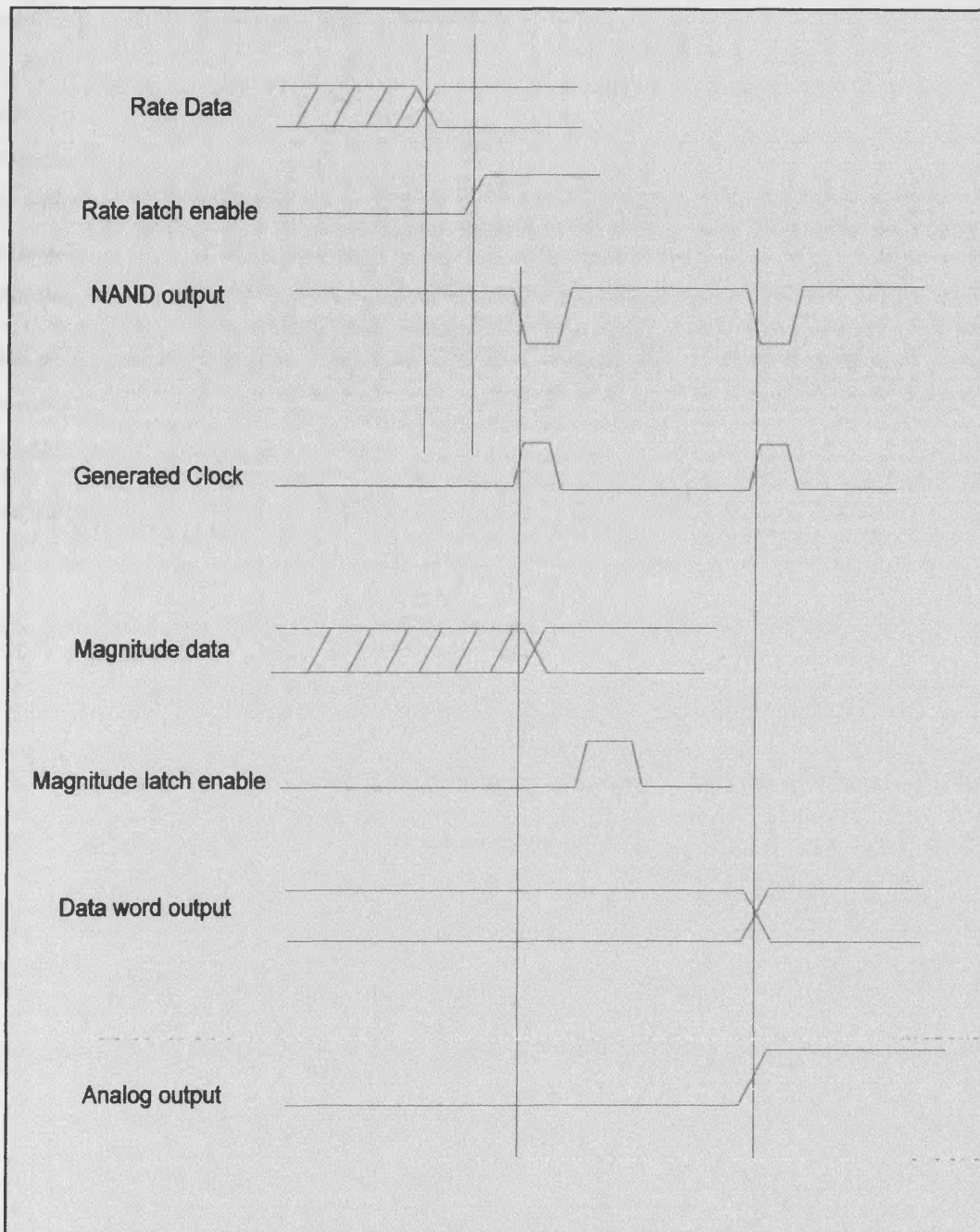


Fig. 4.11 Pulse synthesis timing diagram.

The TDA8702 8-bit DAC used in the project is intended for video applications and when clocked is capable of running at speeds of up to 30 MHz. This is far too slow for this circuit application so the device is used in the free running conversion mode. The full scale conversion time in this mode is quoted at 8ns, which is adequate to derive the fastest pulse edges. The DAC offers single ended or differential analogue outputs. To achieve the best common mode

## CHAPTER 4 INTELLIGENT STIMULATOR DESIGN

noise suppression, the outputs should be configured as a pair of differential outputs and subsequently converted to a single ended output. The single ended signal option is used in this case to remove the need for a differential to single ended conversion stage. The output pulse train requires to be offset by -15V to ensure that the power amplifier is fully turned off during the inter pulse interval and the gain requires to be set to produce reference pulses that will correspond to full scale output pulses of 150V magnitude. A full scale digital magnitude swing with the single ended output option results in a half power rail output swing of 2.5V.

The gain and offset functions may be implemented in a single stage. The single stage conversion requires a fast slew rate operational amplifier, hence the use of the OP42FZ. This ensures that the integrity of the pulse edges is not compromised during this conversion.

The output from the single stage conversion, shown in fig. 4.12, is given by:-

$$V_o = V_{in} \left( 1 + \frac{R_f}{R_g} \right) - V_{ref} \frac{R_f}{R_g} \quad (4.1)$$

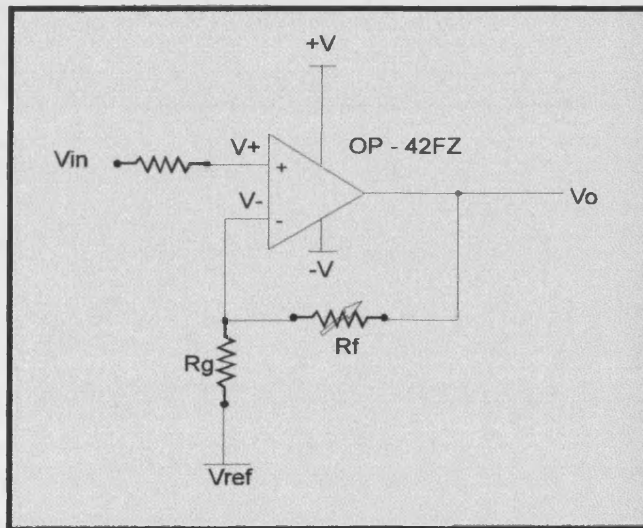


Fig. 4.12 Gain and offset circuit.

### 4. 5. 5 Logic incorporation into a PLD.

The pulse train synthesising circuit design was proved in discrete logic for master oscillator frequencies up to 20 MHz. Oscillator frequencies above this value required the use of either of the following options to guarantee glitch free operation:-

---

## **CHAPTER 4 INTELLIGENT STIMULATOR DESIGN**

---

- 1) The construction of a PCB with impedance matched tracks.
- 2) The incorporation of the discrete logic of the pulse train synthesiser into a programmable logic device (PLD).

The second option was adopted as this solution possesses the additional benefit of a considerable circuit size reduction.

The ispLSI1016 device, manufactured by Lattice Corporation, was the PLD chosen to replace all the discrete logic on the pulse synthesiser board. This device possesses 16 generic logic blocks, 36 input / output lines and may be clocked at frequencies up to 90 MHz, satisfying the requirements for the intended application.

The graphical user interface (GUI) of the programming software includes macros of many common logic circuits, permitting the pulse train synthesising circuit to be directly replicated within the PLD. Logic expressions may also be entered as Boolean expressions if desired. The ispLSI1016, is 'in-circuit' programmable via a seven pin on-board connector, removing the necessity of device removal between subsequent data downloads. Data is sent and verified as well as the device erased under software control, via a PC parallel port and port adapter cabling.

The enclosed section on the circuit diagram, shown in fig. 4.13, shows the discrete logic circuits incorporated in the PLD. The Lattice ispLSI1016 program listing is shown in appendix D.



## CHAPTER 4 INTELLIGENT STIMULATOR DESIGN

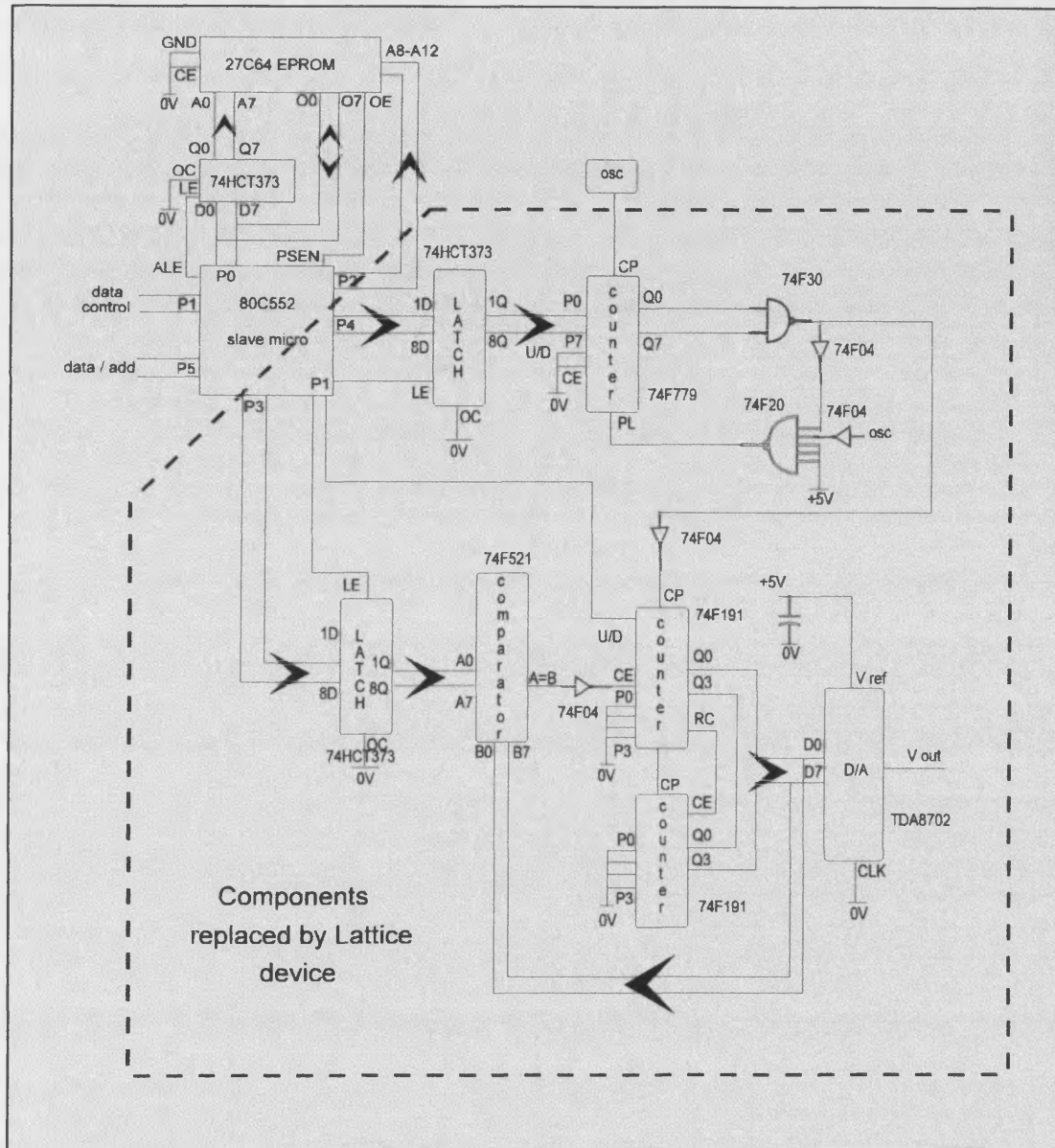


Fig. 4.13 Discrete logic replaced by the ispLSI1016 PLD.

---

## **CHAPTER 4 INTELLIGENT STIMULATOR DESIGN**

---

### **4. 6 Slave microcontroller software.**

#### **4. 6. 1 Requirement for master - slave operation.**

There are a number of reasons why a master - slave system configuration has been chosen for the intelligent stimulator. These are listed below and followed by a brief explanation of each statement.

- To permit a multi-tasking approach to be applied in the control software.
- To enable the easy alteration of the number of chosen stimulator channels.
- To reduce loading on the master microcontroller.
- To permit the decision making instructions to be executed at maximum speed whilst the stimulator outputs stimulation waveforms at a rate consistent with that of the gait cycle.

A multi-tasking approach permits a number of tasks to be undertaken simultaneously. In this case, these tasks are the acquisition of gait data, the interpretation of that data and the generation of the independent stimulation waveforms. The utilisation of the master and slave architecture permits a single master microcontroller to acquire and examine the gait data at the maximum possible rate, whilst the slave microcontroller is tasked with controlling the stimulation waveforms. These waveforms may then be generated at a rate consistent with the patient gait. The new stimulation parameters may be passed to the slave microcontroller when they are required by a handshaking data transfer that permits the two microcontroller cycles to interact.

This method of stimulator control also permits a simple upgrade to further channels by having a single master microcontroller and one slave microcontroller per channel, all of which may be communicated with by the single master microcontroller via a common bus.

The removal of the waveform synthesis functions from the master microcontroller software reduces the loading on this device and permits a number of channels to be added to the system without presenting any significant master microcontroller performance loss due to the extra loading this would otherwise generate.

## CHAPTER 4 INTELLIGENT STIMULATOR DESIGN

### 4.6.2 Slave software overview.

The slave microcontroller software is summarised in fig. 4.14.

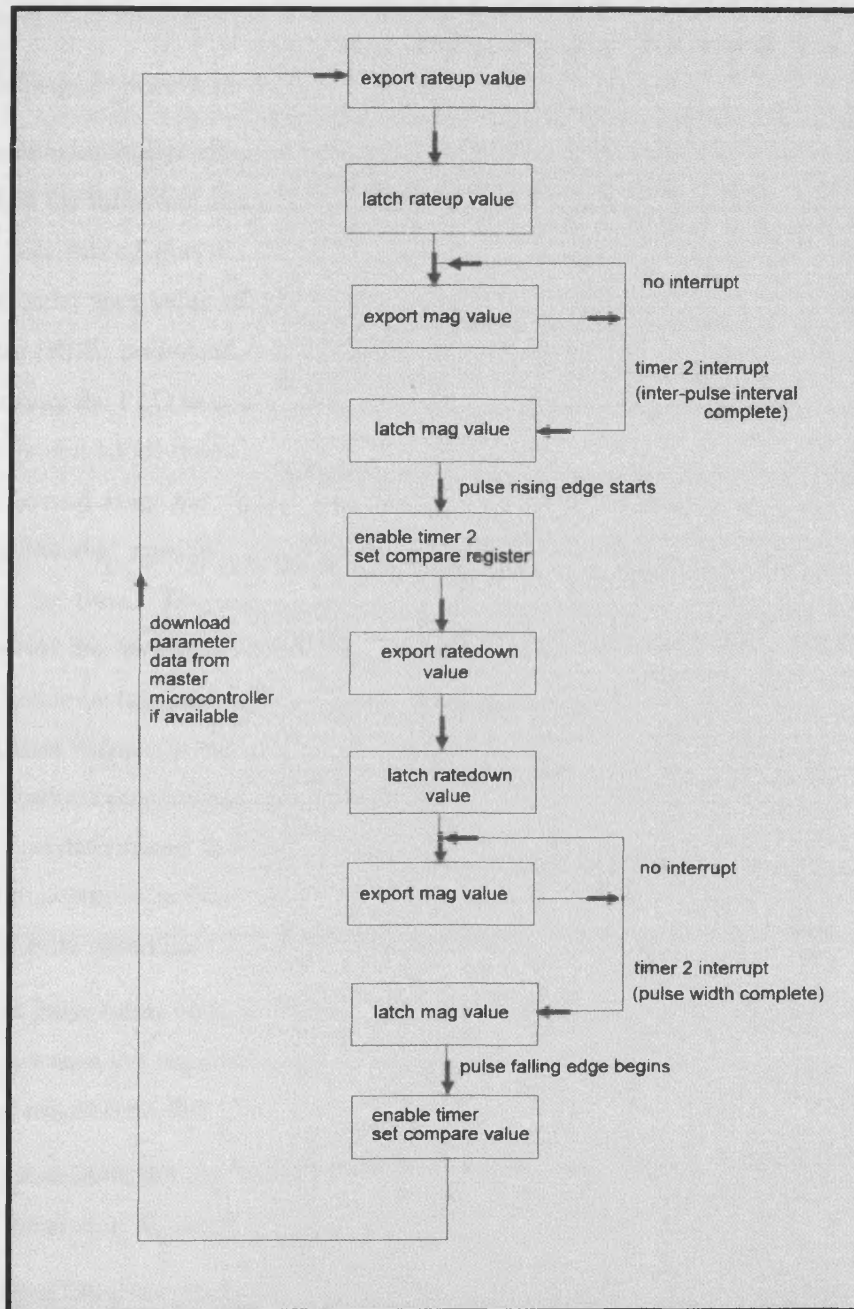


Fig. 4.14 Slave microcontroller software operation.

---

## **CHAPTER 4 INTELLIGENT STIMULATOR DESIGN**

---

The slave microcontroller software performs the following functions :-

- 1) The generation of a setup delay to permit a full system reset to occur.
- 2) The generation of the pulses in the output pulse train.
- 3) The generation of the inter-pulse spacing.
- 4) The exchange of pulse train parameters between the master and the slave microcontroller.

The slave microcontroller effects control of the pulses and inter-pulse spacing of the reference pulse train in the following manner. The rate-up and rate-down value is passed to the PLD via the lower four bits of port 4. These set the rate of rise or fall of the output pulse edges by setting the count start value of the programmable clock generator and are latched by the rate latch enable (RLE) command. With the rate set, the pulse magnitude value is exported and latched, causing the PLD to count to this value. In the case of the inter-pulse spacing, the pulse magnitude is zero at all times. The pulse and inter-pulse lengths are controlled by the use of interrupts derived from the on-board hardware timer 2. This is a hardware function of the microcontroller that runs in parallel with, but without dependency upon, the program being executed at the time. The use of this function ensures that the pulse and space lengths are independent of the length of the software loops and does not require the number of machine cycles utilised to be taken into account. The timer is a sixteen bit counter that is clocked at 1/12 of the oscillator frequency and is set to provide an interrupt when its contents match those of the separately loaded compare registers CM0 and CM1. When this occurs the program counter is forced to a predetermined memory location and program execution continues from this point. The interrupt occurs regardless of any instructions currently being processed with the exception of higher priority interrupts.

In order that pulse trains with particular parameters may be generated, it is necessary to be able to convert between the required pulse train parameter value and the corresponding value output by the slave microcontroller. A derivation of these relationships is performed in Appendix E.

The slave microcontroller software is composed of a number of functions. The action of each of these is detailed in Appendix F.

A full listing of the slave microcontroller software is included in appendix G.

---

## CHAPTER 4 INTELLIGENT STIMULATOR DESIGN

---

### 4. 7 The master microcontroller.

#### 4. 7. 1 Master microcontroller function.

The master microcontroller performs the following three distinct tasks:-

- 1) The control of the digitisation and download of the foot pressure sensor data.
- 2) The calculation of new output pulse train parameters.
- 3) The passing of updated parameter values to the slave microcontroller modules.

#### 4. 7. 2 Master microcontroller circuit details.

The slave microcontroller does not require any external RAM as it runs only a very simple pulse train synthesising program, though the same cannot be said of the master microcontroller. The speed required from the slave microcontroller defines the requirement of a simple program where the internal 255 bytes of RAM are sufficient to store all of the program variables. The master microcontroller program is significantly more complex than the slave device software. This complexity is due to the processing and interpretation of feedback signals and the generation of the waveform synthesis instructions. Therefore, unlike the slave module hardware, 32Kbytes of external SRAM is allocated for storage of the last few seconds of sensor data, to permit interpretation of trends in this data.

The master microcontroller program is located within a 32Kbyte ROM, beginning at address  $0000_{16}$ , permitting a system boot following a reset. The RAM enable is operated by the  $\overline{RD}$  and  $\overline{WR}$  controls, whilst the ROM select is driven by the program store enable control ( $\overline{PSEN}$ ). This permits the differentiation to be made between the two data stores.

The analogue signals resulting from the underfoot pressure sensors are digitised external to the master microcontroller module and clocked into it in serial form, reducing the required cabling and inconvenience to the patient. Three input / output pins are used to implement control of the digitisation. P3.0, P3.1 and P3.2 are used to provide the clock,  $\overline{RST}$  and data functions respectively.

The master microcontroller circuit is shown in fig. 4.15.

## CHAPTER 4 INTELLIGENT STIMULATOR DESIGN

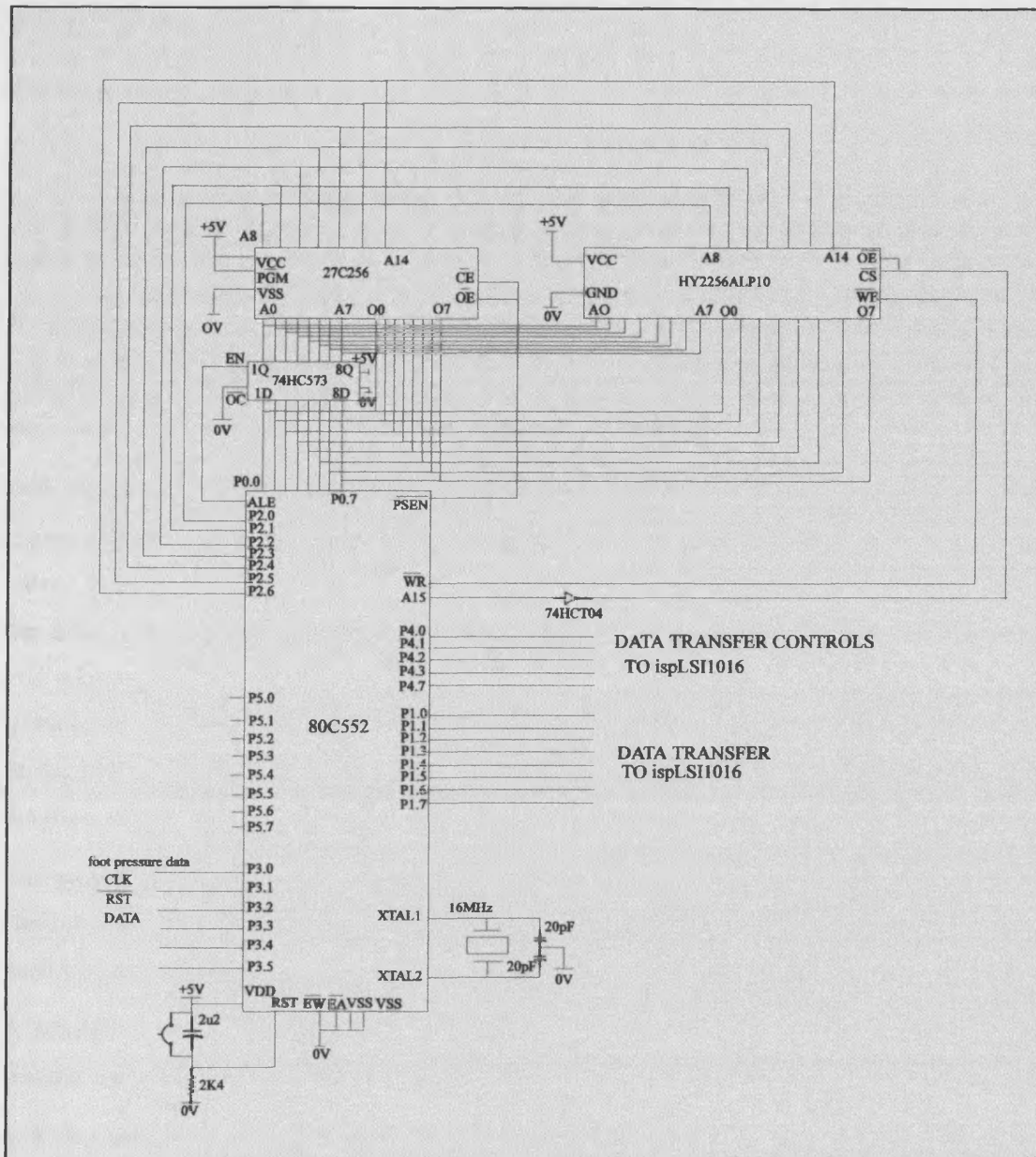


Fig. 4. 15 Master microcontroller circuit.

The 80C552 is clocked at 16MHz, the maximum rated frequency, to permit as much processing as possible to be carried out in a set time, ensuring that the system presents no discernible output lag behind patient movements.

---

## **CHAPTER 4 INTELLIGENT STIMULATOR DESIGN**

---

### **4. 7. 3 Master microcontroller software.**

The functions within the master microcontroller software perform the following actions:-

- 1) Control of the foot pressure data acquisition.
- 2) Interpretation of the acquired foot pressure data and determination of new pulse train parameters.
- 3) Communication of the new pulse train parameters to the slave microcontroller.

This section covers only the communication of the new pulse train parameters to the slave microcontroller. The data acquisition and interpretation are discussed in detail in chapter 5.

Data communication with the slave microcontroller is by means of a handshaking system. The master device continually compares the old value of each parameter with the latest calculated value. When a difference between these values is detected, the master microcontroller signals to the slave microcontroller that it has data to transfer. No action is taken until the slave microcontroller indicates that it is ready to receive data. The master microcontroller then transmits a code to inform the slave device which parameter data will follow. When the slave device has acknowledged receipt of this code, the parameter data is transmitted and once again the slave device will acknowledge the receipt of the data.

This system ensures that both devices are always informed of the receipt of data and permits the slave microcontroller to accept the data at convenient points within its cycle and removes the need to synchronise the cycles of the two microcontrollers.

A detailed description of the master microcontroller software routines concerned with the data transfer are included in Appendix H.

### **4. 7. 4 Master microcontroller circuit layout.**

The master microcontroller circuit was constructed on a double sided PCB, the layout of which is shown in fig. 4.16. Connection to the two slave modules is effected by means of a 25 way ribbon cable and PCB mounted IDC connectors.

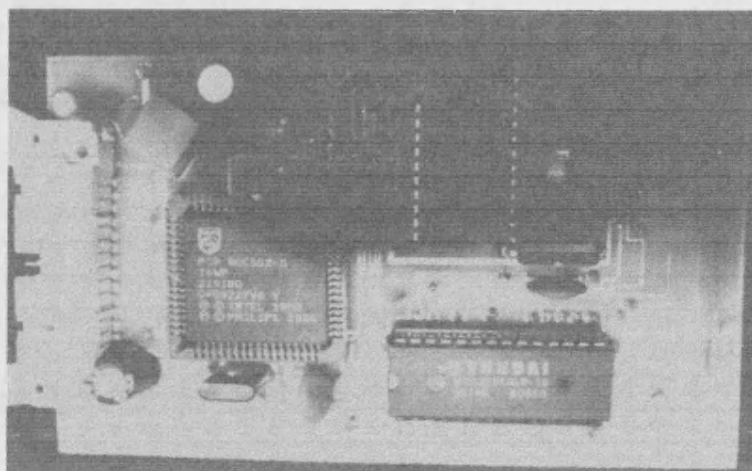


Fig. 4.16 Master microcontroller PCB circuit layout.

### 4.8 The power amplifier.

#### 4.8.1 Power amplifier requirements.

Having decided upon a microprocessor synthesised pulse to permit maximum output flexibility, a power amplifier is necessary to convert this reference signal into a pulse train with sufficient current capability to repeatedly charge and discharge the body capacitance. It is also necessary to electrically isolate the patient from each stimulator channel to prevent currents flowing between channels. These two conditions must be met without compromising the shape of the reference pulse, which should be reflected in the output pulse train.

#### 4.8.2 Possible power amplifier configurations.

A number of possible methods of achieving the requirements of section 4.7.1 have been tried in the past at the University of Bath and they have met with varying degrees of success. The use of a switching amplifier under PWM control has been tried with limited success by Webber [275]. This form of amplifier exhibits high efficiency as on-off control is used resulting in little power dissipation in the output stage. Naturally, the switched output must be smoothed, usually by a reservoir capacitance, to produce a clean output pulse. The problem with this circuit arises when discharging the smoothing capacitance after a pulse has been applied. The discharge into the patient has been found to cause significant overshoot on the negative slope of the pulse and the resulting negative voltage found to obliterate any EMG signals that might be required for



## **CHAPTER 4 INTELLIGENT STIMULATOR DESIGN**

---

control signals. This effect was found by some patients to produce an uncomfortable sensation in addition to reducing the pulse integrity, preventing the analysis of the effects of varying the pulse rise and fall times.

A possible method of overcoming the problem of a high output capacitance is to use PWM techniques along with a fully isolated ring upon which there are two pulse transformers. The ring is on the body side of the isolation barrier and uses one transformer to charge the body capacitance and the other to discharge this, dumping the energy into a supply reservoir rather than the patient. Unfortunately, the turn on and turn off times of MOSFETS do not permit sufficient switching cycles per pulse edge to maintain a close match of the output pulse train to the reference pulse train, so this PWM method of pulse generation was discarded.

The only justification for a switching power amplifier is the associated efficiency, which is of course very desirable in battery powered equipment. This being the case, the likely inefficiency of a linear power amplifier using a switched mode generated supply rail was considered, taking into account that a well designed linear amplifier would closely re-create the pulse shape of the reference input and require no smoothing capacitance.

Consider the pulse parameters to be the nominal values of 30Hz frequency, 300 $\mu$ s pulse width and 30ms inter-pulse interval. Power need only be dissipated in the output stage during the on time, which corresponds to the pulse length time. Therefore, power dissipation in the amplifier devices will nominally occur for :

$$\frac{300\mu S}{30mS} \times 100\% = 1\% \text{ of the time of a pulse train output.} \quad (4.2)$$

This is a negligible percentage of the total operating time, so the pulse edge definition advantage of a linear amplifier was deemed to outweigh the efficiency advantage of a switching amplifier. Consequently, efforts were concentrated on designing a linear power amplifier.

It was decided to use a low voltage rail power amplifier and use the isolation transformer to step up the voltage to the required output level. This has the benefit of safer low voltage power rails and low voltage specification output devices, though the use of a step up transformer does require an increased current capability in the amplifier output stage. A high level schematic of the low voltage rail linear power amplifier is shown in fig. 4.17.

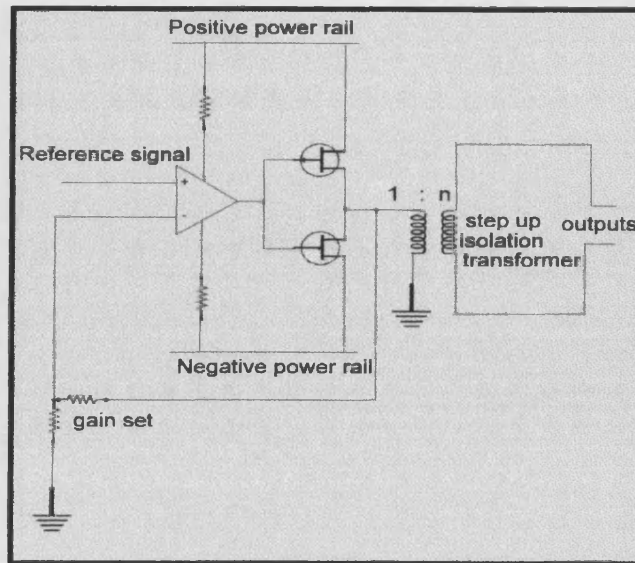


Fig. 4. 17 Linear amplifier schematic.

It was decided to approach the design by the construction and testing of a separate positive and negative transformer driver, using n-channel MOSFET devices in the final transformer driver stage. These devices possess faster response times and are more commonly available than the equivalent p-channel MOSFETs.

#### 4. 8. 3 Stimulator current requirements.

Assuming a 25V primary winding swing to produce the maximum required output to the body, then the output transformer is required to step up the voltage in the ratio 1:6. The power rails used are  $\pm 15V$ , permitting a theoretical 30V swing, though a practical value for the primary winding voltage swing is likely to be nearer to 25V when the voltage drops across the winding resistance, output MOSFET and reservoir capacitance are taken into account. It therefore follows that the primary current will be six times the secondary current. The secondary current must be sufficient to charge the body capacitance in the time required as well as maintain the resistive current into the load during the top of the pulse period.

$$\text{Charge current} \quad I = C \frac{\Delta V}{\Delta t} \quad (4.3)$$

$$I = 0.1 \times 10^{-6} \times 75 \times 10^6 \quad (4.4)$$

$$I = 7.5A \quad (4.5)$$

## CHAPTER 4 INTELLIGENT STIMULATOR DESIGN

This is the secondary current, so a turns ratio of 1:6 results in a primary current of:

$$I_p = 7.5 \times 6 \quad (4.6)$$

$$I_p = 45A \quad (4.7)$$

This assumes a charge time of  $2\mu\text{s}$  at a maximum output of 150V and a body capacitance of  $0.1\mu\text{F}$ . Once charged the resistive current supplied to the body during the pulse is:

$$I_s = \frac{150}{1K} \quad (4.8)$$

$$I_s = 150mA \quad (4.9)$$

therefore  $I_p = 150mA \times 6 \quad (4.10)$

$$I_p = 900mA \quad (4.11)$$

So it can be seen that by far the greater current requirement is the 45A body capacitance charge current. The amplifier must therefore source and sink this value of current and the isolation transformer windings and magnetic circuit must operate at this maximum value.

### 4.8.4 Power amplifier circuit design.

Initially, the upper half of the transformer driver circuit was considered and the schematic for this circuit shown is in fig. 4.18.

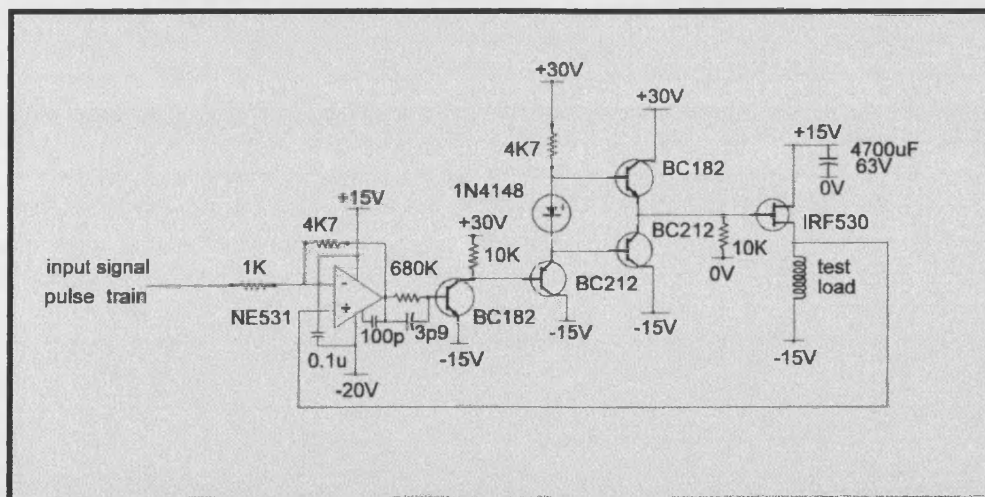


Fig. 4.18 Power amplifier high side schematic.

## CHAPTER 4 INTELLIGENT STIMULATOR DESIGN

This high-side driver is based around an operational amplifier which provides an error signal, forcing the output to the value of the reference signal. A complementary pair of bipolar transistors are used to provide a low impedance gate drive to the MOSFET. The gate drive pair are driven from the operational amplifier output via a biasing network which sets the operating region of the gate driver and prevents the pair of drivers saturating simultaneously, resulting in their destruction. The feedback is taken direct to the amplifier inverting input from the positive side of the load in order to generate a current boosted duplicate of the reference signal.

Although the upper-side transformer driver is capable of driving pulses of current into the transformer windings, it must be remembered that the transformer will present an inductive load to the amplifier. The upper side driver will supply charge current to the windings when required but will only reduce the current flow at a rate governed by the inductance of the transformer windings as there is no discharge path present. To overcome this limitation, a lower side driver with the load in the drain side of the MOSFET was developed. This, like the upper side driver, is a linearly operating circuit, though only operates on pulse turn off to provide a discharge path to the negative supply rail. The schematic of this circuit is shown in fig. 4.19.

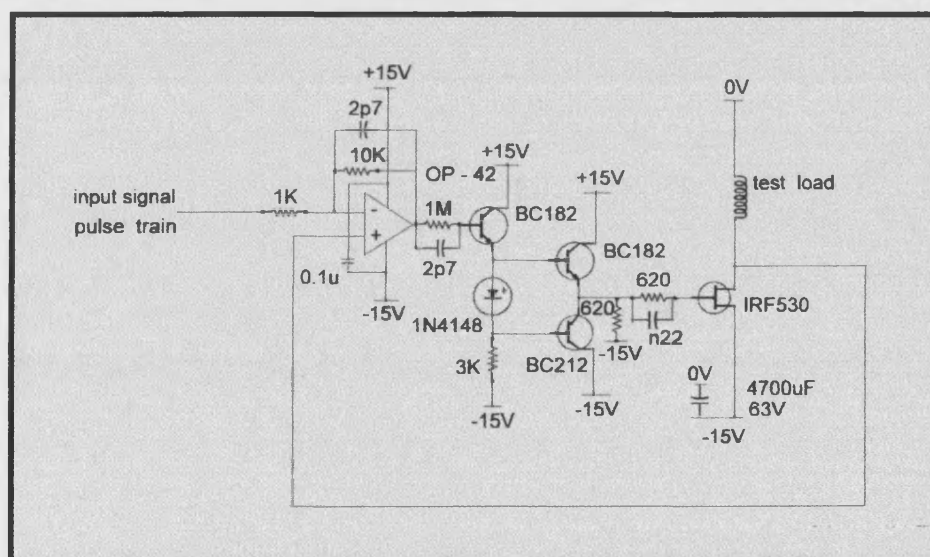


Fig. 4.19 Power amplifier low side schematic.

The power rail to the high-side pre-MOSFET circuitry is +30V, which allows the gate-source MOSFET voltage to attain a maximum value of +15V at full turn on, this is the maximum permissible gate-source voltage and ensures that the device can always be turned fully on. In order to permit the use of standard operational amplifiers with 20V power rails, the extra level

## **CHAPTER 4 INTELLIGENT STIMULATOR DESIGN**

shifting transistor was added to ensure that the operational amplifier would be able to turn off the transistor in the gate driver biasing network.

The high and low side transformer drivers possess stabilising networks to improve their transient response characteristics. The high-side transformer driver was principally stabilised by placing a network in the feedback path of the operational amplifier that limits the low frequency gain of the stage to 4.7 but provides a high frequency boost via the 3.9pF capacitor to ensure fast pulse rise times. Higher gains than 4.7 at this point de-stabilise the circuit, causing glitching on the output pulses. The gain of 4.7 is a compromise between a fast response time and the system transient stability. The 100pF capacitor is present to provide phase compensation to the operational amplifier in accordance with the manufacturers recommendations. The low-side driver has a similar low frequency fixed gain of 10 at the operational amplifier stage, but utilises two high frequency gain boosts, the 2.7pF capacitor which reduces the base impedance of the first bipolar transistor at higher frequencies and the 2.7pF capacitor in parallel with the amplifier feedback path. The low-side driver MOSFET source is tied to the negative rail which results in small gate-source excursions causing very large output fluctuations. The addition of 620R in series with the MOSFET gate limits the low frequency gain of this stage, whilst the 0.22nF capacitor ensures that a fast response to pulse edges is maintained.

The two half drivers were coupled to form the charge and discharge path transformer driver, shown in fig. 4.20. A degree of protection was added to the transformer driver consisting of an output current limit, a shoot-through current limit and a gate-source voltage limiter on the upper driver MOSFET. The output current limit protects against short circuited outputs by reducing the drive to the upper MOSFET when the output current exceeds 50A. The shoot through current limit reduces the drive to the lower half driver MOSFET when the through current exceeds 50A. This limits the current passed by both power devices due to any overlap in switching. The lower half driver cannot supply current to the load, so does not require short circuit output protection. Finally, a transient suppressor is fitted across the gate-source terminals of the MOSFET in the upper driver circuit. This breaks down limiting the voltage across itself to 15V, acting like a high power zener diode. It can be seen that if the reference exhibited a fast minimum to maximum change, then the load side of the MOSFET would be at -15V whilst the gate could briefly be pulled up to +30V, producing a temporary gate-source voltage of 45V. This exceeds the safe gate-source maximum of the devices which is quoted at about 20V. The fast transient suppressor holds this at 15V until the voltage across the load rises, preventing over-voltage damage of the gate-source junction occurring.

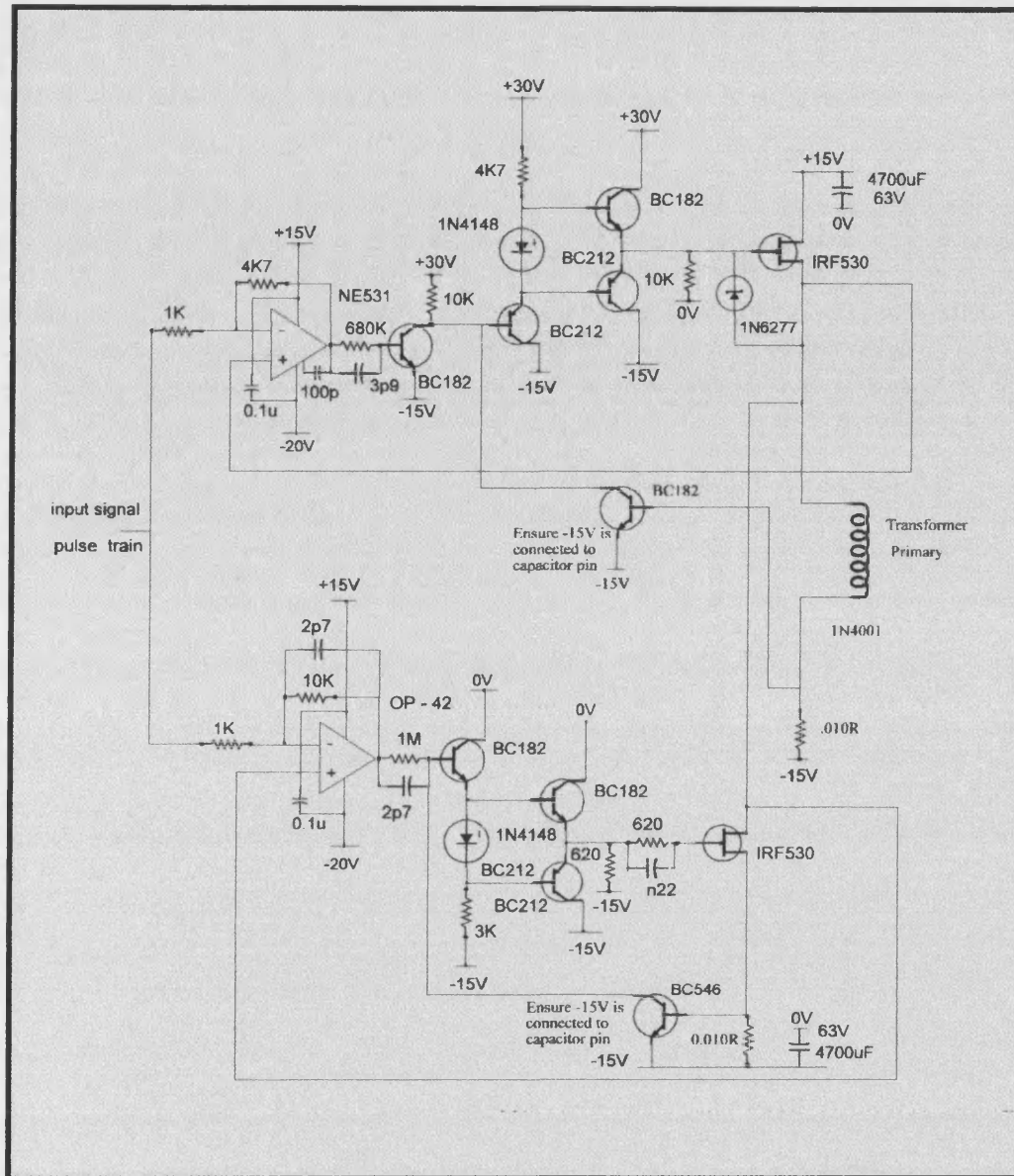


Fig. 4.20 Transformer driver complete schematic.

The complete circuit was tested with the slow and fast edged reference pulses shown in fig. 4.21 and fig. 4.22, the responses to which are shown in fig. 4.23 and fig. 4.24.

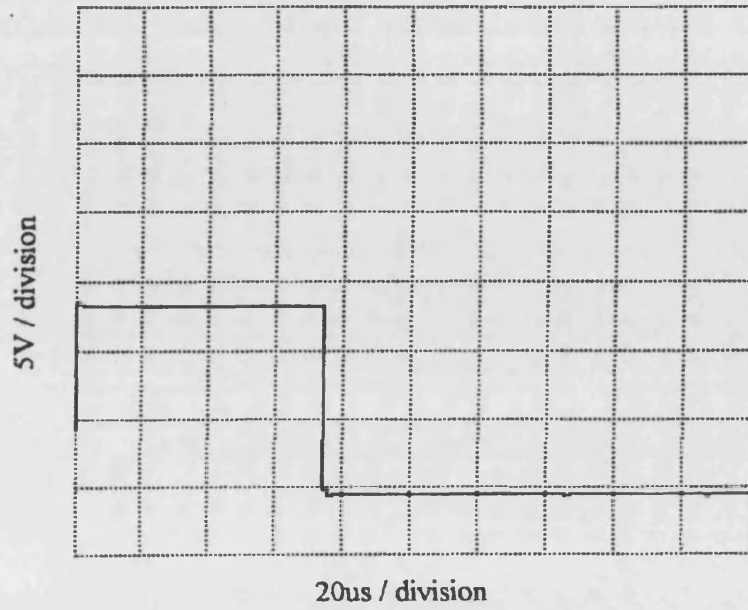


Fig. 4. 21 Fast edged reference pulse.

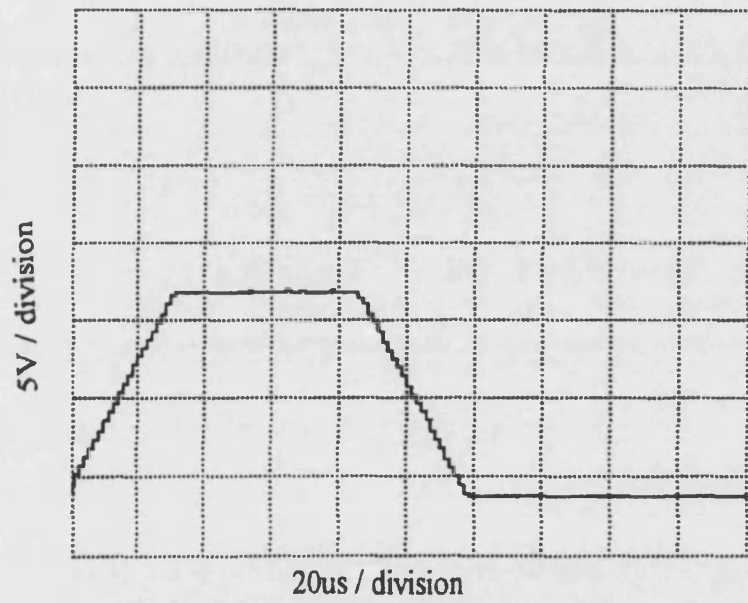


Fig. 4. 22 Slow edged reference pulse.



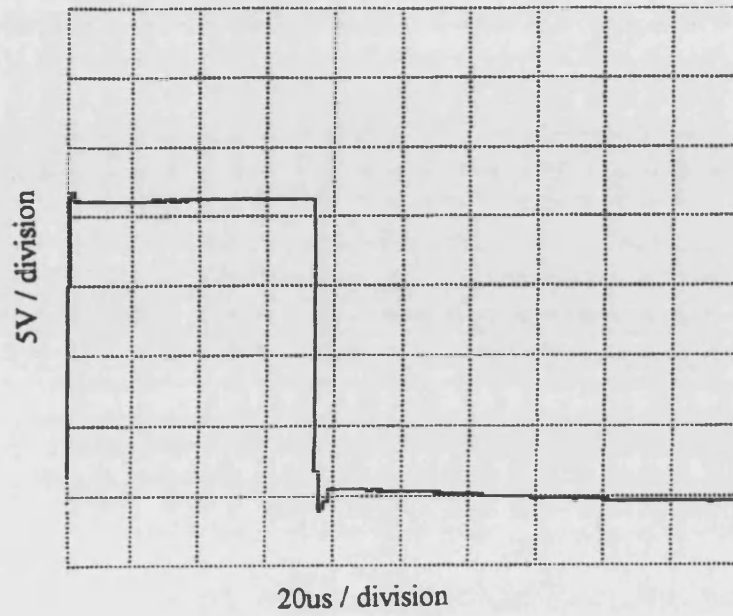


Fig. 4.23 Amplifier output in response to a fast edged reference pulse.

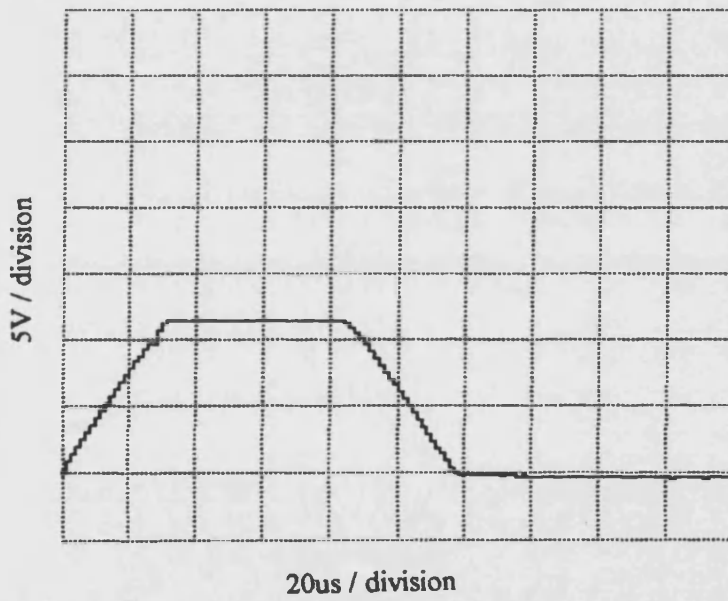


Fig 4.24 Amplifier output in response to a slow edged reference pulse.



---

## **CHAPTER 4 INTELLIGENT STIMULATOR DESIGN**

---

### **4. 8. 5 Feedback arrangement.**

The primary winding wave-shape is maintained by feedback to the transformer driver.

There are three possible feedback arrangements:-

- 1) The use of the high side of the primary winding as the feedback generation point.
- 2) The use of feedback from the secondary winding, opto-isolated to maintain the circuit-patient galvanic isolation.
- 3) the use of a separate sense winding to generate the feedback. This arrangement maintains the required galvanic isolation.

The sense winding alone is not sufficient to effect output control as there is no DC sense component and therefore the amplifier will not switch off fully during the inter-pulse interval. The primary winding feedback and the sense winding feedback may be combined to produce a pulse and DC accurate feedback signal, by connecting the sense winding in series with part of the transformer primary winding. In this way the sense winding output plus a part of the primary winding voltage may be used as the feedback.

The technique of sense feedback was finally discarded in favour of the use of full primary winding feedback as the phase shift incurred across the transformer caused destabilisation of the driver stage. Adequate output responses were gained with the characteristic load connected to the transformer secondary whilst using just primary feedback. These responses are further discussed in section 4.9.

### **4. 9 The output transformer.**

#### **4. 9. 1 Transformer requirements.**

The output transformer serves to provide stimulator-patient isolation on each channel and to step up the voltage to the required output value. The generally accepted transformer equivalent circuit is shown in fig. 4.25 [280], where the secondary parameters have been referred to the primary side of the transformer.

If the primary winding is to pass a high peak current, then the primary resistance needs to be as low as possible in order that most of the primary volts should appear across the primary magnetising inductance and hence appear, via the turns ratio, across the secondary winding.

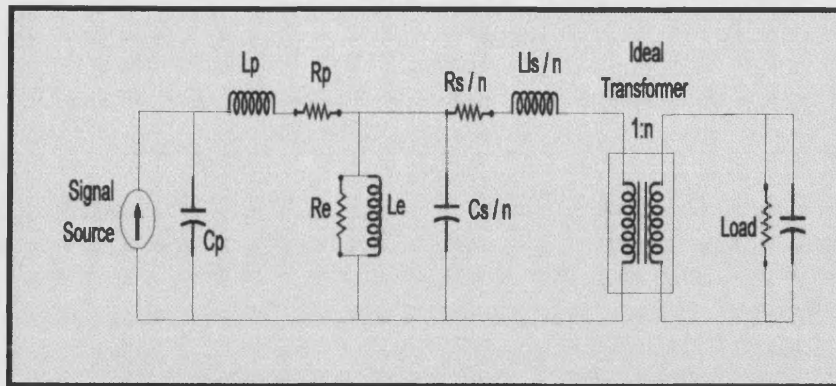


Fig. 4.25 Transformer equivalent circuit.

As a starting point it has been assumed that at full power, 25V will be required across the primary magnetising inductance. It has been assumed that 1V will appear across the FET, 1V across the reservoir capacitor series impedance and that a further 1V may appear across unforeseen parasitic impedances. The maximum pulse magnitude of 25V, therefore results in a maximum permissible voltage drop of up to 2V across the primary winding resistance. At a maximum primary current of 45A:-

$$R = \frac{2}{45} \Omega \quad (4.12)$$

Therefore the maximum permissible winding series resistance = 0.040 ohms.

The transformer core must be of sufficient area and of the correct material to support the maximum flux density driven by the pulses applied to the primary winding. The core must not be allowed to saturate as this produces two undesirable effects. These are the distortion, or flattening, of the pulse when no extra flux can be circulated within the core and the loss of the primary magnetising impedance. If the magnetising impedance falls appreciably, then most of the primary voltage will appear across the winding resistance and a much reduced secondary output will result.

#### 4.9.2 Transformer design introduction.

When designing a transformer, it is necessary to fix the chosen starting parameters and then use the various magnetic circuit and winding relationships to derive the remaining parameters. In this case, the transformer core material and the overall core dimensions were chosen to permit portability of the final unit.

## **CHAPTER 4 INTELLIGENT STIMULATOR DESIGN**

It is necessary to maintain a close match between the shape of the reference pulse train and the transformer secondary pulse train. Assuming that the transformer core is prevented from saturating, the principle reason for waveform distortion is excessive leakage inductance. Leakage inductance is most obviously seen as a reduction in the device transient performance, so should be kept to a minimum value. Consequently, both transformer designs utilise toroidal cores which, with no sharp edges in the structure, ensure that flux leakage is kept to a minimum.

Two separate transformer designs were performed and the resulting devices tested. The initial design used a size 797, type L2 manganese-zinc ferrite core. This is the size of ferrite core required to support the long stimulator pulses as the type L2 possesses a low saturation flux density of typically 0.5T [281].

The second transformer design featured a tape wound silicon-steel core. The silicon-steel used supports a maximum flux swing of 3.0T [282] and therefore requires a smaller core area than a similar ferrite design. The tape wound configuration is a method of producing a laminated core which increases the efficiency of the transformer by reducing eddy currents within the core. It should be noted that the low conductivity of the ferrite material leads to an inherently high efficiency transformer core.

The ferrite and silicon-steel cored transformers were both designed using the procedure shown in Appendix I, which refers to the design for the silicon-steel cored device. The results of this are shown in section 4.9.4. The various secondary side loading arrangements considered for the design are discussed in section 4.9.5 and the test results for both devices are shown in section 4.9.6.

### **4. 9. 3 Pulse train harmonic analysis.**

In order to compensate for the skin effect due to the range of frequencies present in the pulse train waveform, the expected nominal waveform was analysed to determine its frequency content. The frequency content of a trapezoidal waveform may be represented by:-

$$C_n = 2A_{av} \left[ \frac{\sin\left(\frac{n\pi f}{T}\right)}{\left(\frac{n\pi f}{T}\right)} \right] \left[ \frac{\sin\frac{n\pi(f+d)}{T}}{\frac{n\pi(f+d)}{T}} \right] \quad [283] \quad (4.13)$$

The plot shown in fig. 4.25 was produced from equation 4.13 using the PC based software package Excel. The parameters used reflected a typical output pulse with 300µs width, 2µs rise

## CHAPTER 4 INTELLIGENT STIMULATOR DESIGN

and fall time and 30ms spacing. From fig. 4.26 it may be deduced that the harmonic magnitude falls to approximately 1% of the fundamental magnitude at the 3000th harmonic. This defines the highest frequency making an appreciable contribution to the waveform. For  $n = 3000$ , the associated frequency is 100 KHz, therefore, the amplifier and transformer must be capable of supporting frequencies in the range 30Hz to 100KHz.

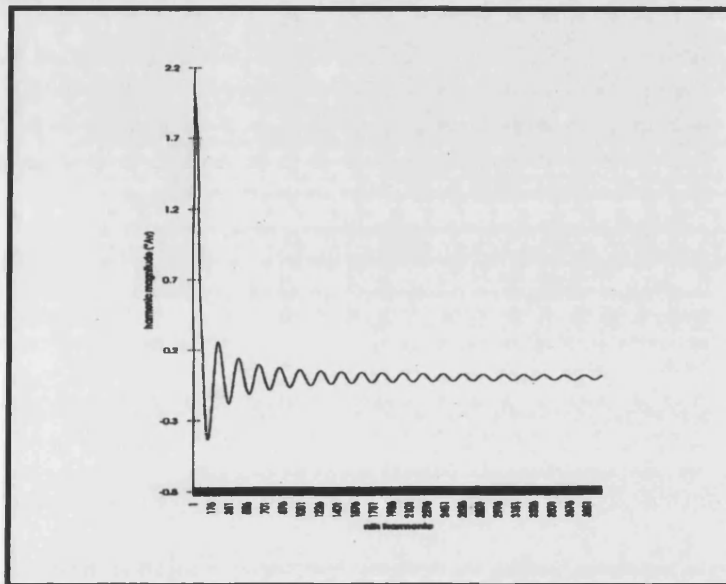


Fig. 4.26 Harmonic analysis of the nominal trapezoidal waveform.

### 4.9.4 Transformer design results.

<u>Parameter</u>	<u>ferrite cored transformer</u>	<u>steel cored transformer</u>
Core diameter	70mm	36mm
Core height	15mm	12mm
Core depth	15mm	12mm
No primary windings	80	27
No secondary windings	480	162
Wire diameter	0.20mm	0.20mm
Winding style	Twisted then wound.	Wound flat and interleaved.

## CHAPTER 4 INTELLIGENT STIMULATOR DESIGN

The bulk of the wire necessary for the ferrite cored transformer winding meant that the strands had to be twisted together first before being wound onto the core and that the primary and secondary windings could not easily be interleaved. The reduced quantity of wire necessary for the steel cored transformer permitted both of these refinements to be easily accomplished.

### 4.9.5 Transformer secondary winding loading arrangement.

The ferrite cored transformer design and the silicon-steel cored design were both evaluated using fast edged reference pulse trains, slow edged reference pulse trains and pulse trains exhibiting both long and short pulse widths. Initially, the characteristic load of a  $1k\Omega$  resistance in parallel with a  $0.1\mu F$  capacitance was used to load the transformer secondary winding, as shown in fig. 4.27.

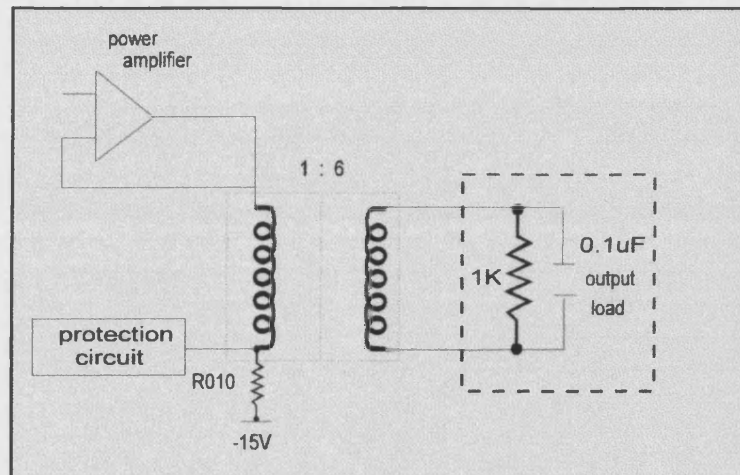


Fig. 4.27 Secondary winding with characteristic load.

This was seen to produce a very oscillatory output from the secondary winding, so an  $80\Omega$  damping resistance was added in parallel with these two loading components to reduce this effect, as shown in fig. 4.28. This arrangement improved the oscillatory behaviour of the secondary winding output but led to a much increased current requirement during the pulse on time as this action reduced the dc impedance placed across the secondary winding to one tenth of the previous value.

## CHAPTER 4 INTELLIGENT STIMULATOR DESIGN

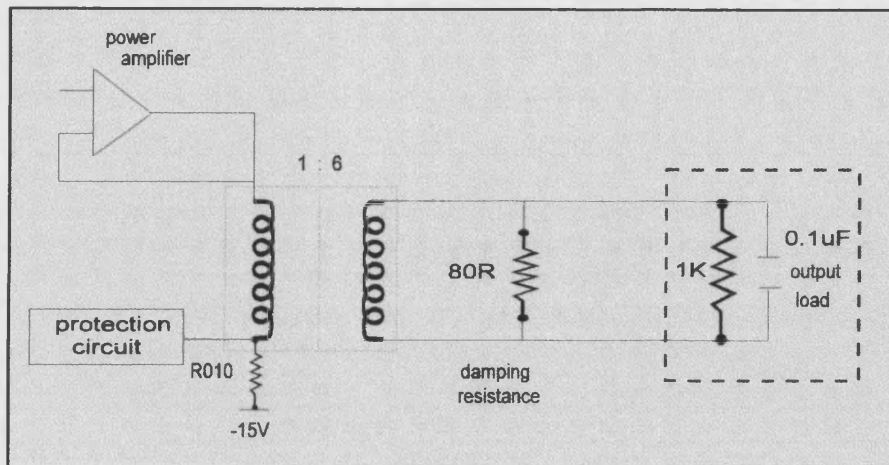


Fig. 4.28 Secondary winding with damping resistance.

This damping resistance was subsequently replaced by the snubber network and diode clamping arrangement shown in fig. 4.29. This snubber arrangement presents high damping to the high frequency pulse edges in addition to a low damping and low current consumption effect during the low frequency flat portion of the pulse. The four diode clamping arrangement restricts the undershoot on each pulse falling edge to a value of 2.5V, a minimum clamp value determined by the core flux reset circuit detailed in section 4.10. This is an acceptable value as the pulse magnitudes will be typically of the order of tens of volts.

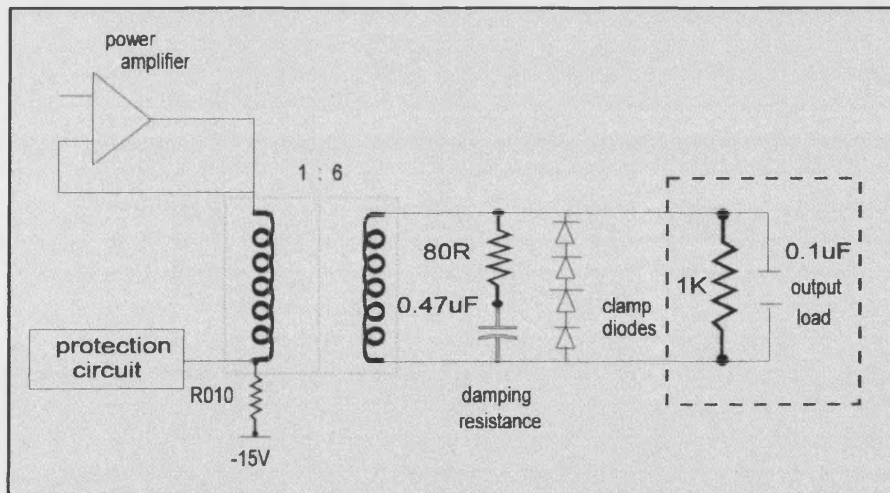


Fig. 4.29 Final pulse transformer secondary loading arrangement.

## CHAPTER 4 INTELLIGENT STIMULATOR DESIGN

### 4.9.6 Transformer evaluation results.

Fig. 4.30 to fig. 4.32 show the ferrite cored transformer secondary winding outputs in response to a  $2\mu\text{s}$  rise time pulse, whilst loaded with the variety of networks shown in section 4.9.5.

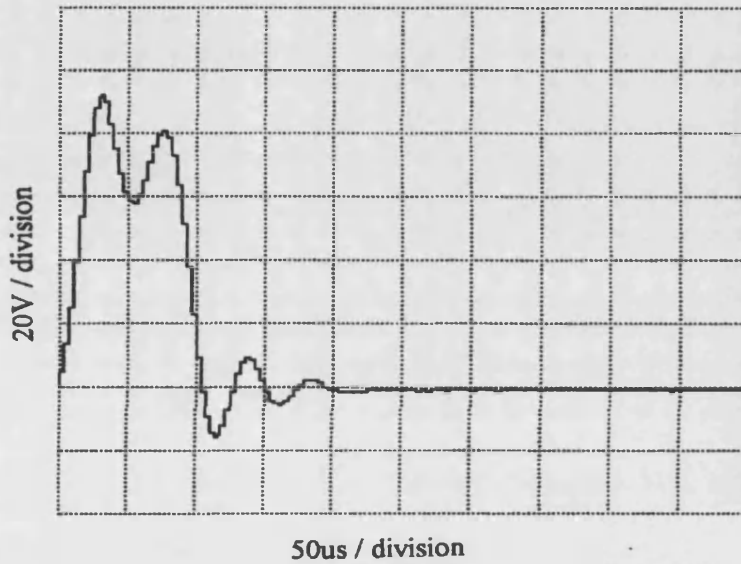


Fig. 4.30 Ferrite cored transformer loaded with the characteristic impedance.

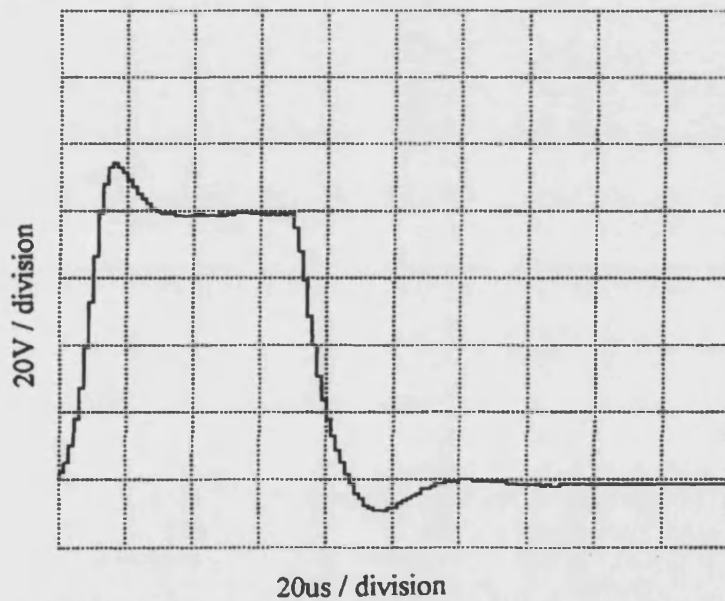


Fig. 4.31 Ferrite cored transformer loaded with additional damping resistance.

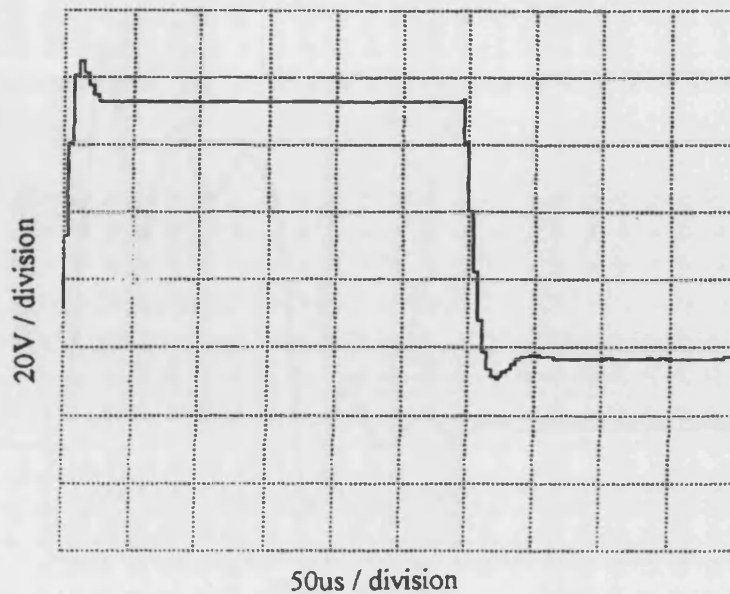


Fig. 4.32 Ferrite cored transformer loaded with the snubber network.

Fig. 4.30 shows the transformer output in response to a reference pulse with the characteristic load connected across the secondary. The output to the load is completely unacceptable due to the obvious oscillatory behaviour and exhibits a poor rise time, coupled with a large overshoot and undershoot.

Fig. 4.31 and fig. 4.32 show the transformer output with an  $80\Omega$  damping resistance added in parallel with the characteristic load. The two output traces show the responses to different applied reference pulse lengths and exhibit far superior waveshape outputs to that of the undamped systems. The settling time, overshoot and undershoot were much improved, though the output to the load was still unacceptable as the pulse rise and fall rates do not duplicate those of the reference pulse.

Fig. 4.33 to fig. 4.36 show the response of the silicon-steel cored transformer to a fast edged ( $2\mu\text{s}$  rise time) reference pulse train with the secondary winding loaded with the variety of networks shown in section 4.9.5.



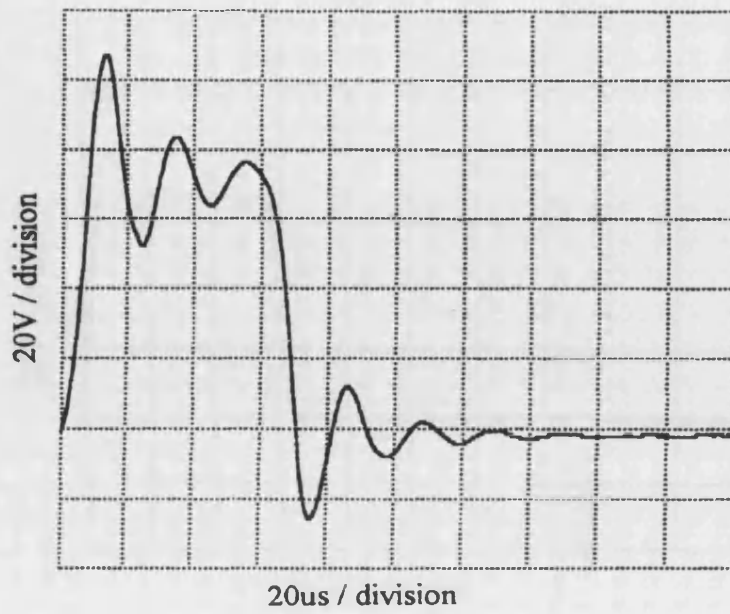


Fig. 4.33 Si-steel transformer loaded with the characteristic impedance.

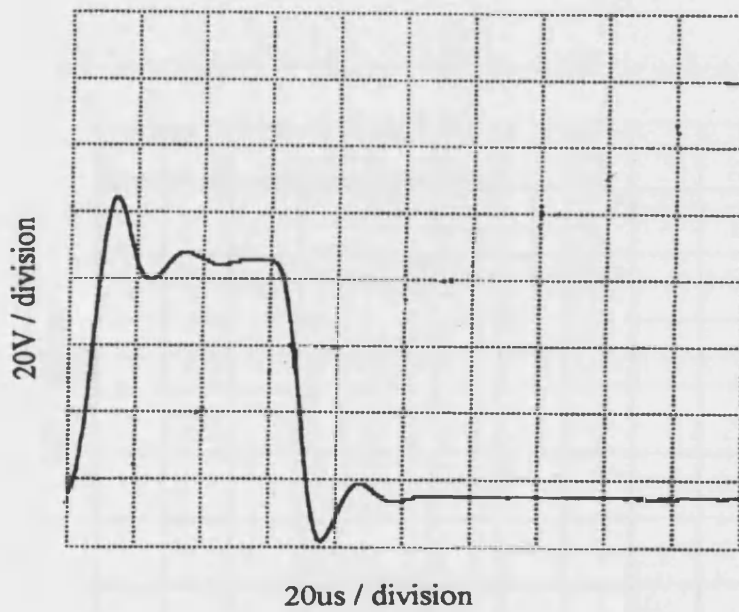


Fig. 4.34 Si-steel transformer with additional damping resistance.

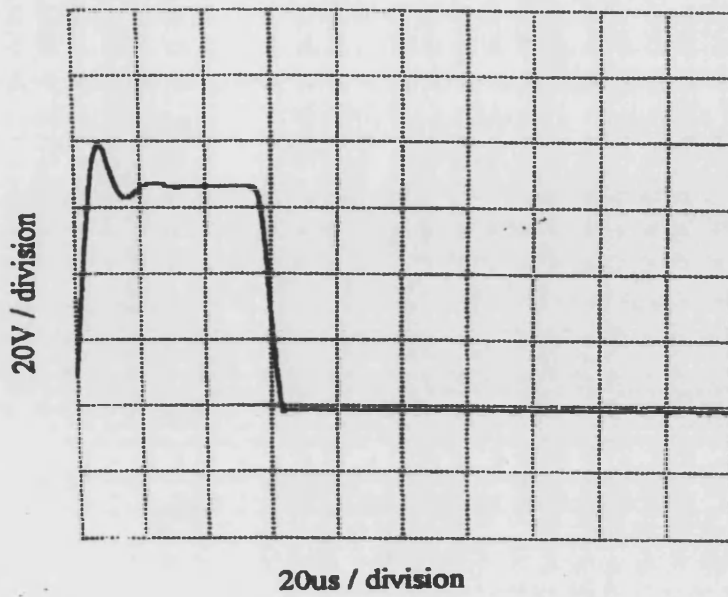


Fig. 4.35 Si-steel transformer with additional damping and diode clamped secondary.

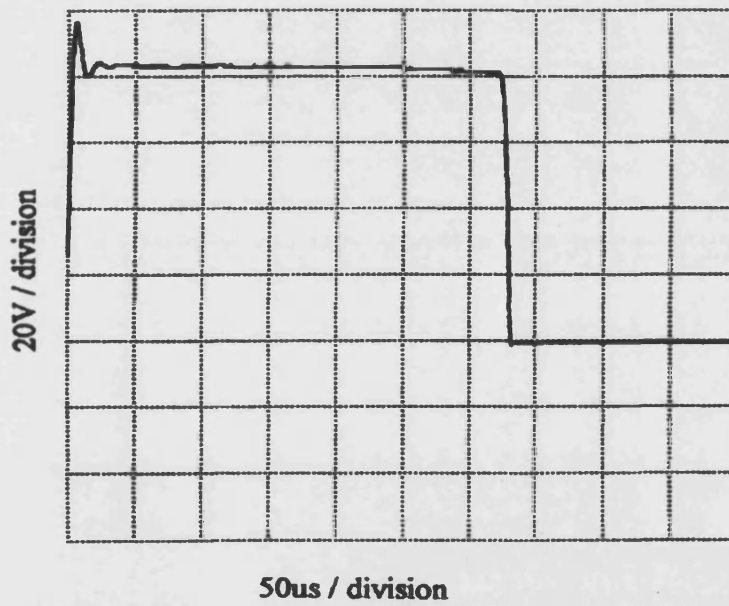


Fig. 4.36 Si-steel transformer with diode clamped secondary and snubber network.

## **CHAPTER 4 INTELLIGENT STIMULATOR DESIGN**

Fig. 4.33 to fig. 4.36 clearly show that the silicon-steel cored transformer produces a superior output to that of the ferrite cored transformer. The inadequacies of the ferrite cored transformer are shown in the responses to test pulses in fig. 4.30 to fig. 4.32. The slow output pulse edges result in the output pulse train not being a close match with the reference pulse train. The poor transient performance of this transformer was most likely due to an excessive leakage inductance, caused by the large number of turns and the twisting of these together before winding. The leakage inductance may be kept to a minimum if the number of turns is minimised and the windings split to achieve several layers of primary and secondary windings, as was performed on the silicon-steel cored transformer.

It can be seen in fig. 4.32 and fig. 4.36 that both transformers responded well to the maximum length reference pulse. The flat top to both pulse responses shows that neither transformer core was driven into saturation by the pulse length as this would have been shown by a rapid droop of the response.

The excellent transient response of the silicon-steel cored transformer, along with the size advantage presented by the use of this device, led to its incorporation within the stimulator design. This transformer was further tested using the snubber network as the secondary load and produced maximum performance parameters of :-

Pulse width = 400 $\mu$ s.

Pulse magnitude = 120V.

Pulse rise time = 3.0 $\mu$ s.

This was considered acceptable for a prototype output transformer, although an improved construction would further reduce the minimum rise and fall times and increase the available output magnitude.

### **4. 10 Transformer core flux reset function.**

Utilisation of the whole of the BH loop, shown in fig. 4.37, is the most efficient method of operation of a transformer, resulting in the smallest core area requirement.

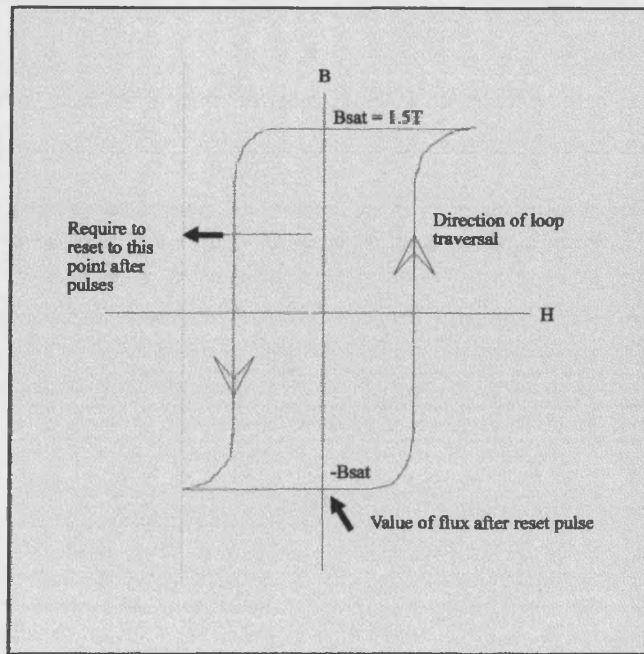


Fig. 4.37 Typical B-H loop for steel.

When applying a unipolar pulse to a transformer, the flux is driven in one direction only. Upon removal of the pulse, the H field falls to zero and the flux level returns, via the hysteresis loop shown, to a point on the positive B axis. If a flux reset is not employed, then only a portion of the first quadrant is traversed, resulting in the utilisation of only a fraction of the possible flux density swing. To minimise the transformer core size, the transformer should be reverse saturated between pulses, to permit a full flux swing to take place at the following pulse.

Saturation of the transformer is governed by the volt-seconds applied to the primary winding by the core flux reset circuit. If the secondary winding is reverse diode clamped as stated, the applied primary voltage will be limited to the diode forward voltage divided by the turns ratio of the transformer. This produces an available reset voltage of approximately 0.1V, which is insufficient to reverse saturate the forward saturated steel core in the available inter pulse interval of 20ms.

The maximum forward applied primary volt-seconds is given by :-

$$V_s = 25 \times 400\mu s. \quad (4.14)$$

$$V_s = 0.01V_s \quad (4.15)$$

The reset applied volt-seconds is required to be double this figure to reset the flux to zero and then to reverse saturate the core. Therefore, the inter-pulse reset must comprise 0.02Vs in the

## CHAPTER 4 INTELLIGENT STIMULATOR DESIGN

reverse direction. The minimum available time for this is 20ms, which sets the reverse voltage requirement at:-

$$V = 0.01 / 20\text{ms} \quad (4.16)$$

$$V = 0.5\text{V} \quad (4.17)$$

This figure is equivalent to the voltage clamped by four diodes in series divided by the turns ratio of the transformer. The supply voltage for the reset winding, one strand of the primary winding, must be higher than the 0.5V clamp voltage though not so high as to cause undue power dissipation in the switching transistor. For convenience, it was decided to use 1.2V as the supply voltage, as this may be conveniently tapped from the first NiCd cell in the supply battery.

The reset was effected by the implementation of the circuit shown in fig. 4.38. This shows both the portion of the circuit incorporated within the ispLSI1016 PLD and the external analogue reset circuit.

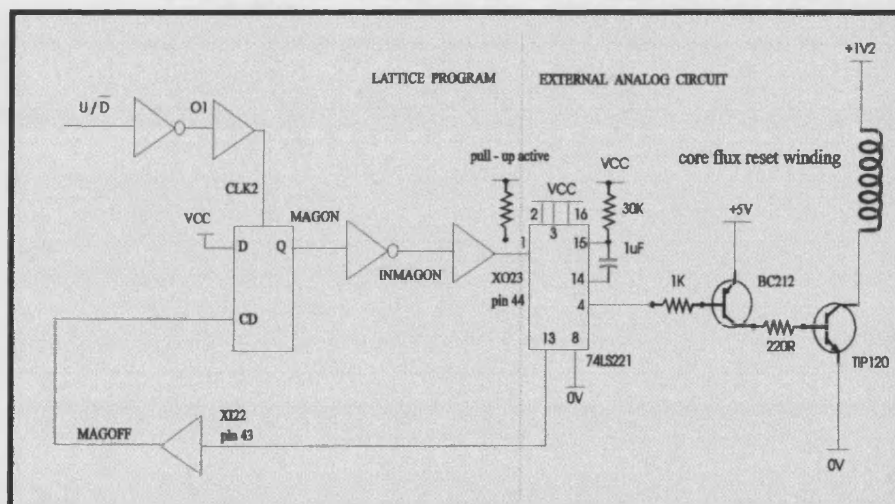


Fig. 4.38 Core flux reset circuit.

The reset is initiated by the PLD internal signal line  $U / \overline{D}$ , which indicates that an output pulse has been completed. This event sets a flip flop which triggers an external monostable, turning on the drive transistor and allowing reverse current to flow through the single strand of the primary winding. The monostable resets after 20ms, resetting the PLD flip flop which turns off the drive transistor in time for the next output pulse. This cycle occurs after every output pulse on every channel.

## CHAPTER 4 INTELLIGENT STIMULATOR DESIGN

The effect of the reset may be observed in the stimulator output pulse train, shown in fig. 4.39. The high magnitude pulses are the transformer output pulses, immediately after which, is the reverse applied voltage collapsing to zero upon reverse saturation of the core. A small spike is present at the reset current turn off, as the flux change induces a small voltage. This is then followed by another output pulse, illustrating the set and reset cycle of the transformer core.

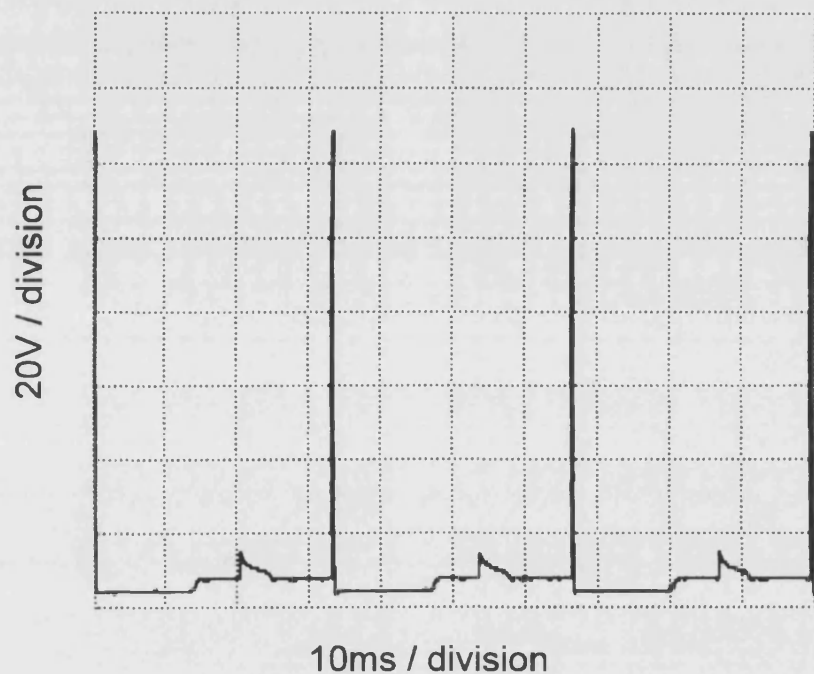


Fig. 4.39 Core flux reset as seen from the secondary winding.

### 4. 11 Stimulator power supply unit.

Power for the whole muscle stimulator unit must be derived from cells in order to fulfil the portability and safety requirements. The rails required are:

- +5V - All logic devices.
- +15V - Operational amplifier positive rails.
  - Power amplifier main power rail.
- 20V - Operational amplifier negative rails.
- +30V - MOSFET drive power rail.
- 15V - Power amplifier main power rail.

These are all derived from 4 series connected NiCd C-Cells, by the circuit shown in fig. 4.40.

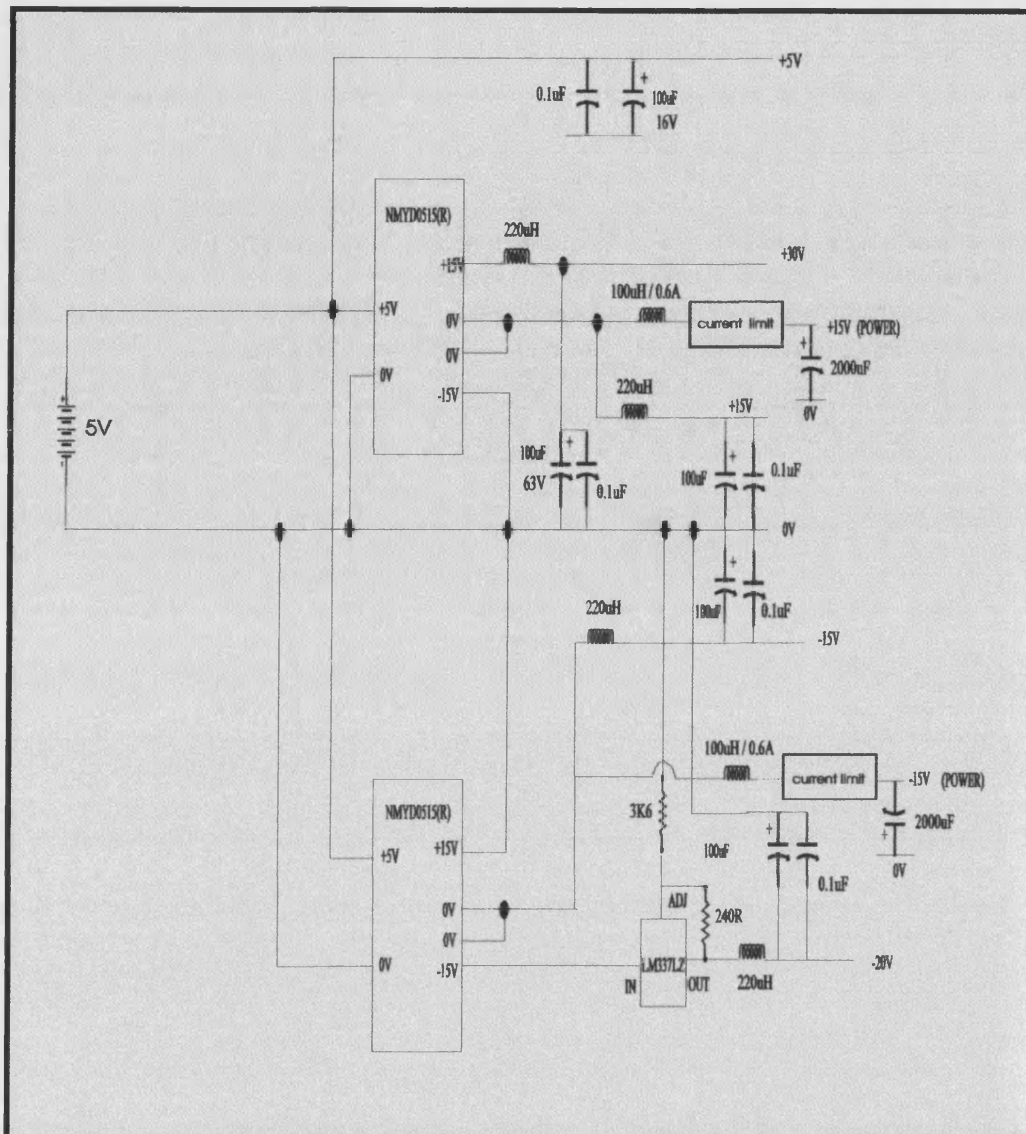


Fig. 4.40 Muscle stimulator power supply circuit.

The supply voltage is boosted, using two DC-DC converters, to  $\pm 30\text{V}$  and  $\pm 15\text{V}$ , referenced to a common 0V rail. The  $-30\text{V}$  supply rail is regulated to  $-20\text{V}$  for use as the operational amplifier negative power rail. Power usage on this rail is low compared to the other three rails, so the 10V drop across the regulator does not cause any heating or dissipation problems. The DC-DC converters are 3W rated with full over-current protection, so no extra protection is required, however current limiting circuits have been designed and installed on the transformer driving  $+15\text{V}$  and  $-15\text{V}$  power rails to permit a possible upgrade to unprotected power converters at a later date.



## CHAPTER 4 INTELLIGENT STIMULATOR DESIGN

The current limiting circuits, set to regulate at 350mA, are shown in fig. 4.41, these also provide protection against power amplifier output short circuits and high capacitor inrush currents.

The power rails other than the two main transformer driving  $\pm 15V$  rails are fitted with LC filtering circuits to minimise the effects due to the switching transients and inrush currents on the high power rails.

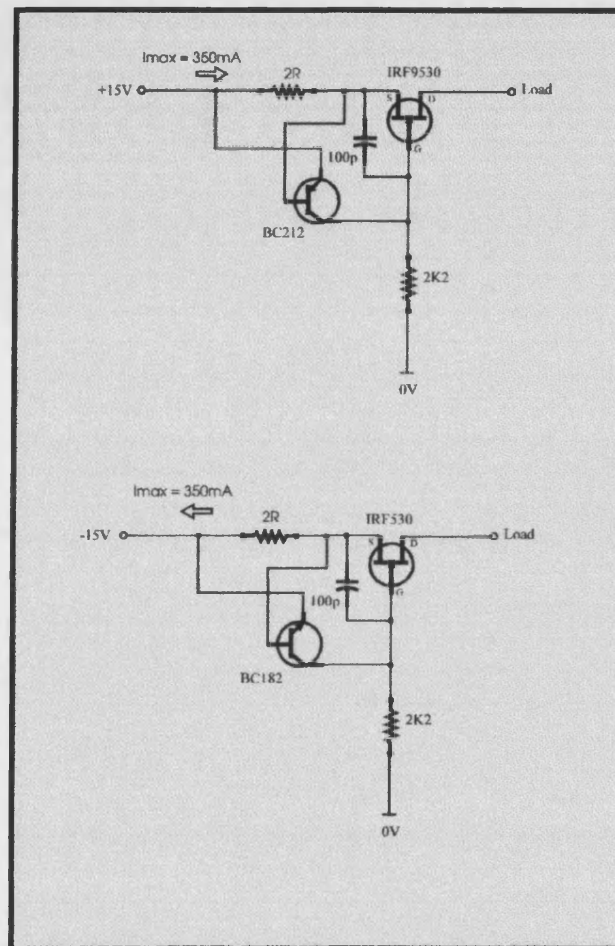


Fig. 4.41 Current limiting circuits.

The large primary winding currents are sourced by the two,  $2000\mu F$ , low ESR capacitors shown in fig. 4.40. These are charged in the inter-pulse interval and supply the extra charge required to maintain the pulse integrity through the step up transformer. At full power, the charge flow may be calculated as follows, assuming a  $100\mu s$  delay before the snubbing network halts the current flow:-

$$Q = I.t \quad (4.18)$$



## CHAPTER 4 INTELLIGENT STIMULATOR DESIGN

---

$$Q = (45 \times 2\mu s) + (400\mu s \times \frac{150}{1K}) + (100\mu s \times \frac{150}{80}) \quad (4.19)$$

$$Q = 350\mu C \quad (4.20)$$

Therefore in the 20ms inter-pulse interval, the required recharge current is:-

$$I = \frac{Q}{t} \quad (4.21)$$

$$I = \frac{350\mu C}{20ms} \quad (4.22)$$

$$I = 18mA \quad (4.23)$$

A supply current of 18mA is required at +15V which creates a power requirement of approximately 0.3W. The 3W DC-DC converter capacity ensures that the other lower power voltage rails are able to be maintained in addition to the charging of the reservoir capacitors.

### 4. 12 Mechanical layout of the stimulator.

The muscle stimulator, consisting of one master and two slave modules, was constructed on three double sided PCBs. A power supply unit, power amplifier, pulse synthesiser and slave microcontroller is present on each slave PCB. The three PCBs are linked by 25 way ribbon cable and IDC connectors, an arrangement that permits expansion by the addition of further slave modules.

The master and slave modules are housed within a semi-enclosed polystyrene box, fitted into grooves that permit easy access and removal of each subsystem. The two transformers are mounted inside the front section of the box, separate to the three modules. The connections to these are by means of screw connectors.

The connections to the outside world are all located on the front panel of the enclosure, shown in fig. 4.42, along with a power switch that connects the power to the output stage, providing an instant shut down control. The power from the battery pack is imported via three 4mm press fit sockets and the electrode conductor connections are also made via 4mm sockets, two per channel to ensure inter channel isolation. A nine way D-socket is provided to transmit signals to and receive data from the sensor controlling circuitry. This method of construction, shown in fig. 4.42 with the PCBs removed for clarity, provides a semi-rugged unit, suitable for laboratory trials, whilst maintaining a modular approach and permitting easy disassembly when required.

## **CHAPTER 4 INTELLIGENT STIMULATOR DESIGN**

---

laboratory trials, whilst maintaining a modular approach and permitting easy disassembly when required.

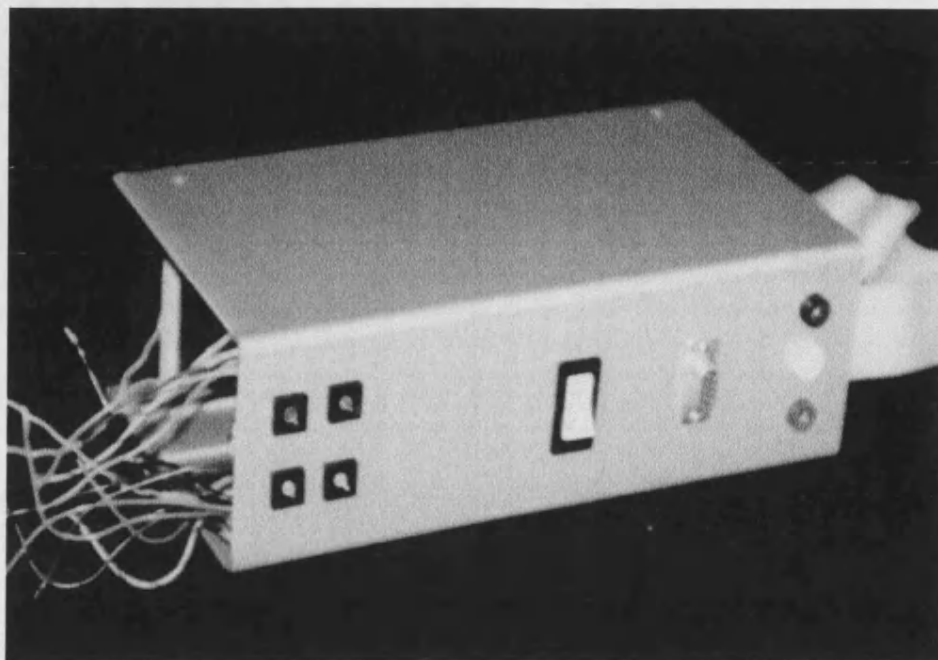


Fig. 4.42 Stimulator unit front panel arrangement.

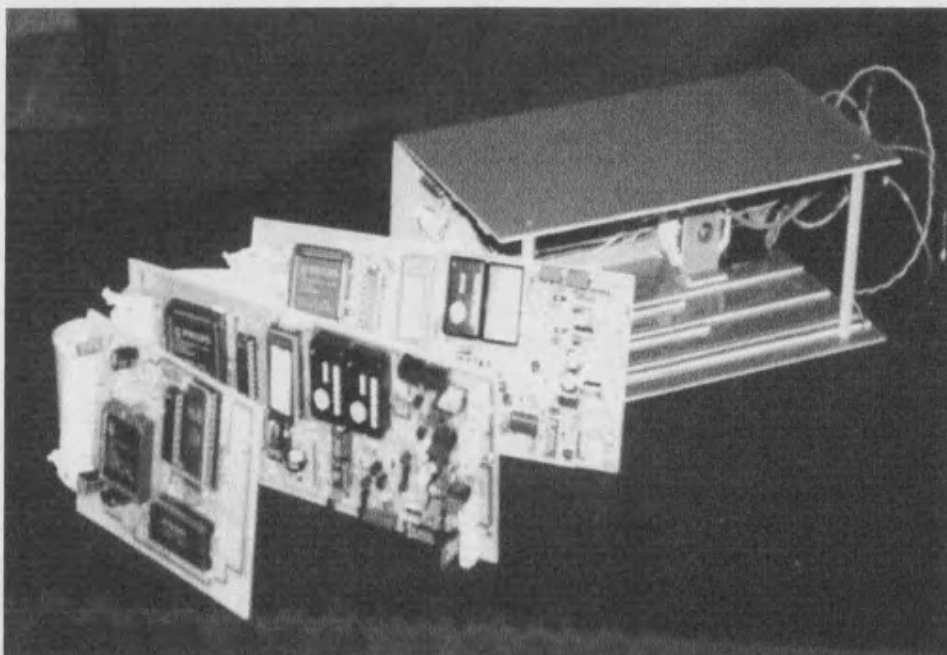


Fig. 4.43 Intelligent stimulator with PCBs removed from unit.

### 4. 13 Stimulator performance.

#### 4. 13. 1 Stimulator output pulses.

The testing of the complete stimulator was initially performed using test programs to produce fixed pulse trains. These were driven into the impedance presented by human tissue via *PALS<sup>TM</sup>* self adhesive electrodes, to demonstrate the functionality and variability of the stimulator output. In each case no feedback was used and the master microcontroller test programs were set to produce a continuously repeating stream of pulses. The parameters of the individual pulses within the streams were varied in each case, though the entire stream was repeated without alteration and captured on a storage oscilloscope. It should be noted that in each case a x10 probe was used to measure the waveforms, so the magnitudes in each case will be ten times greater than those recorded by the oscilloscope.

Fig. 4.44 shows a pulse train generated by the stimulator where the amplitude of successive pulses is adjusted, whilst the remaining parameters are maintained at a constant value. This demonstrates the ability of the stimulator to adjust the output pulse train on a pulse by pulse basis and hence perform the increasing magnitude stimulation strategy suggested by Alfieri [177].

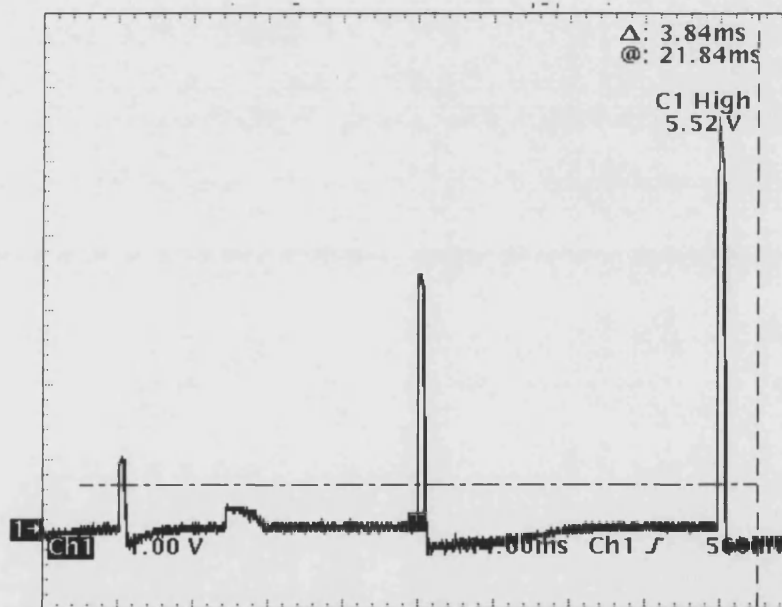


Fig. 4. 44 Amplitude varying pulse train.

Fig. 4.45 shows part of a pulse train produced by the stimulator in which the width of the pulses is gradually increased. Throughout this pulse train, each of the other pulse train parameters is

## CHAPTER 4 INTELLIGENT STIMULATOR DESIGN

maintained at a constant value to illustrate the variability of the width of the pulses. This form of pulse parameter modification is used to increase the strength of the contraction, as longer pulses are thought to recruit further motor units.

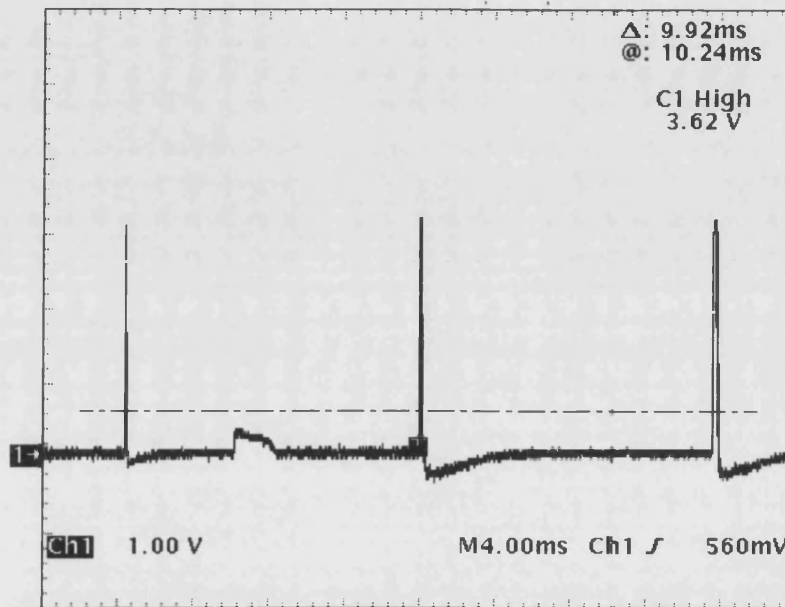


Fig. 4.45 Pulse width varying pulse train.

Fig. 4.46 shows a section of a variable frequency pulse train generated by the stimulator. The stimulator in this trace is producing three separate pulse repetition frequencies in the range 65Hz to 20Hz. This shows that the stimulator is able to produce the type of stimulation proposed by Binder-Macleod and Barker [266], which is considered reduces the fatigue experienced by the patient by making use of the 'catchlike' property of skeletal muscle.

Fig. 4.47 shows a section of a doublet producing pulse train generated by the stimulator. The doublet in the centre of the trace is preceded and followed by a single pulse for comparison. This trace demonstrates the ability of the stimulator to produce the doublets described by Karu [265] and Denslow [259] and used to reduce patient fatigue during FES. Doublets were found by Karu et al [265] to be the most effective of the N-let pulse trains, hence are shown in fig. 4.47, though the stimulator may be programmed to produce N-let pulse trains for any value of N.

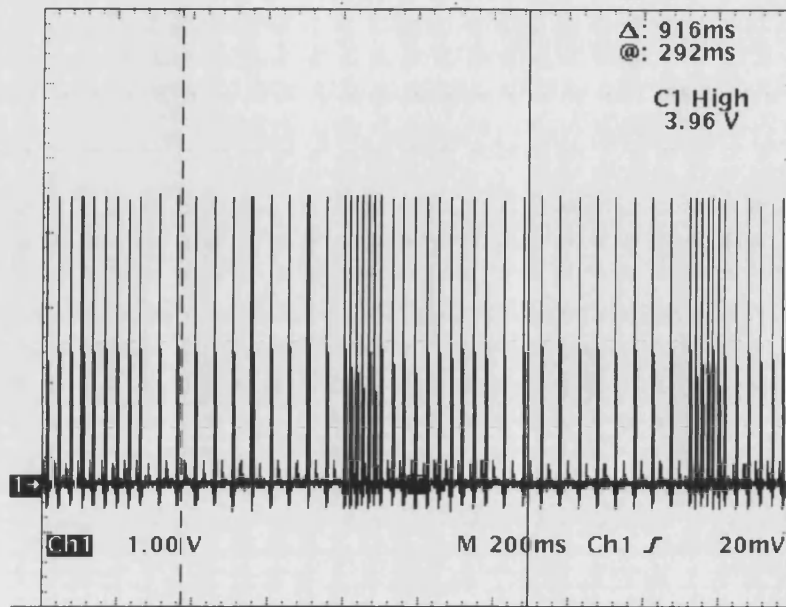


Fig. 4. 46 Variable frequency pulse train.

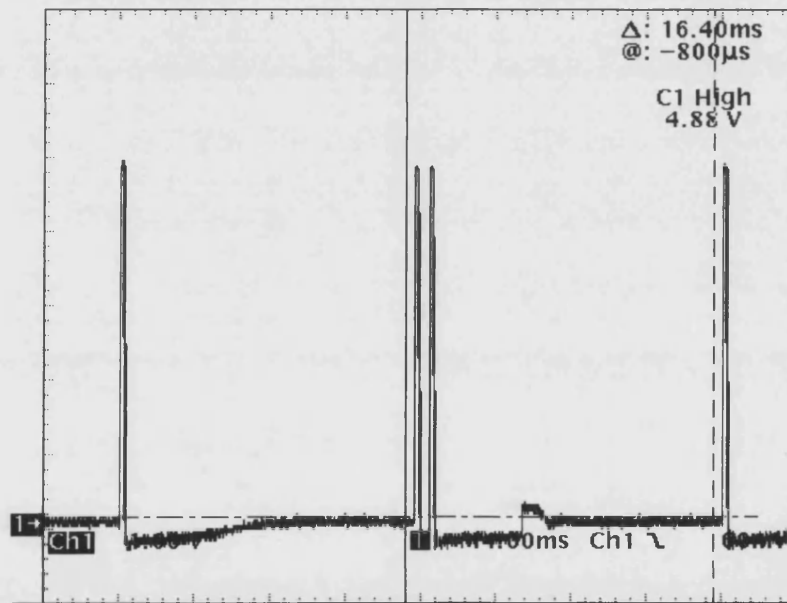


Fig 4. 47 Doublet containing pulse train.

The above traces have shown fixed trains of pulses to demonstrate the variability of the stimulator output. By suitable programming, these parameter variations may be combined to produce any desired stimulation envelope. Naturally, it is not necessary to vary the stimulator output on a pulse by pulse basis, as shown in fig 4.44, although this feature does permit the

## CHAPTER 4 INTELLIGENT STIMULATOR DESIGN

implementation of any future stimulation strategies. Fig. 4.48 shows three pulses of a fixed magnitude and width followed by three pulses of a greater magnitude and then three pulses of an even greater magnitude. The final three pulses exhibit an increased pulse width, showing that the stimulator output need not be varied on a pulse by pulse basis.

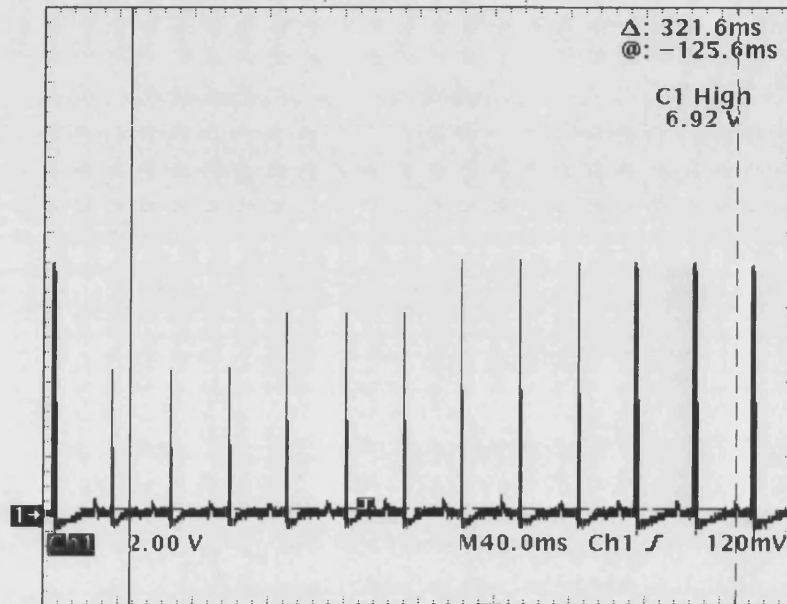


Fig. 4.48 Pulse train with multiple parameter variation.

The traces shown in fig. 4.44 to fig. 4.48 are all of trains of pulses, which demonstrate the variability of the pulse trains but not the shape of the individual pulses. Fig. 4.49 to fig. 4.51 show individual pulses to demonstrate the quality of the waveform delivered to human tissue via the isolation transformers. Fig. 4.49 shows a single fast edged pulse driven into human tissue, demonstrating the ability of the stimulator to drive fast edged pulses into the capacitive load presented by the body.

Fig. 4.50 in contrast to fig. 4.49 shows a pulse with rising and falling edges that are slow when compared to the width of the pulse. Fig. 4.50 also demonstrates that the slow edged pulses may be driven cleanly into the impedance presented by human tissue.

Fig. 4.51 shows how the rate of rise and fall of the edges of the pulses may be set to different values. The pulse shown in fig. 4.51 exhibits a fast rising and slow falling edge, which may be used to combine good wave propagation into the tissue with minimal overshoot and ringing after the pulse.

## CHAPTER 4 INTELLIGENT STIMULATOR DESIGN

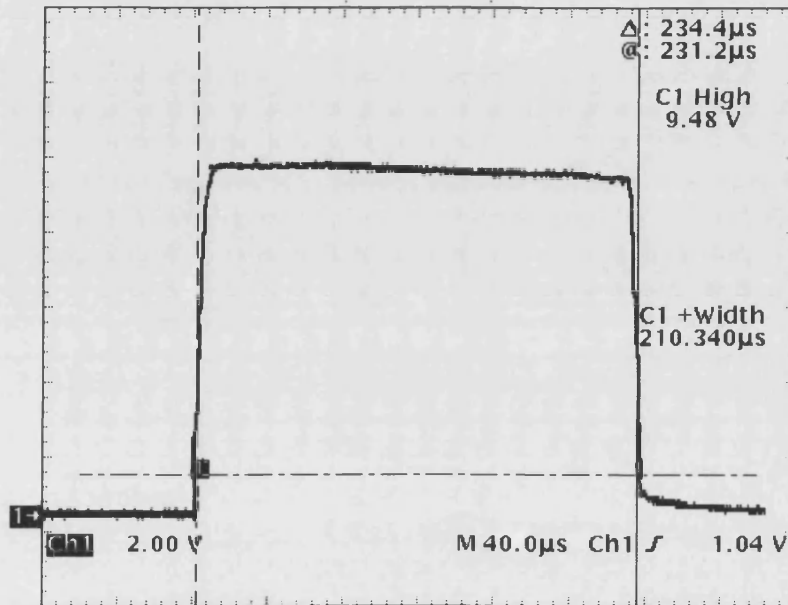


Fig. 4.49 Single fast edged pulse driven into human tissue.

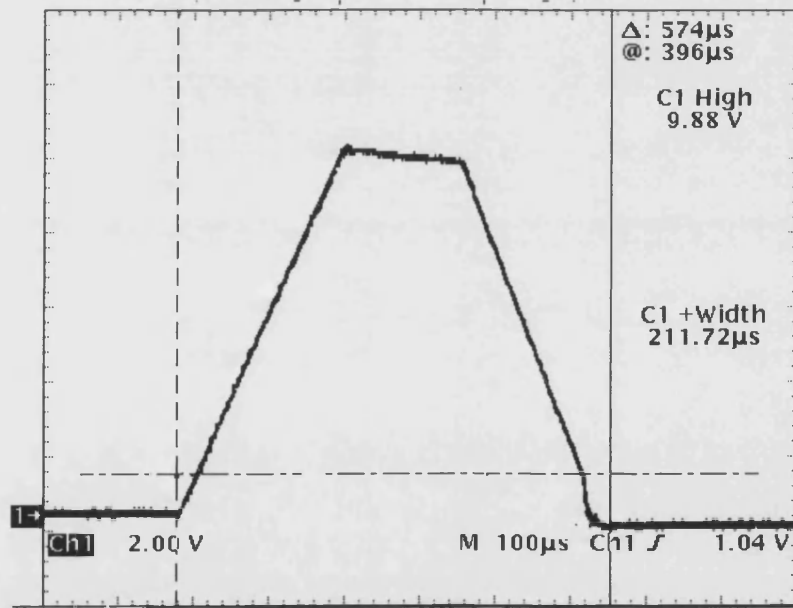


Fig. 4.50 Single slow edged pulse driven into human tissue.



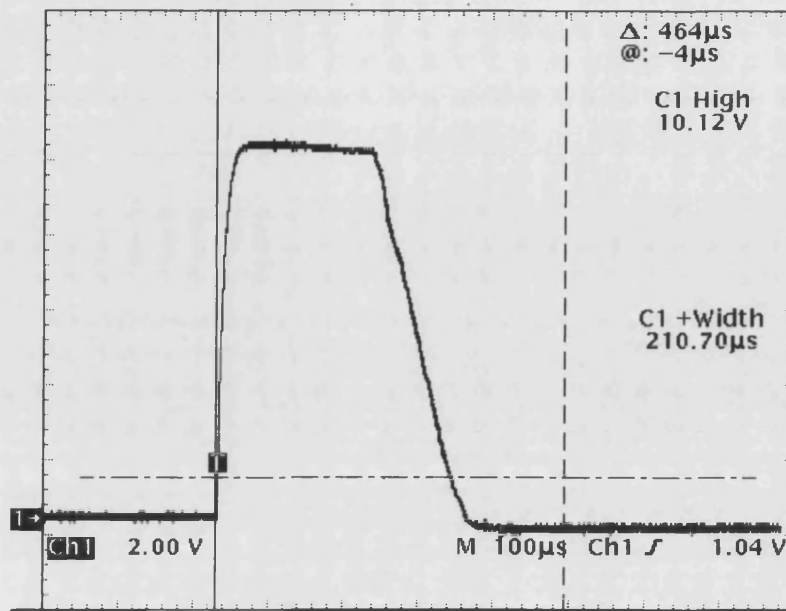


Fig. 4. 51 Single pulse demonstrating different rising and falling edges.

### 4. 13. 2 Stimulator power requirements.

The stimulator whilst operating with two channels active was found to draw a constant current of 1A, supplied at 5V. This was supplied by a NI2020C lithium-ion battery pack with a 4Ah capability and dimensions of 85x70x20 mm, producing a running time of approximately four hours between charges. The lithium-ion technology, manufactured by Energiser, allows the battery pack to maintain its output voltage until very close to the end of its rated life. Charging of the battery pack is accomplished using a proprietary fast charger in one to two hours, permitting useful testing to be carried out with two portable battery packs.

### 4. 13. 3 Movement produced by the stimulator.

The intelligent stimulator was initially tested as a two channel device on healthy subjects with no known physiological defects. A small test routine was written for the master microcontroller permitting serial digitised data to be read from the data acquisition system described in chapter 5 and the pulse width and magnitude to be varied on the output trains. A single potentiometer permitted the DC level at the data acquisition unit to be varied to control the output pulse train change. In this way the level of stimulation was manually varied to test the stimulator.

This simple test setup showed just how effective the stimulator is at producing smooth, precise limb movement. Initial testing used a simple stimulation strategy which was to maintain the stimulation pulse train at a magnitude below that required for a twitch and increase this



## CHAPTER 4 INTELLIGENT STIMULATOR DESIGN

gradually when a contraction was required. This brings on the contraction smoothly and maintains the comfort of the user. At the same time as the magnitude is increased, the pulse width was extended to sustain the contraction and stabilise the limb. The reverse of this procedure was used to reduce the contraction strength with the same smooth, comfortable result. This combination of parameter changes results in a comfortable, smooth precise and sustainable muscle contraction. Fig. 4.52 shows the dorsiflexion of the ankle effected by applying the above stimulation strategy to the common peroneal nerve. The angle of dorsiflexion, measured by an ankle-mounted potentiometer, is shown by the lower trace. The resting angle of the foot was normalised to zero degrees movement and dorsiflexion considered as a positive angular movement. The upper trace shows the stimulation applied to produce this ankle movement. The use of a x10 probe to measure the applied stimulation should once again be noted.

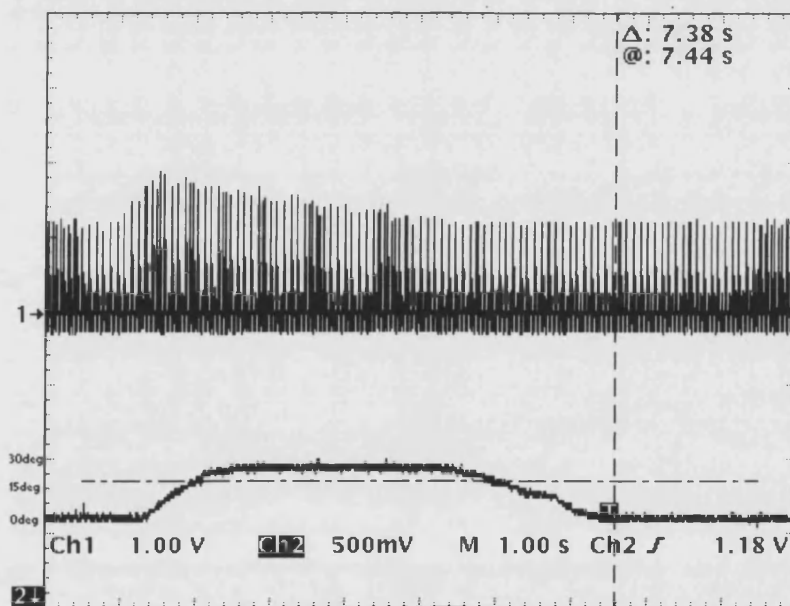


Fig. 4.52 Stimulator induced dorsiflexion..

Subsequent to these tests, the stimulator was used to effect plantarflexion as this may be used to improve push off at the beginning of the swing phase. Fig. 4.53 shows the induced plantarflexion, considered as a negative angular displacement, with the applied stimulation. The stimulation applied to the gastrocnemius / soleus complex is shown in the upper trace, whilst the induced ankle movement is again shown in the lower trace.

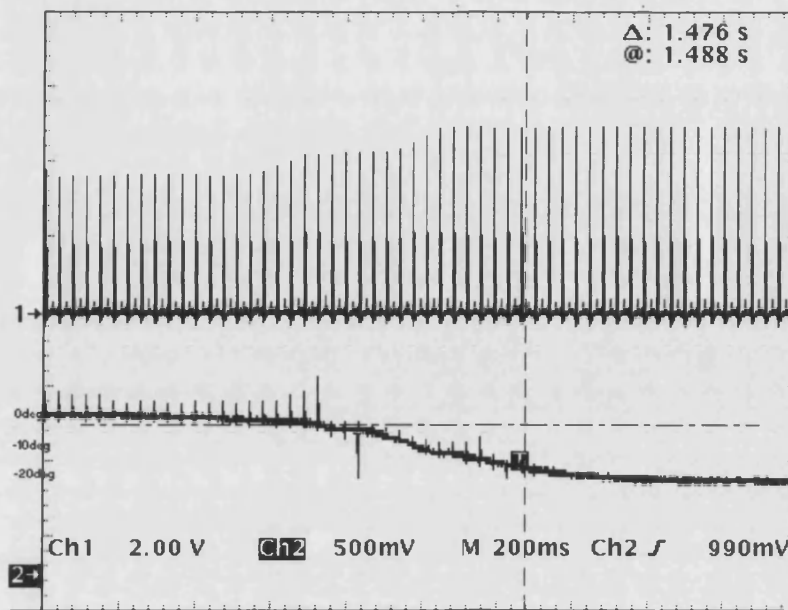


Fig. 4.53 Stimulator induced plantarflexion.

The anterior tibialis was stimulated via the common peroneal nerve and the gastrocnemius / soleus complex by stimulation of the tibial nerve. The following parameters produced a smooth, yet powerful antagonistic movement of the foot.

<u>parameter.</u>	<u>anterior tibialis</u>	<u>gastrocnemius.</u>
Frequency	30Hz	30Hz
Pulse length.	200µs - 300µs	250µs - 350µs
Magnitude	30V - 40V	50V - 60V
rise and fall times	3.0µs	3.0µs

It can be seen that the anterior tibialis requires a lower level of stimulation to effect a contraction. This is most probably due to the stimulation of the site via the common peroneal nerve which is located nearer to the limb surface than the tibial nerve.

#### **4. 14 Intelligent stimulator discussion.**

##### **4. 14. 1 Functionality of the stimulator.**

An intelligent stimulator has been designed and a fully functional prototype unit constructed. The intelligent stimulator is able to monitor a number of feedback generating sensors, make decisions based on the sensor data and synthesise a number of appropriate output pulse trains.

## **CHAPTER 4 INTELLIGENT STIMULATOR DESIGN**

The decision making process and hence the control of the stimulation waveforms relies on the acquisition of gait data by the intelligent stimulator and is therefore discussed, along with the gait data acquisition, in chapter 5.

The number of output channels is presently set to two but is easily upgradeable to  $n$  channels by plugging in further slave cards and effecting a small software alteration. This modular approach maintains the flexibility of the stimulator, allowing its use as a simple one or two channel stimulator or as a multi-channel research tool.

The stimulator prototype was constructed in a portable, semi-rugged form, sufficient for initial testing and evaluation. The unit requires an external battery pack and an external data acquisition unit, normally situated close to the sensors to minimise the pickup of ambient noise. When used to correct foot drop, the intelligent stimulator utilises data from under-foot pressure sensors, acquired from the data acquisition unit via a serial interface.

Each pulse within the output pulse trains is synthesised independently of the preceding or following pulses and independently of the output on any other channel. This allows the stimulator to respond to any sudden and unexpected discontinuities in the sensor data and ensures that any future stimulation strategies may be implemented.

Each channel output is applied to the appropriate muscle group via an output transformer that provides galvanic isolation from the stimulator and isolates each channel from all others. This prevents the risk of physical damage to the patient caused by the flow of inter-channel currents. An additional safety feature, a master cut-off switch, is included to permit the user to switch off power to the amplifier output stage at any time.

### **4. 14. 2 The performance of the stimulator.**

The integrity of the applied pulse trains is excellent, despite the use of the transformer isolation. Tests using characteristic loads and then using Pals self adhesive electrodes attached to the body demonstrated that the synthesised pulse shape is not compromised by the use of the isolation transformer or the required load. Within each pulse train, every parameter is independently variable at any time. This allows the smooth control of any muscle groups by the co-ordinated variation of these parameters. Every pulse parameter may be varied between pre-set limits to provide the required smooth locomotion and to provide a powerful research tool to further investigate the effects of pulse parameter changes, especially the effects of the variation of pulse rise and fall times.

## **CHAPTER 4 INTELLIGENT STIMULATOR DESIGN**

The stimulator maximum performance when attached to the characteristic load or to the body was found to be as follows:-

Maximum output magnitude at 400 $\mu$ s pulse length = 120V.

Maximum output pulse length at 60V magnitude = 500 $\mu$ s.

Minimum output pulse rise time at 100V magnitude = 3.5 $\mu$ s.

Minimum output pulse fall time at 100V magnitude = 3.5 $\mu$ s.

The maximum output pulse magnitude and maximum pulse rise and fall times are dependant on the chosen pulse length. The limiting factor on pulse size is the saturation of the core of the output transformer. Saturation is a function of both applied voltage and time, hence the statement of a pulse magnitude at a particular pulse length.

### **4. 14. 3 Suggested stimulator improvements.**

The three main improvements that will yield the most benefit to the patient are the reduction in size and power consumption of the stimulator and the ability to convert to biphasic operation. A reduction in the power dissipated within the stimulator itself will permit a longer battery life to be obtained between charges and / or a smaller battery pack to be employed. A reduction in the size of the stimulator will enhance the comfort of the user and permit a greater number of channels to be employed for any given final size of stimulator. The conversion to biphasic operation will permit the use of the unit by those patients that cannot tolerate a monophasic stimulation waveform. The first two refinements are closely linked and a reduction in one usually leads to a similar reduction in the other parameter. The possible conversion of the unit to provide a biphasic output waveform is detailed in chapter 6.

Recent innovation in the field of microprocessor design has led to the development of very fast RISC (reduced instruction set computer) microcontrollers capable of processing speeds in excess of 200 MIPS (million instructions per second). The Hitachi HS series and the Digital SA1100 microcontrollers are good examples of such devices. These devices are very powerful, though small in size and low in power consumption due to the RISC architecture. One of these devices could be used to replace the entire master microcontroller board and another to replace the entire digital section of each slave microcontroller board. These devices are powerful enough to directly synthesise a digital representation of the output waveform and would require only the addition of external memory.

---

## **CHAPTER 4 INTELLIGENT STIMULATOR DESIGN**

---

The use of such devices could cut the current consumption of the circuits by half and reduce the size to a fraction of the present size with no change in functionality. The added use of multi-layer PCBs and surface mount components wherever possible will further reduce the required size of the stimulator to the point where a two channel device would be approximately the size of a palmtop computer.

Recent innovation in magnetic materials has led to the production of core materials manufactured by Telcon, that can support peak magnetic flux density swings of 5 - 6 T. This increased flux density support would permit a reduction in the transformer core area and hence reduce the overall size of the isolation transformers to approximately half of their present size, permitting a truly portable unit to be constructed.

## **CHAPTER 5.**

### **CONTROL OF THE INTELLIGENT STIMULATOR.**

#### **5. 1 Introduction to control of the stimulator.**

The development of the intelligent muscle stimulator, detailed in chapter 2, completed the first stage of a system able to restore smooth gait to those exhibiting hemiplegic gait. The pulse synthesiser detailed in chapter 4 cannot be used open loop to effect smooth gait control. A method of monitoring and interpreting the patient gait is needed to provide feedback control of the patient gait. Such a system is described in this chapter.

#### **5. 2 Aims and objectives of chapter 5.**

- Develop and test a gait data acquisition system.
- Show that this system may be used to differentiate pathological gait from normal gait.
- Devise a stimulation strategy for the intelligent stimulator.
- Show how this strategy might be implemented within the master microcontroller.
- Test the principle of this control strategy.

#### **5. 3 Feedback generation methods.**

The generation of gait-related feedback requires the use of sensors to detect the gait events and provide information on the quality of the patient gait. The intelligent stimulator sensors are required to be external to the body, robust and small in size, as cumbersome sensors present a handicap to the patient.

There are a number of possible sources of stance and movement information available on the body of the patient, including:-

- Ankle joint angle measurement.
- Knee joint angle measurement.
- EMG signals from various muscle groupings.

## **CHAPTER 5 INTELLIGENT STIMULATOR CONTROL**

- Pressure on the base of the foot.
- Angle of the toes to the horizontal plane.
- Proximity of the foot to the ground.

All of these parameters may be measured on the affected and unaffected limb.

Joint angles may be measured using goniometers (devices that exhibit a change in resistance with flexion). These devices must be firmly secured in place, however, as errors due to skin movements [284] cannot be tolerated if repeatability is to be maintained.

EMG measurements provide a good indication of the activity of the various muscle groupings but give no indication of the physical position of any part of the limb, though these signals may in future provide a useful addition to the stimulation system when used to estimate patient fatigue, as discussed by Shearn [158], Sime [159] and Carr [160].

A foot-ground proximity measuring subsystem might be employed, consisting of an ultrasonic or optical transducer. This would be used to indicate the distance between the toe and the ground. Such a system may be expanded upon to indicate the position of any or all parts of the foot in three dimensional space. This method of generating feedback appeared complex and likely to result in bulky sensory and processing equipment. For the above reasons, this method of feedback generation was not considered as the main feedback signal generating subsystem.

### **5. 4 Chosen form of feedback.**

The use of a pressure transducer at the foot-ground interface appeared to be the most likely method of fulfilling the requirements of a feedback sensor. It is well understood that the pressure at the foot - ground interface contains information about the postural control of the patient [285]. In addition, there are many foot switches currently in use in foot drop stimulation systems, such as the Odstock two channel stimulator [89]. These switches are thin and robust enough to fit inside the shoe of a patient, where they are used to detect heel strikes and to indicate the onset or cessation of specific phases of gait. It has been declared that the use of an insole worn within the shoe presents an acceptable donning and doffing inconvenience [89] and it was therefore decided to continue the trend of using an underfoot sensing device to permit extensive foot position data to be acquired.

## **CHAPTER 5 INTELLIGENT STIMULATOR CONTROL**

### **5. 5 Underfoot pressure sensing.**

#### **5. 5. 1 Floor mounted pressure sensing.**

The use of the pressure distribution under the foot has been considered as a method of stance and gait analysis since 1882, when Beely placed subjects on a sack filled with Plaster of Paris to observe the imprints left by their feet [286]. In more recent times (1916), Amar [287] introduced the use of a force plate to measure the forces present at the foot - floor interface. Saunders et al. [288] and Jacobs et al. [289] suggested that force plates and associated devices are extremely useful for the study of pathological gait as the information from these highlights any changes in the normal displacement of the body during locomotion.

A number of devices have been devised over the years since Amar introduced the foot plate concept. An early pressure sensing plate devised by Morton, the Kinetograph, was an inked rubber mat that printed at the points of peak underfoot pressure [290,291]. A similar device was also used successfully by Harris and Beath in 1947 to investigate foot ailments in soldiers [292]. This technique has been utilised as recently as 1980, by Grieve [293], in the form of the Foil Pedobarogram. These techniques produced a permanent record of underfoot pressure during gait, whereas Elftman's Barograph [286], using a transparent walkway, produced a dynamic pattern of foot pressure when viewed from beneath the patient. Similarly, Barnett's Plastic Pedograph [293], produced a dynamic visualisation of underfoot pressure by means of driving underfoot plastic rods down into a rubber sheet. The depth of penetration in this case indicated the applied pressure. More advanced methods of pressure measurement such as the C-Ray Scope [294] and the Pedobarograph [295] use an optical method where the interruption of total internal reflection indicates the extent of the applied pressure. A further development of this optical method has been used by Arcan and Bull [221], Leduc et al. [296] and Cavanagh and Michiyoshi [297] where the photoelastic properties of various materials are used to produce pressure dependant interference patterns. A similar method employed by Scranton and McMaster [298] used liquid crystal technology, which exhibits a colour change with applied pressure.

These force plates, including those employed by Cavanagh and Michiyoshi [297], Simkin and Stokes [299], Lo Verde et al. [300], Gerber [301] and Nicol and Hennig [302] have been the most extensively used devices in under-foot pressure measurement [88, 303], although it is clear that only a few steps may be analysed due to the fixed, floor mounted, nature of these devices [88,304]. This type of sensing device is useful in clinical gait studies but cannot be used for



## **CHAPTER 5 INTELLIGENT STIMULATOR CONTROL**

patient gait analysis during everyday activities. In addition, some of the above devices require a method such as photography to store the pressure information in order that a time history of the pressure distributions may be produced. These forms of underfoot pressure measurement are not suitable for use in a simple, portable system that is required to produce an electrical representation of the underfoot pressure distribution. They do, however, illustrate that underfoot pressure has been extensively and successfully used to analyse gait and re-enforces the choice of underfoot pressure sensing as the method of data acquisition for the intelligent stimulator.

### **5. 5. 2 Foot mounted pressure sensing.**

Having determined that underfoot pressure is generally considered to be a good indicator of gait quality, it was decided that a system was required that could be mounted on the patient with minimal inconvenience to that patient. A number of foot mounted systems have been devised and tested in addition to the floor mounted systems described above. Mizayaki and Iwakura [88] suggest that any pressure transducer should have the following attributes:-

- Be able to measure static and dynamic forces simultaneously.
- Impose minimal inconvenience and restraint on the user.
- Be portable.
- Be simple in operation.
- Be reliable.
- Be relatively inexpensive.

These authors [88] developed a shoe sole mounted transducer, consisting of strain gauges mounted on stainless steel plates which bridged two neoprene pillars. Two of these devices were employed per shoe with some success. The use of strain gauges to measure underfoot pressure, also employed by Stott and Soames [305], has been found to introduce poor data due to local bending of the devices [306]. This sensor design allows only two sensors per shoe and requires a specialised constant current drive and amplification circuitry. The location on the outside of the shoe also makes the design liable to damage and contamination and was therefore not considered further in this design.

## **CHAPTER 5 INTELLIGENT STIMULATOR CONTROL**

Pollard et al. [307] have used the change in resistance of a field coil with its displacement relative to a magnet to produce a pressure related signal. Silicon rubber provided the compressive layer that permitted the relative displacement of the coil and magnet.

Hargreaves and Scales [308] used instrumented sports shoes to measure the rates of recovery of hip replacement patients, by observing the underfoot pressure of these patients during walking. These pressure transducers, located within the sole of the sports shoe, were found to present no inconvenience to the patient and to produce underfoot pressure patterns with substantially the same characteristics as those produced by floor mounted force plates [308]. It can therefore be concluded that the use of instrumented footwear instead of force plates does not result in any degradation of the acquired data.

Durie and Shearman devised pressure transducers consisting of conductive rubber sandwiched between brass shims [309]. Applied pressure altered the conductivity of the rubber and this was sensed to provide a time history of the pressure at the site of the transducer. This is a very simple pressure indicating system and was only used for static pressure indication due to excessive hysteresis within the conductive rubber [309]. This limitation reduces the usefulness of this form of sensor in the intelligent stimulator.

An investigation into the relationship between the applied pressure and the temperature of the soles of the feet was carried out by Zilvold [285]. Unfortunately, early indications showed no link between applied pressure and local skin temperature and the work was discontinued.

Capacitive pressure sensors have also been utilised with varying degrees of success. For example, Baumann and Brand [310] taped capacitive pressure sensors to the foot in order to sample peak underfoot pressures. The design of these sensors was later modified by Hennacy and Gunther [311] using piezoelectric crystals, a method also utilised in early work by Schwartz and Heath [312]. These devices, whilst simple and unobtrusive were found to be useful only over a restricted pressure range [285]. Research into the use of capacitive sensors has resulted in the recent Pedar in-shoe pressure measurement system, which consists of shoe insoles instrumented with 99 capacitive sensors [313]. This system requires the use of a PC and a box of support electronics. Whilst this system is undoubtedly useful for detailed gait analysis, it was felt that this number of pressure sensing units per foot was excessive and would require a great deal of processing power if all were to be examined in real time.

The above examples show the popularity of attaching pressure transducers to the base of the foot, the sole of the footwear or incorporating the devices within an insole. It has been stated

## CHAPTER 5 INTELLIGENT STIMULATOR CONTROL

that these methods of obtaining the pressure distributions do not cause inconvenience to the patient [89, 285,308] and that there is a growing trend in the use of parameter measurement techniques at the foot-shoe interface [313]. It has also been stated that the retest reliability of the temporal underfoot pressure variables (using footswitches) is very high [86]. This reliability is further confirmed by the wide use of instrumented insoles and foot mounted switches to provide triggering for various FES systems [235,73, 33,17,86, 94].

The use of an array of pressure sensors permits the underfoot pressure distribution across the base of the foot to be obtained by the master microcontroller in a similar manner to the commercially available system, the Electrodynamogram [314]. This method of data acquisition provides more information than may be obtained from the output of switches and is also considered to be invaluable in overcoming any drift or calibration errors that can occur with use. It was decided that such effects would be best alleviated by utilising the pressure rise and fall events as these will be detectable even if the absolute values of applied pressure have been altered.

The popularity of underfoot pressure detection for generating feedback signals and determining gait quality led to the decision to develop a simple, robust and reliable method of indicating the applied pressure rise and fall by means of an in-shoe system. It was decided that this should be similar in functionality to the magnet and coil system devised by Pollard et al. [307], which combined the attributes of small sensor size and a good resistance to bending-related errors.

### 5. 6 Pressure sensor placement.

There have been a number of sensor arrangements employed in previous research. The single full-sole pressure transducer employed by Hargreaves and Scales [308] produced a single stream of pressure data per foot, with the characteristic shape shown in fig. 5.1.

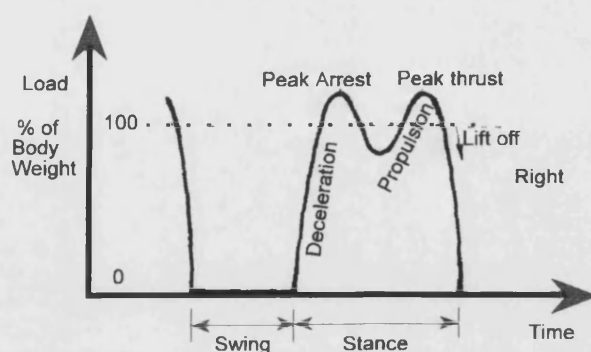


Fig. 5.1 Typical underfoot pressure trace for a single sensor [308].

## CHAPTER 5 INTELLIGENT STIMULATOR CONTROL

Unfortunately, this sensing method does not permit differentiation between pressure changes at different sites on the underside of the foot and therefore relies on a regular pattern of gait related pressure. It is important to be able to sense the pressure changes occurring under different foot regions in order that the different phases of gait may be accurately sensed. A further improvement on the single sensor arrangement is the two sensor system devised by Miyazaki and Iwakura [88]. This produced two data streams per foot, a typical trace of which is shown in fig. 5.2. This is the minimum arrangement that can determine whether or not a correct heel strike and push off have occurred and hence permit the timing between these events to be observed.

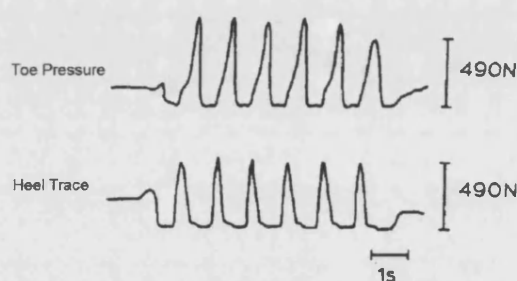


Fig. 5.2 Typical heel and toe trace for a two sensor system [88].

Recently, Granat et al. [90] recommended the use of four sensors (in this case footswitches) per foot for stimulator control. These were placed under the big toe, heel, first metatarsal head and fifth metatarsal head. This positioning was employed to detect the main gait features of heel strike, possible toe strike, and degree of foot inversion. The degree of foot inversion was successfully detected in this case [90] by observing the difference in time of the pressure applied to the sensors below the first and fifth metatarsal head. The inversion was defined as increasing with the length of time that pressure was observed under the fifth metatarsal head compared with that under the first metatarsal head.

This arrangement has been taken slightly further by Pollard et al. [307], by placing pressure sensors under the hallux (big toe), heel, and under all five metatarsal heads. This arrangement produced underfoot pressure traces that largely agreed with those from the equivalent sensors in the above examples, further demonstrating the reliability of this form of gait analysis.

It was decided that the best compromise between gait analysis accuracy and simplicity of operation was afforded by the arrangement described by Granat et al. [90] and it was decided to devise a simple transient pressure sensing system that could be incorporated in an insole in this

---

## **CHAPTER 5 INTELLIGENT STIMULATOR CONTROL**

---

arrangement. This would permit the heel strike to be analysed, check for possible toe strike, analyse push off and allow the degree of foot inversion to be determined.

### **5. 7 Possible methods of under-foot pressure sensing.**

A number of tests with variable capacitance proximity transducers yielded poor results. The proximity of the human body to the simple capacitive systems radically altered the observed capacitance, preventing the acquisition of repeatable values of pressure. From the results of these experiments, the method of capacitive feedback generation was rejected.

An optical method of pressure sensing was also considered but was thought to be very susceptible to ambient light and contamination by the surroundings. The construction of a suitable housing to exclude ambient light and contamination, whilst still permitting accurate pressure sensing movement, was considered to present excessive complexity and likely to result in a system that was too bulky for the user to wear with comfort.

It was eventually decided to use the Hall effect phenomenon as the feedback generation mechanism because of its simplicity, robustness and compactness. This method of gait sensing was used by Pollard et al. [307], where the magnetic field strength was sensed using field coils. The sensing method used in the intelligent stimulator is described in the following section.

### **5. 8 The Hall effect pressure sensing system.**

The pressure sensing system in the intelligent muscle stimulator utilises the Hall effect to detect the strength of a magnetic field, which in turn provides information on the distance of the magnetic field origin from the measurement point.

The principle of the Hall effect is that electrons flowing within a magnetic field experience a force proportional to the strength of that field and will be deflected from their original path unless constraints are imposed upon their movements. The degree of unrestrained deflection may be observed and used to determine the field strength at that point in space [315].

Integrated circuits are available to perform this function within a small package. For example, the UGN3503U is a three leg Hall effect integrated circuit measuring approximately 5mm x 5mm x 2mm. This sensor was chosen to provide the feedback signals for the intelligent stimulator. The Hall effect sensor was used in the arrangement shown in fig. 5. 3.

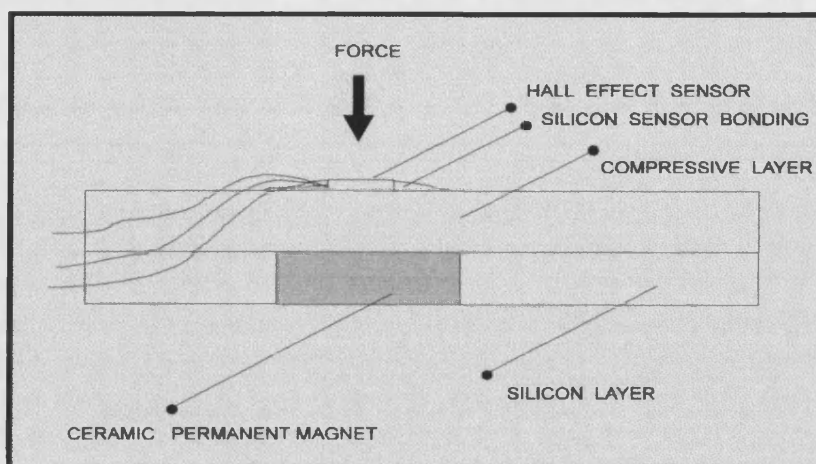


Fig. 5.3 Hall effect pressure sensing arrangement.

The UGN3503U is mounted upon a two layer mat that serves as an insole. The lower layer of this mat is a silicon sheet that exhibits no significant compression or deformation under the expected range of loading. Inserted into voids within this silicon sheet are small ceramic permanent magnets. The Hall effect device is separated from the magnet by a layer of 3.2 mm neoprene placed on top of the silicon sheet. The use of 3.2 mm thickness neoprene in insoles has been suggested by Campbell et al [231], although a number of other materials suited to insole use, including poron and sorbothane, have been listed by Garcia et al. [316]. Compression testing of various materials by Campbell et al. [231] found that open cell neoprene could be classed as 'moderately stiff', a property considered ideal for insole material. Campbell et al. [231] found that this material exhibits a moderate degree of deformation over the expected range of underfoot loading, so was used as the compressive element within the underfoot pressure sensing system. Each device is placed on top of the neoprene, directly over the respective magnet and held in place with silicone sealant. This is also used to bond the two layers of the mat together. Silicone sealant is used because of its excellent bond strength, coupled with a high degree of flexibility without any flexion related stress cracking. This property is extremely important as the mat must flex with the base of the foot to maximise pressure accuracy and user comfort. Many adhesives, such as epoxy resins, fail under repeated flexion and cannot be used for this application. The mat and sensor devices are covered with a thin fabric to minimise wiring damage and to improve the aesthetics of the pressure sensor.

Operation of the system is by compression of the neoprene layer when pressure is applied to a particular section of the mat. At the point of the applied pressure there is the greatest compression of the neoprene layer, which forces the hall effect device closer to the magnet

## **CHAPTER 5 INTELLIGENT STIMULATOR CONTROL**

below. The magnetic field strength experienced by the device varies inversely with the distance from the surface of the magnet, assuming that the adjacent magnets are far enough away to present a negligible contribution to the surrounding field strength. Therefore, as the distance between the magnet and the sensor decreases, the sensor is subjected to an increased field strength and produces a correspondingly higher output, translating the applied pressure into an electrical signal.

The prototype pressure sensing arrangement, described above had an overall thickness of 9 mm and was found to be too thick to easily fit into a shoe and be maintained there in comfort, so holders resembling shoes were constructed to allow an evaluation of this subsystem to be performed. The pressure sensor holders were fabricated from sheet polystyrene, suitably padded with neoprene and fitted with adjustable strap fastening. The sensing mat is placed upon the holder, shown in fig. 5.4, and the user's foot secured on top of this within the holder. The polystyrene sheet is adequately flexible and does not restrict foot movement or flexion and therefore does not significantly affect the acquired pressure readings.

Further improvements to the underfoot pressure sensing mats to enable a more user-friendly insole and data acquisition system to be manufactured are detailed in chapter 6.

The pressure sensing is performed by the pressure sensing mat located within the holder, as shown in fig. 5.5. The holder is then secured to the foot of the user by velcro straps to ensure a secure, yet comfortable, fit.

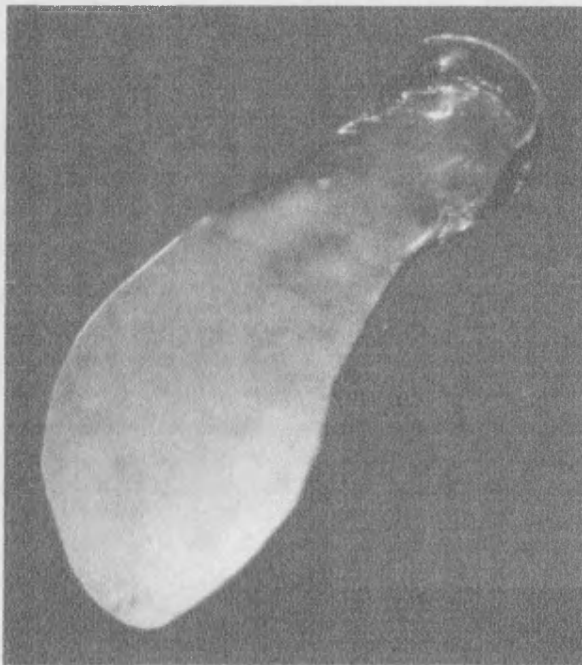


Fig. 5.4 Pressure sensor holder.

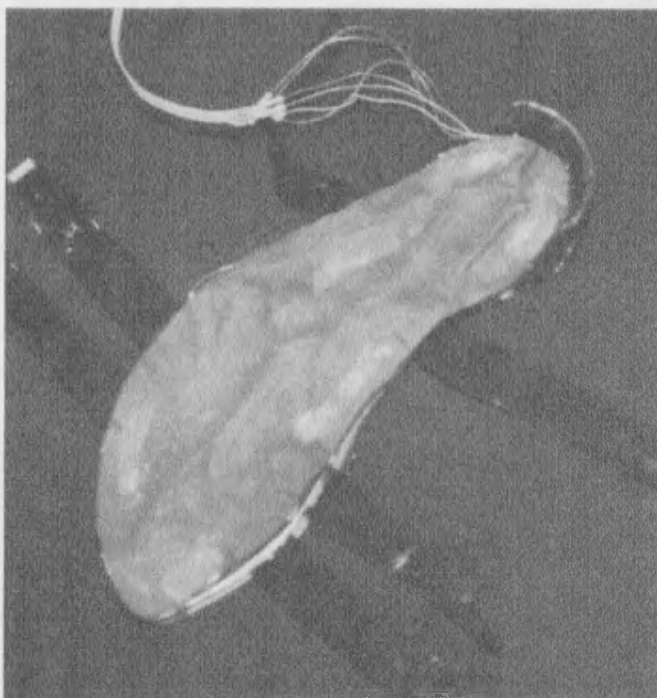


Fig. 5.5 Pressure sensing mat located in the holder.



## CHAPTER 5 INTELLIGENT STIMULATOR CONTROL

The four pressure sensors per mat are located under the following points, as recommended by Granat et al. [90] and shown in fig. 5.6:-

- 1) Big toe.
- 2) Heel.
- 3) First metatarsal.
- 4) Fifth metatarsal.

These are the sites of bony prominences, which result in the high instances of under-foot pressure allowed for in the compression testing of various materials performed by Campbell et al. [231]:-

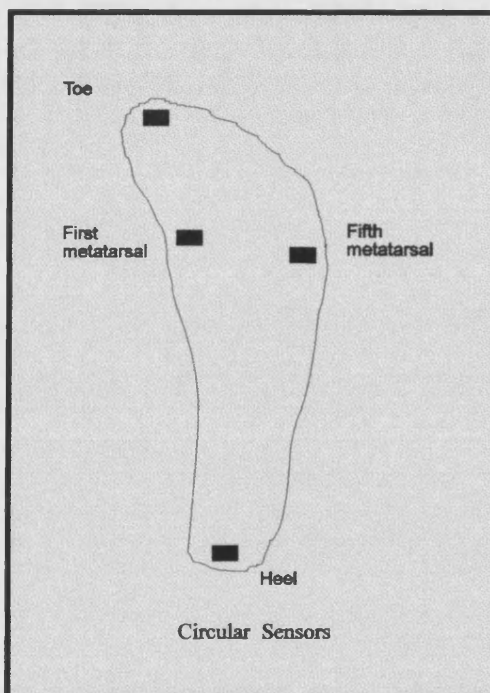


Fig. 5.6 Sensor Placement.

### 5.9 Initial pressure mat testing.

The Hall effect devices used in the arrays described in section 5.8 are powered from a +5V supply. There is no need for filtering or carrier stripping as might be required with a capacitive or inductive system. The output signal is biased at the 2.5V mid-rail point, permitting a simple check to be performed on the functionality of each sensor every time data is sampled.

Initial testing was performed on the underfoot pressure mats by applying pressure to a point directly above the sensor. This compressed the neoprene layer, increasing the output signal. The loading and unloading characteristics of the sensors are shown in fig. 5.7. The pressure

## CHAPTER 5 INTELLIGENT STIMULATOR CONTROL

sensors were tested with applied pressures in the range 0 - 3.5  $Kg/cm^2$  which is the value suggested by Godfrey et al. [317] as the maximum underfoot stress encountered during normal walking.

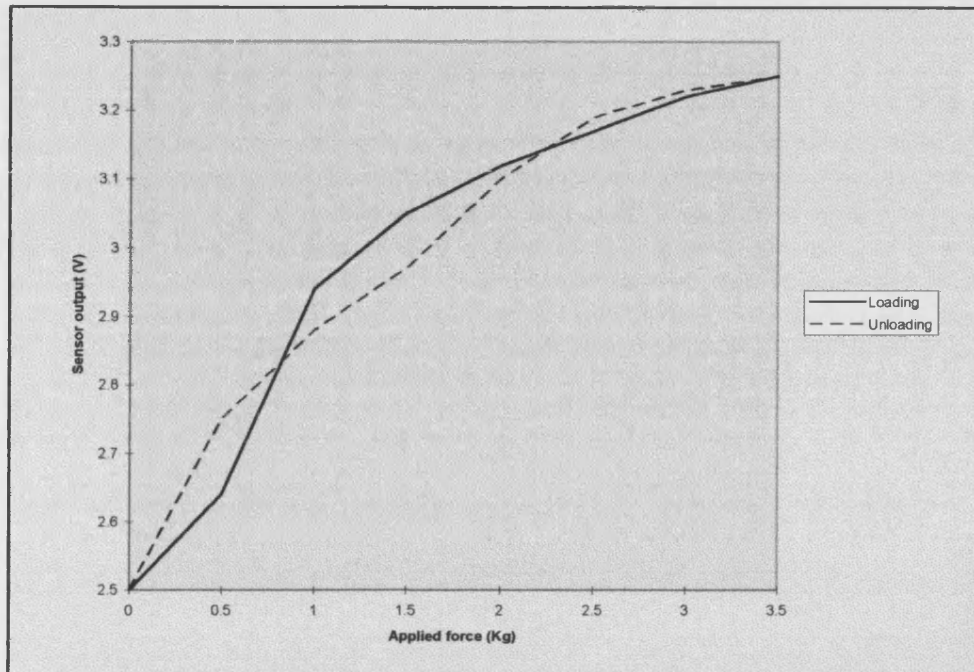


Fig. 5.7 Underfoot pressure sensor tests.

Fig 5.7 shows that the hysteresis associated with this system is acceptable, which ensures that both the rising and falling pressure transitions occurring during gait will be equally detected. Fig. 5.8 shows the response of the system to a suddenly applied and then removed maximum pressure. It can be seen that the response time to this applied pressure is very good and a full scale response is achieved in under 0.1s. The maximum compression resulted in an output signal change of 0.75V. This signal output range is sufficient to permit digitisation without prior gain being applied to increase the signal resolution.

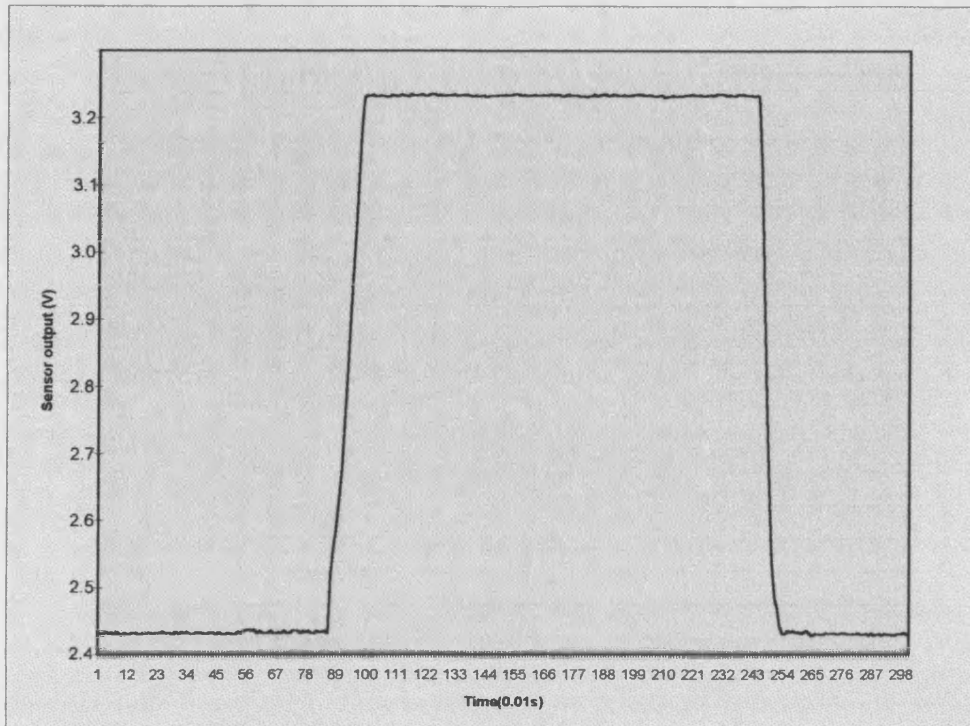


Fig. 5.8 Underfoot pressure sensor response time.

No attempt has been made to perform any absolute pressure calibration of the Hall effect transducer as it was decided to use only the pressure transitions to determine the quality of the gait and provide information to the stimulator. It was decided that the use of these transitions would alleviate many of the problems associated with sensor drift, permanent deformation of the compressive element and initial sensor calibration.

These tests only show the short term functionality of the pressure sensing system. Repeated testing will be required to perform an evaluation of the long term system reliability. Such testing is described by McFadyen et al. [230].

### 5. 10 Pressure distribution data acquisition.

In order to facilitate the investigation of the underfoot pressure patterns, a method of recording the pressure data was required. This permits the acquired data to be logged and plotted to produce a graphical representation of the pressure distribution with time and movement.

The data logger was based on a 386 PC, employing a proprietary analogue to digital conversion (ADC) card mounted in one of the ISA expansion slots. This ADC card, the AD1220 from

## **CHAPTER 5 INTELLIGENT STIMULATOR CONTROL**

Flight Electronics, enables the user to sample up to sixteen single ended analogue channels and, if desired, effect analogue or digital outputs on separate, dedicated output channels. The AD1220 permits throughput rates of up to 100 kHz and is supplied with pre-compiled C routines to enable the data to be sampled. These routines are for inclusion within a DOS-based C program that initiates the sampling and stores the data. The sample and conversion rate of 100 kHz is more than adequate for data sampling during walking which occurs at approximately 1 Hz, permitting up to several thousand data samples per channel per second. This permits the use of the 100 Hz sampling rate successfully used by Kljajic and Krajnik [277] and Jarrett et al. [287] and allows an improvement on the 50 Hz sample rate utilised by Kernozek et al. [313] to record gait information.

The C program written to perform the sampling of the pressure data is included in appendix J and operates in the manner shown in the flow diagram of fig. 5.9.

The program generates a file of data corresponding to each sensor output. Each data entry in the file is carriage delineated so that it can be used in a data analysis software package. The 640 Kbytes DOS file size restriction limits data storage to 3000 samples per channel, which corresponds to 30 seconds of data storage at the 100 Hz chosen sample rate. It was found that 30 seconds of gait data was perfectly adequate for the analysis of gait, as this allows sufficient time for the user to achieve an even stride pattern after the irregularity of the gait initiation.

The PC and acquisition card were used to acquire pressure data to enable the effectiveness of the sensors to be evaluated and to show the underfoot pressure distributions of healthy and stroke affected gait using the Hall effect sensing devices, placed as described in section 5.8.

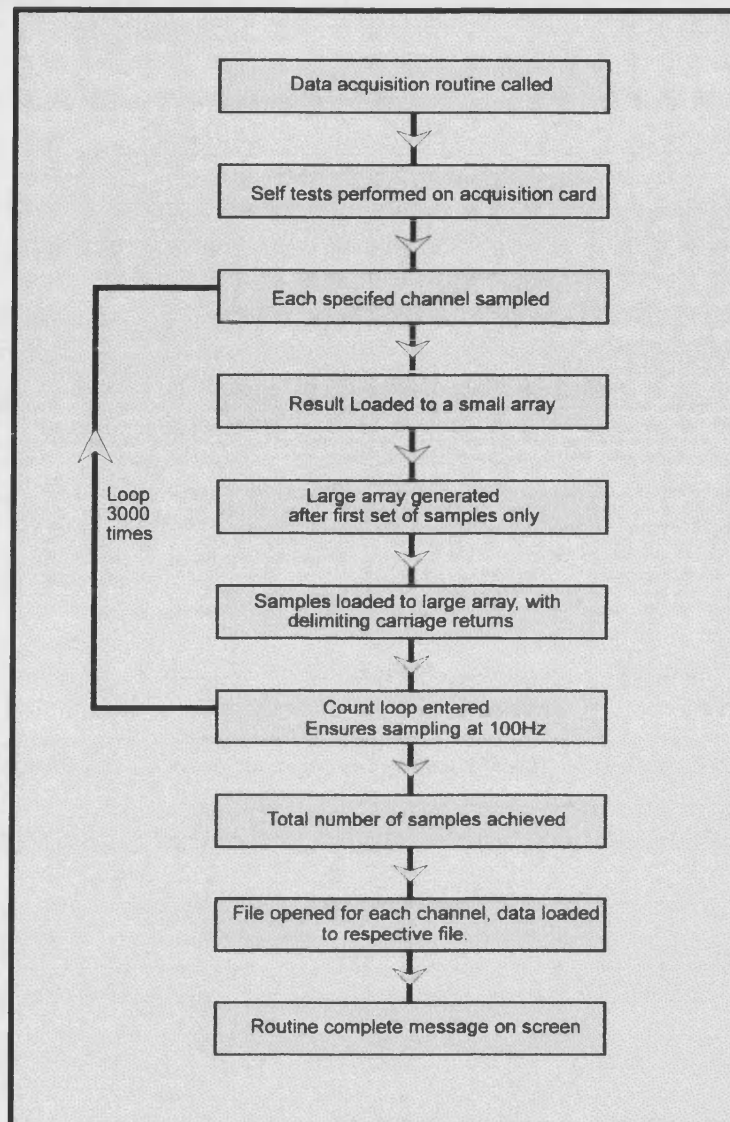


Fig. 5.9 Data acquisition software flow diagram.

The sensor outputs were wired to the acquisition card connector using an umbilical ribbon cable to minimise cable weight. In order to reduce the length of this cable and maximise the available distance for the thirty seconds of stride analysis, the PC and power supply were mounted on a trolley and wheeled along beside the person participating in the tests. This arrangement is shown in fig. 5.10. These tests were either carried out in a corridor to maximise the regularity of the gait pattern or on a treadmill, set to operate at a comfortable speed for the participant. Many of the stroke affected persons had their gait analysed on the treadmill to minimise the risk of injury due to the trailing cables.



Fig. 5.10 Pressure distribution data acquisition in progress.

### 5. 11 Normal gait data observations.

Initially, the variation in the underfoot pressure distribution with time was investigated on healthy persons with no obvious gait abnormalities or history of gait related conditions. This was to verify sensor performance and to develop an understanding of the characteristic pressure patterns produced by normal gait when using the Hall effect underfoot pressure sensing system.

The initial trials were performed on a random sample of fifteen healthy individuals in the age range 23 - 64 years. These trials produced very encouraging results, with the changes in the pressure readings from each of the four sensors occurring in regular patterns. The pressure variation with time from the right heel sensor of one healthy individual during thirty seconds of walking at a pace comfortable to the individual is shown in fig. 5.11 as a line graph. Fig. 5.12 shows the pressure variation on an expanded timebase. It is clear from this graph that the hall



## CHAPTER 5 INTELLIGENT STIMULATOR CONTROL

effect devices and neoprene pressure sensing mats provide reliable and reproducible results in the short term.

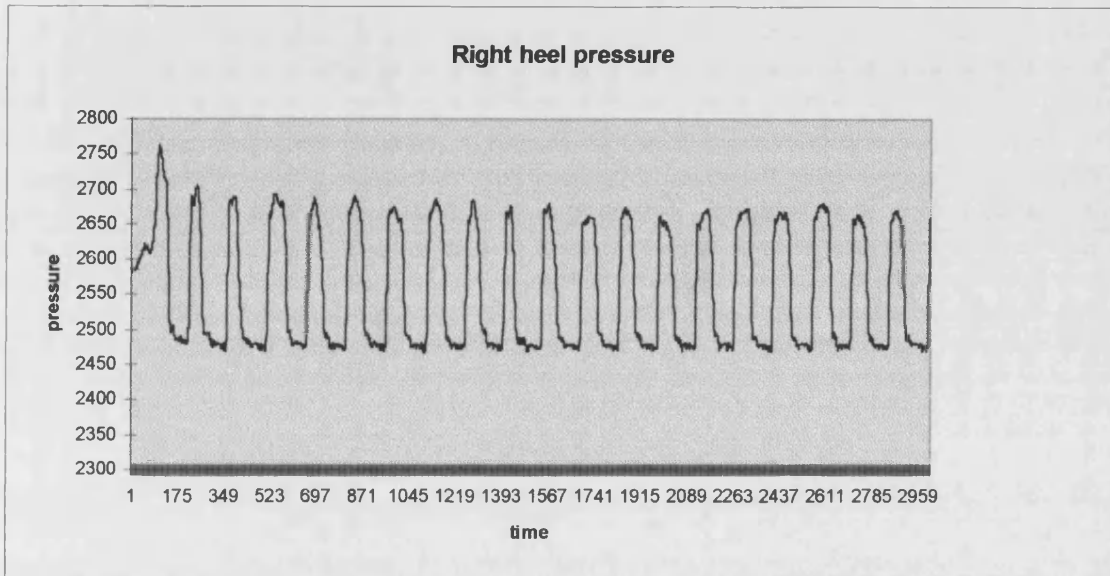


Fig. 5.11 Healthy gait right heel pressure variation with time.

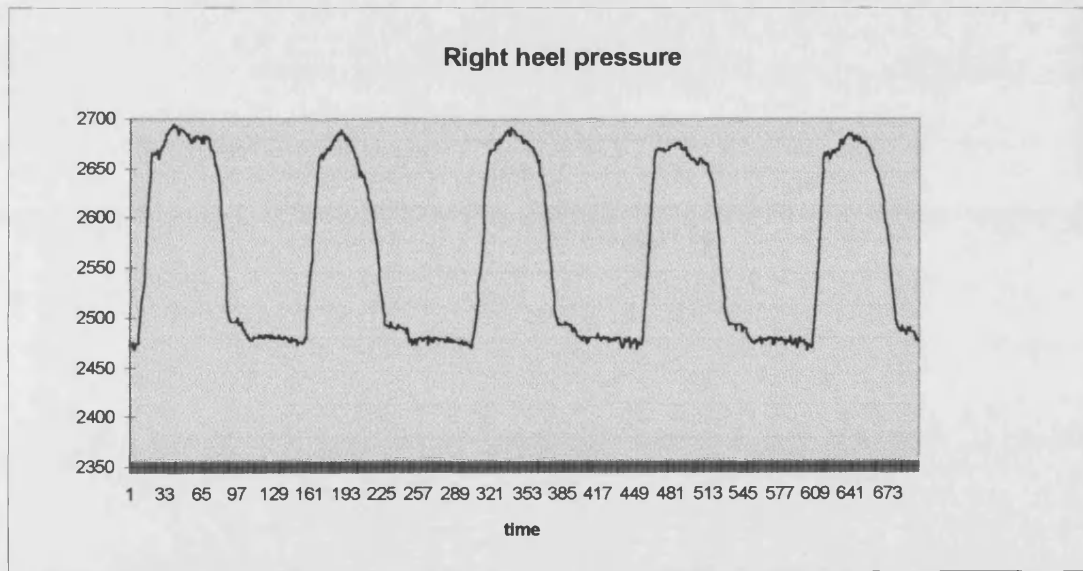


Fig. 5.12 Healthy gait right heel pressure variation with expanded timebase.

## **CHAPTER 5 INTELLIGENT STIMULATOR CONTROL**

It should be noted that the pressure axis values represent uncalibrated, digitised sensor outputs. It may be observed that the patterns shown in the expanded timebase version of the gait conform to a general pattern during the gait cycle but exhibit some differences to the shapes of the pressure traces within this pattern on a stride by stride basis. The phenomenon of small alterations to the underfoot pressure traces associated with normal gait has been observed by Mizayaki and Iwakura [88] and is inferred by Winter [45] who states that slight balance corrections are always being performed by the central nervous system during walking. These underfoot pressure trace differences may therefore be considered as an integral part of normal gait

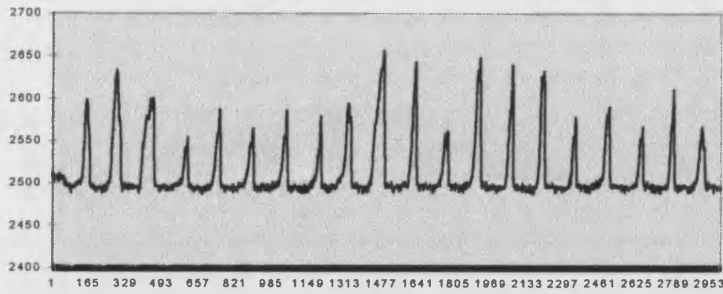
In fig. 5.12, the sharply rising sections following a trough represent the heel strike. The following rounded peak shows how the foot rolls forward and the more gradual descent represents the shift of the body weight towards the front of the foot. The troughs represent the swing phase of the gait, where the foot is clear of the ground. This trace, typical of those from the heel sensor of healthy individuals, bears a close resemblance to that produced by the equipment used by Miyazaki and Iwakura [88], showing that the pressure trace obtained is an accurate representation of the underfoot pressure at this site.

The detail apparent in the pressure variation of fig. 5.12, opened up the possibility of the use of the pressure sensing system as a gait analysis tool to evaluate the effectiveness of all foot drop stimulation systems, as well as for the provision of gait information to the intelligent stimulator. The detail present in the obtained traces resulted in the adoption of this method of gait analysis for the intelligent stimulation system, so further analysis was performed on the gait of both healthy and stroke affected persons.

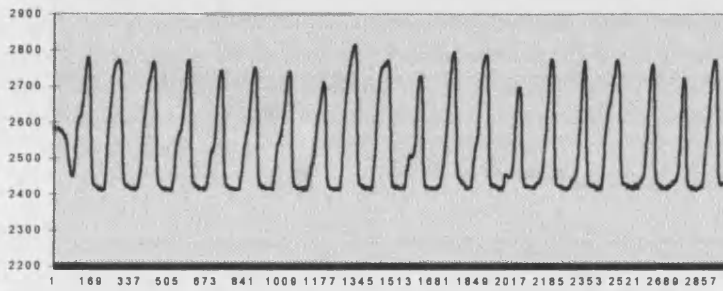
The heel was used in the initial sensor tests as this is the site of the largest pressure excursions, which produces the highest quality outputs. Naturally, to gain a detailed insight into the complete gait cycle, the analysis of all eight sensor outputs is required. Fig. 5.13 shows the output from each of the four right foot pressure sensors during the gait of a normal individual and represents thirty seconds of normal gait. The pressure variation traces are arranged in order to indicate the method by which the pressure is transferred along the foot within the different phases of the gait. The traces in fig. 5.13 show that the patterns produced by the sensors are uniform in nature once a regular stride has been achieved, again confirming that this sensor arrangement is a suitable method of stimulator control. This uniformity is a feature common to all the data obtained, both from those with normal gait and from those with stroke-related abnormal gait.



## CHAPTER 5 INTELLIGENT STIMULATOR CONTROL



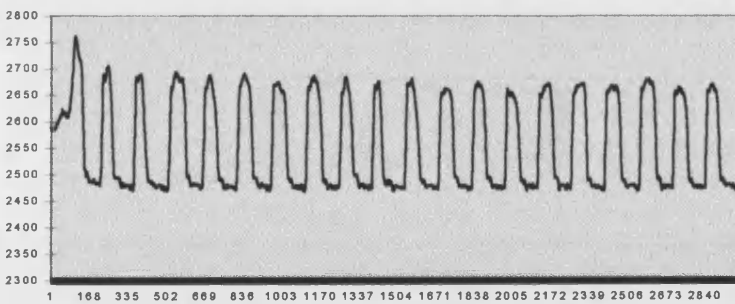
Toe sensor.



First metatarsal.



Fifth metatarsal.



Heel sensor.

Fig. 5.13 Pressure variation under the right foot of a person exhibiting normal gait.

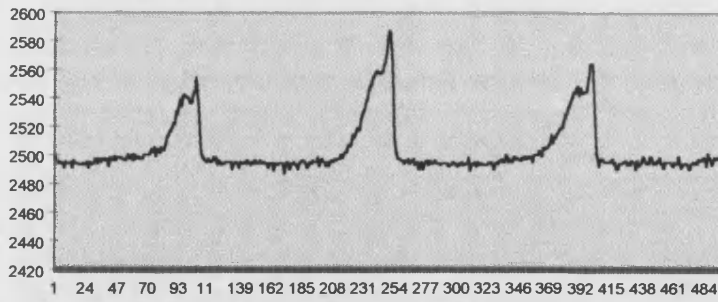
## **CHAPTER 5 INTELLIGENT STIMULATOR CONTROL**

Having established that the pressure variation can be considered as a regularly repeating pattern peculiar to that individual, all data from now on will be shown in the expanded timebase form of fig. 5.12, to ensure clarity and permit the time dependant relationships between the different sensors to be examined. The uniform nature of the data from the sensors removes the need to examine any particular section of this data. When data from several sensors is being compared, it is essential to preserve the phase relationships. Therefore, the compared sections always begin and end with an equivalent data sample, chosen to be at an arbitrary point within the sample range.

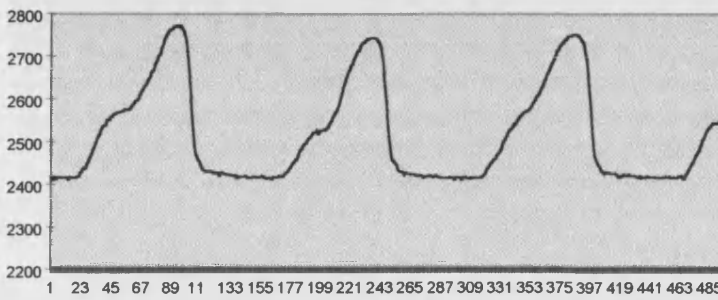
Fig. 5.14 shows an expanded timebase section of the data obtained from under the right foot of a person exhibiting normal gait and permits an examination of the phase relationships between the four sensors. The heel and metatarsal traces of fig. 5.13 and fig. 5.14 show a marked resemblance to the characteristic heel and metatarsal traces detected by the equipment used by Miyazaki and Iwakura [88]. In addition, all four traces closely resemble the results obtained by the multi-sensor instrumented footwear used by Pollard et al. [307]. This further reinforces the accuracy of the Hall effect pressure detection system.

It may be seen in fig. 5.14 that the slight changes in weight distribution do not alter the phasing of the sensor outputs and have no significant effect on the initial pressure rise and fall, reinforcing the decision taken to use the pressure rise and fall data rather than the magnitude data.

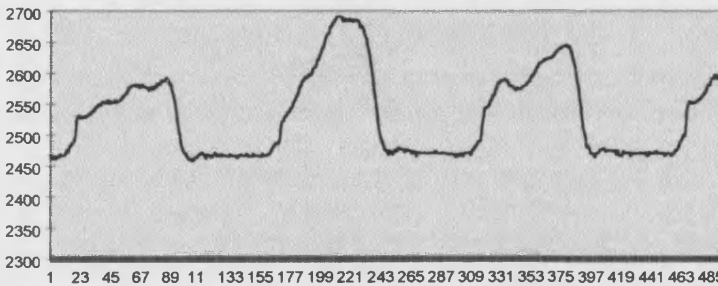
## CHAPTER 5 INTELLIGENT STIMULATOR CONTROL



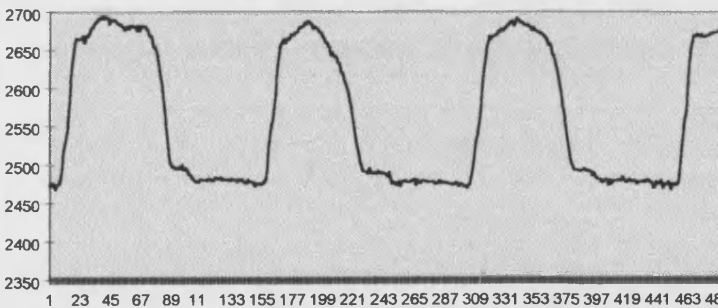
Right toe.



First metatarsal.



Fifth metatarsal.



Right heel.

Fig. 5.14 Right foot pressure variation with normal gait.

## **CHAPTER 5 INTELLIGENT STIMULATOR CONTROL**

---

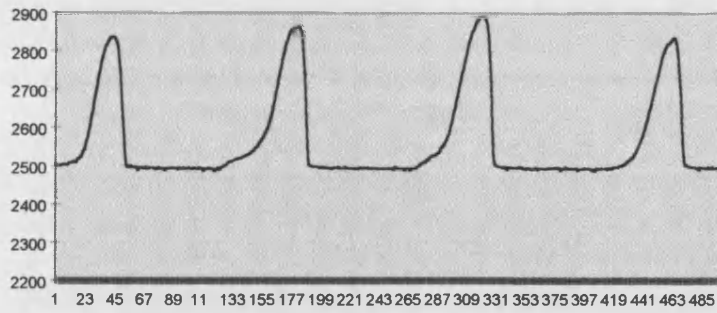
Having shown that the foot pressure data from any one individual is adequately repeatable to be utilised to form the basis of a stimulator control signal, it remains to be demonstrated that the data from different individuals possess significant similarities to enable a global algorithm to be devised to control the stimulator when attached to any patient. Stroke affected patient gait varies radically between individuals, depending upon the severity of the condition. If it can be demonstrated that normal gait between individuals has significant similarities, then one model may be formed to represent normal gait. A control algorithm can then be constructed to enable the stimulation system to alter the patient gait to force this into the pattern of the obtained model of normal gait.

Fig. 5.15 shows the pressure variation with time under the right foot of a second individual with normal gait. It may be observed that the phasing of the sensor outputs and the pressure rise and fall rates are strikingly similar to that seen in fig. 5.14.

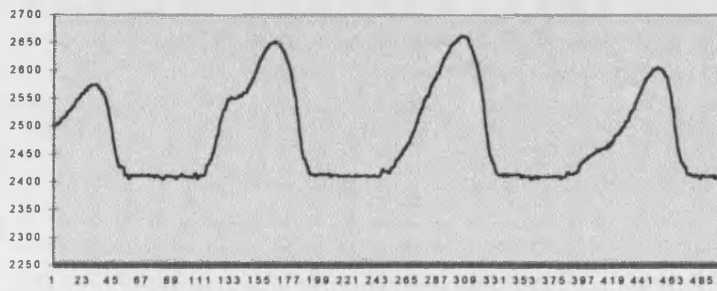
The time pressure variation under the left foot of individuals with normal gait bears the same similarities as that shown under the right foot and may in fact, be considered as a phase shifted version of the right foot pressure data. The pattern observed in the pressure variation under the right foot is maintained in the left foot pressure variation, showing a large degree of symmetry between the two sides of the body during locomotion. The patterns produced by the sensors are never identical, however, as are no two right foot analyses, mainly due to the slight centre of gravity shifts across the metatarsals, caused by the ankle balance strategies described by Winter [45]. The pressure variations under the left foot of those with normal gait will not be discussed further in isolation, rather the two sets of data will now be treated as one extended set of data encompassing the complete gait cycle.

The left and right foot pressure data is shown together in fig. 5.16. Fig. 5.17 and fig. 5.18 show the complete eight sensor pressure variations for a further two individuals. These traces are included to further demonstrate the phase and slope relationship similarities between different individuals with normal gait across the complete gait cycle.

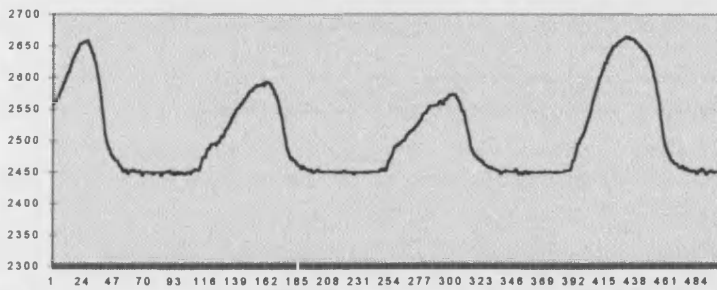
## CHAPTER 5 INTELLIGENT STIMULATOR CONTROL



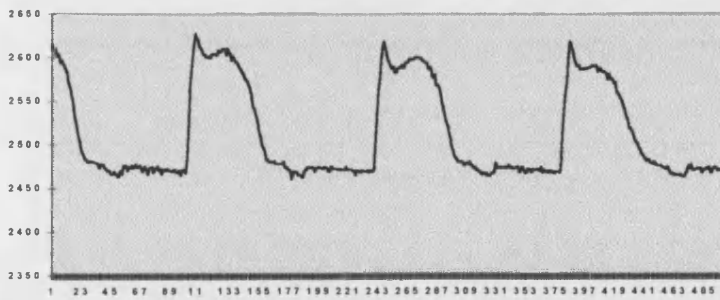
Right toe.



First metatarsal.



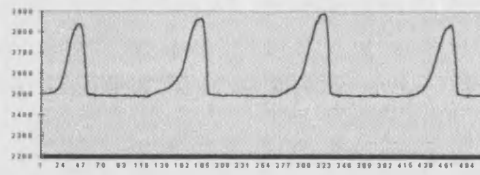
Fifth metatarsal.



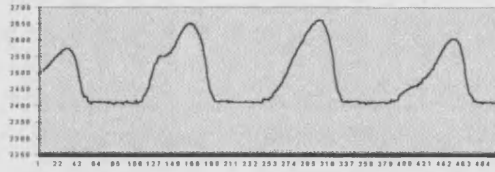
Right heel.

Fig. 5.15 Pressure variation under the right foot during normal gait.

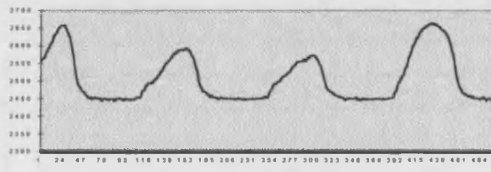
## CHAPTER 5 INTELLIGENT STIMULATOR CONTROL



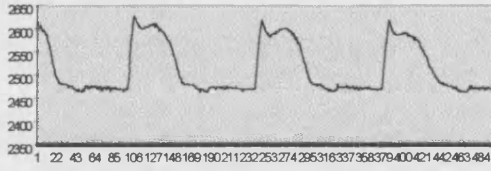
Right toe.



Right 1st metatarsal.



Right 5th metatarsal.



Right heel.



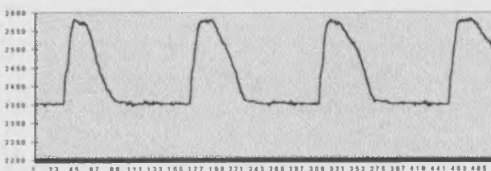
Left toe.



Left 1st metatarsal.



Left 5th metatarsal.



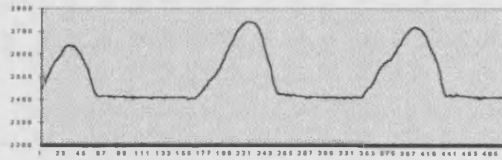
Left heel.

Fig. 5.16 Left and right foot pressure variations for healthy gait.

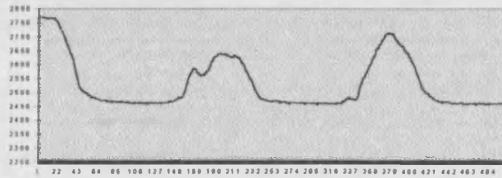
**CHAPTER 5 INTELLIGENT STIMULATOR CONTROL**



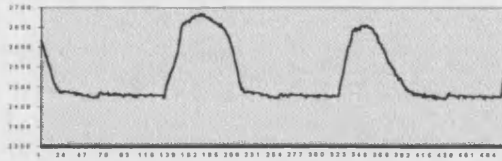
Right toe.



Right 1st metatarsal.



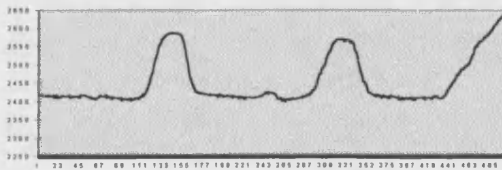
Right 5th metatarsal.



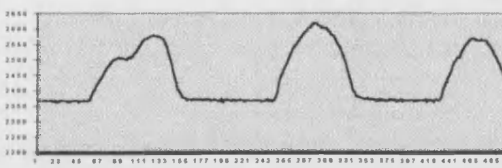
Right heel.



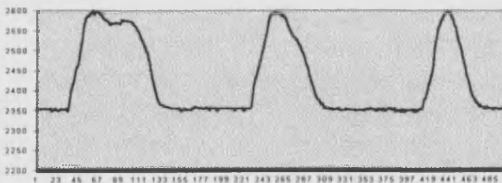
Left toe.



Left 1st metatarsal.



Left 5th metatarsal.

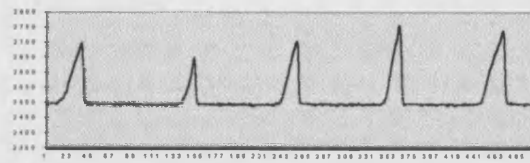


Left heel.

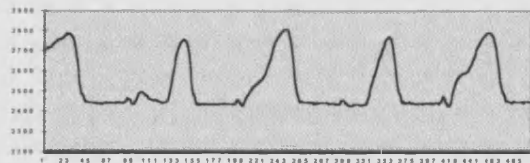
Fig. 5.17 Complete pressure variation for a second normal gait individual.



**CHAPTER 5 INTELLIGENT STIMULATOR CONTROL**



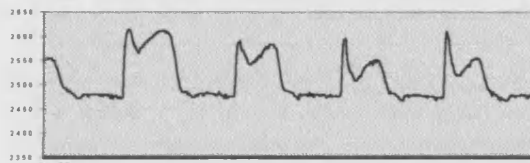
Right toe.



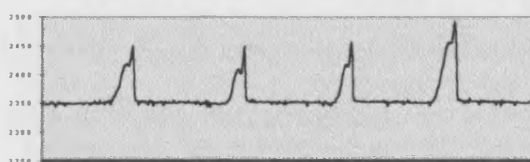
Right 1st metatarsal.



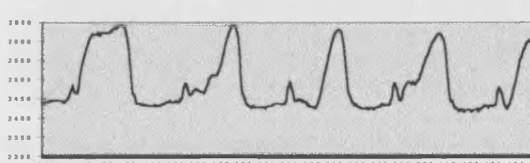
Right 5th metatarsal.



Right heel.



Left toe.



Left 1st metatarsal.



Left 5th metatarsal.



Left heel.

Fig. 5.18 Complete pressure variation for a third normal gait individual.



---

## **CHAPTER 5 INTELLIGENT STIMULATOR CONTROL**

---

The minor pressure variations between like sensor outputs, best illustrated by the first and fifth metatarsal data, show that if any particular sensor output were to be used as a stimulation control in isolation, false stimulator operation would be a likely result. This leads to the requirement to always utilise as many sensor outputs as possible at any one time when effecting a decision. This strategy permits a form of error checking to be incorporated within the structure of the program by always tracking the pressure changes through the gait cycle and corroborating each sensor output by comparison with the data from other sensors.

The fifth metatarsal trace of fig. 5.18 serves to illustrate that occasionally one part of the gait cycle as detected by a particular sensor varies significantly from the general pattern of pressure readings obtained from that sensor. It can be observed from fig. 5.13 to fig. 5.18 that these 'abnormal' pressure readings can occur on any of the sensors due to random alterations in the gait of the individual. It therefore follows that the intelligent stimulator should acquire the gait data over several strides and reject any data vastly different to the other data acquired within that sample period. This data rejection permits the 'filtering out' of any random gait deviations and permits the applied stimulation to be updated every  $\eta$  strides. The value of  $\eta$  is currently set to 5 strides.

### **5. 12 Stroke affected gait observations.**

Having examined the underfoot pressure data from the gait associated with a number of different healthy individuals and discerned that there are certain characteristics common to all normal gait data, it was necessary to perform similar underfoot pressure measurements on those whose gait has been affected by a CVA. This data differed significantly from patient to patient as expected, with the degree of difference from normal gait data dictated by the severity of the CVA and the degree of recovery achieved by the patient.

It should be noted that in all cases the pressure sensing mat must be constructed to ensure a correct fit to the foot of the patient, as stated by Hargreaves and Scales [308]. If an incorrect size of mat is used, then important data is lost as pressure will be applied to incorrect sites upon the mat. If the mat is too short or too long for the foot, then the toe data is usually the first sensor output to be degraded and lost. It was found that one mat size was sufficient for every two shoe sizes i.e. patients with a shoe of size nine or ten could share one size of mat but other shoe sizes required a separate size of sensing mat.

The under foot pressure data shown in fig. 5.19 is derived from the left foot of a left side hemiplegic stroke patient with no applied stimulation and when compared with fig. 5.15, clearly

## **CHAPTER 5 INTELLIGENT STIMULATOR CONTROL**

shows the type of abnormalities common to foot drop gait. This time varying pressure distribution can be seen to be significantly different from the traces obtained from healthy persons, shown in fig. 5.13 to fig 5.18.

The toe pressure data is expressed as an event with slow, approximately equal rise and fall rates. This is due to what may be described as 'flat footed' walking. In normal gait, a slow pressure rise is observed as the foot rolls forward, followed by a fast pressure fall subsequent to push off. The flat footed gait is further confirmed by the slow and approximately equal rate of rise and fall of heel pressure. These details show that the toes are not being raised during the swing phase and hence the foot is landing flat, degrading the heel strike. This degradation is due to the impact impulse being spread over the complete foot area instead of just the heel area. This also results in the commencement of the toe pressure rise in advance of the timing expected from normal gait. A further indication of the foot landing flat is the simultaneous activity of all four of the pressure sensors, showing that the foot has been raised and placed flat and is not exhibiting the characteristic heel to toe progression of normal gait.

The gait anomalies of fig. 5.19 are not especially severe, as there is some pressure activity under the toes, which is often the most easily observed pressure data anomaly in foot drop gait. This can be degraded to such an extent that the toe pressure pattern becomes a mere ripple.

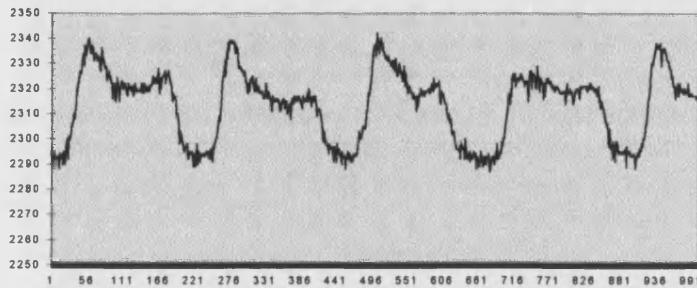
If the right foot pressure data of the left side hemiplegic is examined, as shown in fig. 5.20, it may be seen that the pressure progression is similar to that observed with normal gait. The heel strike is well defined, with the pressure rising on the metatarsals as the pressure under the heel slowly reduces. The toe pressure is seen to ramp up slowly and then fall rapidly, demonstrating that push off is occurring on this foot. Finally, the correct phasing is seen across the data, with the pressure progressing from the heel to the toe. This result is expected, as the right side is the unaffected side of the body and maintains a reasonably normal gait.

The essentially normal gait of the unaffected side reinforces the need to sample the underfoot pressure from both feet as the almost unaffected gait of one side of a hemiplegic becomes a powerful tool when used to supply the stimulator with gait information. The reliable data from the unaffected side ensures that a greater number of correct decisions are made than would have been the case with only the use of abnormal pressure data.

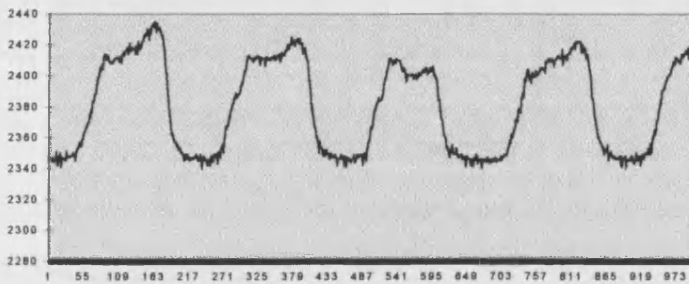
Fig 5.21 to fig 5.23 are examples of the complete, eight sensor, underfoot pressure data variation for three different stroke patients. These illustrate the variability of the gait

## CHAPTER 5 INTELLIGENT STIMULATOR CONTROL

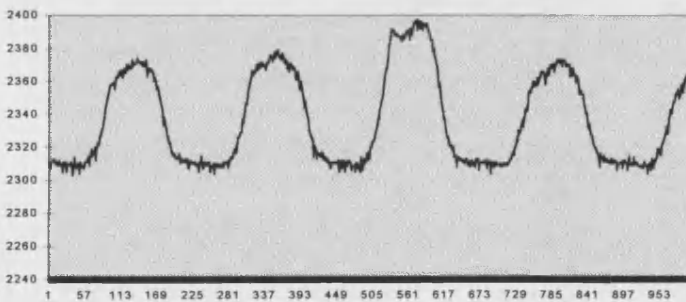
abnormalities and serve to show that definite differences exist between stroke affected gait pressure data and normal gait pressure data.



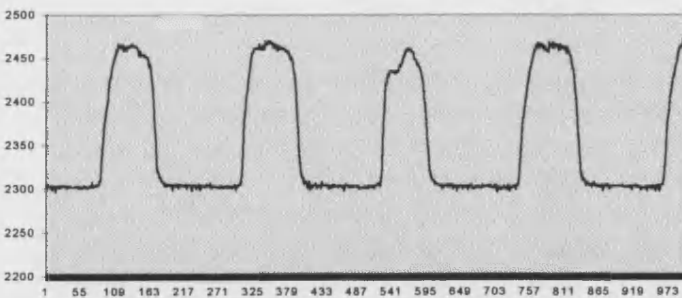
Left toe.



Left 1st metatarsal.

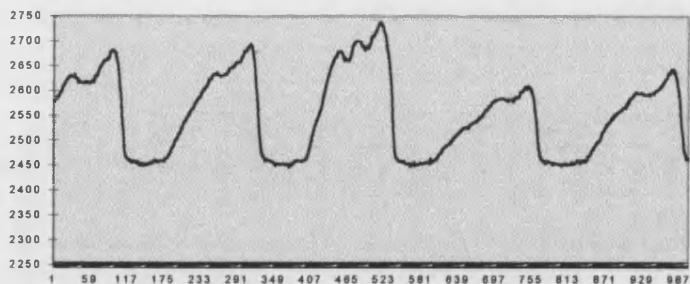


Left 5th metatarsal.

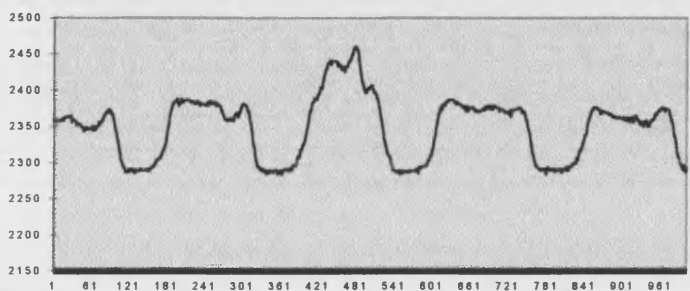


Left heel.

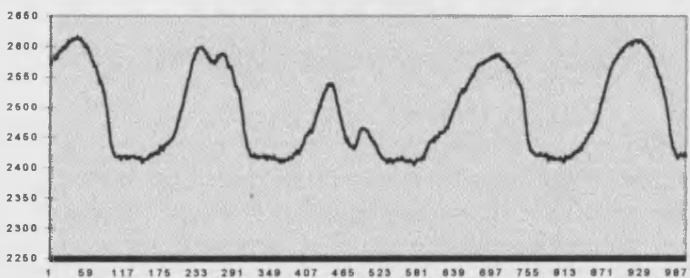
Fig. 5.19 Left foot pressure data from a left side hemiplegic patient.



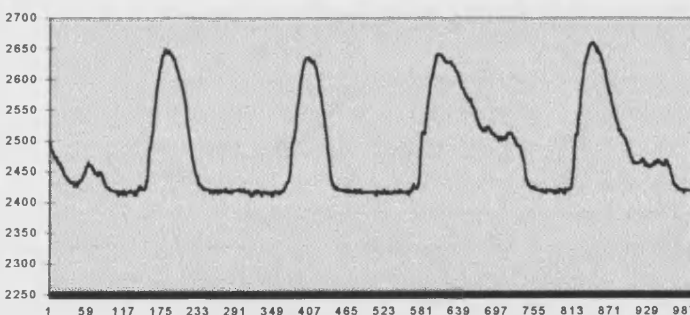
Right toe.



Right 1st metatarsal.



Right 5th metatarsal.



Right heel.

Fig. 5.20 Right foot pressure data from left side hemiplegic.

## **CHAPTER 5 INTELLIGENT STIMULATOR CONTROL**

---

Fig. 5.21 shows the foot pressure variation for a left side hemiplegic whilst walking on the treadmill. The right foot pressure variations are similar to those found in normal gait, though modified slightly due to the burden of the affected side. The right toe pressure is seen to ramp up excessively slowly in relation to its fall time, indicating a lack of push off from the left side which should thrust the bodyweight forward. This is further confirmed by the left toe trace representing little more than a slight pressure variation. It should be noted that the right and left toe pressure traces in fig. 5.21 represent significantly different magnitudes of pressure variation with the left toe trace plotted on an expanded vertical scale.

A comparison of the two heel traces shows a good quality heel strike on the unaffected side, whilst a slower pressure ramp is observed on the affected side, indicating the characteristic flat footed hemiplegic stride.

A further observation is the absence of symmetry between the two foot pressure traces. The affected left side is seen to be in contact with the ground for a far shorter period than the unaffected right side and is due to the uncertain forward movement and placement of the affected side. Great care is being taken by the patient to ensure a careful movement and placement to the stance phase, to fully ensure that the toe clears the ground during the swing phase. Once again, a steady progression of pressure is noted in the unaffected side, whilst the affected side pressure traces rise and fall simultaneously, indicating a flat footed entry to the stance phase.

Fig. 5.21 and fig. 5.22 are both plots of the underfoot pressure variation of left side hemiplegics, so consequently they appear very similar. Fig. 5.23, however, is the underfoot pressure variation from a bilateral foot drop sufferer. The pressure variation characteristics in these plots clearly show that all the previously discussed characteristic gait abnormalities are present under both feet. The decision making in the case of bilateral foot drop patients is more complex than in the hemiplegic patients as there is no longer one set of accurate pressure data to rely on. The foot pressure data is not too dissimilar to that of the affected hemiplegic side and so may be processed in a similar manner.

## CHAPTER 5 INTELLIGENT STIMULATOR CONTROL



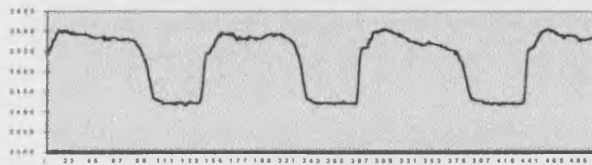
Right toe.



Right 1st metatarsal.



Right 5th metatarsal.



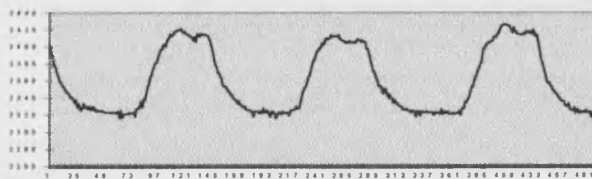
Right heel.



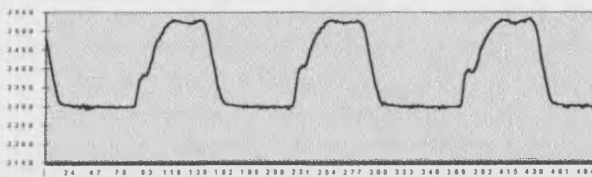
Left toe.



Left 1st metatarsal.



Left 5th metatarsal.



Left heel.

Fig. 5.21 Complete underfoot pressure variation for a left side hemiplegic.

## CHAPTER 5 INTELLIGENT STIMULATOR CONTROL

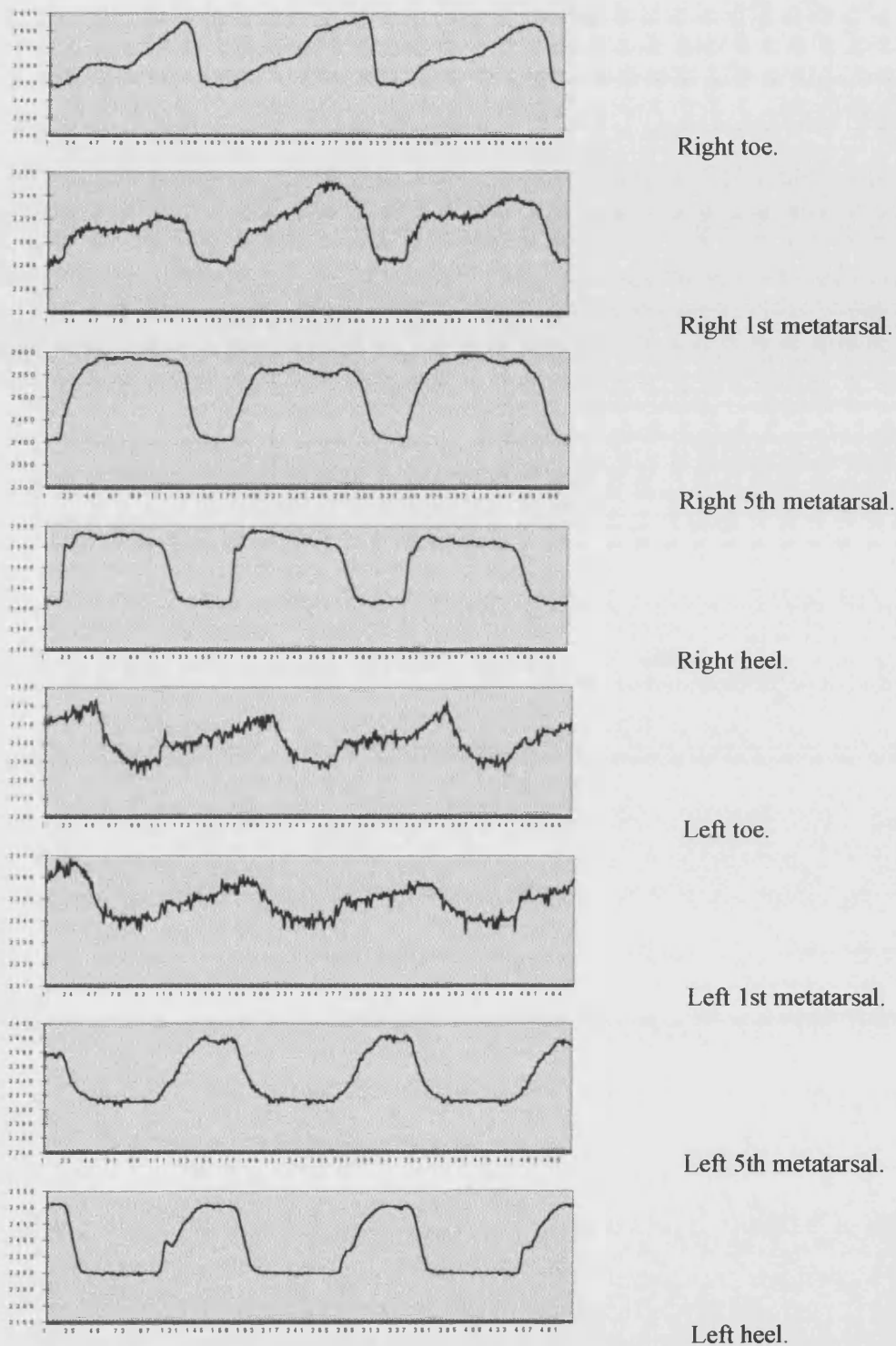


Fig. 5.22 Complete pressure variation for a left sided hemiplegic.

## CHAPTER 5 INTELLIGENT STIMULATOR CONTROL

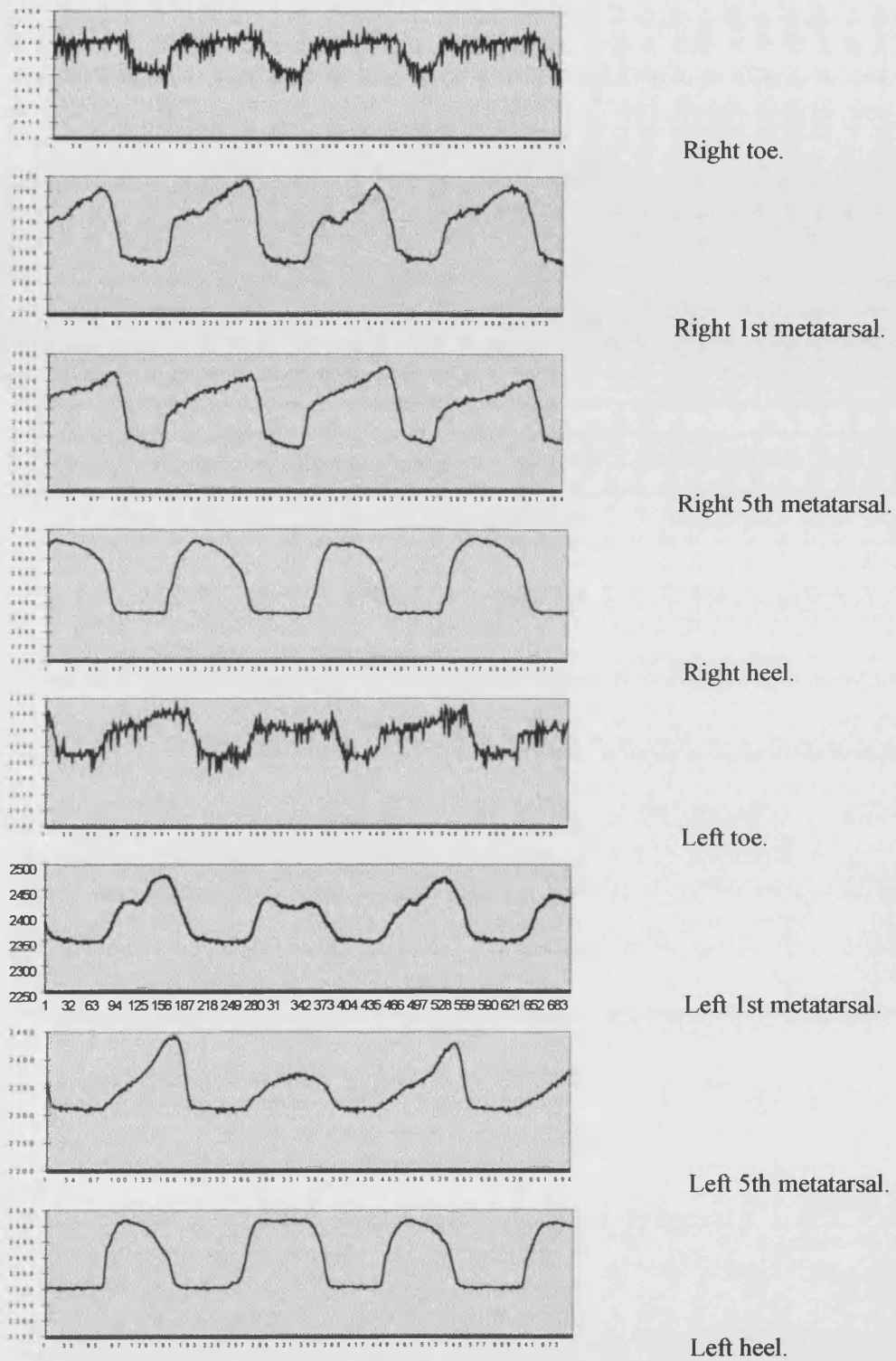


Fig. 5.23 Complete pressure variation for bilateral drop foot patient.



**5.13 Underfoot pressure trace analysis.****5.13.1 Analysis introduction.**

The underfoot pressure traces have been mentioned in a qualitative manner in section 5.13. The general trends in the pressure distribution throughout the gait cycle have been discussed along with the observable differences between the underfoot pressure distributions associated with normal and pathological gait. These comparisons have demonstrated that there are observable differences and it remains to quantify the observed differences so that the master microcontroller is able to numerically evaluate the patient gait.

There were found to be observable differences in the relative timing of the underfoot pressure transitions and the rate of change of pressure at these transitions. These are, therefore, the quantities analysed in this section. The data utilised is from the fifteen stroke patients and fifteen normal volunteers and this permits a comparison to be made between stroke affected and normal gait. The pressure data from both feet of the normal volunteers was utilised in the analysis, although only the data from the affected side of the stroke patients was included. This was done as it has been noted in section 5.13 that the foot pressure data from the unaffected side of the stroke patients bore many similarities to that from the normal volunteers and it was considered that the greatest differences would be produced by the use of the data from the affected side. Naturally, the pressure distributions from the unaffected side are still utilised to provide gait cycle tracking data.

**5.13.2 Underfoot pressure transition relative timing.**

It may be seen by superimposing the pressure transitions from the four sensors under a single foot that the relative timing of the pressure transitions varies considerably between the affected side of stroke patient gait and normal gait. Fig. 5.24 shows a four sensor output plot from a person with normal gait. The pressure transitions can be seen to progress from the heel to the first and fifth metatarsals and then to the toe, as expected with the classic gait phases of heel strike, early stance, mid stance, late stance and push off.

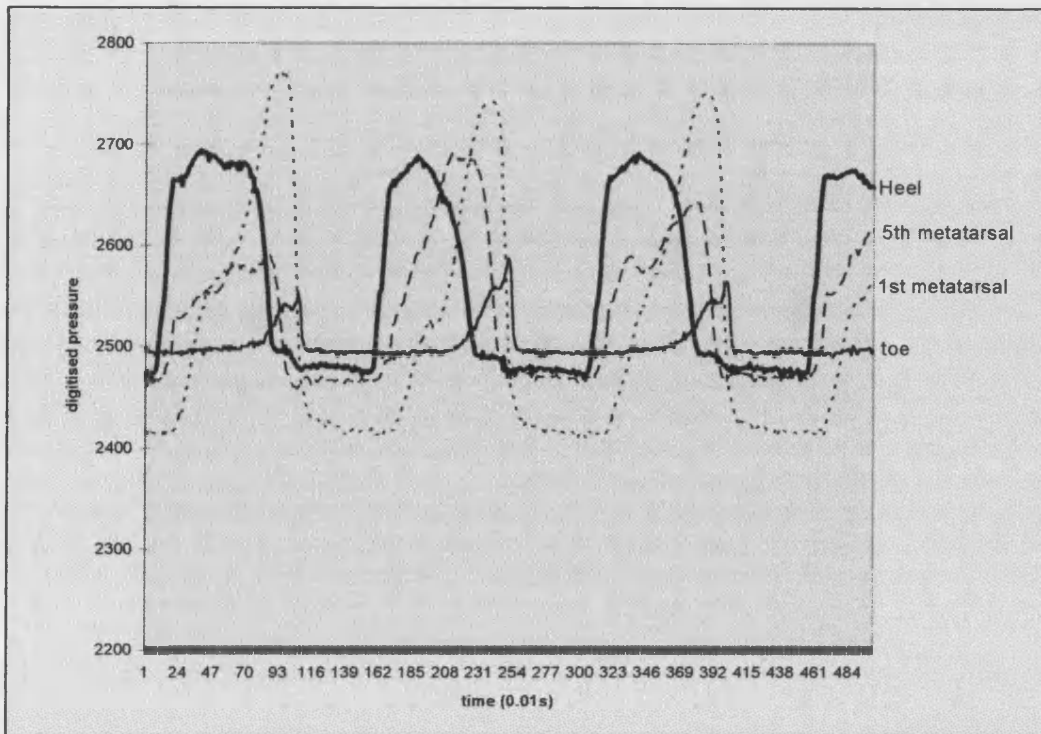


Fig. 5.24 Superimposed four sensor output from normal gait.

The fifth metatarsal pressure rise leads the first metatarsal pressure rise showing a slight tendency to take the bodyweight on the outside of the foot, although this does not affect the heel to toe sequence. Fig. 5.25 shows a four sensor trace where the data was acquired from the affected side of a stroke patient.

This trace shows that a flat-footed gait has been adopted by the patient as the result of insufficient toe lift. It can be seen that the rising pressure transitions from all four sensors occur at the same point within the gait cycle, i.e. at the point at which the foot is placed flat upon the ground. It may also be seen that very little plantarflexion occurs as the toe and metatarsal pressure falls occur at the same point within the gait cycle and the toe pressure rise is very small. This shows a much reduced push off as well as the insufficient toe lift mentioned earlier.

The timing of the gait events was defined as the time elapsed from the heel strike of that foot to the beginning of a rising pressure transition at each of the other three sensors on that foot. In order that different gait speeds might be catered for, the time figures are expressed as a percentage of the time taken for one complete gait cycle, measured from heel strike to ipsilateral heel strike.

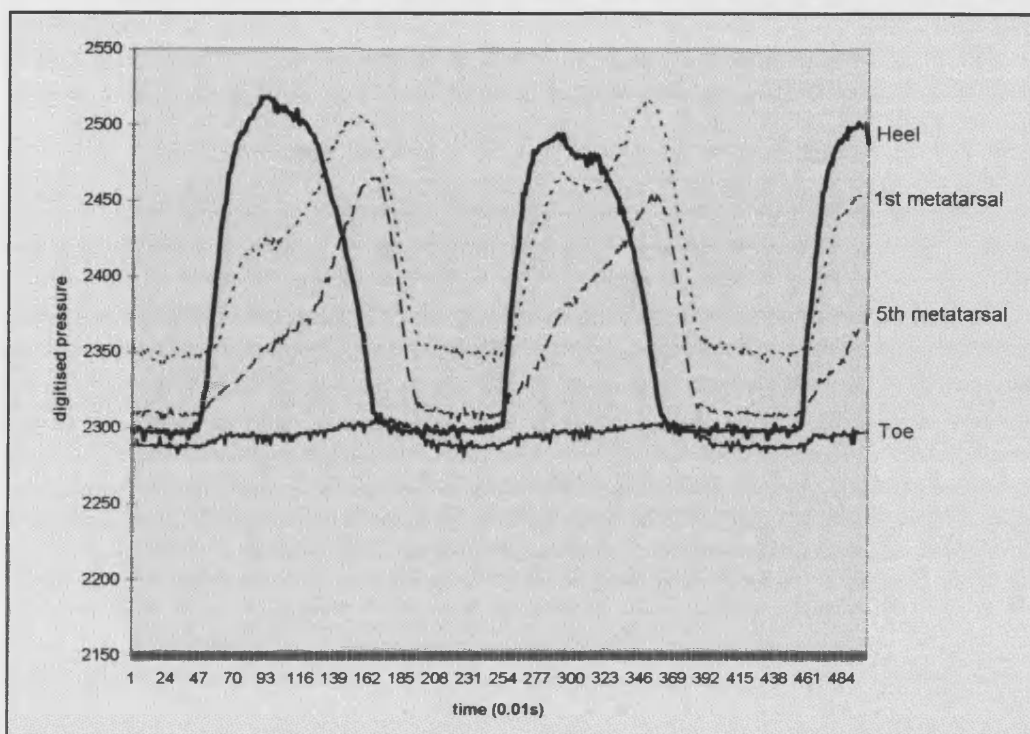


Fig. 5.25 Superimposed four sensor output from stroke gait.

Although the phasing of the stroke affected and healthy gait are very different, it was found that the phasing of the gait of any particular individual was very consistent, once the initial gait initiation stage was complete. This is shown by the following examples from a single normal volunteer and from a stroke patient. In each case, the timing of each of the events that occurred during thirty seconds of walking was used.

**Single Individual normal gait:-**

Time to 1st metatarsal transition.	Average time = 16.5 % of cycle.
	Standard deviation = 6.9 %.
Time to 5th metatarsal transition.	Average time = 6.6 % of cycle.
	Standard deviation = 1.2 %.
Time to toe transition.	Average time = 33.9 % of cycle.
	Standard deviation = 8.4 %.

## **CHAPTER 5 INTELLIGENT STIMULATOR CONTROL**

---

### **Single individual stroke gait:-**

Time to 1st metatarsal transition.	Average time = 1.6 % of cycle. Standard deviation = 2.8 %.
Time to 5th metatarsal transition.	Average time = -3.3 % of cycle. Standard deviation = 1.1 %.
Time to toe transition.	Average time = 1.1 % of cycle. Standard deviation = 3.4 %.

The low figures for the standard deviation (compared to 100 % for a complete gait cycle) show the consistency of the gait exhibited by a single normal and stroke affected individual. Although a single individual for each case is shown to illustrate this consistency, it was found to apply to the underfoot pressure traces of all the healthy and stroke affected individuals whose gait was measured. It should be noted that the positive values are defined as events following the heel strike and negative values as those events preceding the heel strike. Therefore in the stroke gait analysis above, the fifth metatarsal is being placed on the ground prior to the heel showing a flat-footed gait and possibly some foot inversion.

An analysis was then performed on the healthy and stroke affected underfoot pressure data from all fifteen normal volunteers and stroke affected patients, using the data acquired during thirty seconds of walking. The elapsed time is once again stated as the percentage of the gait cycle from the heel strike.

### **Total normal gait analysis:-**

Time to 1st metatarsal transition.	Average time = 16.5 % of cycle. Standard deviation = 7.9 %.
Time to 5th metatarsal transition.	Average time = 5.9 % of cycle. Standard deviation = 2.4 %.
Time to toe transition.	Average time = 34.4 % of cycle. Standard deviation = 13.5 %.

### **Total stroke gait analysis:-**

Time to 1st metatarsal transition.	Average time = -5.4 % of cycle.
------------------------------------	---------------------------------

## **CHAPTER 5 INTELLIGENT STIMULATOR CONTROL**

---

	Standard deviation = 8.0 %.
Time to 5th metatarsal transition.	Average time = -6.0 % of cycle.
	Standard deviation = 6.6 %.
Time to toe transition.	Average time = -7.7 % of cycle.
	Standard deviation = 9.1 %.

This analysis highlights the large differences between the pressure timings of normal and stroke affected gait. The standard deviations result in the following expected ranges for the heel strike to pressure transition timings.

<u>Transition timing</u>	<u>Normal gait.</u>	<u>Stroke gait.</u>
Heel to 1st metatarsal	9.4 % to 23.6 %	-13.4 % to +2.6 %
Heel to 5th metatarsal	3.5 % to 8.3 %	-12.6 % to +0.6 %
Heel to toe	19.9 % to 47.9 %	-16.8 % to +1.4 %

It can be seen that the normal gait range of values are clearly different to the stroke gait range of timing values and that the ranges do not overlap. This permits the master microcontroller to distinguish between normal and stroke related gait by timing the pressure transitions from the heel strike events and adjust the stimulation accordingly.

### **5. 13. 3 Underfoot rate of pressure change analysis.**

In order that compression of the sensor compressive layer over time should not affect the output of the underfoot pressure sensors, it was decided to utilise the rate of change of pressure under the foot during the transition where weight is placed upon or removed from that part of the foot. Section 5.12 has discussed the observable differences in rate of pressure change and the general differences between this parameter in normal and stroke affected gait. It has also been observed that this value is not constant during pressure transitions, demonstrated by the pressure transitions consisting of varying slopes. To overcome the issue of the point at which the pressure gradient should be sampled, it was decided to use the peak rate of change of pressure from each sensor noted for each gait cycle. This produces a single value per sensor per cycle rather than a variety of different rate of change of pressure values.

## CHAPTER 5 INTELLIGENT STIMULATOR CONTROL

It is possible to evaluate the pressure transition gradient on a sample by sample basis according to expression 5.1, where  $S_n$  represents a pressure data sample and  $S_{n+1}$  represents the next sample from that sensor.

$$\text{Gradient} = \frac{(S_{n+1} - S_n)}{0.01} \quad (5.1)$$

This expression produces a value for the gradient at 0.01s intervals. The values produced are in the form of an 8-bit analogue to digital conversion of the sensor outputs, multiplied up to show the rate of pressure change per second. A typical heel sensor output from an individual with normal gait is shown in fig 5.26, with the result of expression 5.1 superimposed upon the pressure trace.

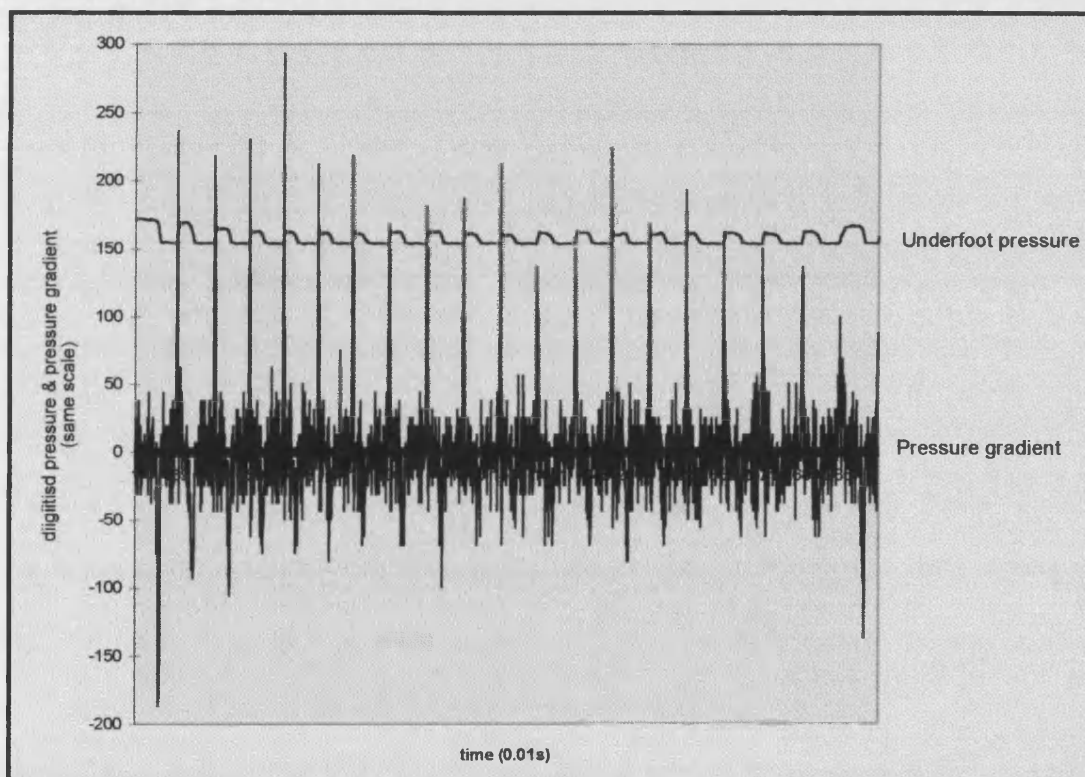


Fig. 5.26 Heel sensor output gradient.

It can be seen that the system noise and the quantisation errors present in the data result in the sample by sample gradient values requiring complex interpretation when the peak rate of pressure change has a low value. This deficiency was overcome by applying a degree of

## CHAPTER 5 INTELLIGENT STIMULATOR CONTROL

smoothing to the gradient expression, using the following expression, where G represents the gradient between successive samples.

$$\text{Smoothed gradient} = \frac{G_n + G_{n+1} + G_{n+2} + \dots + G_{n+10}}{10} \quad (5.2)$$

This averages the gradient over ten samples to show only the true pressure transitions, and may be expressed as:-

$$\text{Smoothed gradient} = \frac{\sum_n^{n+10} S_{n+1} - S_n}{10} \quad (5.3)$$

An example of this treatment of the heel sensor output is shown in fig. 5.27.

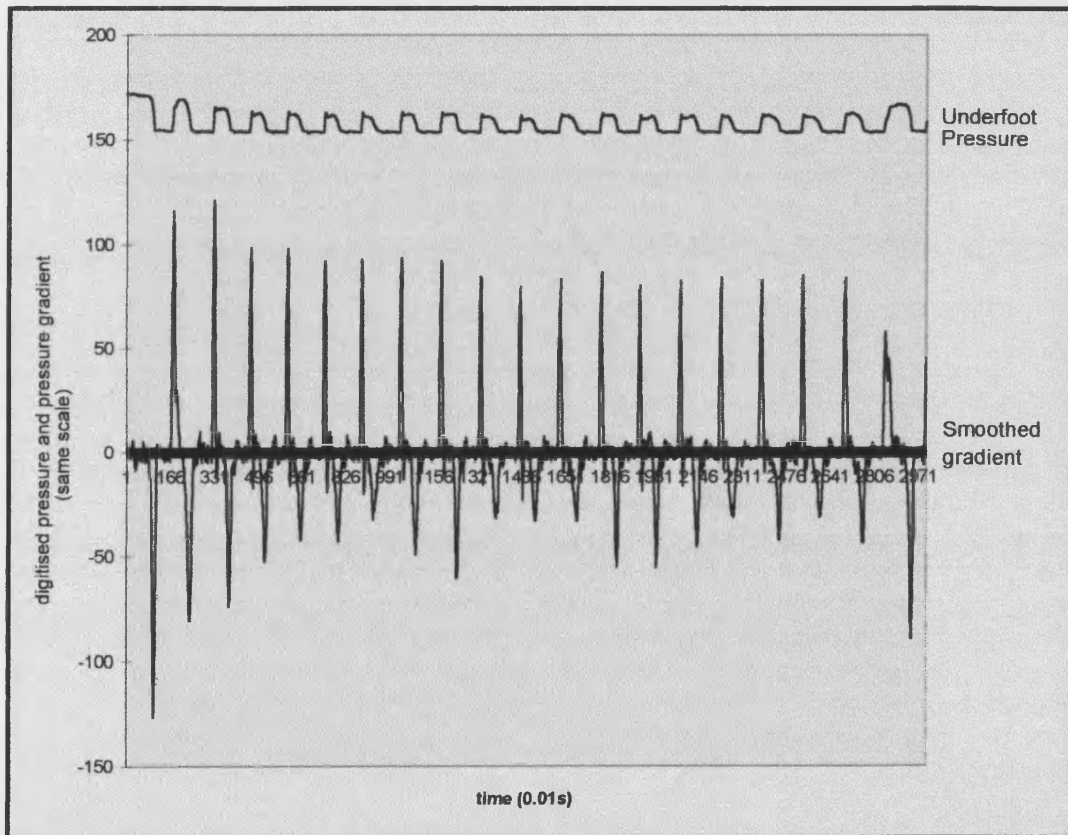


Fig. 5.27 Smoothed heel sensor output gradient.

The effect of this smoothing is to permit those values associated with the pressure transients to be clearly differentiated from the system noise and hence be clearly evaluated.

## **CHAPTER 5 INTELLIGENT STIMULATOR CONTROL**

This operation was performed on the underfoot pressure data gathered from 15 stroke patients and normal volunteers. The peak rate of change of pressure rise and fall per cycle was found to be very different between normal and stroke affected gait but very consistent for any individual during walking. The peak rates of pressure rise and fall per cycle were found from the data acquired during thirty seconds of walking by normal volunteers and stroke patients. An example of the analysis of the peak rate of pressure transitions for a single normal and stroke affected individual is shown below. The low standard deviations with respect to the peak rate of change of pressure magnitude shows the consistent gait exhibited by individuals.

### **Single Individual normal gait:-**

Peak heel pressure rise	Average value = 1770.00 Standard deviation = 95.14.
Peak heel pressure fall	Average value = 1132.50. Standard deviation = 204.73.
Peak 1st metatarsal rise	Average value = 1045.00 Standard deviation = 239.40.
Peak 1st metatarsal fall	Average value = 2782.50. Standard deviation = 255.09.
Peak 5th metatarsal rise	Average value = 760.00 Standard deviation = 181.07.
Peak 5th metatarsal fall	Average value = 1227.50. Standard deviation = 547.83.
Peak toe rise	Average value = 480.00. Standard deviation = 111.68.
Peak toe fall	Average value = 1461.10. Standard deviation = 370.43.

### **Single individual stroke gait:-**

Peak heel pressure rise	Average value = 906.66.
-------------------------	-------------------------



---

## CHAPTER 5 INTELLIGENT STIMULATOR CONTROL

---

	Standard deviation = 129.37.
Peak heel pressure fall	Average value = 1415.38. Standard deviation = 104.85.
Peak 1st metatarsal rise	Average value = 124.68. Standard deviation = 19.10.
Peak 1st metatarsal fall	Average value = 141.38. Standard deviation = 33.06.
Peak 5th metatarsal rise	Average value = 306.56. Standard deviation = 40.60.
Peak 5th metatarsal fall	Average value = 421.66. Standard deviation = 73.64.
Peak toe rise	Average value = 143.88. Standard deviation = 24.22.
Peak toe fall	Average value = 184.70. Standard deviation = 40.75.

The values of peak rate of change of pressure are quoted in digitised pressure value per second.

This operation was performed upon the gait data from all fifteen normal volunteers and stroke patients to compare the data from these two sources and locate the best transitions to use in the qualification of gait quality. The results of these analyses are shown below.

### **Total normal gait analysis:-**

Peak heel pressure rise	Average value = 1714.08. Standard deviation = 376.05.
Peak heel pressure fall	Average value = 969.48. Standard deviation = 319.91.
Peak 1st metatarsal rise	Average value = 824.90. Standard deviation = 319.34.

## **CHAPTER 5 INTELLIGENT STIMULATOR CONTROL**

---

Peak 1st metatarsal fall	Average value = 1580.82. Standard deviation = 636.86.
Peak 5th metatarsal rise	Average value = 738.75. Standard deviation = 401.62.
Peak 5th metatarsal fall	Average value = 1217.80. Standard deviation = 465.06.
Peak toe rise	Average value = 729.68. Standard deviation = 431.59.
Peak toe fall	Average value = 1482.19. Standard deviation = 819.38.

### **Total stroke gait analysis:-**

Peak heel pressure rise	Average value = 976.62. Standard deviation = 237.47.
Peak heel pressure fall	Average value = 1062.50. Standard deviation = 327.51.
Peak 1st metatarsal rise	Average value = 264.06 Standard deviation = 134.44.
Peak 1st metatarsal fall	Average value = 327.61. Standard deviation = 200.68.
Peak 5th metatarsal rise	Average value = 611.38 Standard deviation = 329.13.
Peak 5th metatarsal fall	Average value = 653.49. Standard deviation = 228.20.
Peak toe rise	Average value = 135.89. Standard deviation = 80.78.

## **CHAPTER 5 INTELLIGENT STIMULATOR CONTROL**

Peak toe fall

Average value = 156.04.

Standard deviation = 123.79.

These analyses result in the likely range of peak rate of change of pressure as shown below:-

<u>Event</u>	<u>Normal range</u>	<u>Stroke affected range.</u>
<b>Peak heel pressure rise.</b>	1338.03 to 2090.44	739.15 to 1214.09
Peak heel pressure fall.	649.50 to 1289.39	734.99 to 1390.01
<b>Peak 1st metatarsal rise.</b>	505.50 to 1144.24	129.62 to 398.50
<b>Peak 1st metatarsal fall.</b>	943.96 to 2217.68	126.93 to 528.29
Peak 5th metatarsal rise.	337.13 to 1140.37	282.25 to 940.51
Peak 5th metatarsal fall.	752.74 to 1682.86	425.29 to 881.69
<b>Peak toe pressure rise.</b>	316.06 to 1143.27	55.11 to 216.67.
<b>Peak toe pressure fall.</b>	662.81 to 2301.57	32.25 to 279.83.

The comparison of the expected ranges for the peak rate of change of pressure from each sensor shows those pressure transitions most likely to be of use in the gait evaluation. It can be seen that the heel strike event which gives rise to the peak heel rate of pressure rise may be used to determine the quality of the patient gait as there is no overlap of the normal and stroke affected expected ranges for this event. This is also true of the first metatarsal sensor pressure rise and fall and the toe sensor pressure rise and fall. These ranges are shown in bold type in the above listing for clarity. Clearly, the heel sensor fall and fifth metatarsal sensor rise and fall events do not provide a clear distinction between normal and stroke affected gait and are therefore more useful for the evaluation of gait quality by event timing as discussed in section 5.13.2.

It is therefore suggested that normal gait is effected by the application of stimulation such that the peak rate of change of pressure at the highlighted events is within the range shown for the normal volunteers. The determination of normal gait is likely to be most accurate when the peak rate of change of pressure associated with the first metatarsal pressure fall and the toe pressure fall are used as these two events provide the greatest margin between the expected ranges for normal and stroke affected gait.

## **CHAPTER 5 INTELLIGENT STIMULATOR CONTROL**

### **5.14 Data acquisition for the intelligent muscle stimulator.**

#### **5. 14. 1 Introduction to the data acquisition subsystem.**

The PC utilising the data acquisition card was extremely useful for gaining an insight into the method by which the intelligent stimulator might be controlled, but obviously cannot be used in acquiring the data for the stimulator. Therefore, a small data acquisition subsystem of the type devised by Granat et al. [318] was required to sample the eight data outputs, digitise these signals and make the data available to the master microcontroller.

#### **5. 14. 2 Data acquisition subsystem design.**

It was decided that the data acquisition subsystem should be mounted as close to the site of the pressure sensors as possible. This decision was taken for two reasons:-

- 1) The induced noise on the sensor outputs is reduced if the signal is buffered close to its source.
- 1) The induced noise on the sensor outputs is reduced if the signal is buffered close to its source.
- 2) The wiring, and hence the inconvenience to the patient, is kept to a minimum if the eight output lines from each sensing pad are terminated close to the pad. A method of data transmission utilising a reduced wire count would then be used to transmit the data to the master microcontroller.

These two requirements led to the choice for a serial communication link as the method for transmitting the data to the master microcontroller module. This dramatically reduces the required number of conductors in addition to reducing the input port requirements on the master microcontroller. The above choices led to the system level diagram for the data acquisition system shown in fig. 5.28. The data acquisition system is mounted on the patient just above the ankle.

The ankle location of the acquisition system immediately suggests that this should be small in design and robust in construction. This requirement for the bare minimum of components, led to the use of the Lattice ispLSI1016 - 90LJ PLD to form the logic section and an ADC0838 eight input, multiplexed, serial output, analogue to digital converter to perform the signal conversion. This reduces the component count to two devices plus some external passive components.

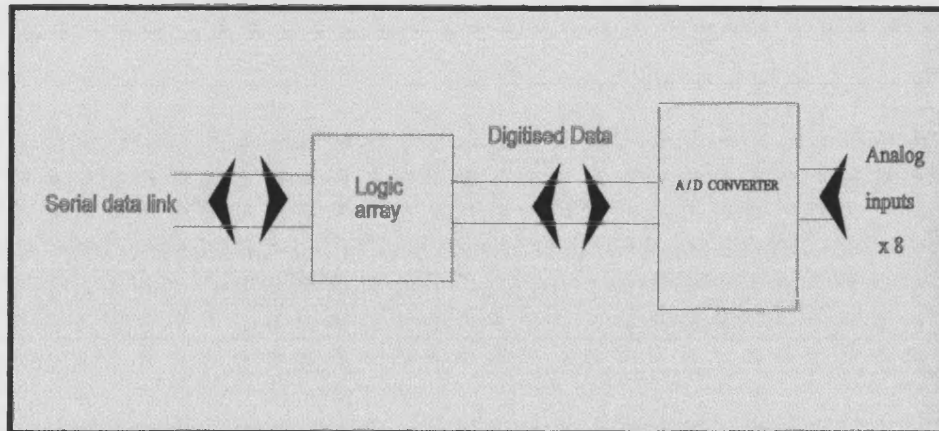


Fig. 5.28 System level diagram for the data acquisition subsystem.

The analogue to digital converter is controlled by the logic block. The logic block shown forms a state machine which, following a reset pulse, is moved through the states by clock pulses from the master microcontroller. A 5-bit serial word is clocked into the converter to set the required input channel and enable the data conversion. Further clock pulses applied to the converter, shift out the data to the master microcontroller via the dedicated data line. When all eight bits have been shifted out of the device, the cycle begins again with the next analogue input selected via an updated 5-bit control word. This method of conversion and transmission allows a 5 wire system to be employed, consisting of data, clock, +5V, ground and reset. The reset is applied subsequent to a full eight input conversion and transmission to ensure that all the logic is reset. This might not be the case if any data corruption had occurred during the previous cycle and would lead to incorrect data being transmitted on the next cycle. The circuit diagram of the acquisition system is shown in fig. 5.29, with the logic incorporated within the Lattice PLD represented by the diagram of fig. 5.30, illustrating the circuit size reduction that becomes possible when using these devices.

## CHAPTER 5 INTELLIGENT STIMULATOR CONTROL

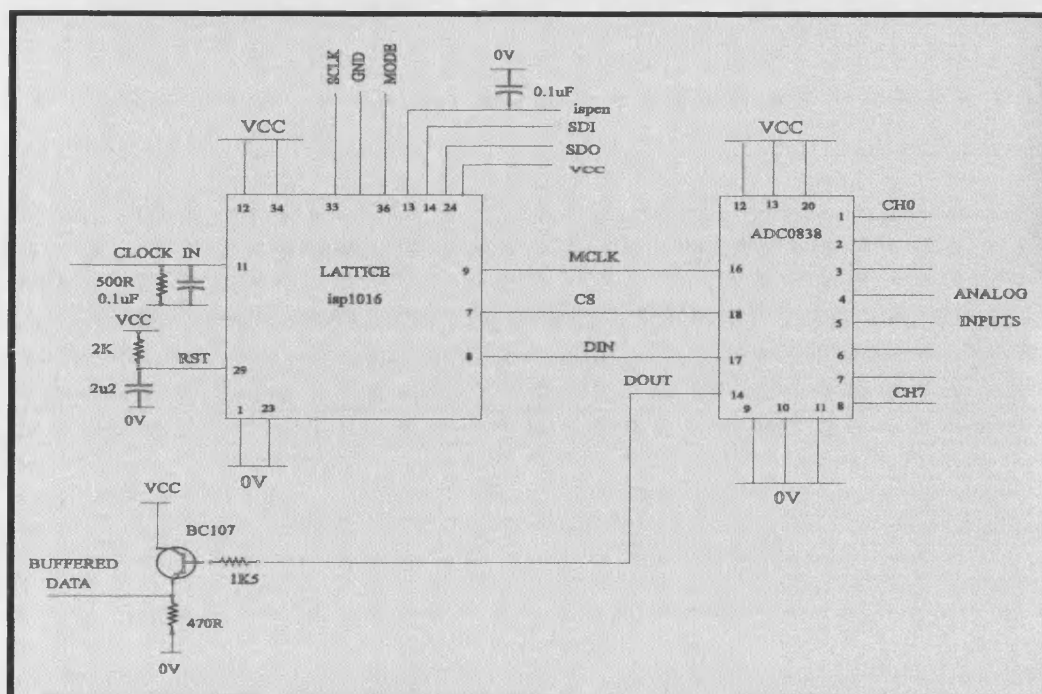


Fig. 5.29 Data acquisition system circuit diagram.

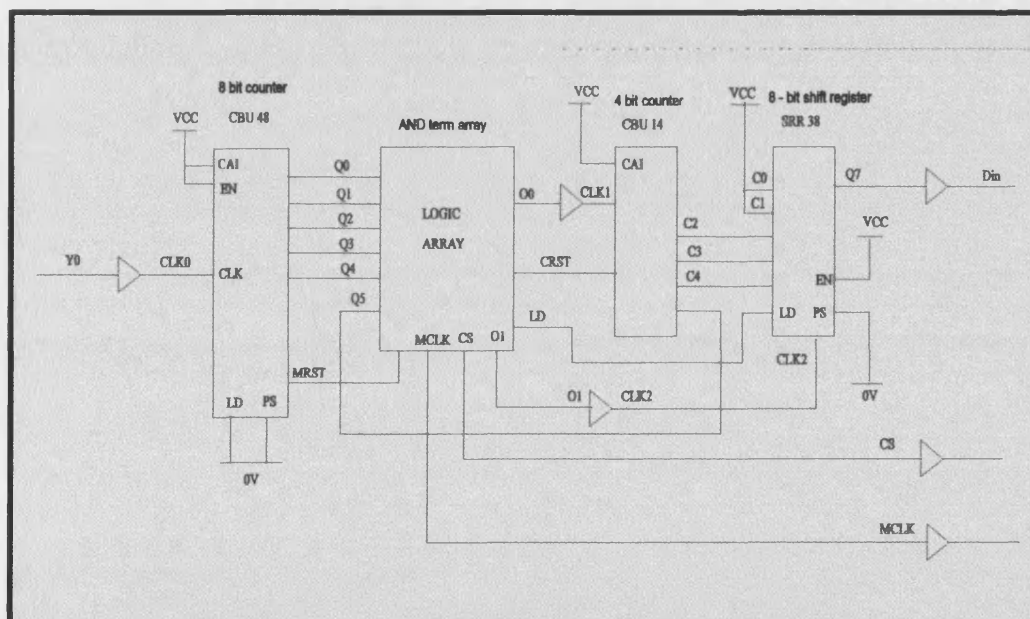


Fig. 5.30 Logic replaced by the use of the Lattice ispLSI1016 PLD.

The arrangement described above requires only a reset pulse followed by a fixed number of clock pulses from the master microcontroller to enable operation. This makes for an extremely simple microcontroller routine consisting of the procedure detailed in fig. 5.31.

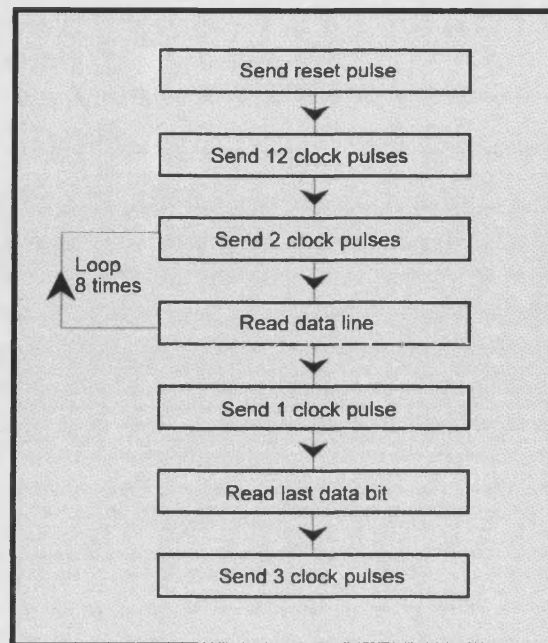


Fig. 5.31 Data acquisition microcontroller routine.

This is then repeated a further seven times to sample the data from all eight sensors.

### 5. 14. 3 State machine operation.

The states used in the state machine incorporated within the Lattice PLD and their effect on the subsystem are detailed in Appendix K. A listing of the PLD code is contained in Appendix L.

### 5. 14. 4 Data acquisition system construction.

For convenience, the data acquisition system was constructed on a single sided PCB and enclosed in an ABS box. Connections to both the pressure sensor outputs and to the microcontroller, via the serial link, are by means of two 9 way D-type connectors. The enclosure affords the necessary protection for initial trials of the complete stimulation system.

The data acquisition subsystem mounted inside the enclosure is shown in detail in fig. 5.32, whilst fig. 5.33 illustrates the serial data connection between the acquisition unit and the main stimulation enclosure.

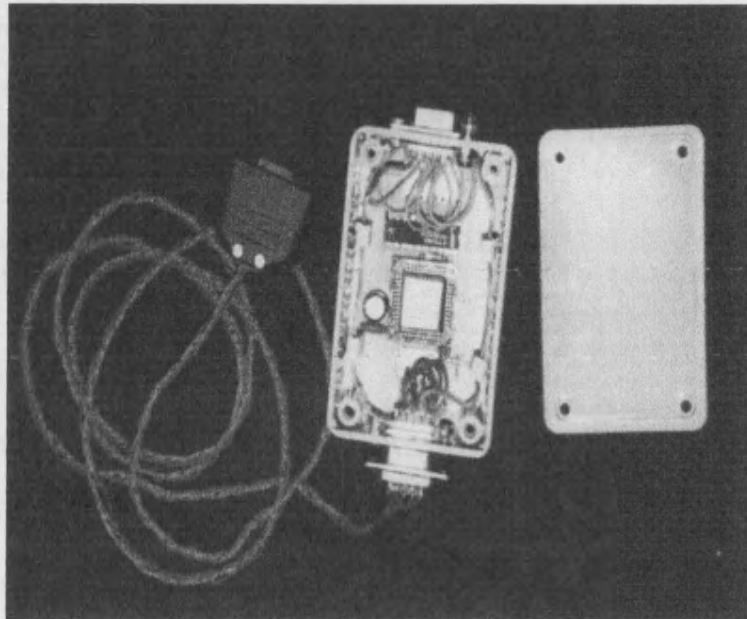


Fig. 5.32 Data acquisition module.

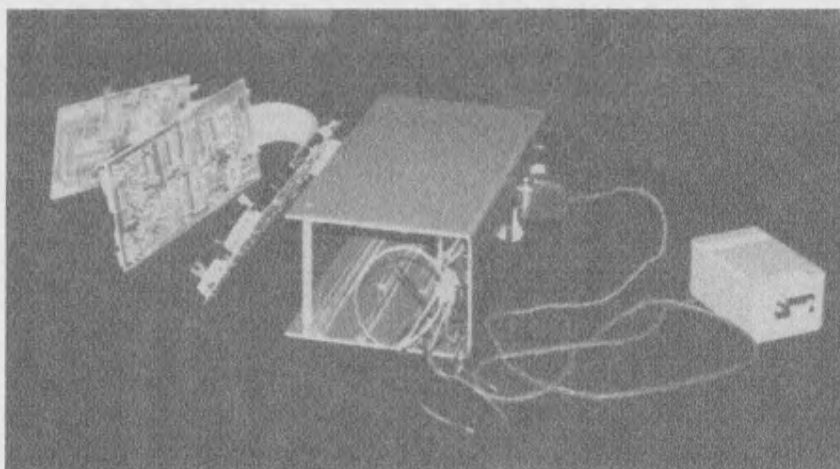


Fig. 5.33 Data acquisition and main stimulator module with serial link in place.



## **CHAPTER 5 INTELLIGENT STIMULATOR CONTROL**

---

### **5. 15 Master microcontroller decision making software.**

#### **5. 15. 1 Software overview.**

The master microcontroller software consists of several modules. Those modules involved with the master to slave data transfer have been functionally described in chapter 4. The remaining functions are associated with data acquisition, gait recognition and stimulation modification.

The decision making software is based upon the method of finite state control, although the states and the mechanism of entry to and exit from each state are not so rigidly defined as in classical finite state control.

Stimulation is applied to the appropriate muscle grouping at the appropriate part of the gait cycle and the parameters of the stimulation waveform are updated every four strides to permit single stride data aberrations to be ignored and not affect an otherwise correct stimulation pattern. A gait tracking framework monitors the gait cycle and tracks the progress of the patient through this cycle. The stimulation instructions are embedded within the gait tracking framework and are then executed as that state, i.e. that portion of the gait cycle, is reached. The data received during the previous four strides is evaluated and used to decide upon the optimum stimulation parameters for the next four paces.

#### **5. 15. 2 Stimulation strategy overview.**

The intelligent stimulator uses digitised underfoot pressure data to make decisions about the gait of the patient and hence determine what correction, if any, is required to the applied stimulation. The new parameters need only be asserted by the master microcontroller and these will be passed to the slave units, which will begin synthesising the new pulse trains with effect from the very next pulse. It can, therefore, be assumed that there is no time lag between the master microcontroller asserting a new parameter value and that stimulation being applied. This is especially important when the stimulation output is altered on a pulse by pulse basis as is the case with the waveforms used to reduce the spastic reflex.

There are a number of parameters that may be extracted from the digitised underfoot pressure data. These are listed as follows:-

- The instance of a pressure rise from any single sensor.
- The instance of a pressure fall from any single sensor.
- The rate of pressure rise from any single sensor.

## **CHAPTER 5 INTELLIGENT STIMULATOR CONTROL**

- The rate of pressure fall from any single sensor.
- The phasing, or order, of the pressure transitions.
- The time between the pressure transitions.

Any one of these parameters may be utilised alone to provide control information to the stimulator, although to reduce the probability of errors occurring, all of these are used together to effect control of the stimulator.

### **5.15.3 Stimulator operating cycles.**

There are a number of cycles to consider when discussing the operation of the intelligent stimulator. The interaction of these cycles is of primary importance in the operation of the stimulator. The cycles to be considered are:-

- The patient gait cycle.
- The master microcontroller program cycle.
- The gait tracking framework cycle.
- The gait calculation cycle.
- The slave microcontroller program cycles.

The patient gait cycle has been discussed in chapter 2 and is considered to occur from heel strike to ipsilateral heel strike. This cycle occurs at the speed of the patient gait and according to the will of the patient. The stimulator is intended to assist with this gait and improve the quality of the gait but make no direct alteration of the rate of the gait cycle. Naturally, an increase in the walking speed of the patient may be seen as a result of the use of the stimulator.

The interaction of the above cycles is represented by the diagram in fig. 5.34.

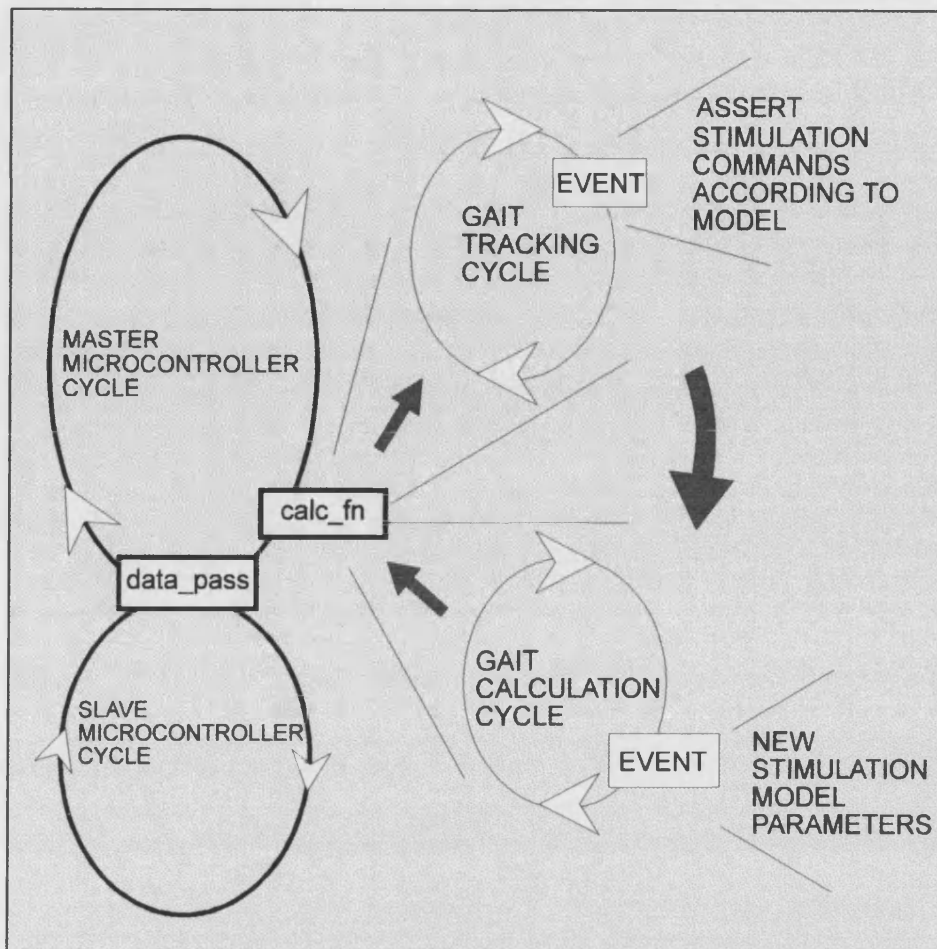


Fig. 5.34 Cycle interactions.

The master microcontroller cycle operates continually and is described in more detail in section 5.15.4. Once per cycle, the function *calc\_fn* is executed and contains all the routines necessary for gait evaluation and stimulation parameter updates. Within this function, two separate cycles are being performed. These are the gait tracking cycle and the gait calculation cycle. The gait tracking cycle, discussed in section 5.15.5, determines by performing tests on the digitised underfoot pressure data the point within the gait cycle that the patient has reached. This cycle is therefore naturally synchronised with the patient gait cycle. The gait calculation cycle, discussed in section 5.15.6, performs separate tests on the underfoot pressure data to determine the quality of the gait and hence determine the necessary changes to the stimulation parameters. The commands to set the stimulation parameters are embedded within the gait tracking cycle and become active as that particular phase of gait is reached.

## CHAPTER 5 INTELLIGENT STIMULATOR CONTROL

The gait tracking cycle asserts stimulation commands according to a pre-set model. This model is then updated on a four stride basis by the gait calculation function.

This method of stimulator control permits the gait tracking framework to track the patient gait cycle and apply levels of stimulation as required by that cycle. These levels begin as default values and are subsequently modified during execution of the gait calculation cycle. This approach permits the master microcontroller to multi-task effectively by collecting gait data, tracking the patient through the gait cycle, analysing the collected gait data and effecting changes in the stimulation parameters within the gait cycle. This multi-tasking approach is taken a stage further when the slave microcontroller units are considered. These units operate independently to the master microcontroller to synthesise the pulse trains, releasing the master unit from the necessity of synchronisation with the patient gait cycle.

### 5.15.4 Master microcontroller cycle.

The top level master microcontroller cycle is shown in fig. 5.35. This shows the outermost program cycle, which operates continually with instructions executed at 16 MHz.

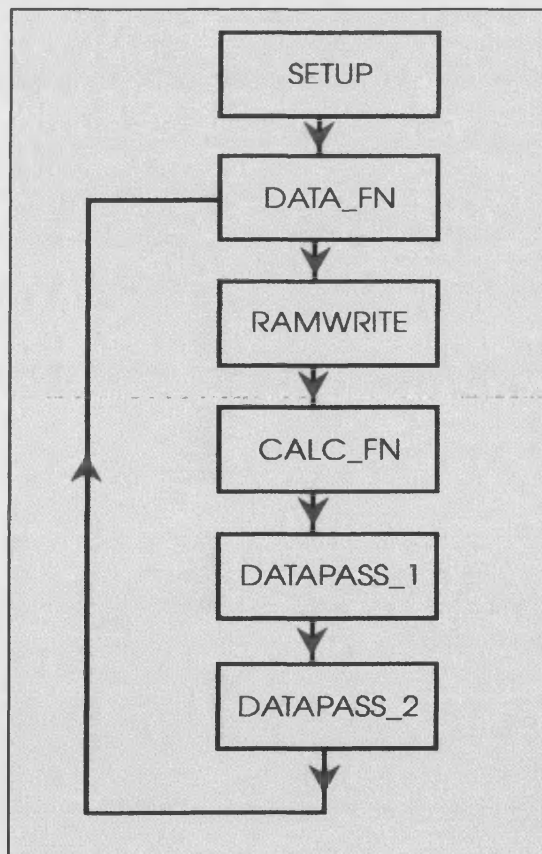


Fig. 5.35 Master microcontroller top level cycle diagram.

## **CHAPTER 5 INTELLIGENT STIMULATOR CONTROL**

An initial setup function initiates the system variables and provides a delay to allow the device to power up and fully reset before commencing program instruction execution. This is then followed by the function *data\_fn*, which is the data acquisition function. This communicates directly with the data acquisition sub-system to initiate the data conversion and clock the data into the microcontroller. The method of data acquisition, along with the associated hardware has been covered in detail in section 5.14.

The acquired data is then stored by the next function, *ramwrite*. This writes the underfoot pressure into the external SRAM to provide a time history of the underfoot pressure data. This function also performs some preliminary processing on this data to detect gait events. The data storage along with the subsequent use of this data will be discussed in more detail in section 5.15.6.

Having performed the preliminary data processing and data storage, the main data processing function *calc\_fn* is entered. Within *calc\_fn* the gait tracking cycle and gait calculation function operate. These two cycles are operated on in turn each time the master microcontroller enters *calc\_fn*, their cycle advanced if necessary and the stimulation parameters updated where necessary. The master microcontroller then continues with its cycle. Stimulation parameters may be updated during the gait tracking cycle according to the stimulation model, which is modified during entry to the gait calculation cycle.

The master microcontroller then compares the latest version of the stimulation parameters with the previous version in the functions *data\_pass 1* and *data\_pass 2*. If there is a difference in these versions of the parameter, the new parameter is passed to the appropriate slave unit, unit 1 in *data\_pass 1* and unit 2 for *data\_pass 2*. The exact mechanism for this data transfer is detailed in chapter 4 and decouples the slave units from the master microcontroller without removing the central control and co-ordination exerted by the master microcontroller.

These separate, but interlinked, cycles are vital to the efficient operation of the stimulator control software. The multi-tasking approach permitted by the use of these cycles allows the master microcontroller to run at the maximum permissible speed but still track the gait cycle and modify the applied stimulation at a rate consistent with patient gait.

### **5. 15. 5 The gait tracking framework.**

The framework, which tracks the patient gait cycle, consists of a structure within which tests are performed to determine which state is active. This structure is operated on by the master microcontroller from the function *calc\_fn*, once per microcontroller cycle. At a point within

## CHAPTER 5 INTELLIGENT STIMULATOR CONTROL

the function *calc\_fn*, the gait tracking framework is entered and tests performed on the underfoot pressure data. These tests determine the location of the patient within the gait cycle and hence the necessary stimulation output parameters. The value of the stimulation parameters at any point within the gait cycle is modified by the gait calculation cycle. This technique of stimulation modification is illustrated by fig. 5.36

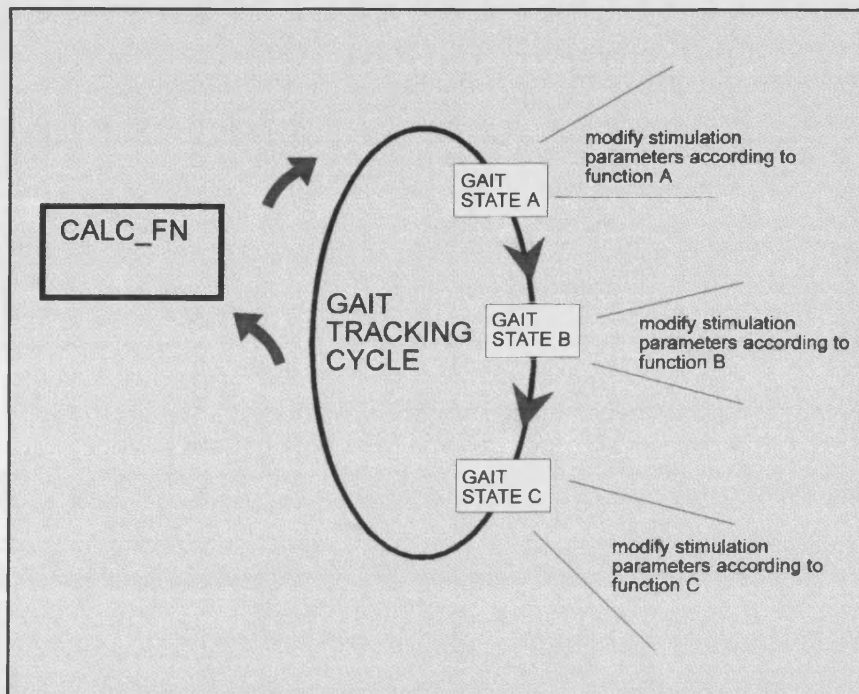


Fig. 5.36 Stimulation modification process.

When the gait tracking framework has been entered, if the first tests to determine the current location within the gait cycle do not produce a true flag then control drops down to the next level of the framework and the following set of tests are commenced.

The cycle is traditionally [186] deemed to start at a left heel strike and finish at the ipsilateral heel strike. Therefore, the last test to be completed is that for the first possible state, the left heel strike. In this way, control has to drop through every set of tests before a true flag may be set. The setting of the true flag prevents this state being re-entered upon subsequent cycles of the program but enables entry to the test section of the prior stage. Control then begins to execute at the top of the framework again and drops down until the next set of tests that produce a true flag are encountered.

## CHAPTER 5 INTELLIGENT STIMULATOR CONTROL

When control drops down to each set of tests, the exclusion flag is tested to see if entry to these tests is permitted, if this is not the case, then no tests are performed and control proceeds around the loop.

The reason for using such a framework to track the gait cycle is to permit the sequential execution of the stimulation modifying instructions embedded within this framework. When a stage is entered and no exclusion flags are set, then the tests for the next state may be performed. If these tests do not produce a true result, then control will fall to the next level which will be fully enterable as the exclusion flag was not set on the previous stage. The stimulation modifying instructions embedded within this stage will be acted upon and control will then continue around the framework. The stimulation modifying instructions take the form of a function that alters the parameters, if necessary, on each entry into that section of the gait tracking framework. The stimulation modification associated with this stage continues until another stage is entered, where the stimulation parameters are varied according to the function particular to that stage. Control cycles from stage to stage in this manner, executing the embedded instructions and modifying the applied stimulation according to the current values of the stimulation parameters.

An example of the stimulation modifying function is shown in fig. 5.37, where the dorsiflexion producing stage subsequent to a push off is examined. The function is executed every time the gait tracking framework is entered and decides that this state is still valid. The stimulation model values  $x$ ,  $y$ ,  $z$ , and  $q$  are set by the gait calculation cycle and updated every four strides to reduce errors due to gait anomalies.

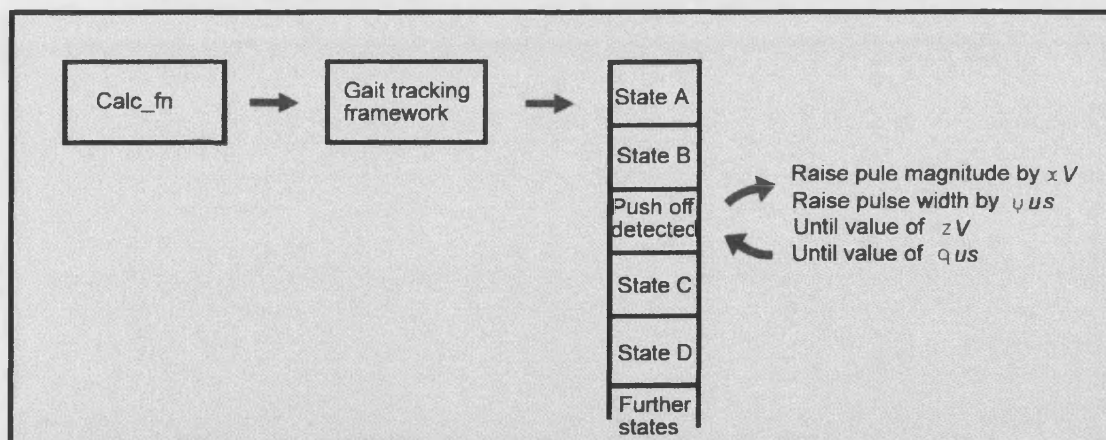


Fig. 5.37 Stimulation modifying function example.



## CHAPTER 5 INTELLIGENT STIMULATOR CONTROL

The gait tracking framework is represented diagrammatically in fig. 5.38, showing stage  $N + 1$  as fully entered on the previous cycle and the effect of the tests in stage  $N + 2$  upon the exclusion of control from the neighbouring stages.

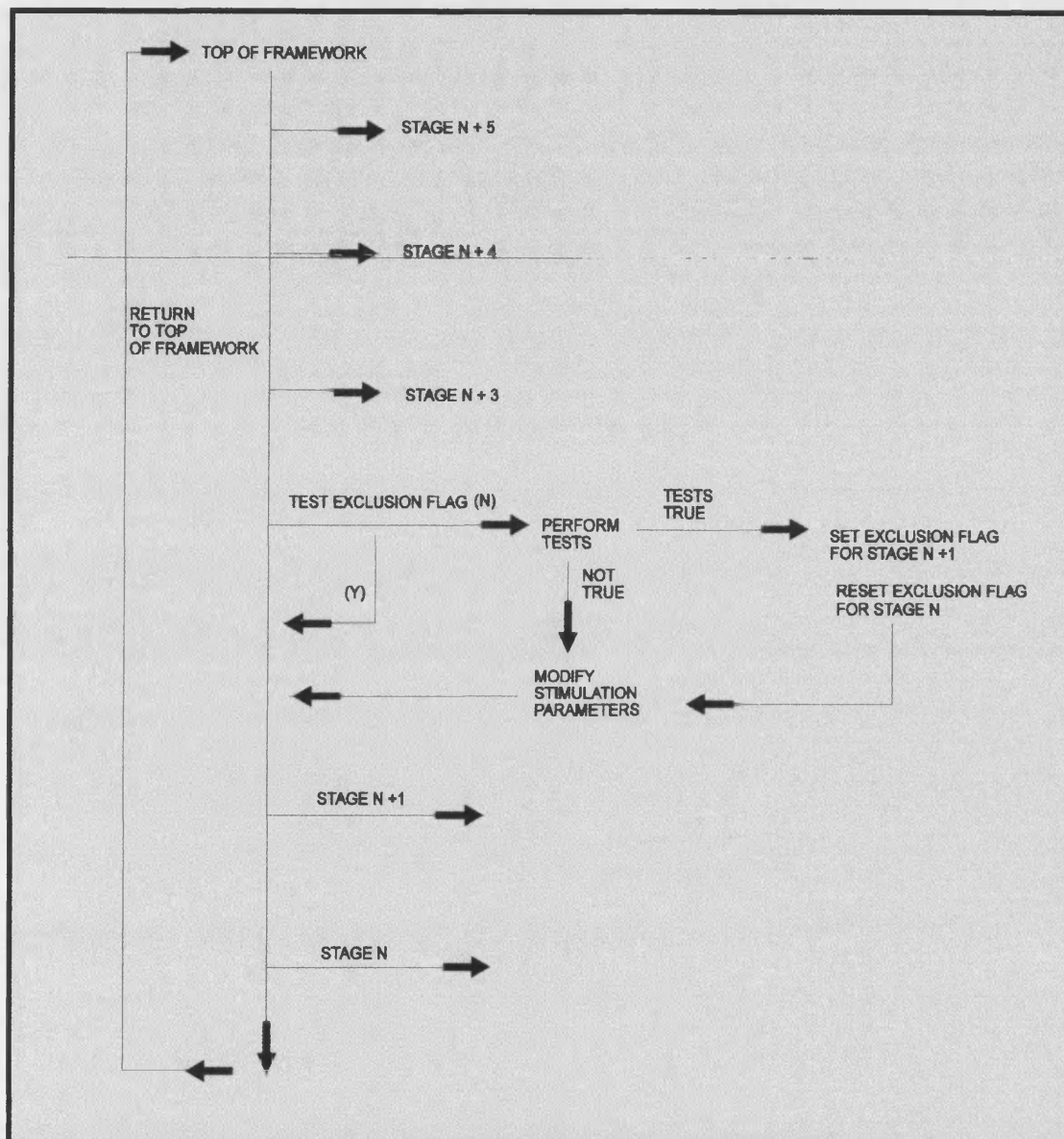


Fig. 5.38 Diagram showing the master microcontroller gait tracking framework.

Stimulation is applied continuously to the muscle groups but when a contraction is not required the magnitude of the stimulation is maintained at a level just below that required to produce a twitch. This permits the stimulation to take effect quickly but without a dramatic rate of magnitude increase, permitting finer, more accurate control of the muscle groups. The



## **CHAPTER 5 INTELLIGENT STIMULATOR CONTROL**

stimulation magnitude is always increased on a pulse by pulse basis, as suggested by Alfieri [177], to produce the required movement with minimal excitation of the spastic reflex.

Having made the increases in stimulation magnitude and pulse width to effect the required muscle activity and assist progression to the next state, the stimulation must be removed, reduced or modified in some way. It would be extremely cumbersome to have to increase the stimulation and then to remove it, as there is no simple way of assessing the rate at which the stimulation should be removed after application. If the stimulation is removed instantly upon entry into the next state, then the result will very likely be a sudden, jerky removal of the contraction. This is to be avoided as is the case with the application of the stimulation.

The solution to the reduction of the applied stimulation was best solved by implementing a 'digital integrator' within the software. The integrator is active at all times within the software and may be compared with a capacitor being charged and discharged in the analogue world. This software routine compares each output parameter with its nominal value. The integrator forces each parameter of the output pulse train towards its nominal value at a preset rate, acting to reduce the applied stimulation. When a stimulation increase is required, the parameter to be altered is forced away from the nominal value at a greater rate than the integrator is able to force this towards the nominal value, by incrementing the magnitude by 1V and the pulse width by 10 $\mu$ s upon every master microcontroller cycle.

The difference in these rates is achieved by calling the integrator function every  $n$  program cycles, whereas the stimulation characteristic is actively altered every  $p$  program cycles. In each case  $n < p$ .

This stabilises the system and ensures that the application and removal of the stimulation is always carried out smoothly and with the maximum of control.

In order that the point in the gait cycle where the stimulation is applied may be altered to bring on the stimulation earlier or later in the gait cycle, a hardware timer on board the master microcontroller is reset on each heel strike to provide a means of triggering the stimulation between pressure transition events. The timer is then checked as a part of the gait tracking framework tests and used in conjunction with the underfoot pressure information.

The tests for the gait states are shown in fig. 5.39. These all utilise the data generated by several different pressure sensors at any one time to minimise false triggering.

## CHAPTER 5 INTELLIGENT STIMULATOR CONTROL

REQUIRED CONDITION		REQUIRED FUNCTION	PHASE OF GAIT
UNAFFECTED SIDE	AFFECTED SIDE		
HEEL STRIKE	1st METATARSAL PRESSURE RISE 5th METATARSAL PRESSURE RISE HEEL PRESSURE FALL	RESET TIMER ALLOW REDUCTION OF ANTERIOR TIBIALIS STIM. INCREASE GASTROC. STIM	MID STANCE (END)
1st METATARSAL PRESSURE RISE 5th METATARSAL PRESSURE RISE HEEL PRESSURE FALL	TOE PRESSURE RISE	CHECK TIMER INCREASE GASTROC. STIM	LATE STANCE
TOE PRESSURE RISE	1st METATARSAL PRESSURE FALL 5th METATARSAL PRESSURE FALL	INCREASE GASTROC. STIM. CHECK TIMER	LATE STANCE (PUSH OFF)
TIMER CONTROLLED	TIMER CONTROLLED	INCREASE ANT. TIB. STIM ALLOW GASTROC STIM TO REDUCE CHECK TIMER	EARLY SWING
TOE PRESSURE RISE 1st METATARSAL PRESSURE FALL 5th METATARSAL PRESSURE FALL	HEEL STRIKE	REDUCE ANT. TIB. STIM. INCREASE GASTROC. STIM.	EARLY STANCE
TOE PRESSURE FALL	1st METATARSAL PRESSURE RISE 5th METATARSAL PRESSURE RISE HEEL PRESSURE FALL	ENTER STABILISATION ROUTINE	MID STANCE

Fig. 5.39 Gait state tests and stimulation functions.

The stance phase stabilisation routine is a routine that examines the toe, heel and metatarsal head sensor pressure data on the affected side and modifies the stimulation applied to maintain a stable stance phase, whilst the unaffected side progresses through the swing phase. In this routine, a pressure rise on the toe sensor causes an increase in the stimulation applied to the common peroneal nerve, to produce some dorsiflexion. Correspondingly, a pressure rise detected on the heel sensor results in an increase of the stimulation applied to the gastrocnemius, to provide some plantarflexion. The system is stabilised by the continual reduction of the applied stimulation carried out by the digital integrator routine.

Whenever the gait tracking cycle is entered, a check is always performed for a heel strike on the unaffected limb. This allows the stimulator to reset the various cycles if any part of the gait cycle has not been clearly detected.

---

## CHAPTER 5 INTELLIGENT STIMULATOR CONTROL

---

### 5. 15. 6 The gait calculation cycle.

#### 5. 15. 6. 1 Introduction to the gait calculation cycle.

The gait calculation cycle is entered from *calc\_fn* within the master microcontroller top level cycle. This cycle is used to make an evaluation of the quality of the gait of the patient and adjust the stimulation parameter model accordingly.

It is not reasonable to perform adjustments on the stimulation parameter model for every master microcontroller program cycle as insufficient data would be gathered during a single cycle to justify a parameter modification. The gait tracking framework is operated upon during each master microcontroller program cycle to ensure an accurate evaluation of the point within the gait cycle and ensure that the stimulation model is applied at the required point. Modification of the model is performed on a four stride basis, with the calculations carried out during the fifth stride. Underfoot pressure data is acquired during four consecutive strides and then processed during the fifth stride. The stimulation parameter model is then modified according to the results of this processing and is applied as the stimulation parameters are varied during the subsequent stride.

The processing of the underfoot data is based around pressure transitions and relies on the data storage facility provided by the SRAM in the master microcontroller circuit. This permits a history of the last four strides to be examined and the relationship between the pressure changes to be compared. The data is stored by the function *ramwrite* earlier in the master microcontroller cycle and is read back from the SRAM during the gait calculation cycle. All of the processing on this data could be performed during this cycle but this would be a particularly inefficient method of processing the data. Instead, some initial pre-processing is performed by the *ramwrite* function, as described in section 5.15.6.2. This pre-processing detects pressure transitions on the data it is loading into the SRAM. When a transition is detected, a marker is set stating the address of the start of the transition, whether the transition is positive or negative and the sensor producing the data. The gait calculation cycle is then able to reference these transition locations to assess the pressure changes without being required to search through the entire 32 Kbytes of memory.

#### 5. 15. 6. 2 Underfoot pressure data pre-processing.

The underfoot pressure data is acquired as stated in section 5.14 and initially stored in an array in the master microcontroller internal memory. This memory is very limited so the pressure information is transferred to the external SRAM and stored in the order shown in fig. 5.40.

## CHAPTER 5 INTELLIGENT STIMULATOR CONTROL

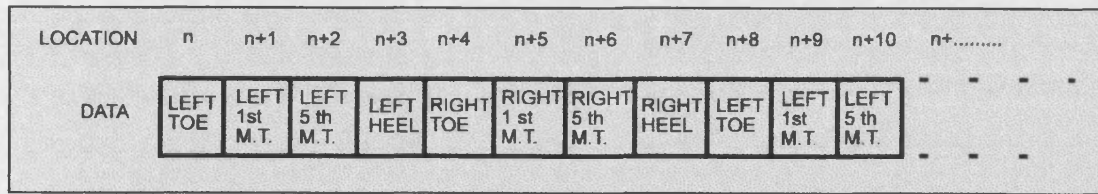


Fig. 5.40 Order of underfoot data storage.

As each byte of data is loaded into its SRAM location, the algorithm shown in equation 5.6 is implemented to determine whether a transition is taking place.

$$\text{Slope between two adjacent samples } (S_n) = ((n+8) - (n)) \times 100 \quad (5.4)$$

$$\text{Smoothed slope} = \sum_n^{n+10} \frac{S_n}{10} \quad (5.5)$$

$$|\text{Smoothed\_slope}| > 30 \quad (5.6)$$

This value was found to be within the range expected for the peak rate of change of underfoot pressure for both normal and stroke affected gait, as discussed in section 5.13.

When a transition is discovered, a check is performed to ensure that there was no transition indicated for the preceding memory location, indicating the beginning of a transition. The memory location of this transition is then stored to provide a transition marker. In this way, the patient gait is reduced to a set of memory locations, which allows a quick reference to the transition data and provides the ideal format for the gait event timing information. The time between gait events may then be found by calculating the number of memory locations separating the appropriate markers and expressed as a percentage of the gait cycle by comparison with the number of memory locations separating heel strikes.

### 5. 15. 6. 3 Gait evaluation and stimulation parameter processing.

Initially, a set of default stimulation parameters are employed by the system to provide a stimulation default model. This model provides the initial stimulation and is subsequently modified as underfoot pressure data is sampled and the gait quality is evaluated.

The intelligent stimulator utilises the temporal relationship between the various underfoot pressure sensor transitions and the pressure rise and fall rates to evaluate the patient gait. This is done by comparison of this data with the expected ranges of values detailed in section 5.13.

## **CHAPTER 5 INTELLIGENT STIMULATOR CONTROL**

It has been stated that the stimulation application and removal throughout the gait phases is partially controlled by an on-board hardware timer that is reset at each heel strike. This permits the stimulation to be applied earlier or later at any point during the cycle, so adjusting the stimulation application time.

The gait is evaluated according to the rules shown in fig. 5.41 and in the order shown. The stimulation parameters, are set within this function and are then used by the stimulation expressions within the gait tracking framework and subsequently the data passing functions.

The primary evaluation is the sensor activation sequence. It was noted in section 5.13.2 that this was an extremely reliable measure of gait quality and showed the most significant difference between normal and pathological gait. It has been shown in this section that normal gait exhibits the following sequence of pressure events across the base of both feet.

Heel sensor activation, first and fifth metatarsal activation, toe sensor activation.

It has also been shown that in normal gait these are separated by the following minimum percentages of the time of one complete gait cycle.

- Heel to 1st metatarsal 9.4 %.
- Heel to 5th metatarsal 3.5 %.
- Heel to toe 19.9 %.

This is expressed as a percentage as patients will walk at a comfortable speed and absolute time values will vary between patients. A reduced dorsiflexion leads to a more flat footed walk with the pressure events brought close together or even brought completely in phase.

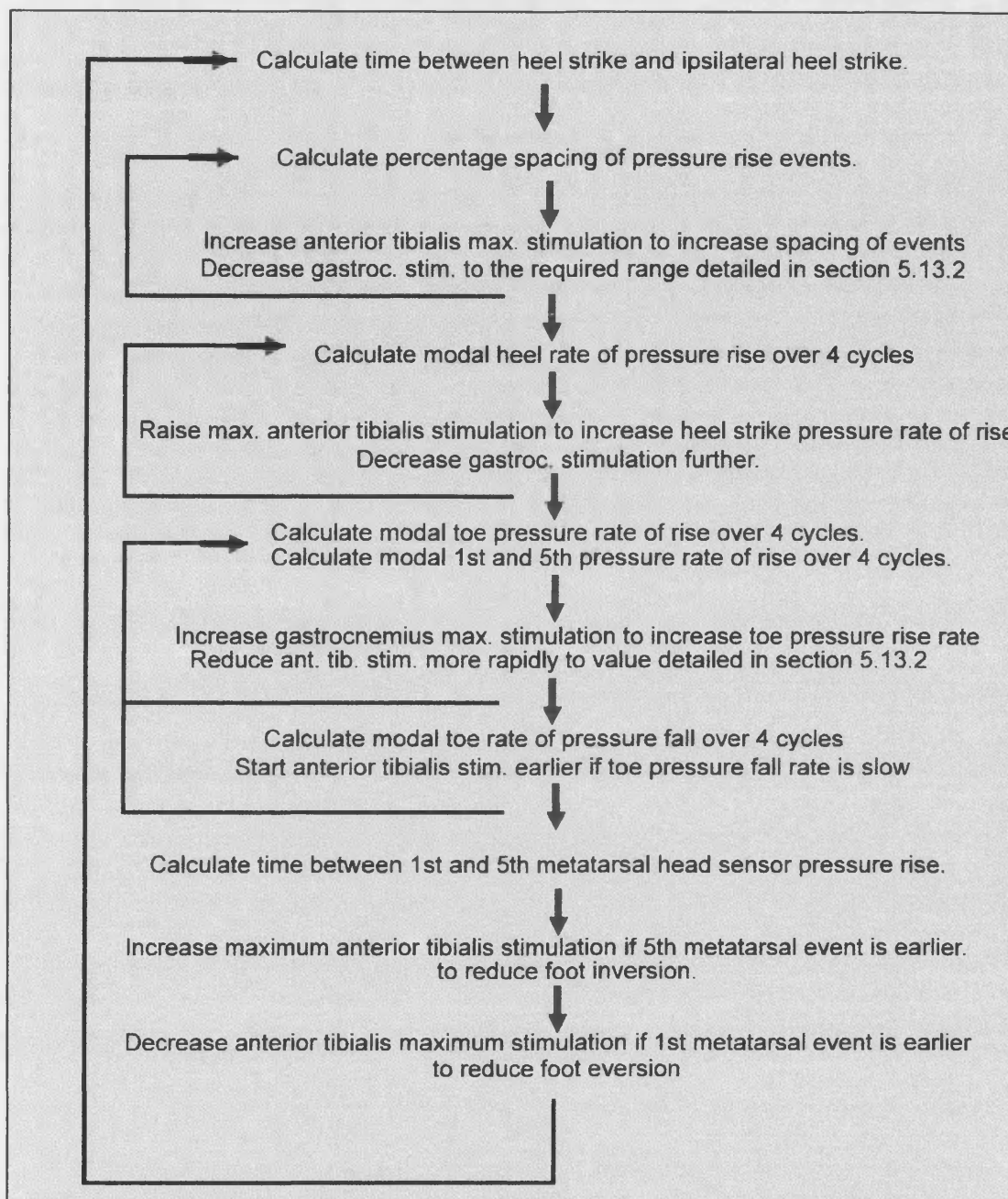


Fig. 5.41 Stimulation model modification..

In order to perform a test for this sensor activation order, it is necessary to calculate the length of a complete gait cycle, defined as heel strike to ipsilateral heel strike. This is performed as follows:-

$$\text{Cycle time} = (\text{Memory location of heel strike} - \text{memory location of prior heel strike}) / 8 \quad (5.7)$$

## **CHAPTER 5 INTELLIGENT STIMULATOR CONTROL**

These locations have been determined by the function *ramwrite* and are referenced by this function. The separation of each of the events may then be evaluated by the following method:-

- Calculate time of complete cycle.
- Separation of event = ( location of metatarsal marker - location of heel marker) / 8.
- Fraction of gait cycle = separation of events / time of cycle.
- This is then repeated for the other event separations.

The sensor rise times and fall times are evaluated using expressions 5.2 and 5.3 shown in section 5.13.3, which correspond to expression 5.4, 5.5 and 5.6 when applied to memory locations. This provides a smoothed rate of pressure rise or fall from the underfoot sensor outputs.

This is performed on data stored at ten memory locations starting with the location indicated by the assigned marker, which indicates the beginning of the transition. The initial location is then incremented and the procedure performed again until the peak rate of change of pressure is found for that transition. The values obtained are compared with those values determined in section 5.13.3 and the maximum stimulation and rate of stimulation application and removal is then increased or decreased correspondingly.

When the result of the calculation requires an earlier or later application of the stimulation, the timer compare value is decreased or increased to produce stimulation that occurs closer to, or further from the heel strike event. The timer value is read on entry to each gait state and the value used to determine whether to alter the stimulation. In this way, the correct part of the gait cycle is tested for as well as the time lapse from the heel strike associated with that foot.

These calculations permit the values of maximum stimulation, minimum stimulation, rate of application of stimulation, rate of removal of stimulation and the timing of the stimulation within the stimulation model to be altered to vary the patient gait as required.

### **5. 16 Initial stimulator tests utilising the underfoot pressure feedback.**

Initially, testing was performed to ensure the correct functionality of the stimulator in response to feedback from the Hall effect underfoot pressure sensing array. A simple test stimulation routine was written and embedded within the gait tracking framework to ensure that the stimulator would respond to pressure sensor transitions.

## CHAPTER 5 INTELLIGENT STIMULATOR CONTROL

This stimulation routine was embedded within the gait tracking framework at the point where a rising pressure transition was detected on the right toe sensor output. This would correspond to the nominal timing of the required dorsiflexion for the swing phase of the gait cycle. When this transition was detected, the magnitude of the channel 1 output was increased on a pulse by pulse basis to a new fixed value. The digital integrator was then allowed to reduce the magnitude of the stimulator output to its original value.

The result of this test, shown in fig. 5.42, shows the stimulator output along with the analogue right toe pressure sensor output, as captured by a digital storage oscilloscope. The use of x10 oscilloscope probes should be noted.

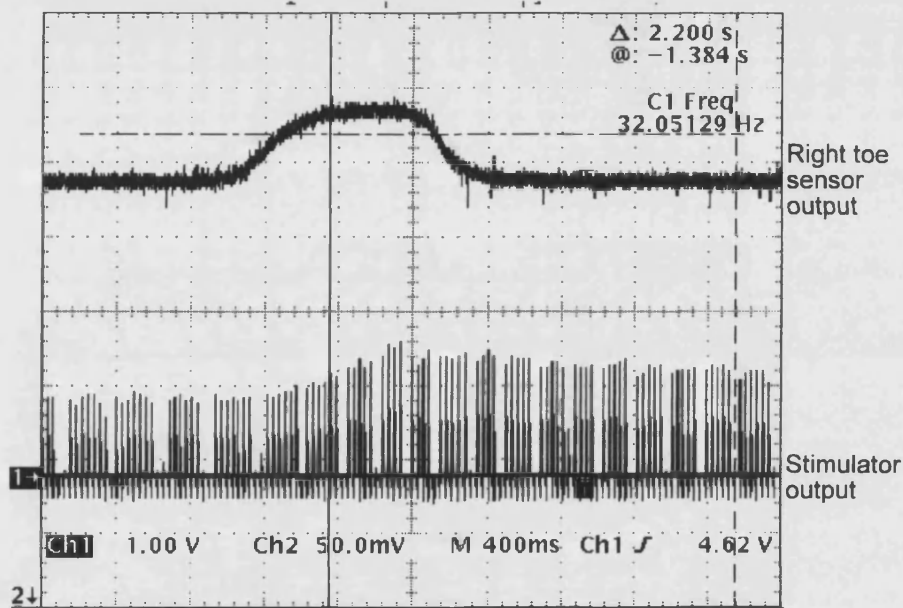


Fig. 5.42 Response of the stimulator to a rising pressure transition.

Fig. 5.42 shows that the master microcontroller gait tracking framework is able to detect the state of push off via a rising pressure transient on the right toe sensor and modify the stimulation waveform at the required time. The subsequent decay in the observed stimulator output shows the digital integrator function is operating correctly to reduce the output waveform parameters to their original values.

A further development of these initial tests was the use of the intelligent stimulator to stabilise the stance phase. The stance phase of either limb is required to provide a solid base to support the weight of the body during the swing phase of the contralateral limb. During the swing phase of the affected limb, the limb with the normal range of voluntary movement is able to provide



---

## **CHAPTER 5 INTELLIGENT STIMULATOR CONTROL**

---

the necessary support, by activation of both the gastrocnemius / soleus complex and the anterior tibialis simultaneously to minimise ankle movement. An initial burst of anterior tibialis activity has been observed on entry to the stance phase to arrest the forward movement of the bodyweight [188]. This then gives way to the activity of both the gastrocnemius and tibialis anterior to stabilise the bodyweight [188]. When the hemiparetic limb is required to provide the stable support, stimulation of both of these muscle groups may be used to produce this effect. The applied stimulation must provide only sufficient muscle force to stabilise the foot without causing further movement.

A section of the master microcontroller program was devised to provide this stabilisation upon entry of the affected limb to the mid stance phase after three full gait cycles to ensure that gait initiation is complete.

The level of stimulation necessary to produce dorsiflexion and plantarflexion of the foot are set by the values determined for adequate toe lift and push off during the swing and late stance phase of the gait cycle. During the mid stance phase, these values are applied to the anterior tibialis and gastrocnemius / soleus simultaneously. The pressure under the affected limb is monitored constantly and adjustments to the stimulation level made as required. Rising pressure detected on the metatarsal heads or toe sensors or falling heel sensor pressure leads to an increase in the anterior tibialis stimulation level and a decrease in the gastrocnemius stimulation level to produce some ankle dorsiflexion. A rising pressure detected on the heel sensor or a falling pressure output from the metatarsal head or toe sensors results in a corresponding increase in the gastrocnemius stimulation level and a decrease in the tibialis anterior stimulation level to plantarflex the ankle slightly. The correction provided is prevented from over correcting the weight shifts by the action of the digital integrator which reduces the applied stimulation towards the value set on entry to the mid stance phase.

The master microcontroller code to provide the stance phase stabilisation is included in appendix M.

The result of testing this section of the stimulator control is shown in fig 5.43, where the intelligent stimulator was fitted to a normal volunteer, who initiates gait and then stops walking during the right leg stance phase. This demonstrates the action of the gait tracking framework in detecting entry to the stance phase and then applying and modifying the stimulation in response to weight shifts over that limb.

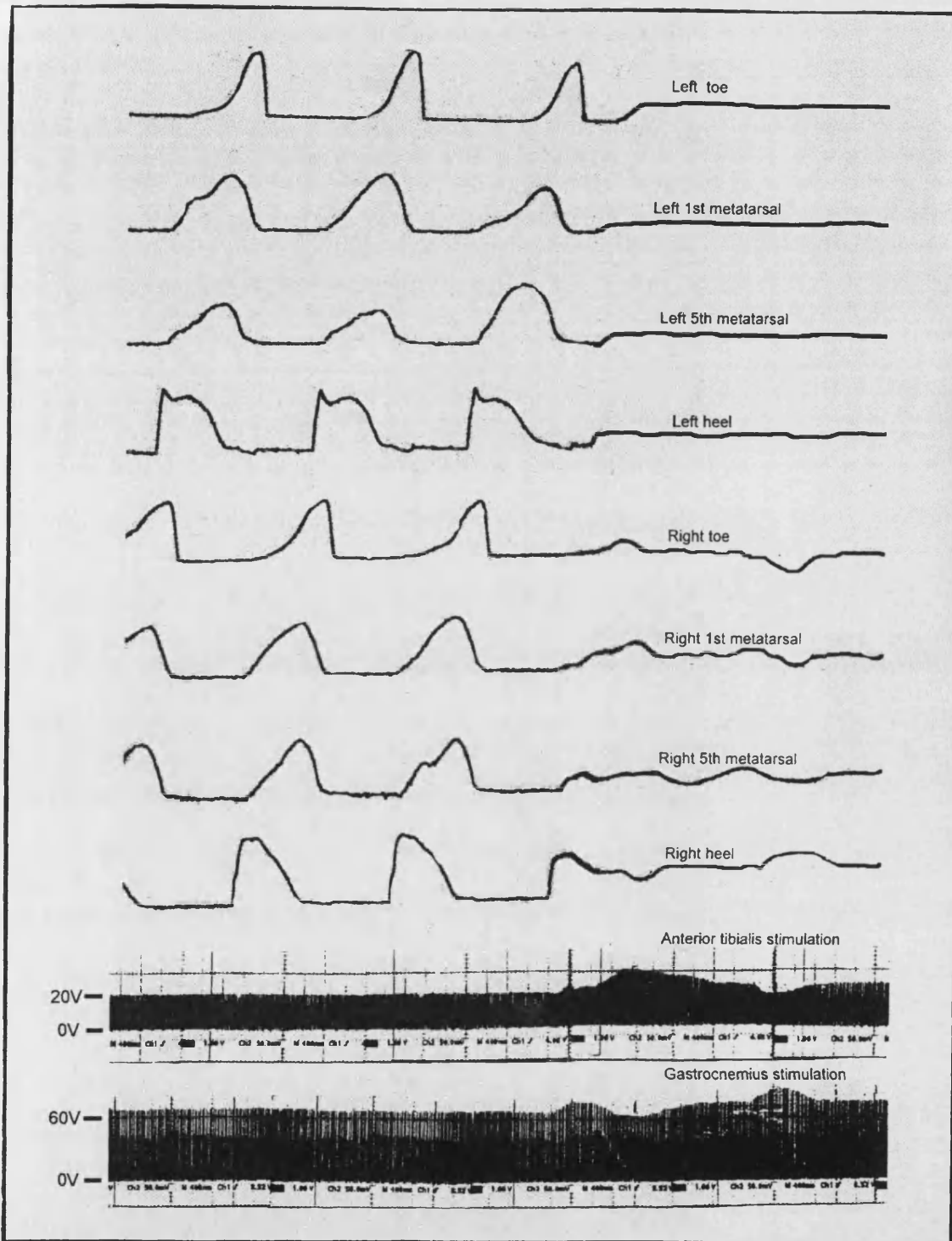


Fig. 5.43 Stance phase stabilisation.

## **CHAPTER 5 INTELLIGENT STIMULATOR CONTROL**

This demonstrates the correct functionality of the master microcontroller, slave microcontroller, underfoot pressure sensing system and data acquisition system in effecting control of the lower limb by the application of intelligent decision making microcontroller software.

### **5. 17 Discussion.**

An investigation has been performed into methods of providing information on patient gait as feedback for the intelligent muscle stimulator. This is essential if closed loop control is to be provided. The gait information is used to determine the corrective stimulation required and this stimulation applied to the appropriate muscle groupings.

After consideration of several methods of providing sensory feedback information on the patient gait, it was decided that the use of a permanent magnet and hall effect transducer offered the best combination of size, repeatability and simplicity. The use of this arrangement as an insole has been used to provide data on the time variance of the under-foot pressure distribution.

The time varying underfoot pressure distribution of persons with normal gait and hemiplegic drop-foot stroke patients has been recorded, analysed and compared. After an initial push off the stride pressure distribution pattern was found to settle into a regular series of peaks and troughs within one gait cycle. The pressure variations observed in normal gait are never identical, although similar enough across a range of different individuals to be employed as a general gait reference. In each case, the relative timing of the pressure transitions and the peak rate of change of underfoot pressure of stroke affected patients were seen to exhibit significant differences to the corresponding variations from those with normal gait. This effect was found to be especially pronounced in the rising output of the heel and first metatarsal pressure sensor and in the falling output of the toe pressure sensor. In each case, the pressure variations under the affected limb were especially different from those exhibited by normal volunteers. The pressure variations under the limbs of stroke patients unaffected by the stroke bore a strong resemblance to those exhibited by normal individuals and play an important role in determining the position of the patient within the gait cycle.

The bulk of the PC based gait data acquisition system prevented its use in the intelligent stimulator, so a compact data acquisition system was developed to present the under-foot pressure variations to the master microcontroller in digital form. This was accomplished via a serial data link and was found to operate reliably.

The likely variations of the stroke gait from normal gait, permitted the control software to be developed. This takes the form of a number of cycles running in parallel to permit the master

## **CHAPTER 5 INTELLIGENT STIMULATOR CONTROL**

microcontroller to multi-task effectively. In this way, the gait tracking framework that detects gait events by monitoring the progression of the under-foot pressure distribution is able to function and apply stimulation as determined by a calculation routine, which analyses the timing and peak rate of change of pressure of the underfoot pressure transitions. The underfoot pressure data acquired during the previous four gait cycles is always stored and used to evaluate the relative timing and peak rate of change of pressure values from each sensor. The stimulation parameter values are then modified as necessary. The use of the four gait cycles to assess the patient gait allows the occasional anomalies observed in all gait to be ignored and therefore prevents false alteration of the stimulation parameters when the gait is otherwise of an acceptable quality.

Error detection is applied by ensuring that the output from more than one sensor is always considered and by looking ahead for the next expected gait state and ignoring unexpected events. In this way the master microcontroller can successfully track the patient through the entire gait cycle. The rise and fall of the pressure sensor outputs is detected in each case and absolute pressure values are never used. This counteracts the problems associated with sensor drift and permanent deformation of the sensor compressive element.

The gait modifying stimulation instructions are embedded within the framework and are only executed upon entry to the correct gait state as shown by the pressure distribution variation. Reduction of the applied stimulation is effected smoothly by means of a constantly operating algorithm. This ensures that the stability of the system is maintained.

To summarise: A method of acquiring accurate, repeatable gait data has been developed that may be used to evaluate the quality of a person's gait and used to provide the feedback signals for the intelligent stimulator. The intelligent stimulator is able to successfully track the patient throughout the entire gait cycle and has been used to stabilise the stance phase, demonstrating the use of underfoot pressure feedback and showing the correct operation of the intelligent stimulator.

## **CHAPTER 6.**

### **CONCLUSIONS AND FURTHER WORK.**

#### **6. 1 Balance aid conclusions.**

##### **6. 1. 1 Balance aid philosophy.**

The development of the balance aid, described in chapter 3, represents a new stroke patient rehabilitation approach. The 'take home and use' approach is likely to be more efficient in aiding patient recovery than the present hospital based approach and this presents the first step in a move towards the on-line monitoring of patient performance without the need for exhausting and inconvenient travel to hospitals. Previous treatment of these patients has always been by direct physiotherapist contact during hospital appointments, both for instruction and for progress monitoring. It is considered that this approach to the restoration of the patient's balance could be improved upon to increase the efficiency of treatment and the recovery rate at a time when the patient can very quickly lose confidence in their own ability. The balance aid provides a method of overcoming many of the shortcomings in conventional balance re-training methods by increasing the available patient treatment time and providing training in a convenient environment for the user. It is also considered that use of the balance aid will significantly improve the utilisation of the physiotherapist's time by providing more patient evaluation data than was previously available and provide data acquired during a period that is more representative of the life of the patient.

The balance aid is a compact, portable and lightweight balance re-training aid, based on prior research performed at Bath University, that patients may use within their own homes to provide a convenient high intensity re-training routine. The balance aid utilises visual balance feedback, a method utilised to good effect by a number of authors and suggested to improve the recovery of patients by providing to them an indication of their progress. The feedback is derived from balance sensing pads incorporating novel, robust optical pressure sensors developed for this application and described in chapter 3. The patient stands upon these pads and practices balance adjustment as indicated by the instruction on a LCD screen. The pads are only 25mm in height and exhibit minimal movement whilst sensing the patient's centre of balance, so

## **CHAPTER 6 CONCLUSIONS AND FURTHER WORK**

maintain the patient's feeling of security at all times. This is extremely important as the confidence of the user is likely to be at a low level in the first few weeks following the stroke.

The balance aid may be utilised to re-train patients in the skill of static balance, which has been stated by a number of researchers to be an essential pre-requisite to the recovery of locomotion. There have been some doubts raised on the worth of static balance training following stroke, but the necessity for the dynamic control of the body centre of mass and hence the underfoot centre of pressure are now well documented and it is this aspect of balance re-training that the work reported here concentrates upon. The microcontroller based design of the balance aid permits the balance aid to be flexible enough to run two program options. In the first of these, static balance training may be undertaken and in the second, dynamic balance training to practice the documented weight shifts to initiate gait may be practised.

It is intended that the intensive training permitted by the use of balance aid within the home at the convenience of the patient, will reduce the time taken for the patient to achieve the necessary balance proficiency for progression to the next stage of the rehabilitation. This could be the fitting of a stimulator, so the development of the balance aid is an important precursor to the development of intelligent stimulation systems. The reduced recovery time likely when using this system would permit the faster return to an active lifestyle, minimising confidence loss, tissue wastage and patient frustration.

### **6. 1. 2 The balance aid system.**

The balance aid prototype was constructed to a build standard considered adequate to permit the unit to undergo full trials. The system is fully portable and will pack into two suitable sized cases, one to contain the main processing unit and the other to hold the two footpads. The balance aid is extremely simple to use and requires no instruction manuals or assembly instructions. The polarisation and variation of the connectors used within the balance aid prevents the unit from being assembled incorrectly. Once assembled, the unit need only be powered up to begin operation. Full instruction in the use of the unit is provided by on-screen instruction at the appropriate time, removing the need to remember how to perform any of the operations.

The balance aid shows the user the location of their centre of balance in relation to their ideal centre of balance. The user is then instructed in the balance adjustment required to adjust their balance to align this with an ideal centre of balance. Five 'skill levels' are included to ensure that the user is always provided with a challenging, but not unrealistic, task whilst training.

## **CHAPTER 6 CONCLUSIONS AND FURTHER WORK**

The static balance re-training program, which has been found by researchers to improve the balance confidence of stroke patients, maintains the ideal centre of balance stationary in the centre of the screen and prompts the user to align their true centre of balance with this ideal centre of balance. The dynamic balance re-training option moves a reference box around the screen in the manner documented as the movement of the centre of underfoot pressure required for the initiation of gait. The patient is then instructed to maintain, by means of dynamic weight shifts, the cross representing their ideal centre of balance within the reference box. A score is generated representing the percentage of the time that the ideal centre of balance was within the reference box and stored to provide a history of the progress of the patient. This permits the patient to practice the skill of dynamic weight shifts to and from the hemiparetic side.

The balance aid may be used by any person of any foot size, height or weight. The centre of balance sensing pads feature internal over-force limits to prevent damage by excessive dynamically applied force. This permits a single design to be manufactured in high volume and used by all patients without customisation to individual physiological needs.

The balance aid operates both from the mains and from the internal cells, which permit a 3 hour training session between charges. Charging then takes place overnight whilst the unit is in a power down state. This permits the unit to be used at a preferred location within the home, removing the constraints of mains outlet positioning. The balance aid incorporates a self test routine that may be invoked by the user as a general functional test or for use when a specific defect is suspected. This removes the need for a 'return-to-base' schedule for periodic functional testing, as the user is able to determine whether a fault exists without the need for any additional equipment, further adding to their confidence in the unit. This removal of the need for specialised testing is extended to the calibration of the balance aid. Many systems suffer from a need to ensure regular calibration of the sensors and associated driving circuitry. The balance aid removes the need for this procedure by implementing an internal calibration upon the output of each sensor within the system. This procedure is recommended at the beginning of each balance re-training session.

### **6. 1. 3 Suggested balance aid improvements.**

Research is suggested into further programming to permit more balance related games to be implemented on the system, especially the requirements of games for different patient age ranges. Currently available balance re-training systems are not particularly suited to intensive use by the patient, so do not exhibit the option to upgrade the system to run balance related

## CHAPTER 6 CONCLUSIONS AND FURTHER WORK

games. The current balance indication software is perfectly adequate for balance indication, though more challenging and interesting games will only serve to hold the interest and attention of the patient for longer and lead to an increased use of the system. The implementation of further games on balance aid is highly recommended to maintain the interest of the patient throughout the high intensity training that it is envisaged the balance aid will provide.

The SRAM incorporated within the balance aid permits the memory unit to be interrogated for balance performance data by another balance aid unit held by the physiotherapist. This permits the patient to bring or send the memory unit to the physiotherapist so that their performance may be assessed.

The memory unit requires to be battery backed at all times to maintain this information at present. The recent availability and increased storage capacity of flash memory suggests its implementation within the unit to record the progress of the patient and suggest appropriate skill levels or game levels at the beginning of a training session. The use of this non-volatile storage medium then removes the need to provide a battery backed memory unit and allows the unit to be completely powered down without any loss of performance or current skill setting data.

A further development suggested to improve the transfer of the performance data to the physiotherapist is the addition of a modem to the balance aid. The availability of single chip modem solutions permits the simple addition of the modem to the flexible microcontroller based system, as suggested in fig. 6.1. The balance aid might then be connected to the telephone system and interrogated by the physiotherapist's PC at a convenient time, removing the need for transport of any part of the balance aid.

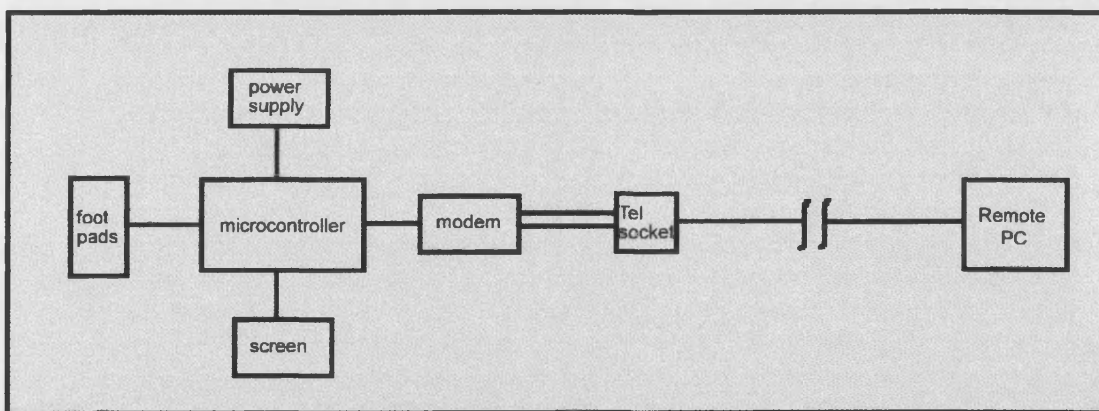


Fig. 6.1 Balance aid modem modification.



## **CHAPTER 6 CONCLUSIONS AND FURTHER WORK**

### **6. 1. 4 Suggested further balance aid investigation.**

It is suggested that investigation be made into the possibility of incorporating the balance aid into a system that permits the patient re-training to be monitored as it occurs. Section 6.2.1 details the 'next step' where the attachment of a modem permits the interrogation of the unit to obtain the balance re-training results. It is recommended that this development be expanded upon to permit the physiotherapist to monitor the balance re-training as it occurs, by transmitting the balance data via the telephone line to the physiotherapist. This will allow a remote assessment of the patient progress to occur and permit advice to be given to the patient as it is required without the need for the patient to leave their home. In addition, modified training programs could be downloaded to the balance aid when the physiotherapist monitoring the training decides these are required. Recent modem technology advances mean that this is an achievable goal and would ensure that continual patient assessment and the implementation of personalised re-training procedures could be achieved whilst the patient remains in the comfort of their home.

The ability of the balance aid to receive program data would then allow the monitoring physiotherapist to select a particular training program from a range of possible training schemes to suit the balance deficiencies of each particular patient. This would allow specific deficiencies to be targeted such as initiation of gait, termination of gait or particular weight shifts. In this way, the patient would always be performing training designed to assist them to develop the balance skills required from a few days to several weeks after the stroke.

Research should then be undertaken to compare the recovery rates of stroke patients using conventional therapy with those using the balance aid at home, with the obvious comfort and extended use that this system provides. A shortened time to recovery when using the balance aid would be powerful evidence in support of a move towards the implementation of 'take home' equipment, such as the balance aid.

### **6. 1. 5 Balance aid summary.**

Balance aid is a system devised to permit stroke patients to practise balance training at home at their convenience, permitting a much increased training schedule intensity to be achieved over conventional therapy. Balance aid permits re-training of both static and dynamic balance skills to be performed. Balance aid permits the balance progress to be stored in preparation for the next training session, permitting progress to be continued by the patient over a number of training sessions. The memory of balance aid may be interrogated by another such machine to

---

## **CHAPTER 6 CONCLUSIONS AND FURTHER WORK**

---

permit a physiotherapist to observe the balance training progress achieved by the patient. The flexibility of the microcontroller based system permits the further development of balance aid to produce a portable on-line re-training device.

### **6. 2 Intelligent muscle stimulator conclusions.**

#### **6. 2. 1 Intelligent stimulator philosophy.**

The intelligent muscle stimulator represents an entirely new method of applying corrective gait stimulation to those stroke patients suffering from foot drop. This concept involves monitoring feedback signals generated by an underfoot pressure sensing array and synthesising stimulation pulse trains to produce the necessary gait correction. Current stimulation systems suffer from the application of fixed stimulation patterns that are often triggered from only a single underfoot sensor. These systems cannot adapt to changes in the patient gait, patient physiology or the terrain and require the applied stimulation to be altered by the patient or a physiotherapist when such changes do occur. It has been observed that the requirement for an initial set up on such systems can require a lengthy consultation time with the physiotherapist, after which there is no guarantee that the ideal stimulator settings have been achieved. The development of the intelligent stimulator is the first step in the process of removing some of the shortcomings experienced by current stimulation equipment.

The intelligent stimulator processes data generated by a pressure sensing array located under each of the patient's feet. These sensors consist of a novel hall effect system incorporated within a compressive medium, forming insoles worn inside specially designed holders. The sensors are a development of earlier research into the use of magnetic field sensing to determine the quality of the patient gait. There are four sensors per foot which are constantly monitored to indicate the exact point of the patient within the gait cycle at any particular instant. These sensors are placed at the heel, big toe and first and fifth metatarsal heads as indicated by prior research. Decisions are always based on the information from not less than three of these sensors over a four stride period to provide a means of error correction by cross referencing of the sensor outputs. This prevents the problems of incorrect stimulator outputs due to unexpected patient movement. This effect is more likely to appear in current stimulators that feature only a single heel switch as the gait detection mechanism. The stimulator then applies multi-tasking software algorithms to determine the required stimulation and synthesise the appropriate monophasic pulse trains.

---

## **CHAPTER 6 CONCLUSIONS AND FURTHER WORK**

---

The stimulation parameters are calculated by utilising the relative timing and the peak rate of change of pressure of the underfoot pressure transitions. Transitions in the outputs from the sensors are always used to avoid problems that may otherwise occur with sensor drift and permanent deformation of the compressive layer.

A gait tracking framework within the master microcontroller software monitors the underfoot pressure sensor outputs and determines the point of the patient within the gait cycle. Stimulation waveform parameters are contained within a stimulation model and are passed to the slave units, which generate the stimulation pulse trains, as the necessary point within the gait cycle is detected. A gait calculation function analyses the patient underfoot pressure sensor data and alters the stimulation model parameter values as necessary to enhance the patient gait.

It was found by a comparison of normal and stroke affected gait that the time from the heel strike to a pressure rise on each of the other three underfoot sensors permitted a clear differentiation between normal and stroke affected gait to be made. The analysis of the peak rate of change of pressure per stride of the heel, toe and first metatarsal head sensor also permitted a clear differentiation to be made between normal and stroke affected gait. These quantities are extracted from the underfoot pressure sensor data and used to determine the gait quality of the patient by the gait calculation routine. The gait calculation routine then modifies the stimulation model parameters which are applied at the appropriate point within the gait cycle by the gait tracking framework. This modification occurs on a four stride basis, using the modal value of the above parameters to ensure that the expected occasional gait aberrations do not affect the stimulator output when the patient gait is otherwise acceptable.

This approach to the stimulation calculation and application decouples the decision making process from the gait cycle, permitting the master microcontroller to run at a high speed whilst the gait cycle proceeds at a relatively low speed. This effect is also utilised by the master and slave relationship, where the master microcontroller program execution is decoupled from the waveform generation activity yet maintains control over the complete system.

### **6. 2. 2 The intelligent stimulator.**

The intelligent stimulator exhibits a modular construction, permitting expansion by the addition of further output channels. This permits the expansion of the stimulator during future research to effect finer control of the patient gait by the control of additional muscle groups. Each output channel is transformer isolated to ensure the prevention of inter-channel current flow. The stimulator is able to synthesise the required pulse train on any of the attached output

## **CHAPTER 6 CONCLUSIONS AND FURTHER WORK**

channels at any time. Within the output pulse train, every parameter of the train may be varied from one pulse to the next, completely independently of the parameters of the previous or following pulses. This flexibility ensures that the stimulator is able to adapt the applied stimulation to suit the physiology of the patient and to provide a good quality correction to the gait of that person. Previous stimulator designs have not permitted this dynamic update of pulse parameters

The stimulator design ensures that the shape of every pulse is maintained when driven through the isolation transformer and into the capacitive load presented by the body. This ensures that every parameter of each pulse train may be accurately varied without distortion of the waveform. In this way the intelligent stimulator may be used as a research tool to investigate the effects of pulse parameter changes, especially the rise and fall times of the stimulation pulse edges.

The pressure sensors used to indicate the variation in under-foot pressure have proved to be an extremely useful gait analysis tool when attached to a data logging PC. In short term tests, the sensor arrays produced excellent gait information without excessive hysteresis or any evidence of permanent deformation of the compressive element. The peak rate of change of the detected pressure and the timing of the pressure transitions alone were used to remove the need for any form of calibration of the sensor arrays. The sensor arrays without the stimulation unit were used to great effect to determine the gait pressure patterns of healthy individuals and the likely variations from these of the gait pressure patterns of stroke affected individuals.

The intelligent stimulator becomes a very powerful tool when used with the under-foot pressure sensing arrays. Information from these arrays is digitised close to the sensors and transmitted in serial form to the intelligent stimulator. This minimises wiring and hence inconvenience to the user. The stimulator is able to monitor the patient gait and determine the current point within the stride. The 'gait tracking framework' implemented within the software, successfully implements this function by analysis of all eight pressure sensor outputs. Corrective stimulation is then applied utilising the 'digital integrator' function to stabilise the applied stimulation. This regulation routine within the software successfully ensures that excessive stimulation is not applied before the stimulation site is able to produce a response.

Initial tests were performed at a particular phase of the gait cycle, the stance phase. The stance phase was seen to be stabilised by the antagonistic stimulation of the anterior tibialis and the gastrocnemius / soleus complex. This proved the correct operation of the intelligent stimulator

## **CHAPTER 6 CONCLUSIONS AND FURTHER WORK**

and showed the importance of the 'digital integrator' technique in ensuring that the complete system remained stable.

Testing of the intelligent stimulator on healthy individuals found that the stimulation applied took effect smoothly without any jerkiness and produced no sudden extreme contractions. This is achieved jointly by the implementation of a pulse by pulse stimulation increase thought to aid suppression of the spastic reflex and the reduction of the stimulation to a value just below that required to produce a twitch when stimulation is not required. The movement produced by the stimulator when regulated by the 'digital integrator' was found to be precise and very controllable. This shows that the stimulator is an extremely powerful tool when used to combat foot drop, as well as being fully programmable to permit stimulation of any other site, following a software update.

### **6. 2. 3 Suggested Intelligent stimulator hardware modifications.**

These suggested modifications are considered necessary to prepare the intelligent stimulator for long term trials. These require a simple to use, compact and robust unit.

The first step in the next stage of the development of the intelligent stimulator should be to reduce the size of the stimulator, now that its effectiveness in producing variable outputs has been proven. The master and slave PCBs should be reconstructed using multi layer techniques and, where possible, surface mount components. Many of the discrete transistors used in the design may be replaced by transistor arrays, the use of which, coupled with the use of microcontrollers with an internal flash ROM, will result in a considerable unit size reduction. In addition, recent high specification microcontrollers may be used to replace much of the digital circuitry, to reduce both size and overall power consumption.

The recent introduction of magnetic materials able to support peak flux densities in excess of 5T allow the construction of smaller transformers, without a reduction in the available stimulator output. This development will also serve to reduce the size of the stimulator and improve it's ease of use.

The pressure sensing mats are presently only in prototype form and would not be viable for use in a finished muscle stimulation system. The next stage of the sensor development is to reduce the mat thickness and replace the neoprene sheet used as the compressive element. This will undoubtedly undergo permanent compression in time, eventually leading to a reduced sensor accuracy.

## CHAPTER 6 CONCLUSIONS AND FURTHER WORK

Discussion with Broadland Plastics, a polymer manufacturer, has shown that the compressive neoprene element used in the pressure sensors may be replaced with a closed cell aerated silicon layer. These may be cold-cast and tailored to the required stiffness by the addition of different percentages of the aeration ingredient. The availability of such materials means that the sensors and associated wiring may be cast into the polymer insole, increasing the reliability and decreasing the overall thickness of the pad. The ability to cold cast the insoles removes the risk of damage to the electronic components, which might occur if the insoles were cast from molten polymers. Such a sensor pad modification might incorporate a thin magnetic sheet as the base layer, as shown in fig. 6.2, removing the need for bulky individual magnets. This would lead to an improved sensor and magnet placement accuracy.

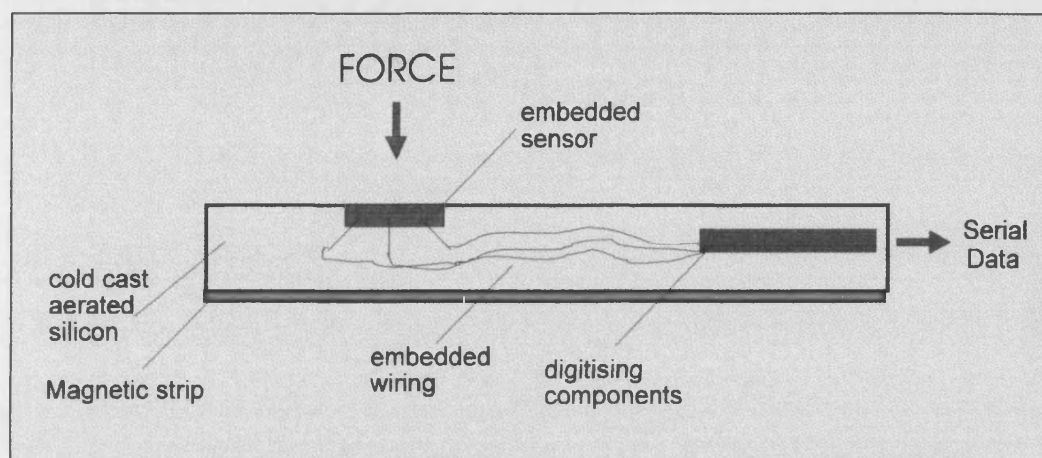


Fig. 6. 2 Possible future pressure sensing mat construction.

A further progression from the incorporation of the sensing elements into a single moulding is the incorporation of the analogue to digital conversion circuitry into this moulding. These components should be placed under the arch of the foot, a pressure free area of sufficient size to permit the placement of surface mount sized components within the polymer. A further modification to enhance the convenience to the user is to consider modulating the data from the sensors onto the 5V power line. This would then reduce the data transfer requirements to a two wire system, a far more convenient arrangement for the user.

These modifications would result in an estimated insole thickness of 4-5mm, a size and robustness more in line with the requirements for use in long term trials.

The stimulator output stage delivers a purely monophasic pulse train. Testing has shown this to work extremely well and produce fine control when used at normal pulse magnitudes. If high pulse magnitudes are likely to be continuously applied to stimulation sites, then it is

## CHAPTER 6 CONCLUSIONS AND FURTHER WORK

recommended that a biphasic output stage be designed for the stimulator in order to minimise excessive ion transport at the site requiring the high magnitude stimulation. Recent innovation in the semiconductor industry has produced solid-state high power relays with change over times in the region of  $50\mu\text{s}$ . These may be used to provide the intelligent stimulator with a biphasic output, as shown in fig 6.3, by alternately switching the polarity of the output after each pulse in the pulse train. The high speed of these devices makes them suitable for the stimulator when doublets are being produced, as the output polarity may be reversed for the closely following second pulse of the doublet. The signal for the polarity reversal is an existing signal used to signal the end of a complete pulse and trigger the core flux reset. It is suggested that this signal is used to drive a flip flop, which in turn alters the output polarity by energising switches A and then switches B on a pulse by pulse basis. This produces a single positive pulse followed by a single negative pulse, a true biphasic output which reduces the ion transfer effect associated with monophasic pulse trains.

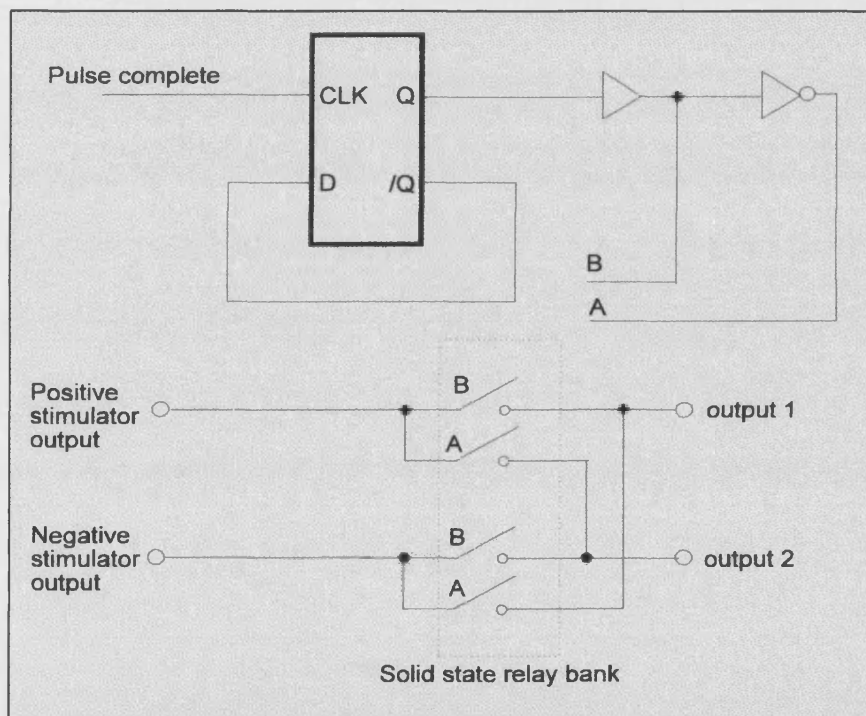


Fig. 6. 3 Biphasic stimulator conversion.

## **CHAPTER 6 CONCLUSIONS AND FURTHER WORK**

---

### **6. 2. 4 Suggested intelligent stimulator further investigation.**

The initial requirement is the undertaking of trials and the subsequent modification of the stimulator master microcontroller software to cater for the results of such trials.

Extensive testing should be performed to ensure that the system is able to quickly recover and re-orientate itself within the gait cycle, should there be a large anomaly in the patient gait at any time. This might require the addition of further tests for unexpected sensor output combinations. These combinations would represent sensor outputs expected for states in the cycle other than the expected next state. Many such tests would permit a fast adjustment of the stimulator outputs, when events such as the user stopping suddenly or stumbling occur.

An investigation is required into the effect and usefulness of the ramp up and ramp down function on each output pulse. The adjustable ramp down function may be utilised to produce a slower ramp than the applied rising ramp. This will alleviate any overshoot problems and provide a definite pulse off indication, allowing EMG measurements to be made without ringing from a fast pulse turn off causing interference on the small EMG signals. A signal line from the pulse synthesising PLD may be used to indicate the pulse off point and commence EMG measurement or latch the EMG data for collection by a processor at its next sample point. The variability of the rising edge of the output pulses also requires detailed investigation. It should be ascertained whether the variation now possible on this pulse edge may be used to produce a more comfortable stimulation than the injection of a train of approximately square pulses. The faster edges of an applied pulse produce a more efficient wave propagation into the body tissue, so an investigation into the alteration of this ramp time to vary the applied stimulation is required. This may be an alternative to increasing the pulse magnitude, or may be used in conjunction with the pulse magnitude and pulse width alterations.

It is suggested that further investigation into the analysis of the underfoot pressure traces of both normal and stroke affected individuals is performed. In this investigation, the gait event timing and peak rate of change of pressure has been employed to evaluate the quality of the patient gait. It is suggested that an investigation be performed into whether any other quantities may be extracted from the under-foot pressure data to further highlight the differences between normal and stroke affected gait. These may then be used in conjunction with the quantities stated above.

It is also suggested that an investigation should be performed into the incorporation of a form of EMG measurement into the intelligent stimulator. This could be used to provide extra



---

## **CHAPTER 6 CONCLUSIONS AND FURTHER WORK**

---

feedback to the stimulator about muscle activity and the degree of spasticity present. This may be found by the comparison of the muscle activity with the movement obtained. The incorporation of the EMG measurements might also be used to provide an indication of the degree of patient fatigue.

These features would permit the analysis of further forms of feedback, producing a more complete picture of the gait quality and the physiological condition of the patient gait than is available with the current feedback scheme. It is suggested that the incorporation of further feedback techniques and increased processing power could result in a stimulator able to apply stimulation, interpret the results and alter the stimulation strategy accordingly. As an example, such a strategy alteration could involve the change to a reduced fatigue strategy, such as a variable frequency pulse train, or a spastic reflex suppressing waveform, such as a pulse-by-pulse magnitude increase, if excessive fatigue or spasticity is detected.

The ability of the intelligent stimulator to select the correct stimulation strategy in addition to providing the necessary gait correction stimulation waveforms would then result in a stimulation system that could genuinely be described as a 'zero set up time solution' for every patient.

Finally, the complete stimulation system may be converted, with suitable sensor and master microcontroller software changes, to provide stimulation to any muscle grouping, to effect correction of any movement deficiency, making it a truly general purpose stimulation system.

## APPENDIX A. BEAM CALCULATIONS

The calculation of the cantilever beam parameters utilises three separate equations, one for the stored strain energy within such a beam, the second representing the deflection of the end of a loaded cantilever beam and the third equation giving an expression for the second moment of area of a rectangular beam.

These derivations require the following assumptions:

- 1) The beam deflection is small, resulting in no permanent set.
- 2) No buckling of the beam occurs, so that the second moment of area remains unchanged.

Consider the cantilever beam diagram shown in Fig. A. 1.

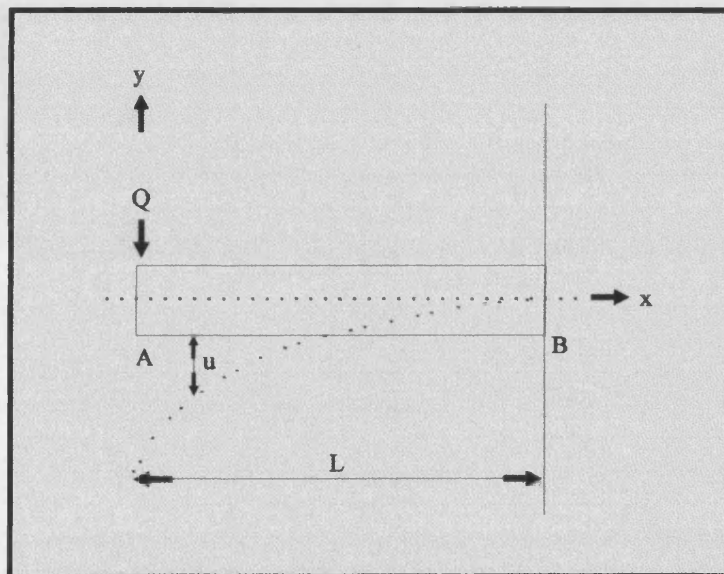


Fig. A. 1 Cantilever beam diagram.

The maximum stress within the beam is given by the expression:-

$$f_o = \sqrt{\frac{3Q^2 l^3}{IV}} \quad [319] \quad (A.1)$$

Taking moments about the point B, the fixed end of the cantilever beam:-

At a distance x  $M = -Qx$  (A.1)

$$M = Elu''_y \quad [320] \quad (A.2)$$

## APPENDIX A BEAM CALCULATIONS

---

Therefore  $-Qx = EIu'_y$  (A.3)

Integrating once  $\frac{-Qx^2}{2} + C_1 = EIu'_y$  (A.3)

At  $x = L$ , slope  $u'_y = 0$  [320] (A.4)

Therefore  $\frac{-QL^2}{2} + C_1 = 0$  (A.5)

$$C_1 = \frac{QL^2}{2} \quad (A.6)$$

$$EIu'_y = \frac{-Qx^2}{2} + \frac{QL^2}{2} \quad (A.7)$$

Integrating once more produces :-

$$EIu_y = \frac{-Qx^3}{6} + \frac{QL^2x}{2} + C_2 \quad (A.8)$$

At  $x = L$

$$u_y = 0 \quad (A.9)$$

Therefore  $0 = \frac{-QL^3}{6} + \frac{QL^3}{2} + C_2$  (A.10)

$$\therefore C_2 = \frac{-QL^3}{3} \quad (A.11)$$

Substituting this back into the equation produces:

$$EIu_y(x) = \frac{-Qx^3}{6} + \frac{QL^2x}{2} - \frac{QL^3}{3} \quad (A.12)$$

$$u_y(x) = \frac{-QL^3}{3EI} \left[ \frac{1}{2} \left( \frac{x}{L} \right)^3 - \frac{3}{2} \left( \frac{x}{L} \right) + 1 \right] \quad (A.13)$$

Then at  $x = 0$

$$u_y = \frac{-PL^3}{3EI} \quad (A.14)$$

## APPENDIX A BEAM CALCULATIONS

This represents the maximum value of the deflection of the beam.

The maximum value of stress within the beam is given by the expression:-

$$f_o = \sqrt{\frac{3Q^2 I^3}{IV}} \quad [319] \quad (A.15)$$

In order to represent this expression in more convenient quantities, it is necessary to further resolve the second moment of area.

The diagram A. 2 refers to the second moment of area of a rectangular beam.

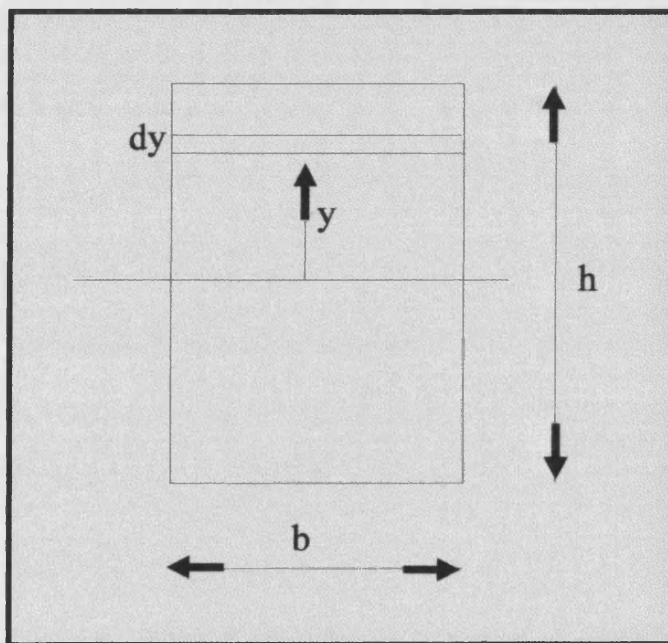


Fig. A. 2 Second Moment of Area for a rectangular beam.

$$I \text{ for a rectangular beam} = \iint y^2 dA \quad [321] \quad (A.16)$$

$$I = 2 \int_0^b \int_0^y y^2 db dy \quad (A.17)$$

$$I = 2 \int_0^b \left[ \frac{y^3}{3} \right]_0^y db \quad (A.18)$$

## APPENDIX A BEAM CALCULATIONS

---

$$I = 2 \frac{by^3}{3} \Big|_0^y \quad (\text{A.19})$$

$$I = \frac{by^3}{3} \quad (\text{A.20})$$

But from diagram A. 2 it can be seen that:-

$$y = \frac{h}{2} \quad (\text{A.21})$$

Therefore

$$I = \frac{bh^3}{12} \quad (\text{A.22})$$

This resulting expression for I can now be substituted into the equation for the maximum beam stress equation (A. 15) noting also that :

$$V = bhl \quad (\text{A.22})$$

$$f_o = \left( \frac{3Q^2 l^3 12}{bh^3 bhl} \right)^{\frac{1}{2}} \quad (\text{A.23})$$

$$f_o = \sqrt{\frac{36Q^2 l^2}{b^2 h^4}} \quad (\text{A.24})$$

$$f_o = \frac{6Ql}{bh^2} \quad (\text{A.25})$$

An expression for the deflection of the end of the beam has already been stated as:

$$u_y = \frac{Ql^3}{3EI} \quad (\text{A.26})$$

Substituting I produces:

$$u_y = \frac{4Ql^3}{Ebh^3} \quad (\text{A.27})$$

This provides us with two equations, one for the maximum stress in the beam and the other for the deflection of the free end of the beam. Both of these equations are in terms of the dimensions of the beam.

## **APPENDIX A BEAM CALCULATIONS**

Within the expressions for the maximum stress and end deflection, certain term combinations may be replaced by constants for a particular material.

The deflection is given by : 
$$u_y = \frac{4Ql^3}{Ebh^3} \quad (\text{A.28})$$

Which may be written as : 
$$u_y = \frac{K_1 l^3}{bh^3} \quad (\text{A.29})$$

With 
$$K_1 = \frac{4Q}{E} \quad (\text{A.30})$$

The maximum strain is given by : 
$$f_o = \frac{6Ql}{bh^2} \quad (\text{A.31})$$

Which may be written as: 
$$f_o = \frac{K_2 l}{bh^2} \quad (\text{A.32})$$

With 
$$K_2 = 6Q \quad (\text{A.33})$$

The fixed parameters are: 
$$Q = 300\text{N} \quad (\text{A.34})$$

$$u_y = 1 \times 10^{-3} \text{m} \quad (\text{A.35})$$

For mild steel 
$$f_o = 250 \times 10^6 \text{Nm}^{-2} \quad [322] \quad (\text{A.36})$$

allowing a margin of  $50 \text{Nm}^{-2}$

For mild steel 
$$K_1 = 5.714 \times 10^{-9} \quad [322] \quad (\text{A.37})$$

$$K_2 = 1800 \quad (\text{A.38})$$

When a value for length of beam is selected, the expressions can be further simplified to:

$$bh^3 = K_3 l^3 \quad (\text{A.39})$$

$$K_3 = \frac{bh^3}{l^3} = \frac{K_1}{u_y} \quad (\text{A.40})$$

$$bh^2 = K_4 l \quad (\text{A.41})$$

$$K_4 = \frac{bh^2}{l} = \frac{K_2}{f_o} \quad (\text{A.42})$$

For mild steel 
$$K_3 = 1.90 \times 10^{-6} \quad (\text{A.43})$$

---

## APPENDIX A BEAM CALCULATIONS

---

$$K_4 = 7.2 \times 10^{-6} \quad (\text{A.44})$$

The two above expressions may be divided to produce a relationship between  $l$  and  $h$  :

$$\frac{bh^3}{bh^2} = \frac{K_3 l^3}{K_4 l} \quad (\text{A.45})$$

$$\text{Reducing to } h = K_5 l^2 \quad (\text{A.46})$$

$$\text{Where } K_5 = \frac{K_3}{K_4} \quad (\text{A.47})$$

$$\text{For mild steel } K_5 = 0.264 \quad (\text{A.47})$$

$$\text{From the above expressions: } bh^3 = K_3 l^3 \quad (\text{A.48})$$

$$b^3 h^6 = K_4^3 l^3 \quad (\text{A.49})$$

$$b^2 h^3 = \frac{K_4^3}{K_3} \quad (\text{A.50})$$

$$h = \sqrt[3]{\frac{K_4^3}{K_3 b^2}} \quad (\text{A.51})$$

$$h = \sqrt[3]{\frac{K_4^3}{K_3}} \frac{1}{b^{2/3}} \quad (\text{A.52})$$

This expression relates  $b$  to  $h$ .

Having established the relationships between  $h, l$  and  $b$  the constants may be calculated for any material and graphs plotted to show if the required size of beam for the given constraints is possible.

For a steel beam, a graph was plotted for all values of  $l$  and  $b$  with  $h$  given and varying in the range 0mm to 3mm. This is shown in Fig. A. 3.

## APPENDIX A BEAM CALCULATIONS

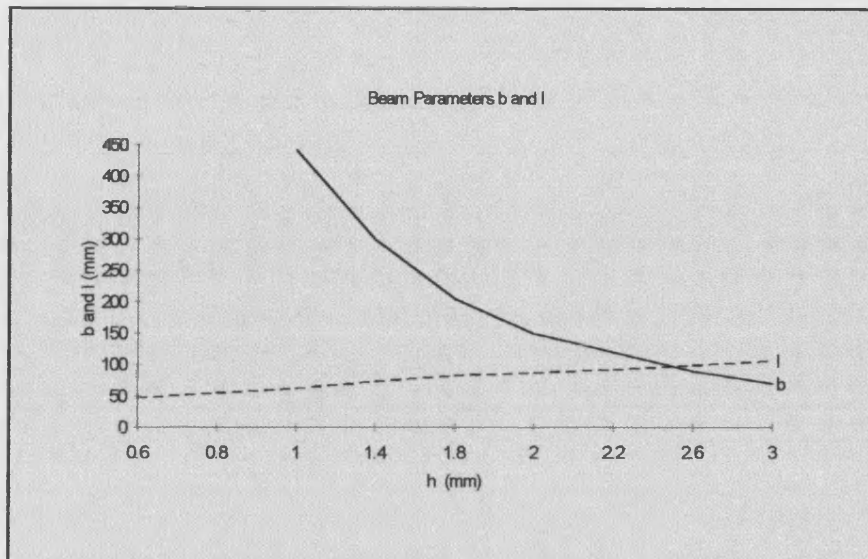


Fig. A. 3 Mild steel cantilever beam parameters.

From the graph it can be seen that the optimum dimensions available for a mild steel beam are:-

$$h = 3\text{mm}, \quad l = 100\text{mm}, \quad b = 70\text{mm}$$

This is not a practical size of sensor to fit within a footpad, so mild steel was discarded as the cantilever beam material.

The same process was repeated for brass to produce the following constants:-

$$E = 100 \times 10^9 \text{ Pa [322]}, \quad f_o = 450 \times 10^6 \text{ Pa [322]}, \quad K_1 = 12 \times 10^{-9}$$

$$K_2 = 1800, \quad K_3 = 4 \times 10^{-6}, \quad K_4 = 4.5 \times 10^{-6}, \quad K_5 = 0.889$$

A graph was plotted, as before, to show the values of  $l$  and  $b$  for given  $h$  varying between 0 mm and 3.4 mm. This graph is shown in Fig. A. 4 and indicates an optimum size of :-

$$h = 3.0\text{mm}, \quad l = 57 \text{ mm}, \quad b = 20\text{mm}$$



## APPENDIX A BEAM CALCULATIONS

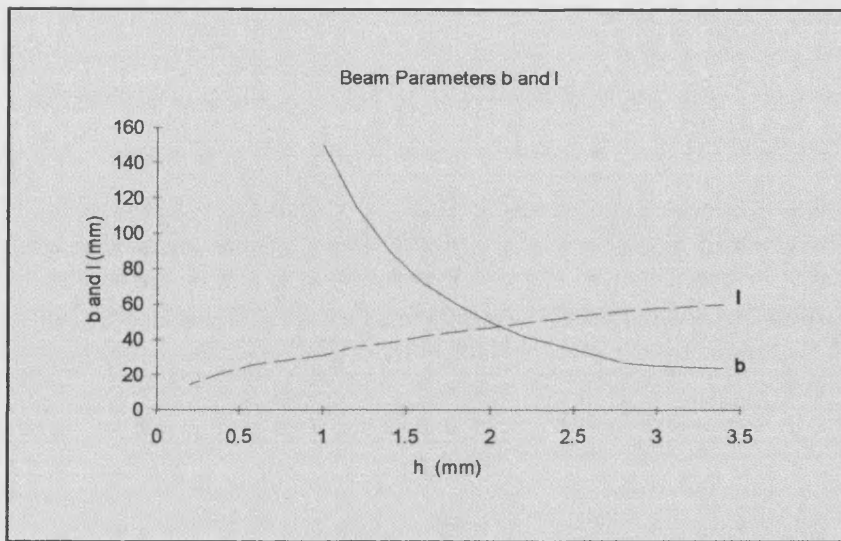


Fig. A. 4 Brass cantilever beam parameters, maximum deflection 3mm.

This is very close to a usable size, so it was decided to reduce the maximum deflection value and repeat the exercise.

So, for a brass beam, now with maximum deflection set at 2mm, the constants have the values:

$$K_1 = 12 \times 10^{-9}, \quad K_2 = 1800, \quad K_3 = 6 \times 10^{-6}, \quad K_4 = 4 \times 10^{-6}, \quad K_5 = 15$$

The graph of  $b$  and  $l$  for values of  $h$  varying between 0mm and 3mm is shown in Fig. A.5 and indicates an optimum beam size of:-

$$h = 3.0 \text{ mm}, \quad l = 45 \text{ mm}, \quad b = 19 \text{ mm}$$

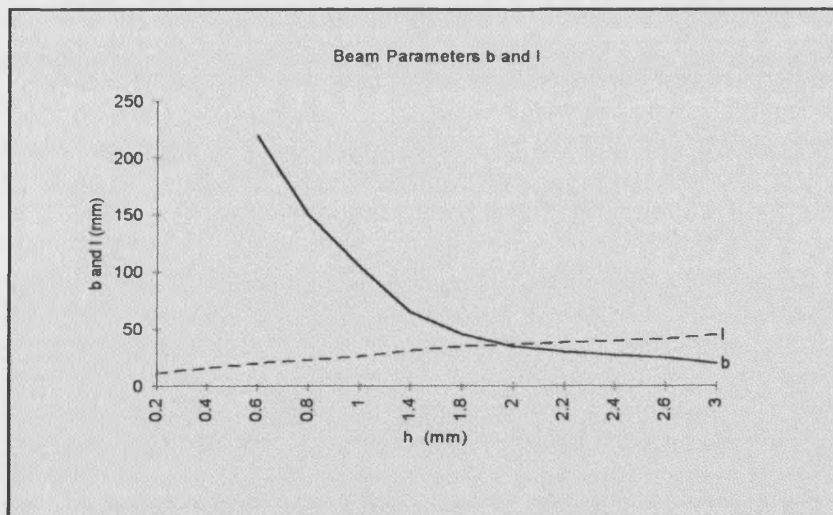


Fig. A. 5 Brass cantilever beam parameters, maximum beam deflection 2mm.

## APPENDIX A BEAM CALCULATIONS

This is a workable solution for the dimensions of the beam, although a maximum deflection of 1mm or 1.5 mm would result in a further decrease in beam size.

A maximum beam deflection of 1.5 mm results in the following constants:-

$$K_1 = 12 \times 10^{-9}, \quad K_2 = 1800, \quad K_3 = 8 \times 10^{-6}, \quad K_4 = 4 \times 10^{-6}, \quad K_5 = 2$$

From the graph of  $l$  and  $b$  for  $h$  varying between 0mm and 3mm, shown in Fig. A. 6, it can be seen that the optimum beam size is:-

$$h = 3.4 \text{ mm}, \quad l = 41 \text{ mm}, \quad b = 14 \text{ mm}$$

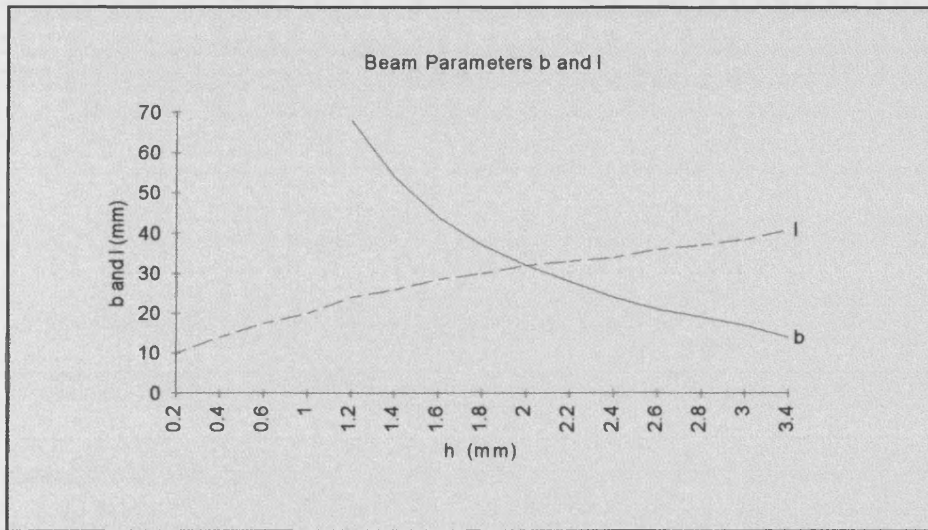


Fig. A. 6 Brass cantilever beam parameters, maximum deflection 1.5mm.

This is an ideal size for use within the footpads and 1.5 mm deflection was seen to produce a usable linear output in the sensor output tests.

Further plots were produced for a brass beam with 1mm maximum permissible deflection and for a nickel - steel alloy beam with 3mm deflection. These graphs are shown in Fig. A. 7 and Fig. A. 8 respectively.

## APPENDIX A BEAM CALCULATIONS

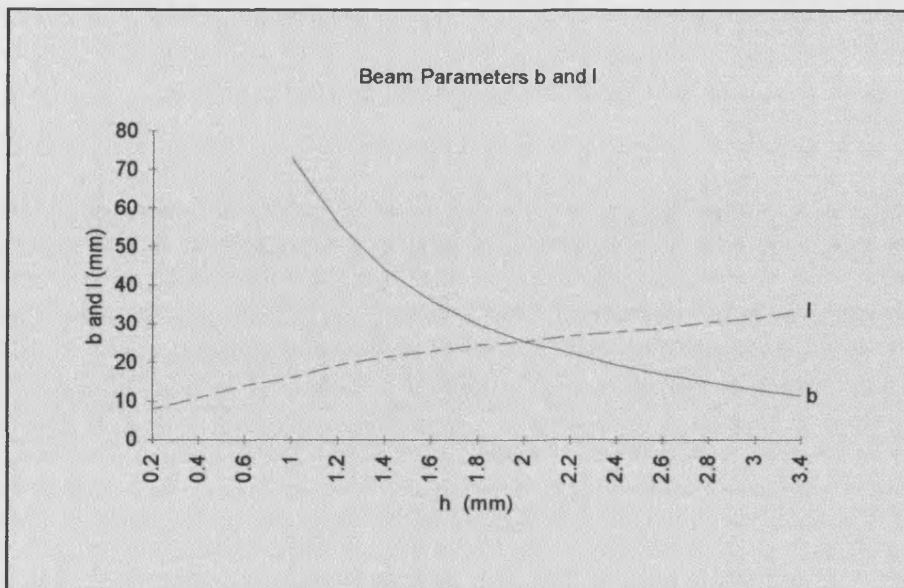


Fig. A. 7 Brass cantilever beam parameters, maximum deflection 1mm.

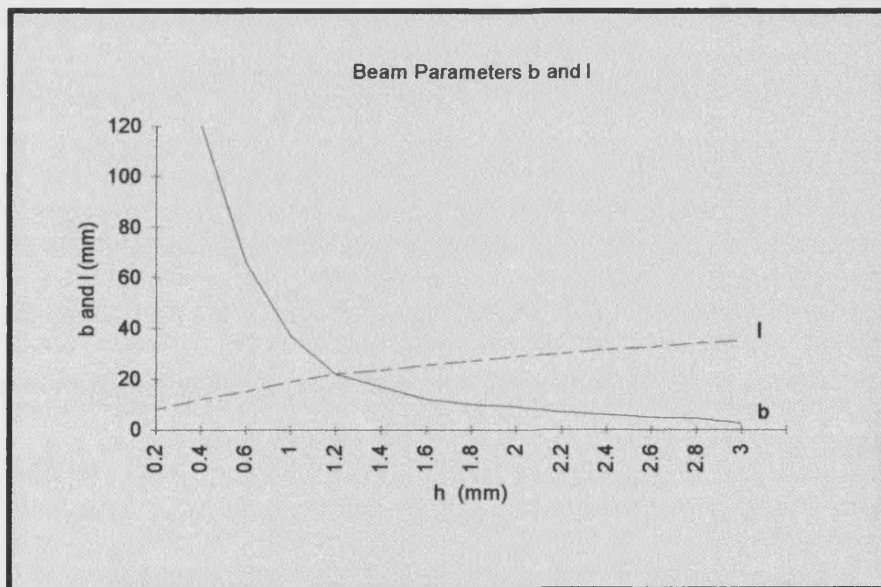


Fig. A. 8 Nickel steel cantilever beam parameters.

It can be seen that the materials more suited to this application are those with a high maximum stress value which tend to permit deflection without permanent deformation occurring. Aluminium has a comparatively low maximum stress value of  $f_o = 71 \times 10^9 Pa$ , so will produce less ideal beam dimension values than the mild steel and was not considered further.

---

## **APPENDIX A BEAM CALCULATIONS**

---

The nickel steel alloy has an extremely high maximum stress value of  $f_o = 1200 \times 10^6 Pa$  and so produced by far the most usable beam dimensions as can be seen from the graph in Fig. A. 8. This material would permit the use of a beam deflected by up to 3mm, with dimensions of:

$$h = 2 \text{ mm}$$

$$b = 12 \text{ mm}$$

$$l = 29 \text{ mm}$$

Unfortunately, this material was rejected in favour of a brass beam due to the prohibitive cost of nickel steel.

**Summary:** A brass beam with maximum deflection of 1.5 mm and the following dimensions was chosen:-

$$h = 3.4 \text{ mm}, \quad b = 14 \text{ mm}, \quad l = 41 \text{ mm}$$

This choice was considered to present the best compromise between size, sensor output and cost of the unit.

---

## **APPENDIX B. BALANCE AID SOFTWARE**

### **APPENDIX B. BALANCE AID SOFTWARE.**

#### **ROOT.**

This module does not contain any actual balance aid running software but rather controls the manner in which the whole program will be executed. The 8051 assembly code must be assembled to Intel hex, stored in the EPROM and acted upon by the microcontroller. The META assembler carries out this process by considering the root file and assembling the files named within it in the order stated. Root also presents such information to the META system as whether a printout or listing is required and how the operating system fields are presented on the screen. To summarise, root contains all the parameters required by the assembler.

#### **DEFVARS.**

DEFVARS is a module introduced exclusively to define the variables used within the software. The first section of the module assigns constant or initial values to variables so that a variable name may be used in preference to a number within the program. The second section of the module assigns internal flags to specific functions. These flags are mainly concerned with status indications and interrupts to the on board analogue to digital converter. The third and by far the largest section of the DEFPARS module is concerned with the allocation of the 256 bytes of internal memory. Labels are allocated numbers corresponding to memory locations and may then be used whenever a variable is to be stored, improving the readability of the program listing. These locations are all within the internal RAM.

#### **SETUP.**

SETUP is a two line module informing the assembler, by use of the ORG command, that the program should start at  $0000_{16}$ , so that upon boot up the program counter is reset to zero.

#### **INTRO.**

INTRO is the first module to produce any output apparent to the user. An initial output port reset is performed, with a delay loop, to ensure a full reset precedes the rest of the module. The introductory screen, is then displayed, introducing the user to the balance aid and prompting a switch press to continue. The calibration routine, CAL, is then called to reset the pressure sensor outputs to zero, thereby removing any offsets. CAL will be described as a separate module. Upon completion of the CAL routine, a jump back to INTRO is performed and the user is then presented with a screen page offering a footpad test routine. If the test button is pressed, the

## **APPENDIX B. BALANCE AID SOFTWARE**

module TEST is called and will be executed. TEST will also be described as a separate module. If a test procedure is not required or the test routine has been completed, then a jump is made to MAIN, the software central module.

### **MAIN.**

The module MAIN controls the operation of the balance aid. It achieves system control by calling all the remaining routines and modules when required. Each of these, upon completion of the particular task, return control to MAIN at the point following that particular call. MAIN initially calls the CHKFEET module to determine the user's foot position, which, when correct, will permit a return to MAIN.

Having achieved correct positioning of the user's feet on the footpads, the final screen page is printed on the LCD screen.

Within MAIN, *Padchk* is the first routine called to perform a check on foot position. This call is within the MAIN loop to permit a foot position check for every cycle of the program. If no problems are flagged by this check, then the routine *strain* is called to take a reading from each of the pressure sensors and update the previous values stored in the internal RAM. With this information now available, the module COFG is called to interpret the pressure sensor readings and determine the position of the user's centre of balance. When the co-ordinates of the centre of balance are available, the routine *show* is called to delete the old centre of balance indicating cross and draw in the updated cross to indicate the current position of the user's centre of balance.

This completes one cycle of the program, after which, provision is made to quit the program or change the skill level and display the new skill level value. After completion of the skill level update, MAIN returns to the point where the *padchk* routine is called to begin another cycle of centre of balance calculation and screen updating.

### **CHKFEET.**

The CHKFEET module performs the foot position checking functions by accessing and interpreting the data from the footpads. When the user permits continuation of the program, the routine *strain* is called. This routine acquires, digitises and stores the output from each pressure sensor at the time of sampling. When the data acquisition is complete, CHKFEET checks each reading to ensure that it is above a threshold, which is set above the noise level of the system. When each sensor outputs a value greater than this threshold, it is assumed that the user has both

## **APPENDIX B. BALANCE AID SOFTWARE**

feet reasonably well centred upon the footpads. Until this is the case, the screen will continue to display the opening message of the module and will not permit further progress.

When the user has both feet reasonably well placed, the routine *ftpad* is called to acquire the foot position data generated by the strips running horizontally across the footpads. The information conveyed to the microcontroller is the position of the frontmost and rearmost part of each foot. A comparison of the new data to that acquired during the previous cycle is performed to see if any changes have occurred in the positioning of the feet since the last software cycle. If no changes have occurred, then no screen update is required and the flicker effect of a constantly updated display is minimised.

Two footpad outlines are drawn on the screen and the position of the foot on each pad is represented within these by rectangles of varying length and position. Once the foot positions have been drawn on the screen, checks are carried out to determine whether or not the foot placement is ideal. This is accomplished by comparing the distance from the toes to the front of the footpad with the distance between the heel and the rear of the footpad. If either is three or more times greater than the other, then that foot is deemed to be out of position and then the required error message is printed on the screen above the relevant footpad outline. Typical screens displaying some of the possible error messages are shown in fig. B.1. Until the above criteria are met, the program will cycle through the foot position data acquisition and analysis, displaying the positions of the feet and any error messages required. When the feet are correctly positioned on the footpads, the user is informed by an on screen message and, when ready, may progress to the next part of MAIN.

## APPENDIX B. BALANCE AID SOFTWARE

---

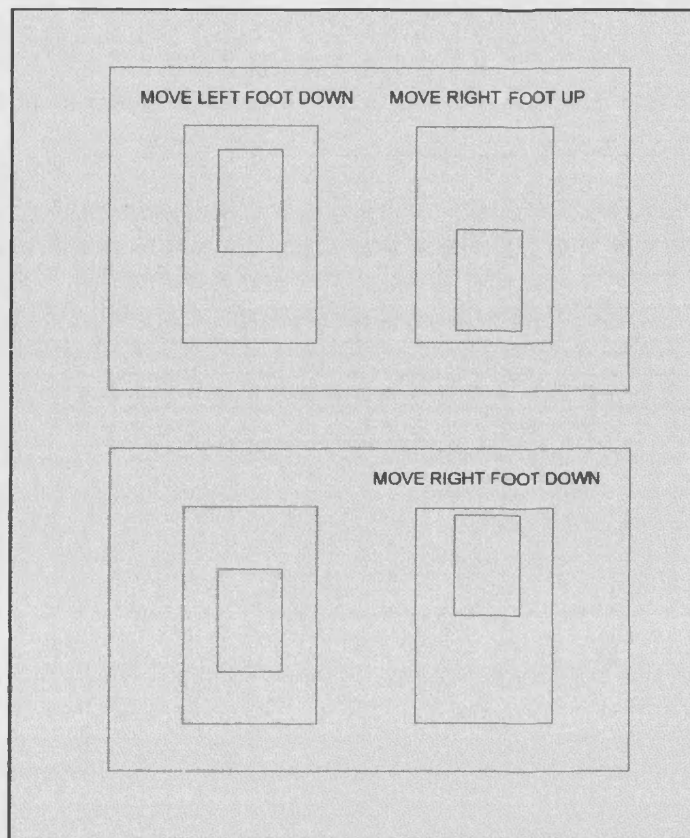


Fig. B.1 Screen display showing possible foot positions.

### INPUT.

This module contains all the routines necessary to gather data from the footpads and switches. The first routine within INPUT, *switch*, stores the logic value relevant to the state of the latched skill level switches and the test routine initiating switch. Note that the state of the quit button is ignored at this point so that accidental quitting of the session does not occur.

The second routine, *strain* uses ADCON, the 80C552 analogue to digital converter control register, to select an input from port 5 and perform a conversion on that analogue signal. The value of this register at any time controls the conversion. The output from each pressure gauge in turn is selected and digitised in the following order:-

Left footpad front left sensor, rbr, lbl, rfr, lbr, rfl, lfr, rbl.

Subsequent to each conversion, the digitised offset recorded during calibration is subtracted from the corresponding sensor value. If this result should ever be negative due to drift, then the result is set to zero to ensure wrap around register problems do not occur. The third routine, *fipad*, acquires the foot position data. A parallel load signal is transmitted to the footpads to



## **APPENDIX B. BALANCE AID SOFTWARE**

effect the load of fresh data into the shift registers. The first data bit is read in by the microcontroller and followed by the output of a clock signal to make the next bit available. The data bits are stored at the required memory location when four bits have been loaded. The four bit words represent the frontmost or rearmost positions of the feet, producing sixteen possible positions for each half of each foot. The above sequence is repeated a further three times to produce four 4-bit words coding for the positions of the extremities of both feet. These are acquired and stored in the following order:

Right back, right front, left back, left front.

INPUT is not called as a module but as separate routines within the module. A return to the calling module is effected upon completion of any of the three routines contained within this module.

### **COFG.**

This module is responsible for calculating the centre of gravity of the patient, using the readings obtained from the pressure sensors within each footpad. The pseudocode, shown in appendix C corresponds to the centre of gravity position generating algorithm.

Initially, the sensor readings from the left and right footpad are added and divided by four to produce an average sensor reading for each footpad. These two values are then subtracted from each other to deduce which is the greater, indicating whether the user's weight is concentrated to the left or the right of an imaginary point between the two footpads. The result of the subtraction is multiplied by the skill level and divided by a scaling factor, set at  $0B_{16}$ . A check is performed to see whether the result of all of the above would cause the centre of balance of the user to lie outside the screen. If this is the case, then the left or right offset is set to the limiting value of  $14_{16}$ . If the cross lies within the boundary of the screen, then the value of the offset is maintained. The horizontal offset is then stored in a dedicated memory location.

The average readings for the four front pressure sensors and the four rear pressure sensors are then found. As with the horizontal offset calculation, these average readings are subtracted from each other to show whether the user's weight is acting to the front or the rear of the footpad centre point. The result of the subtraction is multiplied by the skill level and divided by a scaling factor, set at  $03_{16}$ . The final vertical offset is either stored if it is within the limit for the screen, or failing this the vertical offset is assigned the limiting value of  $4B_{16}$ .

## APPENDIX B. BALANCE AID SOFTWARE

The final screen position of the cross is calculated by use of the horizontal and vertical offsets calculated previously. It can be seen in fig. B.2, that the screen addresses number horizontally from the top left corner to the bottom right corner.

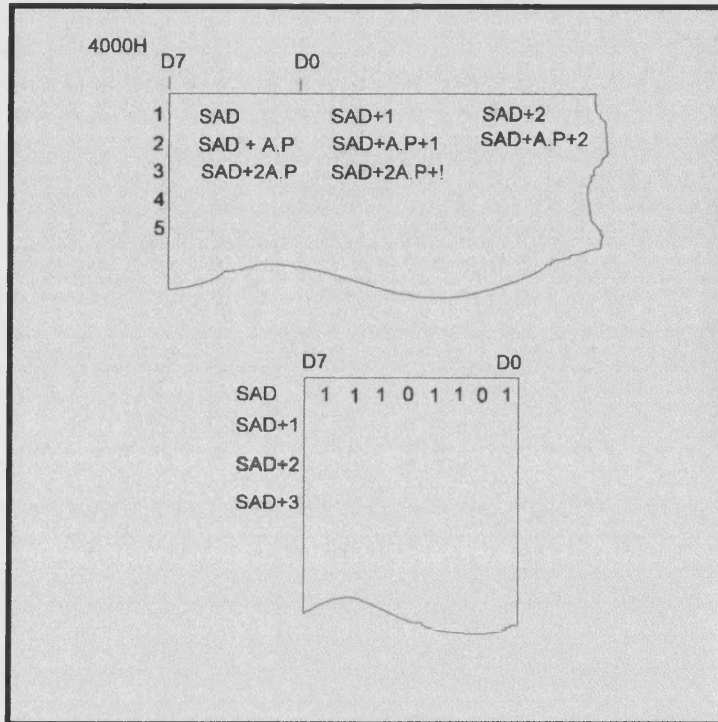


Fig. B.2 Screen addressing progression and memory mapping.

The centre of the screen is situated at  $595F_{16}$  and the cross position is calculated with respect to this point. Each screen line is comprised of 40 blocks of 8 dots, addressable in single blocks. The vertical offset is multiplied by  $50_{16}$  to convert to a whole number of screen lines and added to, or subtracted from, the centre point co-ordinate depending upon whether the centre of balance is to the rear or the front of the centre point of the footpads. This produces a screen co-ordinate at a point directly above or below the screen centre. The horizontal offset is then added to the co-ordinate produced for centre of balance offsets to the right and subtracted for balance offsets to the left. The result is the final cross screen position and is stored as two, 2-digit hex numbers.

### GFXLIB.

This module comprises just two routines and is concerned with writing graphics to the LCD screen. The routine *scrwrite* is called from the *clrscr* routine within the GFXUTIL module and sends the necessary control codes and data to the SED 1330 screen controller, which in turn drives the LCD screen.

## **APPENDIX B. BALANCE AID SOFTWARE**

The second routine, *tabaddr*, is called whenever text is to be placed on the screen. For ease of use, the screen position is referenced to the co-ordinate (0,0) in the bottom left screen corner, whereas in reality the character screen starts at  $0000_{16}$  in the top left corner. This routine converts between these two methods of addressing the screen.

### **GFXUTIL.**

This 'graphics utilities' module contains a number of routines concerned with output to the screen. The routine *text* is called whenever text is to be sent to the LCD screen. Data consisting of the text and its position on the screen is read by this routine. *Text* then sends the control characters required for cursor positioning to the screen driver, followed by the data to be printed on the screen. The routine *char* performs an identical function to *text* but acts on single characters rather than on a string of characters.

The routine *horiz* draws horizontal lines on the screen according to the start and finish co-ordinates specified after the routine call. A data list after the routine call specifies how many lines are to be drawn and contains the 16-bit co-ordinates of the two ends of the line. The order of the list is as follows:

start point low byte, start point high byte, finish point low byte, finish point high byte.

In order to draw a horizontal line, the start position is sent to the screen driver using the appropriate preceding control code and the cursor is positioned accordingly. A block of eight dots is then printed at this point, the cursor position incremented and the process repeated until the end co-ordinate is reached. In this way a line is formed by continuous blocks of dots. The whole routine then repeats to draw as many lines as there are data lists.

The routine *vert*, which is used to draw vertical lines on the screen, operates in a similar fashion to *horiz*. Start and finish co-ordinates are either available in data lists or have been pre-calculated. The cursor is positioned at the uppermost co-ordinates of the line and a single dot is printed. The cursor is advanced one complete line and another dot is printed, forming a vertical line. Both *horiz* and *vert* may be used to erase previously drawn lines by overwriting with blank characters. In order to avoid erasing sections where vertical lines meet horizontal lines, the screen data is read and the single dot of the vertical line at that point is ORed with that data. The result is then sent to the screen as data so that vertical lines are printed alongside any existing data.

## **APPENDIX B. BALANCE AID SOFTWARE**

The *clrscr* routine sets the cursor to the top left corner of the screen and then sends the control code to erase all screen data following the cursor address.

A cross is drawn on the screen to indicate to the user the position of his centre of balance. The routine, *show*, erases the old cross if the user's centre of balance has changed since the last program cycle. It determines this by XORing both bytes of the old and new cross centre position, the result being a 1 if there has been a change in the cross position. If a change has occurred, the existing cross centre position is converted to line start and finish co-ordinates and the lines erased using the technique outlined above.

A similar procedure is used to determine the start and finish addresses of the two sections of the new cross, which is then drawn using the routines *horiz* and *vert*.

The box in the centre of the screen is re-drawn as deletion of the old cross often removes sections of this box.

### **MATHLIB.**

This module contains four routines that are called whenever 16-bit arithmetic is necessary, as the 80C552 microcontroller used in this application is only capable of mathematical operations on 8-bit numbers. The four bytes to be added, subtracted, multiplied or divided are loaded into the appropriate registers before the required routine is called. The 16-bit result is returned in 2-byte form in two separate registers. These routines are called whenever screen addresses are calculated, significantly reducing the volume of coding.

### **SCRSET.**

This module is initiated subsequent to a reset and performs all the LCD screen initialisation required prior to writing data to the screen. A detailed explanation of all the screen commands with all the coding necessary to achieve a variety of screen configurations is given in the SED 1330 LCD Preliminary Instruction Manual [41] on pages 17 to 40.

### **TEST.**

The test module is a single routine, called whenever the operator chooses to perform a test on the operation of the footpads. The option is offered in the module INTRO and may only be called from this module. TEST initially presents a title page of instructions and the test routine will commence when the user signifies his readiness by pressing any button.

## APPENDIX B. BALANCE AID SOFTWARE

Two footpad outlines are drawn on the screen when the routine begins and, upon the operator applying point pressure to the footpads as instructed, functional foot detection strips are shown by horizontal bars printed within the outlines. These are produced by calling the routine *fpad*. Initially, the module TEST converts the strip number corresponding to the left front foot position into a 16-bit screen start and finish address and the horizontal bar is drawn on the screen. The position of the left rear foot position is processed next and a similar horizontal bar drawn. The start and finish screen addresses of these lines are then used to draw in two vertical lines to form a diagrammatic representation of a foot outline. An identical cycle is performed for the right footpad. This is similar to the routine in the CHKFEET module that displays the user's foot position but not identical as in this case no horizontal lines are deleted. The routine cycles, alternately updating the left and right footpad outlines until the user indicates that he no longer wishes this part of the test to continue. Non functioning foot detection strips show up as missing horizontal bars on the footpad outline and indicate a failure at that position on the footpad. A typical screen midway through this test is shown in fig. B.3.

The second part of the test module concerns testing of the pressure sensing units. The screen is cleared and instructions for this part of the test printed on the screen. When the user has pressed any button to signify that he is ready to begin this section, the screen is cleared and two footpad outlines are displayed. The routine displays the digitised sensor output as a 3-digit decimal number in the relevant corner of the footpad outline. A continuous cycle is entered, whereupon the routine *strain* is called to produce the digitised sensor outputs. The previous sensor reading is updated with the current sensor output if :

Previous value < current value

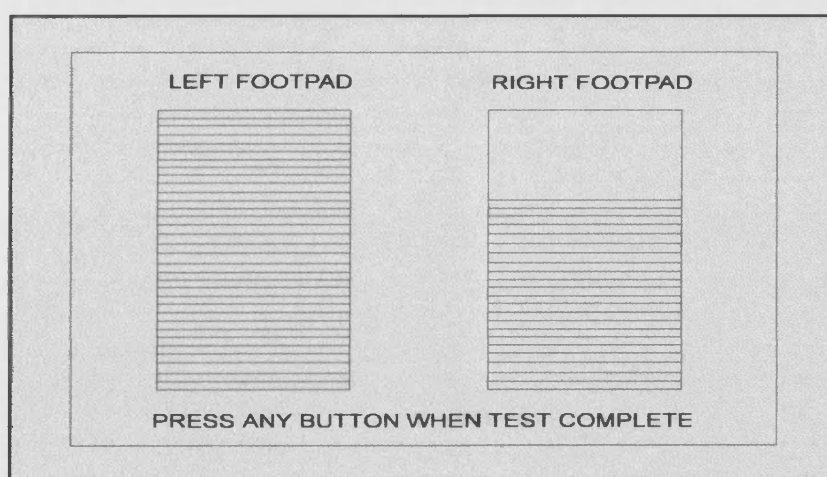


Fig. B.3 Screen display midway through foot location subsystem test.

## APPENDIX B. BALANCE AID SOFTWARE

---

At the end of every cycle, the value of the temporary store is converted to its ASCII value by calling the routine *ascii*. This is then printed in 3-digit decimal form on the screen. This results in the highest output from each sensor being displayed in the relevant corner of the footpad so that the minimum initial value and maximum final value of each sensor may be examined. A typical screen midway through this test is shown in fig. B.4.

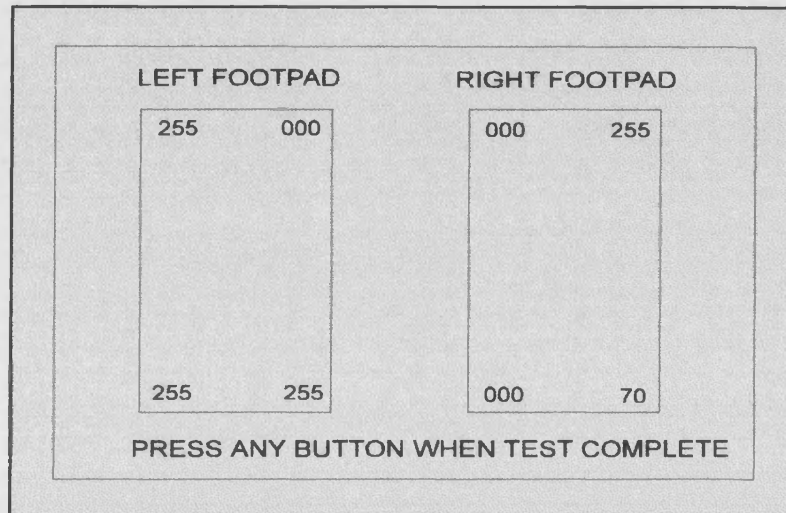


Fig. B.4 Screen display midway through a pressure sensor test.

The user may press any button when satisfied that the test is complete, to return to the main program and proceed to the foot positioning routines.

### CAL.

This routine is called from the module INTRO at the beginning of each balance aid session. The routine begins with an instruction page, which remains until the user presses any button to show readiness to continue. Calibration should be carried out with both feet clear of the footpads so that the only sensor readings are due to footpad weight and sensor offsets. After the instruction page, the A / D converter control register, ADCON, is set to receive the input from the left pad front left sensor (lfl) and a conversion initiated. A loop causes the routine to wait until the end of the conversion is signalled and then the result is stored in internal RAM (IRAM) as the lfl sensor offset. This is subtracted from all further readings from this sensor to correct any offsets in the device output. The routine then repeats this operation for each of the other seven sensor outputs, storing each offset value in a separate IRAM store. Once complete, CAL returns control to the module INTRO without waiting for any operator prompt.

## APPENDIX C C. of G. CALCULATION

---

### APPENDIX C. C. of G. CALCULATION.

$lfl+lfr+lbl+lbr$  = total of left footpad sensors.

$rfl+rfr+rbl+rbr$  = total of right footpad sensors.

$\frac{total\_left}{4}$  = Average left footpad sensor output.

$\frac{total\_right}{4}$  = Average right footpad sensor output.

$lfl+lfr+rfl+rfr$  = total of front footpad sensors.

$lbl+lbr+rbl+rbr$  = total of rear footpad sensors.

$\frac{front\_total}{4}$  = Average front footpad sensor output.

$\frac{rear\_total}{4}$  = Average rear footpad sensor output.

If left average - right average  $< 0$  weight is to the right side.

then:  $\frac{(Rav - Lav) \times skill}{scaling\_const}$  = right offset

otherwise :  $\frac{(Lav - Rav) \times skill}{scaling\_const}$  = left offset

If screen limit - offset  $< 0$  then offset = limit

If front average - rear average  $< 0$  weight is acting to the rear.

then:  $\frac{(Backav - frontav) \times skill}{scaling\_const}$  = rear offset

otherwise :  $\frac{(Frontav - backav) \times skill}{scaling\_const}$  = front offset

If screen limit - offset  $< 0$  then set offset = limit

Screen centre position  $\pm$  [vertical offset x 50<sub>16</sub>] = vertically offset cross position.

Vertically offset cross pos  $\pm$  [horizontal offset] = final screen cross position.

## APPENDIX D. PULSE SYNTHESIS PLD CODE

---

# APPENDIX D. PULSE SYNTHESIS PLD CODE.

```
// Sat Apr 12 17:15:50 1997
// C:\thesis\thesapps\PSYN6.ldf generated using Lattice pDS Version 2.20
LDF 1.00.00 DESIGNLDF;
DESIGN PSYN6;
PART isplSI1016-90LJ;
DECLARE
END; //DECLARE
SYM GLB A0 1 ;
CBUD4 ([Q0..Q3],CAO,[R1..R4],VCC,CLK0,GND,PL1,VCC,GND,GND,GND);
END;
SYM GLB A2 1 ;
NAND4(OSC,[Q0..Q3])
AND2(PL1,[DCLK,IOSC])
INV(DCLK,OSC)
INV(O0,OSC)
END;
SYM GLB A3 1 ;
CBUD8 ([OP0..OP7],CAO2,[D0..D7],VCC,CLK1,GND,GND,CE,UD,GND,RST);
END;
SYM GLB B2 1 ;
MAG8 (GT,EQU,LT,[M0..M7],[OP0..OP7],GND,VCC,GND);
END;
//No ldf text found for cell: A6
//No ldf text found for cell: A7
//No ldf text found for cell: B7
//No ldf text found for cell: B6
//No ldf text found for cell: B5
SYM GLB B4 1 ;
INV (CE,EQU);
INV(IOSC,ACLK)
END;
//No ldf text found for cell: A4
//No ldf text found for cell: A5
SYM GLB B0 1 ;
BUF(CLK1,O0)
BUF(IOCLK0,O2)
BUF(CLK2,O1)
END;
SYM GLB B3 1 ;
INV (O1,UD);
FD21 (MAGON,VCC,CLK2,MAGOFF);
INV (INMAGON,MAGON);
END;
//No ldf text found for cell: A1
SYM IOC IO24 1 ;
XPIN IO XI24 LOCK 3 ;
IL11 (R1,XI24,IOCLK1);
END;
SYM IOC IO25 1 ;
XPIN IO XI25 LOCK 4 ;
IL11 (R2,XI25,IOCLK1);
END;
SYM IOC IO26 1 ;
XPIN IO XI26 LOCK 5 ;
IL11 (R3,XI26,IOCLK1);
END;
SYM IOC IO27 1 ;
XPIN IO XI27 LOCK 6 ;
IL11 (R4,XI27,IOCLK1);
END;
SYM IOC IO0 1 ;
XPIN IO XI0 LOCK 15 ;
IL21 (M0,XI0,IOCLK0);
END;
SYM IOC IO1 1 ;
```



## **APPENDIX D. PULSE SYNTHESIS PLD CODE**

---

```
XPIN IO XI1 LOCK 16 ;
IL21 (M1,XI1,IOCLK0);
END;
```

```
SYM IOC IO2 1 ;
XPIN IO XI2 LOCK 17 ;
IL21 (M2,XI2,IOCLK0);
END;
SYM IOC IO3 1 ;
XPIN IO XI3 LOCK 18 ;
IL21 (M3,XI3,IOCLK0);
END;
SYM IOC IO4 1 ;
XPIN IO XI4 LOCK 19 ;
IL21 (M4,XI4,IOCLK0);
END;
SYM IOC IO5 1 ;
XPIN IO XI5 LOCK 20 ;
IL21 (M5,XI5,IOCLK0);
END;
SYM IOC IO6 1 ;
XPIN IO XI6 LOCK 21 ;
IL21 (M6,XI6,IOCLK0);
END;
SYM IOC IO7 1 ;
XPIN IO XI7 LOCK 22 ;
IL21 (M7,XI7,IOCLK0);
END;
SYM IOC IO30 1 ;
XPIN IO XI30 LOCK 9 ;
IB11 (UD,XI30);
END;
SYM IOC IO29 1 ;
XPIN IO XI29 LOCK 8 ;
IB11 (RST,XI29);
END;
SYM IOC IO8 1 ;
XPIN IO XO8 LOCK 25 ;
OB11 (XO8,OP0);
END;
SYM IOC IO9 1 ;
XPIN IO XO9 LOCK 26 ;
OB11 (XO9,OP1);
END;
SYM IOC IO10 1 ;
XPIN IO XO10 LOCK 27 ;
OB11 (XO10,OP2);
END;
SYM IOC IO11 1 ;
XPIN IO XO11 LOCK 28 ;
OB11 (XO11,OP3);
END;
SYM IOC IO12 1 ;
XPIN IO XO12 LOCK 29 ;
OB11 (XO12,OP4);
END;
SYM IOC IO13 1 ;
XPIN IO XO13 LOCK 30 ;
OB11 (XO13,OP5);
END;
SYM IOC IO14 1 ;
XPIN IO XO14 LOCK 31 ;
OB11 (XO14,OP6);
END;
SYM IOC IO15 1 ;
XPIN IO XO15 LOCK 32 ;
OB11 (XO15,OP7);
END;
```

```
SYM IOC Y0 1 ;
XPIN CLK Y0 LOCK 11 ;
IB11 (CLK0,Y0);
END;
```

```
SYM IOC Y2 1 ;
XPIN CLK Y2 LOCK 33 ;
IB11 (IOCLK1,Y2);
END;
SYM IOC IO31 1 ;
XPIN IO XI31 LOCK 10 ;
IB11 (O2,XI31);
END;
SYM IOC IO28 1 ;
XPIN IO XI28 LOCK 7 ;
IB11 (ACLK,XI28);
END;
SYM IOC IO23 1 ;
XPIN IO XO23 LOCK 44 ;
OB11 (XO23,INMAGON);
END;
SYM IOC IO22 1 ;
XPIN IO XI22 LOCK 43 ;
IB11 (MAGOFF,XI22);
END;
SYM IOC IO16 1 ;
XPIN IO XO16 LOCK 37 ;
OB11 (XO16,EQU);
END;
END; //LDF DESIGNLDF
```

## **APPENDIX E STIMULATOR PARAMETER DERIVATION**

### **APPENDIX E. STIMULATOR PARAMETERS.**

The pulse rise time ( $t_r$ ) is dependant on the value of the pulse magnitude number ( $M$ ), the applied rate value ( $R$ ) and the applied oscillator frequency ( $f$ ).

Considering the clock divide section of the circuitry:

$$\text{The number of counts to a parallel load} = (255 - R) \quad (\text{E.1})$$

$$\text{Therefore the period of one generated clock cycle } (t_{clk}) = \frac{(255 - R)}{f} \quad (\text{E.2})$$

Pulses are always generated from zero magnitude (stimulator off) to the desired final magnitude, utilising a number of counts ( $M$ ). This value sets the final magnitude of the pulse.

$$\text{Therefore the rise time } t_r = (M) \left( \frac{255 - R}{f} \right) \quad (\text{E.3})$$

$$\text{and similarly the fall time } t_f = (M) \left( \frac{255 - R}{f} \right) \quad (\text{E.4})$$

Note that  $R$  may be different for the rising and falling edges of the pulse to produce non-identical rise and fall times.

The pulse rising and falling edges are initiated by internal timer interrupts to the slave microcontroller. These interrupts occur when the on-board hardware timer value matches the value in the timer compare register.

The following derivation provides the relationship between the compare value and the waveform parameters.

$$\text{Pulse length timing compare function time period} = t_p + t_r \quad (\text{E.5})$$

$$\text{where } t_p + t_r = T_1 \rightarrow T_3 \text{ with the timer enabled at } T_1 \quad (\text{E.6})$$

$$t_p + t_r = t_p + \left[ M \left( \frac{255 - R}{f} \right) \right] \quad (\text{E.7})$$

$$\text{where } t_p \text{ may be expressed as } \frac{N_1}{f_2}$$

## APPENDIX E STIMULATOR PARAMETER DERIVATION

$f_2$  = frequency of timer clock

$N_1$  = number of clock cycles for pulse top

Similarly the interval  $T_3 \rightarrow T_5$  may be expressed as:-

$$t_f + t_s = t_s + \left[ M \left( \frac{255 - R}{f} \right) \right] \quad (\text{E.8})$$

where  $t_s$  may be expressed as  $\frac{N_2}{f_2}$

$N_2$  = number of clock cycles for off period

When programming the stimulator,  $f$  and  $f_2$  will be fixed in hardware and it will be convenient to specify the time  $t_p$  and  $t_s$  as well as  $t_r$  and  $t_f$ .

$$\text{So if } T_{timer} = t_p + t_r \quad (\text{E.9})$$

$$\text{and } T_{timer} = \frac{K_1}{f_2} \quad (\text{E.10})$$

$K_1$  = number of counts between timer reset and beginning of falling edge.

$$\text{Then } \frac{K_1}{f_2} = t_p + \left[ M \left( \frac{255 - R}{f} \right) \right] \quad (\text{E.11})$$

$$\text{so } K_1 = f_2 \left[ t_p + \left[ M \left( \frac{255 - R}{f} \right) \right] \right] \quad (\text{E.12})$$

$$\text{Similarly } \frac{K_2}{f_2} = t_f + t_s \quad \text{for the stimulator off period.} \quad (\text{E.13})$$

$$\text{so } \frac{K_2}{f_2} = t_s + \left[ M \left( \frac{255 - R}{f} \right) \right] \quad (\text{E.14})$$

$$\text{Therefore } K_2 = f_2 \left[ t_s + \left[ M \times \left( \frac{255 - R}{f} \right) \right] \right] \quad (\text{E.15})$$

## **APPENDIX E STIMULATOR PARAMETER DERIVATION**

Finally, the magnitude value  $M$  may be calculated by:-

$$\text{step size} = \frac{\text{Maximum\_output\_required}}{\text{Chosen\_number\_of\_counts}} \quad (\text{E.16})$$

$$\text{then } M = \frac{V_{out}}{\text{step\_size}} \quad (\text{E.17})$$

The rate number  $R$  may be calculated by manipulation of the expression for  $t_r$  and  $t_f$  to produce:-

$$R = 255 - \left( \frac{f \times t_r}{M} \right) \quad \text{for a rising pulse edge.} \quad (\text{E.18})$$

$$\text{and } R = 255 - \left( \frac{f \times t_f}{M} \right) \quad \text{for a falling pulse edge.} \quad (\text{E.19})$$

Generally,  $f$  will be fixed at 64MHz,  $f_2$  will be fixed at 16/12 MHz and  $t_r, t_f, t_p$  and  $t_s$  will be specified as pulse parameters. Calculations of the unknowns should proceed as follows:-

- 1) Choose the number of counts from zero to the stimulator maximum value.
- 2) Calculate the value of  $M$ .
- 3) Calculate rising and falling values of  $R$ .
- 4) Calculate the compare register values for pulse width  $K_1$  and pulse spacing  $K_2$ .

## **APPENDIX F. SLAVE SOFTWARE ROUTINES.**

### **SETUP.**

The function *setup* initialises the microcontroller internal control registers that require values other than the reset default values. The ports P1, P3 and P4 are reset, as is the magnitude counter within the ispLSI1016 and preparations are made for the first pulse. At this time, the pulse parameters will all be default values as the slave microcontroller program is not receiving data. The rateup value and the magnitude latch enable signal (MLE), presently inactive, are exported via port 4 and the rateup value is then latched. The first pulse magnitude is exported and the timer activated by the setting of the relevant bits within TM2CON, the timer control register. The count direction is set to up in advance of the first pulse. Setup is called once only at the beginning of main. Control is returned to main at the end of setup.

### **INIT\_PULSE.**

This function invokes the execution of the initial pulse. This is performed by a separate routine as there can be no interrupt to start the initial pulse as no definite time has elapsed prior to its synthesis. This function exports the magnitude value by latching it to the ispLSI1016 which starts the synthesis of the pulse and resets the timer. The pulse length governing interrupt is enabled for a match with the timer compare register CM0. Upon detection of the completion of the rising edge, the fall rate is exported, latched and the zero magnitude value exported. The count direction is then set to down, ready for next magnitude change. Control then returns to *main*, where an infinite loop is entered. Break out from the loop from this point onwards is by compare register match interrupt only.

### **PULSE.**

This function is identical to *Init\_pulse* but called exclusively by an interrupt caused by a timer 2 match with the timer compare register CM1. The value of CM1 corresponds to the length of the inter pulse interval.

### **INTER\_PULSE.**

This interrupt called function generates the inter pulse spacing and interrogates port 1 for new parameter data. Upon entry into the function, the inter-pulse length governing interrupt is enabled, the new rate and magnitude data exported and the count direction set to up. Plenty of time remains to accept new data as the inter pulse spaces are always of far greater length than the

## **APPENDIX F SLAVE SOFTWARE ROUTINES**

pulses themselves. Once the above tasks have been completed, the data transfer request line is monitored until the line is active, which causes entry to the data download routine, or until a timer compare register match causes an interrupt.

### **INFO\_IN.**

This function, which interrogates the data transfer and control ports, is called at the beginning of the *inter-pulse* routine to ensure that there is sufficient time for a full data transfer between the master and slave microcontrollers, should this be required.

At the beginning of the function, a test is performed on the data to transfer flag which, if active, will initiate a data transfer. The data transfer will continue until this flag is de-activated, ensuring a complete data transfer within one inter-pulse interval.

Subsequent to a 'data to transmit' signal being detected, the slave system waits for an address request signal to be activated. The slave system then assigns the value placed on port 5 by the master microcontroller to the variable 'address'. This variable specifies which parameter is to be updated by the forthcoming data, as only the pulse parameters requiring to be updated are transmitted. An address acknowledge signal is then activated to inform the master device that the address has been received. The slave microcontroller then waits for a data request signal before comparing the previously loaded address value with known parameter addresses. The current data is then loaded as the appropriate parameter. A data acknowledge signal is then activated to end the data transmission. This cycle will be repeated up to seven times to update as many parameters as require alteration within that inter-pulse period. The cycle is terminated by the removal of the data to transmit flag and control is returned to the *inter\_pulse* function. Each pulse parameter on each slave module is allocated a unique address, permitting all data to be transferred by a single common data bus.

The addresses associated with the seven pulse parameters are as follows:-

<b><u>Parameter</u></b>	<b><u>Slave Module 1</u></b>	<b><u>Slave Module2</u></b>
magnitude	10	15
rateup	20	25
ratedn	30	35
comp0lo	40	45
comp0hi	50	55
comp1lo	60	65
comp1hi	70	75

## APPENDIX F SLAVE SOFTWARE ROUTINES

Fig. F.1 shows the timing associated with a single pulse parameter data transfer between the master microcontroller and the slave microcontroller.

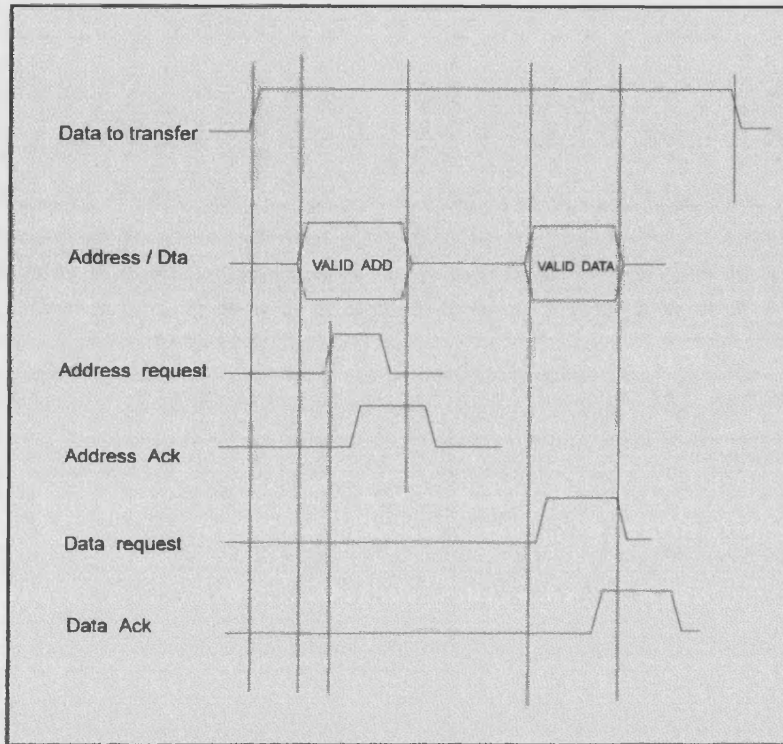


Fig. F.1 Data transfer timing diagram.

### MAIN.

*Main* calls the routines *setup* and *init\_pulse* once only, then waits within an infinite loop for the matches between timer 2 and the timer compare registers CM0 and CM1 to effect interrupts.

## APPENDIX G. SLAVE SOFTWARE LISTING.

```

#include <stdio.h>
#include <register.h>
void setup (void); /* function definition */
void info_in (void);
void init_pulse (void);
/***** general information *****/
/* P4.5 = RST
P4.4 = MLE
P4.7 = RLE
P4.6 = U/D
P4.0 to P4.3 = Rate value
P3.0 to P3.7 = Magnitude value
P1.0 to P1.7 = Data control port
P1.5 = timer 2 reset RT2
P5 = data / address input only
P1.0 = address request
P1.1 = data request
P1.2 = address acknowledge
P1.3 = data acknowledge
P1.4 = end of pulse rising edge detection
P1.7 = data to transfer flag
*/
/***** variable declarations *****/
int delay = 0; /* reset delay loop variable */
int rateup = 0x0E; /* rate up count value set to default */
int ratedn = 0x0E; /* rate down count value at default */
int mag = 0x1E; /* magnitude value at default */
int comp0lo = 0x68; /* compare register 0 low byte - default */
int comp0hi = 0x01; /* compare register 0 high byte - default */
int comp1lo = 0xFF; /* compare register 1 low byte - default */
int comp1hi = 0xA0; /* compare register 1 high byte - default */
int mleval = 0x10; /* value of MLE bit */
int mleudval = 0x50; /* mle plus ud bit value */
int wait = 0; /* forever delay */
int address; /* data transfer byte recognition number */
int adtest; /* masked address byte for valid add test */
/***** setup function *****/
void setup (void)
{
/***** internal register set up *****/
TM2CON = 0x00; /* timer 2 enable, ext reset enable */
IEN0 = 0x80; /* general interrupt enable */
IEN1 = 0x00; /* disable compare 0 and compare 1 interrupts */
IP1 = 0x30; /* priority to compare interrupts */
TM2IR = 0x00; /* T2 interrupt flags reset */
/***** reset ports to zero *****/
P1 = 0x00;
RT2 = 1; /* write 1 to set as an input */
P10 = 1;
P11 = 1;
P17 = 1;
P14 = 1;
P12 = 1; /* set outputs high - active low */
P13 = 1; /* to avoid bus contention */
P3 = 0x00;
P4 = 0x00;
PCON = 0x10; /* watchdog reset */
T3 = 0x00; /* watchdog reset */
/***** start of actual prog *****/
RST = 1;
MLE = 1;
RST = 0;
P4 = rateup | mleval; /* output rate value OR MLE bit */

```



## APPENDIX G SLAVE MICROCONTROLLER SOFTWARE.

```
RLE = 1;          /* remove rate latch */
RLE = 0;          /* set rate latch */
UD = 0;          /* set to count up */
P3 = mag;        /* output magnitude */
CML0 = comp0lo;
CMH0 = comp0hi;  /* compare registers set */
CML1 = comp1lo;
CMH1 = comp1hi;
TM2CON = 0x21;   /* timer start - zero at start */
return ;
}                /* end of setup function */
/*****8 init_pulse function *****/
void init_pulse(void)
{
IEN1 = 0x10;     /* enable CM0 interrupt */
MLE = 0;         /* remove latch enable */
MLE = 1;         /* set latch and reset timer */
while (P14 == 0) /* wait for end of rising edge */
{
}
P4 = ratedn | mlevel; /* output new rate value OR mle */
RLE = 1;
RLE = 0;
P3 = 0x00;       /* output zero magnitude */
UD = 1;          /* set to count down */
return;
}                /* end of pulse function */
/***** pulse function *****/
void pulse(void) interrupt 12 using 2
{
PCON = 0x10;     /* watchdog reset */
T3 = 0x00;
TM2IR = 0x00;    /* reset timer interrupt flag */
IEN1 = 0x10;     /* enable CM0 interrupt */
MLE = 0;         /* remove latch enable */
MLE = 1;         /* set latch and reset timer */
while (P14 == 0) /* wait for end of rising edge */
{
}
P4 = ratedn | mlevel; /* output new rate value OR mle */
RLE = 1;
RLE = 0;
P3 = 0x00;       /* output zero magnitude */
UD = 1;          /* set to count down */
}                /* end of pulse function */
/***** inter_pulse function *****/
void inter_pulse(void) interrupt 11 using 3
{
TM2IR = 0x00;    /* reset timer interrupt flag */
PCON = 0x10;
T3 = 0x00;       /* watchdog reset on inter
pulse section - time to perform */
IEN1 = 0x20;     /* set compare interrupt CM1 */
MLE = 0;         /* latches zero magnitude */
MLE = 1;         /* resets timer */
while (P14 == 0) /* wait for count to stop */
{
}
info_in(); /* calls port communication function when slaved */
PCON = 0x10;     /* watchdog reset */
T3 = 0x00;
CML0 = comp0lo; /* loads new timer values */
CMH0 = comp0hi;
CML1 = comp1lo;
CMH1 = comp1hi;
P4 = rateup | mleudval; /* rate val OR mle plus ud bit */
RLE = 1;         /* remove rate latch */
RLE = 0;         /* set rate latch */
```

## APPENDIX G SLAVE MICROCONTROLLER SOFTWARE.

```
UD = 0;          /* set to count up */
P3 = mag;        /* output magnitude value */
}                /* end of function */
/* ***** port interrogation routine ***** */
void info_in (void)
{
    PCON = 0x10; /* watchdog reset */
    T3 = 0x00;
    while (P17 == 1) /* data to transfer flag active */
    {
        while (P10 == 0 && P17 == 1) /* wait for an address request */
        {
            /* or leave loop if P17 is low */
        }
        if (P17 == 0) /* jump to return if P17 is low */
            break;
        address = P5; /* read first address word */
        adtest = address & 0x0F; /* masking of top 4 bits of address */
        if (adtest != 0x05) /* test for valid address - all board 1 addresses end in 5 */
            break;
        P12 = 0; /* address acknowledged - active low */
        while (P11 == 0 && P17 == 1) /* wait for data request */
        {
            /* leave loop if P17 is low */
        }
        if (P17 == 0)
            break; /* jump to return if P17 is low */
        switch (address)
        {
            case 0x15: mag = P5; /* load port */
                break;
            case 0x25: rateup = P5; /* to variable */
                break;
            case 0x35: ratedn = P5; /* according to */
                break;
            case 0x45: comp0lo = P5; /* address */
                break;
            case 0x55: comp0hi = P5;
                break;
            case 0x65: comp1lo = P5;
                break;
            case 0x75: comp1hi = P5;
                break;
        }
        P13 = 0; /* data acknowledged - active low */
        P12 = 1; /* address ack reset */
        while (P11 == 1) /* wait until data request is off */
        {
        }
        P13 = 1; /* reset data acknowledge */
    } /* end of while loop */
}
return;
}
/* ***** main program ***** */
void main(void) /* start at address 0 */
{
    int delay = 0; /* start up delay 100 counts */
    while (delay < 100)
        delay++;
    PCON = 0x10; /* watchdog reset */
    T3 = 0x00;
    setup (); /* call setup */
    PCON = 0x10; /* watchdog reset */
    T3 = 0x00;
    init_pulse (); /* call init_pulse routine */
    PCON = 0x10; /* watchdog reset */
    T3 = 0x00;
    while (1)
    {
        /* infinite loop */
    }
    /* interrupt driven from here on */
}
```

## **APPENDIX H. DATA TRANSFER ROUTINES.**

### **SETUP.**

This routine is called once only following a system reset to define the initial port settings and variable values.

### **DATA\_PASS\_1 and DATA\_PASS\_2.**

These routines effect pulse parameter updates to the slave microcontroller of channel 1 and 2. Initially, as the master microcontroller requires to update the slave microcontroller's pulse parameters, the data to transfer line (P4.7) is taken high. The data control tasks are assigned to port 4 and the data and address transfers take place via port 1. The data to transfer line remains high for the whole time that parameters are passed between the two devices. The slave microcontroller will ignore this control line until there is time available for a complete transfer, then test that line and, if active, accept addresses and data. Subsequent to activating the data to transfer line, a test is performed on each parameter, to determine whether or not any updates are necessary. The test is to compare the previous value of each parameter with the latest value. A difference in value causes the transfer of the parameter data to take place. If there is no difference in value, a similar test is performed on the next parameter and so on throughout all seven parameters. When a difference is detected between the old and new versions of a parameter, the address associated with that parameter is published on port 1 and the address request line (P4.1) is taken high to signal to the slave that the address is available. This address informs the slave microcontroller which parameter will follow as data. When the slave device has stored this address, it activates the address acknowledge line to signal that it has done so. This is received by the master device on P4.2 and is followed by the replacement of the address with the parameter data and the activation of the data request line. The master device will then wait until a data acknowledge signal is received on P4.3 before proceeding to the next parameter and repeating the complete cycle. Upon completion of each cycle, the variable holding the 'old' version of the transferred parameter is updated with the value of the parameter passed to the slave device.

### **MAIN.**

This is the control allocation function that calls each function at the required time. When each function has performed the relevant tasks, control is returned to *main*.

## APPENDIX I TRANSFORMER DESIGN

### APPENDIX I. TRANSFORMER DESIGN.

Considering the primary winding:-

$$N\phi = Vt \quad \text{According to the volt second balance.} \quad (I.1)$$

$$NBA = Vt \quad \text{where } \phi = BA = \text{total flux} \quad (I.2)$$

Now, given that  $V_{\max} = 25V$  and the nominal pulse length will be  $300\mu s$ :

$$N_p = \frac{Vt}{BA} \quad (I.3)$$

The silicon-steel core has a diameter of 36mm, with the toroid section measuring 12mm by 12mm. This produces a core area of  $0.144 \times 10^{-3} m^2$

$$N_p = \frac{25 \times 300 \times 10^{-6}}{3.0 \times 0.144 \times 10^{-3}} \quad (I.4)$$

$$N_p = 27 \quad \text{primary turns.} \quad (I.5)$$

Therefore the winding requirement is 0.040 ohms and 27 turns.

One turn of wire around the 12x12mm core requires 48mm of wire, therefore 27 turns requires:

$$l = 27 \times 48 \times 10^{-3} \quad (I.6)$$

$$l = 1.29m \quad (I.7)$$

When choosing a primary wire diameter, it is necessary to consider the current carried and skin effects due to the applied high frequency pulses. The harmonic analysis performed in section 4. 8. 3 shows that a maximum frequency of 100KHz must be considered.

The skin effect associated with this frequency is most usefully expressed as a depth of penetration, given in cm by:

$$\delta = \frac{6.6}{\sqrt{f}} \quad [282] \quad (I.8)$$

$$\text{Therefore } \delta = 0.208mm \quad (I.9)$$

Multi stranded k - filar winding is the accepted method of overcoming the skin effect in windings. For each strand the wire diameter must be at least equal to the depth of penetration, so that  $d > \delta$ .

## **APPENDIX I TRANSFORMER DESIGN**

$$\text{Therefore } d \geq 0.208\text{mm.} \quad (\text{I.10})$$

A convenient wire size available in enamelled copper is 0.20mm and considering that a resistance of 40mΩ is required with a wire length of 1.29m:-

$$R = \frac{\rho l}{A} \quad (\text{I.11})$$

$$\text{for copper wire } \rho = 1.7 \times 10^{-8} \Omega\text{m}^{-1} \quad [\text{323}] \quad (\text{I.12})$$

$$\text{so } A = \frac{1.7 \times 10^{-8} \times 1.29}{40\text{m}\Omega} \quad (\text{I.13})$$

$$A = 0.55\text{mm}^2 \quad (\text{I.14})$$

This is the full conductor area required to satisfy the above requirements. The cross sectional area of 0.2mm copper wire is 0.0314mm<sup>2</sup> [323]. Therefore, to achieve the required area of conductor, 17 strands of 0.20mm wire are required. In this way most of the conductor area of each strand is utilised instead of a fraction of the area of one large conductor. These strands are insulated from each other and are wound in parallel.

The current capability of 0.20mm copper wire is 0.35A [323]. The pulse maximum current values are 45A for 1μs, 900mA for 300us and zero for the rest of the cycle. This results in a maximum average current of:

$$I_{av} = \frac{315\text{usA}}{30000\text{us}} \quad (\text{I.15})$$

$$I_{av} = 10\text{mA} \quad (\text{I.16})$$

So, although the peak current is far in excess of the rated wire value, its short duration prevents any undue heating of the winding.

The use of a 1:6 turns ratio results in 162 turns on the transformer secondary. So, to ensure that both windings will fit within the core window area:-

Assuming a single primary conductor winding depth, 17 conductors, 27 primary turns and a conductor external diameter of 0.20mm, the total conductor winding width is calculated to be:-

$$w = 27 \times 17 \times 0.20\text{mm} \quad (\text{I.17})$$

$$w = 91.80\text{mm} \quad (\text{I.18})$$

The steel core inside diameter is 12mm, which results in an internal circumference of :

## **APPENDIX I TRANSFORMER DESIGN**

---

$$C = \pi \times 12\text{mm} \quad (\text{I.19})$$

$$C = 37.68\text{mm} \quad (\text{I.20})$$

Therefore the number of complete layers required to produce the primary winding is :

$$\text{number of layers} = \frac{91.80\text{mm}}{37.68\text{mm}} \quad (\text{I.21})$$

$$\text{number of layers} = 2.5 \quad (\text{I.22})$$

Therefore the winding depth at the deepest point will be:

$$\text{depth} = 3 \times 0.20\text{mm} \quad (\text{I.23})$$

$$\text{depth} = 0.60\text{mm} \quad (\text{I.24})$$

The area associated with this winding is :

$$\text{area} = 0.60 \times 37.68 \quad (\text{I.25})$$

$$\text{Area} = 22.60\text{mm}^2 \quad (\text{I.26})$$

It is convenient to use the same wire to form the secondary winding as the penetration depth will have the same value in this winding. Using 162 turns wound k-filar and still assuming 48mm for the length of one turn, the length of wire required for 162 turns is:

$$\text{length} = 162 \times 48\text{mm} \quad (\text{I.27})$$

$$\text{length} = 7.7\text{m} \quad (\text{I.28})$$

With the maximum secondary current set at 7A, it was considered that 7V would be an acceptable voltage drop across the secondary winding resistance. This results in a resistance value for the secondary of  $1\Omega$ .

Now for  $1\Omega$  winding resistance using  $R = \frac{\rho l}{A}$  (I.29)

$$\text{conductor area} = \frac{1.7 \times 10^{-8} \times 7.1}{1} \quad (\text{I.30})$$

$$\text{conductor area} = 0.1306\text{mm}^2 \quad (\text{I.31})$$

Using 0.20mm copper wire of area  $0.0314\text{mm}^2$  [45], the required number of strands will be:

$$\text{number of strands} = \frac{0.1306}{0.0314} \quad (\text{I.32})$$

## **APPENDIX I TRANSFORMER DESIGN**

$$\text{number of strands} = 4 \quad (\text{I.33})$$

The number of layers occupied by this winding is found by:

$$\text{winding width} = 4 \times 0.20 \times 162 \quad (\text{I.34})$$

$$\text{winding width} = 130\text{mm} \quad (\text{I.35})$$

Continuing to use the assumption of an internal core circumference of 37.68mm, the number of layers required is:

$$\text{number of layers} = \frac{130}{37.68} \quad (\text{I.36})$$

$$\text{number of layers} = 3.5 \text{ layers.} \quad (\text{I.37})$$

Therefore there are 4 layers at the deepest point in the winding.

The additional area occupied by this winding is :

$$\text{winding area} = 4 \times 0.20 \times 37.68 \quad (\text{I.38})$$

$$\text{winding area} = 30.14\text{mm}^2 \quad (\text{I.39})$$

So, the total winding area within the core window of the primary and secondary winding is given by :

$$\text{Total area} = \text{Primary area} + \text{secondary area} \quad (\text{I.40})$$

$$\text{Total area} = 22.60\text{mm}^2 + 30.14\text{mm}^2 \quad (\text{I.41})$$

$$\text{Total area} = 52.74\text{mm}^2 \quad (\text{I.42})$$

The available core area is given by :-

$$\text{Area} = \pi \times \left[ \frac{12}{2} \right]^2 \quad (\text{I.43})$$

$$\text{Area} = 113.04\text{mm}^2 \quad (\text{I.44})$$

This shows that the windings will fit within the window area of the initially chosen core. It should be noted that the above calculations are to estimate the fit of the windings only and do not take into account the reduction in core internal diameter as the window area fills up with the windings.

## APPENDIX J. DATA ACQUISITION SOFTWARE

```

#include <stdio.h>                /* printf Prototype */
#include <ad1200.h>               /* card header file */
#include <dos.h>                  /* dos for time function */
unsigned int y = 0;
int x;
unsigned int a;
unsigned int k;
long int q;                      /* loop variable for pause */
int count = 0;                   /* No cycles before back up */
unsigned int cycles = 0;         /* total no cycles to date */
int chan;                        /* channel number */
unsigned num;                    /* returned val of No system drives */
FILE *fp;                        /* set file pointer */
int n;                           /* loop number */
int adspace[16];                /* A/D result storage */
int *dpoint;                    /* pointer to data array */
unsigned int bigarrayno;
unsigned int arrayno;
int adnumber;                   /* a/d value from array */
unsigned int storage [30000];    /* big array definition */
char whichfile [10][7]
= {"data0","data1","data2","data3","data4","data5","data6","data7","data8","data9"};
void store (void);              /* store function def */
void array_store (void);        /* data to big array fn */

/***** main function *****/
main ()
{

/***** This section supplied with AD 1220 card *****/

int r,v,id,i;                   /* return value, version, card id digin data*/
int PassFail[14];              /* Put Diagnostic test results here*/
v=Version();
printf("\nDriver Major.Minor Version :=%x.%x", v / 0x100, v % 0x100);
printf("\nCopyright Message :=%s",HelloMsg());
BaseSet(0x218);                /* set base address */
printf("\nBase I/O Address Read Back :=%x",BaseGet() );

/* EVERY PROGRAM SHOULD PERFORM THE DIAGNOSTIC TEST */
id=Diag(PassFail);
if (id==ADERR)
{
printf("\nError: Card Failed Diagnostic Test \nExit Program");
return;
}
else printf("\nCard Passed All Tests, Card Type := AD%4d\n",id);
printf ("\n");                 /* print blank line */
/*Only Need To Use IntrSet and DmaSet if not using factory default*/
r=IntrSet(5);                  /* Set up Interrupt Line */
if ( (id==1200) || (id==1201))
r=DmaSet(3);

/***** main prog additions to sample prog *****/

while (cycles < 3000)         /* loop until 12K array is full */
{
chan = 0;                     /* set first channel */
while (chan < 10)             /* sample each input */
{
r = ADIn(chan, &adspace[chan] ); /* sample data and store in array */
if (r==ADOK)                 /* check for good conversion */
chan++;                      /* increment channel number */
}
chan = 0;                    /* reset to channel zero */
}

```



## APPENDIX J DATA ACQUISITION SOFTWARE

---

```
array_store(); /*data to big array */
for (n=0;n<6000;n++) /* delay loop for 25MHz 386 PC*/
{
}
cycles++; /* increment loop variable*/
} /* end of sampling function*/
printf ("data samples complete\n"); /* screen message */
store(); /*file function */
printf ("file operations complete\n"); /* screen message */

} /* end of main */

/***** data to big array function *****/
void array_store (void)
{
    x = 0; /* initialise to first array value */
    while (x < 10)
    {
        dpoint = &adspace [x]; /* get value from conversion array */
        bigarrayno = *dpoint;
        /* printf ("%d,%d\n",bigarrayno,cycles); */ /* print to screen */
        storage[y] = bigarrayno; /* put value in big array */
        y++; /* next value in big array */
        x++; /* next value in conversion array */
    }

    return;

} /* end of function */

/***** file operation routine *****/

void store (void)
{
    _dos_setdrive (3,&num); /* set for drive C */
    a=0; /* start point in big array */

    for (n=0;n<10;n++) /* loop for 16 data files */
    {
        fp = fopen (whichfile[n],"a"); /* open first data file */
        k = a; /* set start point */
        while (k < 30000)
        {
            dpoint = &storage[k];
            arrayno = *dpoint; /* load big array data to files */
            fprintf (fp,"%d\n",arrayno);
            /* printf ("file operations\n"); */
            k = k + 10; /* next data */
        }
        fclose (fp); /* close that file */
        a++; /* next start point */
    }

    return;

} /* end of function */
```

## APPENDIX K STATE MACHINE OPERATION

---

### APPENDIX K. STATE MACHINE OPERATION.

<u>State</u>	<u>Action</u>	<u>Comments</u>
0	CS high	Initialise converter
1	CS low + PL high	Enable device
2	PL high + O1 high	Load 0 to 4 - bit counter (Clock required for load)
3	MCLK high	Output master clock pulse
4	O1 high	clock shift register
5	MCLK high	
6	O1 high	
7	MCLK high	
8	O1 high	
9	MCLK high	
10	O1 high	
11	MCLK high	All data sent to converter
12	No action	
13	MCLK high	MSB output to uC
14	No action	Data read by uC
15	MCLK high	
16	No action	
17	MCLK high	
18	No action	
19	MCLK high	
20	No action	
21	MCLK high	
22	No action	
23	MCLK high	
24	No action	
25	MCLK high	
26	No action	
27	MCLK high	
28	No action	LSB read by uC
29	O0 high	Clk 4 - bit counter
30 + Q5	CRST high	Reset 4 - bit counter
31	MRST high	Reset master counter

## APPENDIX L DATA ACQUISITION PLD CODE.

# APPENDIX L. DATA ACQUISITION PLD CODE

```
// Sat Apr 12 19:00:02 1997
// C:\thesis\thesapps\addriv.ldf generated using Lattice pDS Version 2.20
LDF 1.00.00 DESIGNLDF;
DESIGN ADDRIV;
PART pLS11016-90LJ;
OPTION Y1_AS_RESET ON;
DECLARE
END; //DECLARE
SYM GLB A0 1 ;
CBU48 ([Q0,Q1,Q2,Q3,Q4,OP5,OP6,OP7],CARRY,[D0..D7],VCC,CLK0,GND,GND,VCC,MRST);
END;
SYM GLB A4 1 ;
CBU14 ([C2,C3,C4,Q5],CAO,VCC,CLK1,CRST);
END;
// No ldf text found for cell: A5
SYM GLB A6 1 ;
SRR38 ([DA0..DA7],[C7,C6,C5,C4,C3,C2,C1,C0],VCC,CLK2,GND,PL,VCC,GND);
END;
SYM GLB B7 1 ;
SIGTYPE CS OUT;
SIGTYPE PL OUT;
SIGTYPE O0 OUT;
SIGTYPE CRST OUT;
EQUATIONS
CS = !Q0 & !Q1 & !Q2 & !Q3 & !Q4 & !Q5;
PL = Q0 & !Q1 & !Q2 & !Q3 & !Q4 & !Q5
    # !Q0 & Q1 & !Q2 & !Q3 & !Q4 & !Q5;
O0 = Q0 & !Q1 & Q2 & Q3 & Q4 & !Q5;
CRST = !Q0 & Q1 & Q2 & Q3 & Q4 & Q5;
END
END;
SYM GLB B6 1 ;
SIGTYPE O1 OUT;
SIGTYPE MRST OUT;
EQUATIONS
O1 = !Q0 & !Q1 & Q2 & !Q3 & !Q4 & !Q5
    # !Q0 & Q1 & Q2 & !Q3 & !Q4 & !Q5
    # !Q0 & !Q1 & !Q2 & Q3 & !Q4 & !Q5
    # !Q0 & Q1 & !Q2 & Q3 & !Q4 & !Q5
    # !Q0 & Q1 & !Q2 & !Q3 & !Q4 & !Q5;
MRST = Q0 & Q1 & Q2 & Q3 & Q4 & !Q5
END
END;
SYM GLB B4 1 ;
BUF (C0,VCC)
BUF (C1,VCC)
BUF (C5,VCC)
BUF (C6,VCC)
END;
SYM GLB B5 1 ;
SIGTYPE MCLK OUT;
EQUATIONS
MCLK = Q0 & Q1 & !Q2 & !Q3 & !Q4 & !Q5
    # Q0 & !Q1 & Q2 & !Q3 & !Q4 & !Q5
    # Q0 & Q1 & Q2 & !Q3 & !Q4 & !Q5
    # Q0 & !Q1 & !Q2 & Q3 & !Q4 & !Q5
    # Q0 & Q1 & !Q2 & Q3 & !Q4 & !Q5
    # Q0 & !Q1 & Q2 & Q3 & !Q4 & !Q5
    # Q0 & Q1 & Q2 & Q3 & !Q4 & !Q5
    # Q0 & !Q1 & !Q2 & !Q3 & Q4 & !Q5
    # Q0 & Q1 & !Q2 & !Q3 & Q4 & !Q5
    # Q0 & !Q1 & Q2 & !Q3 & Q4 & !Q5
    # Q0 & Q1 & !Q2 & Q3 & Q4 & !Q5
    # Q0 & !Q1 & !Q2 & Q3 & Q4 & !Q5
    # Q0 & Q1 & !Q2 & Q3 & Q4 & !Q5
END;
END
SYM GLB B0 1 ;
BUF (CLK1,O0);
BUF (CLK2,O1);
END;
SYM GLB B3 1 ;
BUF (C7,VCC)
END;
// No ldf text found for cell: A1
// No ldf text found for cell: A2
// No ldf text found for cell: A3
// No ldf text found for cell: A7
SYM IOC IO8 1 ;
XPIN IO XO8 LOCK 8;
OB11 (XO8,DA7)
END;
SYM IOC IO7 1 ;
XPIN IO XO7 LOCK 7;
OB11 (XO7,CS)
END;
SYM IOC IO9 1 ;
XPIN IO XO9 LOCK 9;
OB11 (XO9,MCLK);
END;
SYM IOC Y0 1 ;
XPIN CLK Y0 LOCK 11;
IB11 (CLK0,Y0);
END;
END; //LDF DESIGNLDF
```

## APPENDIX M. MASTER SOFTWARE

```

#pragma small                                /* small memory model */
#include <reg2.h>
#define XBYTE ((unsigned char *) 0x20000L)    /* ext read / wr def */
void data_fn (void);                         /* function definitions */
void data_pass1 (void);
void calc_fn (void);
void setup (void);
void ramwrite (void);
void ramread (void);
void data_pass2 (void);
void error_pres (void);
void slope_detect (void);
void speed_detect (void);
void watchdog (void);
void add (void);
void subtract (void);
void add_bytes (void);
void regulate_stim (void);
/***** general information *****/
P1.0 to P1.7 -- data and address transfer (o/p)
P1.7 -- external 10K pullup fitted.
P4.0 -- address request (o/p)
P4.1 -- data request (o/p)
P4.2 -- address ack (i/p)
P4.3 -- data ack (i/p)
P4.7 -- data to transmit indicator (o/p)
*/
int delay = 0; /* start up delay variable */
/* slave board 1 variables */
unsigned char mag = 0x58; /* magnitude value to pass to slave */
unsigned char newmag = 0x1E; /* latest magnitude value */
unsigned char rateup = 0x0D; /* ramp up value to pass to slave */
unsigned char newrateup = 0x0D; /* latest ramp up value */
unsigned char ratedn = 0x0D; /* ramp down value to pass to slave */
unsigned char newratedn = 0x0D; /* latest ramp down value */
unsigned char comp0lo = 0x5E; /* comparator 0 low byte value to pass to slave */
unsigned char newcomp0lo = 0xE0; /* new comparator 0 low byte value */
unsigned char comp1lo = 0xAB; /* comparator 1 low byte value to pass to slave */
unsigned char newcomp1lo = 0x8C; /* latest comparator 1 low byte value */
unsigned char comp0hi = 0x02; /* high byte comparator 0 to pass to slave */
unsigned char newcomp0hi = 0x01; /* latest high byte for comparator 0 */
unsigned char comp1hi = 0x88; /* comparator 1 high byte value to pass to slave */
unsigned char newcomp1hi = 0xB9; /* latest comparator 1 high byte value */
/***** slave board 2 variables *****/
unsigned char mag2 = 0x58; /* magnitude value to pass to slave */
unsigned char newmag2 = 0x14; /* latest magnitude value */
unsigned char rateup2 = 0x0D; /* ramp up value to pass to slave */
unsigned char newrateup2 = 0x0D; /* latest ramp up value */
unsigned char ratedn2 = 0x0D; /* ramp down value to pass to slave */
unsigned char newratedn2 = 0x0D; /* latest ramp down value */
unsigned char comp0lo2 = 0x68; /* comparator 0 low byte value to pass to slave */
unsigned char newcomp0lo2 = 0xE0; /* new comparator 0 low byte value */
unsigned char comp1lo2 = 0xE6; /* comparator 1 low byte value to pass to slave */
unsigned char newcomp1lo2 = 0xE6; /* latest comparator 1 low byte value */
unsigned char comp0hi2 = 0x02; /* high byte comparator 0 to pass to slave */
unsigned char newcomp0hi2 = 0x01; /* latest high byte for comparator 0 */
unsigned char comp1hi2 = 0xAA; /* comparator 1 high byte value to pass to slave */
unsigned char newcomp1hi2 = 0xAA; /* latest comparator 1 high byte value */
unsigned char mask = 0x10; /* mask for adci value */
unsigned char readloop; /* loop for 8 sensor reads */
unsigned char clkloop; /* loop for lattice clocks */
unsigned char datloop; /* loop to read 1 sensor data */
unsigned char input = 0; /* temporary store for input data bit */
unsigned char sensor = 0; /* final rotated byte from sensor */
unsigned char psns[8]; /* array to hold 8 sensor readings */

```

## APPENDIX M MASTER SOFTWARE

```
unsigned int ramloop;          /* ram access loop variable */
unsigned int startaddr;       /* start address of RAM block to be accessed */
unsigned char location;       /* 0 - 7 value of RAM write address within block */
unsigned char sig_in_1;      /* value read back from RAM */
unsigned char sig_in_2;      /* value read from RAM */
unsigned char chan;          /* input channel number 0 - 7 for read */
unsigned int ramaddr;         /* ram value to be read from */
unsigned char samp[10];      /* array of data read from RAM */
unsigned char n;              /* read loop variable */
unsigned char cycle_no;      /* number of loops to call calc_fn */
unsigned char timer_control = 0; /* counter value in walking speed meas */
unsigned int speed_count = 0; /* increasing loop time variable init val */
unsigned char speed_val = 20; /* final scaled time loop variable */
unsigned char lo;            /* lo byte of 16 bit operation */
unsigned char hi;            /* hi byte of 16 bit operation */
unsigned int byte_total;     /* 16 bit version of hi and lo */
unsigned char loop;         /* integrator count down rate */
unsigned char magmax = 0x47; /* ch1 max value */
unsigned char magmin = 0x1D; /* ch1 min value */
unsigned char mag2max = 0x24; /* ch2 max value */
unsigned char mag2min = 0x10; /* ch2 min value */
unsigned char magnom = 0x32; /* ch1 nominal value */
unsigned char mag2nom = 0x14; /* ch2 nominal value */
unsigned int byte_total_max = 0x0258; /* ch max pulse width */
unsigned int byte_total_min = 0x00B4; /* ch min pulse width */
unsigned int byte_total_nom = 0x01C2; /* ch1 nom pulse width */
unsigned int byte_total_nom2 = 0x0190; /* ch2 nom pulse width */
bit upslope;                /* true / false slope up */
bit dnslope;                /* true / false slope down */
bit flata;                  /* true / false level detected */
bit flatb;                  /* true / false level detected */
bit flat;                  /* overall level detect bit */
bit error = 0;              /* broken wire fault flag */
bit lsenflat = 1;           /* left sensors flat bit */
bit lhrise = 0;             /* left heel pres rising bit */
bit lbrise = 0;             /* left ball pres rising bit */
bit rtrise = 0;             /* right toe pres rising bit */
bit rtfall = 0;            /* right toe pres fall bit */
bit rtlev = 0;              /* right toe pres level bit */
bit rhrise = 0;            /* right heel pres rising bit */
bit ltrise = 0;            /* left toe pres rising bit */
bit levflag = 0;           /* used as store for level bit */
bit levbit = 0;            /* bitwise and of flat and levflag */
bit speedheel1 = 1;        /* 1st heel strike access flag */
bit speedball1 = 0;        /* ball pressure rise access flag */
bit speedheel2 = 0;        /* 2nd heel strike access flag */
bit speedheel3 = 0;        /* 1st heel ramp down access flag */
bit heel_bit;
bit ball_bit;               /* temp stores for slope detect results */
bit outer_bit;
/* ***** */
void setup(void)            /* data transfer initial port settings */
{
    P40 = 0;                /* set outputs to zero */
    P41 = 0;
    P47 = 0;
    P1 = 0x00;
    P42 = 1;                /* set inputs to 1 */
    P43 = 1;
return;
}
/* ***** */
void calc_fn(void)          /* calculation function */
{
    if (startaddr < 72)    /* check if 10 blocks available */
    {
        startaddr = startaddr + 8; /* move to start of next block */
        return;             /* back to main */
    }
}
```

## APPENDIX M MASTER SOFTWARE

---

```
}
if ( timer_control < 2)
{
    speed_detect(),          /* call speed detect / initialising */
                          /* 2 heel strikes noted */
    goto exit;              /* update start address */
}
/* performed once only */
/***** first section of control statements *****/
if (ltrise == 1)          /* enter if bit set */
{
    chan = 1;              /* right ball */
    ramread();
    slope_detect();
    ball_bit = upslope;    /* rising right ball pressure */
    chan = 4;              /* left toe input data from RAM */
    ramread();             /* call ram reading to array function */
    slope_detect();        /* call slope detection function */
    if (upslope == 1 || ball_bit == 1) /* check for pressure rise */
    {                       /* on left toe / right ball */
        lsenflat = 1;      /* set next entry level flag */
        rhrise = 0;        /* reset entry flag */
        ltrise = 0;        /* reset entry bit to prevent entry next cycle */
    }
    if (rhrise == 0)
    {
        newmag = 0x23;     /* end of cycle - reset to default */
        newmag2 = 0x19;    /* next layer stabilises foot */
        newcomp0lo = 0x5E;
        newcomp0lo2 = 0x5E;
        newcomp0hi = 0x01;
        newcomp0hi2 = 0x01;
    }
    if (rhrise == 0)      /* only if this layer active */
        goto exit;       /* escape to address inc */
}
/* ***** next section of control statements *****/
if (rhrise == 1)        /* enter if bit set */
{
    chan = 3;             /* right heel input data from RAM */
    ramread();            /* call ram reading to array function */
    slope_detect();       /* call slope detection function */
    if (upslope == 1)    /* check for pressure rise rt heel strike */
    {
        ltrise = 1;      /* set next entry level flag */
        rtlev = 0;       /* reset entry flag */
    }
    chan = 1;            /* right ball */
    ramread();
    slope_detect();
    if (upslope == 0 && rtlev == 0) /* until pressure on right ball */
    {                               /* ie foot stable */
        lo = comp0lo2;
        hi = comp0hi2;
        add_bytes();                /* to 16 bit format */
        if (byte_total > 0x00B4)
        {
            subtract();             /* reduce pulse width */
            newcomp0lo2 = lo;
            newcomp0hi2 = hi;
        }
        if (mag2 > 0x14 && byte_total < 0x014A)
            newmag2 = mag2 - 1;     /* reduce amplitude when */
                                    /* halfway to min width */

        lo = comp0lo;
        hi = comp0hi;
        add_bytes();                /* to 16 bit format */
        if (byte_total < 0x01E0)
        {
            add();                  /* increment pulse width */
            newcomp0lo = lo;
        }
    }
}
```

## APPENDIX M MASTER SOFTWARE

---

```
newcomp0hi = hi;
}
if (mag < 0x2E && byte_total > 0x014A)
    newmag = mag + 1;          /* increase ch 1 to stabilise foot */
}                               /* when halfway to max pulse width */
}
/* ***** next section of control statements***** */
if (rtlev == 1)                /* enter if bit set */
{
    chan = 0;                  /* right toe input data from RAM */
    ramread();                 /* call ram reading to array function */
    slope_detect();           /* call slope detection function */
    levbit = flat;            /* temp store */
    chan = 1;                  /* right ball */
    ramread();
    slope_detect();
    ball_bit = flat;          /* temp store */
    chan = 2;                  /* right outside */
    ramread();
    slope_detect();
    if (flat == 1 && levbit == 1 && ball_bit == 1)
    {
        /* ball outer and toe flat */
        rhrise = 1;           /* set next entry level flag */
        rtfall = 0;           /* reset entry flag */
        /* no action required */
    }
}
/* next section of control statements */
/* into swing phase now - toe lifting */
if (rtfall == 1)               /* enter if bit set */
{
    chan = 6;                  /* left outside */
    ramread();
    slope_detect();
    outer_bit = upslope;       /* temp store */
    chan = 5;                  /* left ball data */
    ramread();
    slope_detect();
    ball_bit = upslope;        /* temp store */
    chan = 0;                  /* right toe input data from RAM */
    ramread();                 /* call ram reading to array function */
    slope_detect();           /* call slope detection function */
    if (dnslope == 1 || outer_bit == 1 || ball_bit == 1)
    {
        /* check for right toe lift */
        /* or left outer or ball fall */
        rtlev = 1;            /* set next entry level flag */
        rtrise = 0;           /* reset entry flag */
    }
    for (loop = 0; loop < 20; loop++)
    { regulate_stim();         /* return toward nominal params */
    }
}
chan = 0;                      /* right toe channel */
ramread();
slope_detect();
levflag = flat;                /* transfer flat value to store */
chan = 1;                      /* right ball */
ramread();
slope_detect();
levbit = levflag & flat;       /* if toe and ball flat */
/* both 1 if level ie foot off ground */
if (levbit == 0 && mag2 < 0x24 && rtrise == 0)
    /* right toe and ball both flat */
    /* if not lift toe during swing phase */

newmag2 = mag2 + 1;
lo = comp0lo;
hi = comp0hi;                  /* check current pulse width */
add_bytes();
if (byte_total < 0x01E0 && mag2 > 0x24 && levbit == 0 && rtrise == 0)
```



## APPENDIX M MASTER SOFTWARE

---

```
{
    add();
    newcomp0lo = lo;
    newcomp0hi = hi;
}
}
/* ***** next section of control statements ***** */
/* checks for toe push off on right foot */
if (rtise == 1)
    /* enter if bit set */
    {
    chan = 0;
    ramread();
    slope_detect();
    if (upslope == 1)
        /* check for pressure rise */
        /* ie toe push off complete */
        {
        rtfall = 1;
        lbrise = 0;
        speed_val = 20;
        }
    if (rtfall == 1)
        regulate_stim();
    }
/* ***** next section of control statements ***** */
/* entered if left ball, outer or heel lift noted */
if (lbrise == 1)
    /* enter if bit set */
    {
    chan = 5;
    ramread();
    slope_detect();
    ball_bit = upslope;
    chan = 6;
    ramread();
    slope_detect();
    outer_bit = upslope;
    chan = 7;
    ramread();
    slope_detect();
    if (dnslope == 1 || ball_bit == 1 || outer_bit == 1)
        /* left heel lift, outer or ball rise */
        {
        rtrise = 1;
        lhrise = 0;
        speed_val = 10;
        }
    chan = 1;
    ramread();
    slope_detect();
    ball_bit = upslope;
    chan = 2;
    ramread();
    slope_detect();
    outer_bit = upslope;
    chan = 0;
    ramread();
    slope_detect();
    if (upslope == 0 && ball_bit == 0 && outer_bit == 0 && lhrise == 0)
        /* until rise on right ball or toe or outer */
        {
        if (mag < magmax)
            /* increment ch1 pulse magnitude */
            newmag = mag + 1;
        lo = comp0lo;
        hi = comp0hi;
        add_bytes();
        if (byte_total < byte_total_max)
            /* convert to 16 bit format */
            {
            add();
            newcomp0lo = lo;
            newcomp0hi = hi;
            /* increment ch1 width */
            }
        }
    if (mag2 > mag2min)
        /* reduce ant tib stim */

```



## APPENDIX M MASTER SOFTWARE

---

```
newmag2 = mag2 - 1;
lo = comp0lo2;
hi = comp0hi2;
add_bytes();          /* change to 16 bit format */
if (byte_total > byte_total_min)
{
    subtract();       /* decrement ch2 pulse width */
    newcomp0lo2 = lo;
    newcomp0hi2 = hi;
}
}
}
/***** next section of control statements *****/
/* left heel strike or right heel lift to enter */
if (lhrise == 1)     /* enter if bit set */
{
    chan = 7;        /* left heel input data from RAM */
    ramread();       /* call ram reading to array function */
    slope_detect(); /* call slope detection function */
    heel_bit = upslope; /* temp store */
    chan = 3;        /* right heel */
    ramread();
    slope_detect();
    if (dnslope == 1 || heel_bit == 1) /* check for heel pressure rise */
    {
        lbrise = 1; /* set next entry level flag */
        lsenflat = 0; /* reset entry flag */
        speed_val = 10; /* increase sample speed */
    }
    chan = 5;        /* set for left ball */
    ramread();
    slope_detect();
    ball_bit = upslope; /* temp store for ball sensor */
    chan = 6;        /* left foot outer */
    ramread();
    slope_detect();
    outer_bit = upslope; /* outer bit temp store */
    chan = 7;        /* left heel */
    ramread();
    slope_detect(); /* check for press drop */
    if (dnslope == 0 && ball_bit == 0 && outer_bit == 0 && lsenflat == 0)
    {
        /* until ball or outer pressure rises */
        /* or heel pressure falls */
        /* ch1 increase */
        if (mag < magmax)
            newmag = mag + 1;
        if (mag2 > mag2min)
            newmag2 = mag2 - 1; /* relax stim on ant tib */
        lo = comp0lo; /* load variables for fn call */
        hi = comp0hi;
        add_bytes(); /* convert to 16 bit format */
        if (byte_total < byte_total_max)
            /* extend ch1 pulse length */
            {
                add();
                newcomp0lo = lo; /* increment ch1 pulse length */
                newcomp0hi = hi;
            }
        lo = comp0lo2; /* load variables for fn call */
        hi = comp0hi2;
        add_bytes(); /* to 16 bit format */
        if (byte_total > byte_total_min)
            {
                subtract(); /* reduce ch2 pulse width */
                newcomp0lo2 = lo;
                newcomp0hi2 = hi;
            }
    }
}
else
    lhrise = 0; /* prevent re-entry if ball or */
                /* outer pressure rise noted */
```

## APPENDIX M MASTER SOFTWARE

---

```
}
/* last section of control statements */
/* closed loop control here */
if (lisenflat == 1) /* enter if bit set */
{
    chan = 5; /* left ball input data from RAM */
    ramread(); /* call ram reading to array function */
    slope_detect(); /* call slope detection function */
    ball_bit = flat; /* temp store */
    chan = 7; /* left heel */
    ramread();
    slope_detect();
    levbit = flat; /* temp store */
    chan = 4; /* left toe */
    ramread();
    slope_detect();
    if (flat == 1 && levbit == 1 && ball_bit == 1) /* check for level */
    { /* ball, heel, toe */
        /* lhrise = 1; set next entry level flag */
    }
    chan = 1; /* action to take */
    ramread(); /* stabilising effect */
    slope_detect();
    ball_bit = dnslope; /* temp store of result */
    chan = 2; /* right outer sensor */
    ramread();
    slope_detect();
    outer_bit = dnslope; /* temp result store */
    chan = 3; /* right heel */
    ramread();
    slope_detect();
    if (upslope == 1 || ball_bit == 1 || outer_bit == 1) /* heel pressure rising */
    { /* or ball pres falling */
        lo = comp0lo; /* to 16 bit format */
        hi = comp0hi;
        add_bytes();
        if (byte_total < byte_total_max)
        { /* increment width */
            newcomp0lo = lo;
            newcomp0hi = hi;
        }
        if (mag < magmax) /* or outside pres falling */
            newmag = mag + 1; /* increase magnitude */
        lo = comp0lo2; /* to 16 bit format */
        hi = comp0hi2;
        add_bytes();
        if (byte_total > byte_total_min) /* decrease ch2 pulse width */
        { subtract();
            newcomp0lo2 = lo;
            newcomp0hi2 = hi;
        }
        if (mag2 > mag2min) /* decrease ant tib stim */
            newmag2 = mag2 - 1;
    }
    chan = 1; /* right ball */
    ramread();
    slope_detect();
    ball_bit = upslope; /* temp store */
    chan = 3; /* right heel */
    ramread();
    slope_detect();
    heel_bit = dnslope; /* temp store */
    chan = 0; /* toe sensor */
    ramread();
    slope_detect();
    if (upslope == 1 || heel_bit == 1 || ball_bit == 1) /* ball pressure rising */
    { /* or toe pres rising */
```

## APPENDIX M MASTER SOFTWARE

---

```

                                /* or heel pres falling */
                                /* to 16 bit format */
lo = comp0lo;
hi = comp0hi;
add_bytes();
if ( byte_total > byte_total_min) /* decrement pulse width */
{
    subtract();
    newcomp0lo = lo;
    newcomp0hi = hi;
}
if (mag > magmin )
    newmag = mag - 1;          /* decrease stim */
lo = comp0lo2;                /* to 16 bit format */
hi = comp0hi2;
add_bytes();
if (byte_total < byte_total_max) /* increment ch2 width */
{
    add();
    newcomp0lo2 = lo;
    newcomp0hi2 = hi;
}
if ( mag2 < mag2max)          /* increase ant tib stim */
    newmag2 = mag2 + 1;
}
if (loop == 10)              /* every ten cycles */
{
    regulate_stim();          /* call dig integrator fn */
    loop = 0;
}
loop++;
}
exit: startaddr = startaddr+8; /* move to next block for write to RAM */
                                /* next block starts at startadd now */
if ( startaddr > 31999)
{
    startaddr = 0;            /* reset at limit of RAM */
}
                                /* leaves locations for storage */
return;
}
/* ***** serial data collection function ***** */
void data_fn (void)
{
    P32 = 0;                  /* reset to Lattice */
    P32 = 1;                  /* reset off */
    P30 = 0;                  /* clock low */
for (readloop = 0; readloop < 8; readloop++) /* 8 sensor reads */
{
    for (clkloop = 0; clkloop < 14; clkloop++)
    {
        P30 = 1;              /* 14 clocks to lattice */
        P30 = 0;
    }
    P31 = 1;                  /* set high to allow read */
for (datloop = 0; datloop < 8; datloop++)
{
    if (P31 == 1)
        sensor++;            /* add bit to sensor */
    if (datloop < 7)
        /* do not rotate left on */
        /* last digit */
        sensor = 2 * sensor; /* rotate left 1 posn */
    P30 = 1;
    P30 = 0;                  /* clock lattice */
    P30 = 1;
    P30 = 0;                  /* clock again */
}
                                /* loop for next bit */
    P30 = 1;
    P30 = 0;
    P30 = 1;
    P30 = 0;                  /* last clock of cycle */
    psens [readloop] = sensor; /* store sensor reading in array */
}
}

```

## APPENDIX M MASTER SOFTWARE

---

```
    sensor = 0;                /* reset sensor */
}                               /* end of 1 sensor read loop */
return;
}                               /* end of function */
/*****data passing function to board 1*****/
void data_pass1 (void)
{
    /* magnitude data transmission */
    P47 = 1;                    /* data to transfer signal to slave */
    if (mag != newmag)          /* test to see if data has changed */
    {
        P1 = 0x10;              /* mag indicator word */
        P40 = 1;                /* address request bit */
        while (P42 == 1)        /* wait for acknowledge */
        {
        }
        P40 = 0;                /* reset request */
        P1 = newmag;            /* export new data */
        P41 = 1;                /* data request */
        while (P43 == 1)        /* wait for acknowledge */
        {
        }
        P41 = 0;                /* reset data request */
        mag = newmag;           /* update mag value */
    }                             /* mag data transmitted */
    /* rateup data transmission */
    if (rateup != newrateup)    /* test to see if data has changed */
    {
        P1 = 0x20;              /* rateup indicator word */
        P40 = 1;                /* address request bit */
        while (P42 == 1)        /* wait for acknowledge */
        {
        }
        P40 = 0;                /* reset request */
        P1 = newrateup;         /* export new data */
        P41 = 1;                /* data request */
        while (P43 == 1)        /* wait for acknowledge */
        {
        }
        P41 = 0;                /* reset data request */
        rateup = newrateup;     /* update rateup */
    }                             /* rateup data transmitted */
    /* ratedn data transmission */
    if (ratedn != newratedn)    /* test to see if data has changed */
    {
        P1 = 0x30;              /* ratedn indicator word */
        P40 = 1;                /* address request bit */
        while (P42 == 1)        /* wait for acknowledge */
        {
        }
        P40 = 0;                /* reset request */
        P1 = newratedn;         /* export new data */
        P41 = 1;                /* data request */
        while (P43 == 1)        /* wait for acknowledge */
        {
        }
        P41 = 0;                /* reset data request */
        ratedn = newratedn;     /* update ratedn */
    }                             /* ratedn data transmitted */
    /* comparator 0 low byte data transmission */
    if (comp0lo != newcomp0lo) /* see if data has changed */
    {
        P1 = 0x40;              /* comp0lo indicator word */
        P40 = 1;                /* address request bit */
        while (P42 == 1)        /* wait for acknowledge */
        {
        }
        P40 = 0;                /* reset request */
    }
}
```

## APPENDIX M MASTER SOFTWARE

---

```
P1 = newcomp0lo;          /* export new data */
P41 = 1;                  /* data request */
while (P43 == 1)          /* wait for acknowledge */
{
}
P41 = 0;                  /* reset data request */
comp0lo = newcomp0lo;     /* update comp0lo */
}                          /* comp0lo data transmitted */
/* comp0hi data transmission */
if (comp0hi != newcomp0hi) /* see if data has changed */
{
P1 = 0x50;                /* space indicator word */
P40 = 1;                  /* address request bit */
while (P42 == 1)          /* wait for acknowledge */
{
}
P40 = 0;                  /* reset request */
P1 = newcomp0hi;          /* export new data */
P41 = 1;                  /* data request */
while (P43 == 1)          /* wait for acknowledge */
{
}
P41 = 0;                  /* reset data request */
comp0hi = newcomp0hi;     /* update comp0hi */
}                          /* comp0hi transmitted */
/* comp1lo data transmission */
if (comp1lo != newcomp1lo) /* see if data has changed */
{
P1 = 0x60;                /* space indicator word */
P40 = 1;                  /* address request bit */
while (P42 == 1)          /* wait for acknowledge */
{
}
P40 = 0;                  /* reset request */
P1 = newcomp1lo;          /* export new data */
P41 = 1;                  /* data request */
while (P43 == 1)          /* wait for acknowledge */
{
}
P41 = 0;                  /* reset data request */
comp1lo = newcomp1lo;     /* update comp1lo */
}                          /* comp1lo transmitted */
/* comp1hi data transmission */
if (comp1hi != newcomp1hi) /* see if data has changed */
{
P1 = 0x70;                /* space indicator word */
P40 = 1;                  /* address request bit */
while (P42 == 1)          /* wait for acknowledge */
{
}
P40 = 0;                  /* reset request */
P1 = newcomp1hi;          /* export new data */
P41 = 1;                  /* data request */
while (P43 == 1)          /* wait for acknowledge */
{
}
P41 = 0;                  /* reset data request */
comp1hi = newcomp1hi;     /* update comp1hi */
}                          /* comp1hi transmitted */
P47 = 0;                  /* data transfer indicator off */
return;
}                          /* end of function */
/* ***** data passing function to board 2 ***** */
void data_pass2 (void)
{
P47 = 1;                  /* magnitude data transmission */
if (mag2 != newmag2)      /* data to transfer signal to slave */
{                          /* test to see if data has changed */

```

## APPENDIX M MASTER SOFTWARE

---

```
P1 = 0x15;          /* mag indicator word */
P40 = 1;           /* address request bit */
while (P42 == 1)  /* wait for acknowledge */
{
}
P40 = 0;          /* reset request */
P1 = newmag2;     /* export new data */
P41 = 1;         /* data request */
while (P43 == 1) /* wait for acknowledge */
{
}
P41 = 0;         /* reset data request */
mag2 = newmag2;  /* update mag value */
}                /* mag data transmitted */
/* rateup data output */
/* test to see if data has changed */
if (rateup2 != newrateup2)
{
    P1 = 0x25;     /* rateup indicator word */
    P40 = 1;      /* address request bit */
    while (P42 == 1) /* wait for acknowledge */
    {
    }
    P40 = 0;      /* reset request */
    P1 = newrateup2; /* export new data */
    P41 = 1;     /* data request */
    while (P43 == 1) /* wait for acknowledge */
    {
    }
    P41 = 0;     /* reset data request */
    rateup2 = newrateup2; /* update rateup */
}                /* rateup data transmitted */
/* ratedn data transmission */
/* test to see if data has changed */
if (ratedn2 != newratedn2)
{
    P1 = 0x35;     /* ratedn indicator word */
    P40 = 1;      /* address request bit */
    while (P42 == 1) /* wait for acknowledge */
    {
    }
    P40 = 0;      /* reset request */
    P1 = newratedn2; /* export new data */
    P41 = 1;     /* data request */
    while (P43 == 1) /* wait for acknowledge */
    {
    }
    P41 = 0;     /* reset data request */
    ratedn2 = newratedn2; /* update ratedn */
}                /* ratedn data transmitted */
/* comparator 0 low byte data transmission */
/* see if data has changed */
if (comp0lo2 != newcomp0lo2)
{
    P1 = 0x45;     /* comp0lo indicator word */
    P40 = 1;      /* address request bit */
    while (P42 == 1) /* wait for acknowledge */
    {
    }
    P40 = 0;      /* reset request */
    P1 = newcomp0lo2; /* export new data */
    P41 = 1;     /* data request */
    while (P43 == 1) /* wait for acknowledge */
    {
    }
    P41 = 0;     /* reset data request */
    comp0lo2 = newcomp0lo2; /* update comp0lo */
}                /* comp0lo data transmitted */
/* comp0hi data transmission */
/* see if data has changed */
if (comp0hi2 != newcomp0hi2)
{
```

## APPENDIX M MASTER SOFTWARE

```

P1 = 0x55;          /* space indicator word */
P40 = 1;           /* address request bit */
while (P42 == 1)  /* wait for acknowledge */
{
}
P40 = 0;          /* reset request */
P1 = newcomp0hi2; /* export new data */
P41 = 1;         /* data request */
while (P43 == 1) /* wait for acknowledge */
{
}
P41 = 0;         /* reset data request */
comp0hi2 = newcomp0hi2; /* update comp0hi */
/* comp0hi transmitted */
}
/* comp1lo data transmission */
if (comp1lo2 != newcomp1lo2) /* see if data has changed */
{
P1 = 0x65;      /* space indicator word */
P40 = 1;       /* address request bit */
while (P42 == 1) /* wait for acknowledge */
{
}
P40 = 0;       /* reset request */
P1 = newcomp1lo2; /* export new data */
P41 = 1;       /* data request */
while (P43 == 1) /* wait for acknowledge */
{
}
P41 = 0;       /* reset data request */

comp1lo2 = newcomp1lo2; /* update comp1lo */
/* comp1lo transmitted */
}
/* comp1hi data transmission */
if (comp1hi2 != newcomp1hi2) /* see if data has changed */
{
P1 = 0x75;      /* space indicator word */
P40 = 1;       /* address request bit */
while (P42 == 1) /* wait for acknowledge */
{
}
P40 = 0;       /* reset request */
P1 = newcomp1hi2; /* export new data */
P41 = 1;       /* data request */
while (P43 == 1) /* wait for acknowledge */
{
}
P41 = 0;       /* reset data request */
comp1hi2 = newcomp1hi2; /* update comp1hi */
/* comp1hi transmitted */
}
P47 = 0;       /* data transfer indicator off */
return;
}
/* end of function */
/* ***** */
void ramwrite (void) /* RAM access function */
{
for (location = 0; location < 8; location++)
{
ramloop = startaddr + location;
XBYTE[ramloop] = psens[location]; /* write to RAM */
}
return;
}
/* end of function */
/* ***** */
void ramread (void) /* last 10 samples to array function */
{
for (n=0;n<10;n++)
{
ramaddr = startaddr - (8*n) + chan; /* address of data */
}
}

```



## APPENDIX M MASTER SOFTWARE

---

```
samp[n] = XBYTE[ramaddr];          /* read data to array */
}

if (samp[0] < 50) /* check most recent value for broken wires */
{
    error = 1;
}
return;
}
void error_pres (void) /* shutdown routine */
{
    newmag = 0x05;
    newmag2 = 0x05;
return;
}
/* ***** */
void slope_detect (void) /* slope detection function */
{
    /* 10 samples used */
    upslope = samp[0]>samp[2] && samp[1]>samp[3] && samp[2]>samp[4]
    && samp[3]>samp[5] && samp[4]>samp[6] /* && samp[5]>samp[7]
    && samp[6]>samp[8] && samp[7]>samp[9]*/;
    dnslope = samp[9]>samp[7] && samp[8]>samp[6] && samp[7]>samp[5]
    && samp[6]>samp[4] && samp[5]>samp[3] /* && samp[4]>samp[2]
    && samp[3]>samp[1] && samp[2]>samp[0] */;
    flata = samp[9]>(samp[8]-25) && samp[9]<(samp[8]+25) && samp[9]>(samp[7]-25)
    && samp[9]<(samp[7]+25) && samp[9]>(samp[6]-25) && samp[9]<(samp[6]+25)
    && samp[9]>(samp[5]-25) && samp[9]<(samp[5]+25) && samp[9]>(samp[4]-25);
    flatb = samp[9]<(samp[4]+25) && samp[9]>(samp[3]-25) && samp[9]<(samp[3]+25)
    && samp[9]>(samp[2]-25) && samp[9]<(samp[2]+25) && samp[9]>(samp[1]-25)
    && samp[9]<(samp[1]+25) && samp[9]>(samp[0]-25) && samp[9]<(samp[0]+25);
    flat = flata && flatb;
return;
}
/* ***** */
void speed_detect (void) /* determine walking speed function */
{
    /* counts time between left heel strikes */
    /* at start of use only */

    if (speedheel3 == 1)
    {
        chan = 5; /* left ball */
        ramread();
        slope_detect();
        ball_bit = upslope; /* temp store */
        chan = 6; /* left outer */
        ramread();
        slope_detect();
        if (upslope == 1 || ball_bit == 1) /* check for ramp up */
        {
            timer_control++; /* now = 2 */
        }
    }
    if (speedheel2 == 1) /* look for second heel strike */
    {
        chan = 7; /* select left heel */
        ramread();
        slope_detect();
        if (upslope == 1)
        {
            speedheel3 = 1; /* reset flag */
            speedheel2 = 0; /* set entry level flag */
        }
    }
    if (speedball1 == 1) /* look for left ball rise */
    {
        chan = 5; /*select left ball */
        ramread();
        slope_detect();
        ball_bit = upslope; /* temp store */
    }
}
```



## APPENDIX M MASTER SOFTWARE

---

```
chan = 6; /* left outer */
ramread();
slope_detect();
if (upslope == 1 || ball_bit == 1) /* ball or outer rise */
{ speedheel2 = 1; /* set next entry level flag */
  speedball1 = 0; /* reset flag */
}
}
if (speedheel1 == 1) /* look for first heel strike */
{
  chan = 7; /* select left heel input */
  ramread();
  slope_detect();
  if (upslope == 1) /* increment on slope up */
  {
    timer_control++;
    speedball1 = 1; /* set next entry level flag */
    speedheel1 = 0; /* reset flag */
  }
}
watchdog(); /* refresh watchdog */
speed_count++; /* count cycles to next strike */
if (timer_control == 2)
  speed_val = speed_count / 100; /* scale to suit */
speed_val = 20; /* default value at present */
return;
}
/* ***** */
/* watchdog refresh function */
void watchdog (void)
{
  PCON = 0x10;
  T3 = 0x00;
  return;
}
/* ***** */
/* 16 bit increment */
void add (void)
{
  if (lo < 0xFA) /* check for full lo register */
    lo = lo + 5; /* if not add 2 */
  if (lo > 0xFA) /* if full carry 1 */
  { lo = 0x00;
    hi++;
  }
  return;
}
/* ***** */
/* 16 bit decrement */
void subtract (void)
{
  if (lo > 0x05) /* check for lo byte zero */
    lo = lo - 5; /* if not decrement */
  if (lo < 0x05) /* if 0 - 5 borrow from hi byte */
  { lo = 0xFF;
    hi--;
  }
  return;
}
/* ***** */
/* convert to 16 bit */
void add_bytes (void)
{
  byte_total = hi; /* load upper 8 bits */
  byte_total = byte_total << 8; /* shift left 8 times */
  byte_total = byte_total | lo; /* place lo in low byte */
  return;
}
}
```

## APPENDIX M MASTER SOFTWARE

---

```
/* ***** */
/* digital integrator function */
void regulate_stim (void)
{
    if (mag > magnom)
        newmag = mag - 1;    /* bring ch1 closer to nominal value */
    if (mag < magnom)
        newmag = mag + 1;
    if (mag2 > mag2nom)
        newmag2 = mag2 - 1; /* bring ch2 closer to nom value */
    if (mag2 < mag2nom)
        newmag2 = mag2 + 1;
    lo = comp0lo;
    hi = comp0hi;           /* to 16 bit format */
    add_bytes();
    if (byte_total > byte_total_nom) /* bring nearer to nom pulse width */
    {
        subtract();
        newcomp0lo = lo;       /* update parameters */
        newcomp0hi = hi;
    }
    if (byte_total < byte_total_nom)
    {
        add();                 /* update parameters */
        newcomp0lo = lo;
        newcomp0hi = hi;
    }
    lo = comp0lo2;          /* to 16 bit format */
    hi = comp0hi2;          /* ch 2 */
    add_bytes();
    if (byte_total > byte_total_nom2) /* bring closer to nom pulse width */
    {                           /* ch2 */
        subtract();
        newcomp0lo2 = lo;
        newcomp0hi2 = hi;
    }
    if (byte_total < byte_total_nom2) /* bring closer to nom pulse width */
    {                           /* ch2 */
        add();
        newcomp0lo2 = lo;
        newcomp0hi2 = hi;
    }
    return;
}
/* ***** */
/* start of main program */
main()
{
    while (delay < 100)
    {
        delay++;              /* start up delay */
    }
    setup();                  /* call port initial settings function */
    while (1)                 /* infinite loop */
    {
        watchdog();          /* watchdog register refresh */
        data_fn();           /* call data gathering function */
        watchdog();          /* watchdog refresh */
        ramwrite();          /* call RAM access function */
        watchdog();          /* watchdog refresh */
        if (cycle_no == speed_val) /* call every nth loop */
            /* defined by walking speed */

        {
            calc_fn();        /* call calculating function */
            /* ramread called from within function */
            cycle_no = 0;     /* reset loop */
        }
        cycle_no++;          /* increment loop */
    }
}
```

## APPENDIX M MASTER SOFTWARE

---

```
if (error == 1                                /* shutdown proc for hardware error*/
{
  while (1)                                    /* trap in loop to stop prog */
  {
    watchdog();                               /* watchdog refresh */
    error_pres();
    data_pass1();
    data_pass2();
  }
}
watchdog();                                   /* watchdog refresh */
data_pass1();                                 /* call data passing function board 1 */
watchdog();                                   /* watchdog refresh */
data_pass2();                                 /* call data passing function board 2 */
watchdog();                                   /* watchdog refresh */
}                                              /* end of infinite loop */
}                                              /* end of main */
```

## **APPENDIX N. CONFERENCE PAPER.**

**The Development of an Intelligent FES System For The Treatment of Foot Drop.  
John R. Williams, University of Bath.**

**Presented at the 5th IPEMB Clinical Functional Electrical Stimulation Meeting, Odstock Hospital, Salisbury on 13th March 1997.**

### **Synopsis.**

A Functional Electrical Stimulation System implementing closed loop control has been developed in order to reduce the effort required to set up such systems and effect a smoother, more natural gait than is produced by currently available systems. The system is driven entirely by software and has been designed with flexibility as a high priority, to enable it to function as a general FES research tool in addition to its use in the treatment of foot drop.

### **Introduction.**

The large variation in patient parameters and the day to day variation in electrode positioning results in time consuming set up procedures for FES systems, which can eventually become such an inconvenience that the patient decides to discontinue use of the system.

Present stimulator parameters are set for each individual patient and there is no mechanism for the stimulator to assess the effect of its output upon the gait of the patient and modify this accordingly. The patient does possess a degree of control over the level of applied stimulation, though manual control of this parameter on a stride by stride basis is neither practical, nor desirable, so is instead made a fundamental requirement of this stimulation system.

In order to effect a much reduced set up time for each patient and to maintain a smooth gait regardless of patient parameter changes, a system has been devised that monitors the outputs of sensors mounted upon the feet, modifying its outputs according to the rules contained within the controlling software.

### **The Stimulator System Configuration.**

This stimulation system has been developed around the Intel 80C552 microcontroller, which provides a good combination of program execution speed and input / output availability.

The system is comprised of a master module, based around the 80C552, which receives data from the foot mounted sensors and makes decisions about the required output based upon this data. The master module is coupled to n slave modules by a common data bus, where n represents the required number of output channels. The slave units, identical in all respects with the exception of small software alterations that permit each channel to be addressed independantly of all the other channels, synthesise the pulse trains to be applied to the muscle groups. Any number of slave modules or channels may be added to produce finer control of patient movements by the stimulation of further muscle groups.

The pulses to be applied to the patient by each channel are synthesised digitally, beginning with default parameters and subsequently being modified as the data from the sensors is interpreted in response to gait irregularities. These pulses are converted to analog form and amplified for

## **APPENDIX N CONFERENCE PAPER**

---

application to the patient via an isolation transformer. The digital synthesis of each individual pulse permits total control of all pulse parameters to be effected, therefore allowing any combination of these parameters to be applied to the muscle group at any time, regardless of those parameters previously allocated.

### **System Pulse Train Variability.**

The parameters of any individual pulse may be defined as follows:-

<u>Parameter</u>	<u>Typical Value</u>	<u>Limiting Value</u>
Magnitude	40 V	10V - 120V
Pulse width	300us	100us - 400us
Inter pulse spacing	30ms	20ms - no limit.
Pulse rise time	5us	4us dependant on width
Pulse fall time	5us	4us - no limit.

Every one of these parameters is variable from one pulse to the next, independantly from all other parameters and all other channels.

### **Feedback Generating Sensors.**

The sensors developed to generate the necessary feedback signals register the pressure beneath each of the patient's feet. Each sensor pad utilises the Hall effect principle and consists of four ceramic permanent magnets separated from four Hall effect sensors by a layer of closed cell neoprene. A pressure change across the pad alters the separation of these devices which in turn alters the magnetic field strength at the Hall effect sensor. The output of this device depends on its surrounding magnetic field strength, therefore the output reflects the pressure applied to the mat. No signal conditioning circuitry is required to interpret the pressure applied and once digitised, pressure rise and fall rates are calculated within the master unit to avoid the need for sensor calibration and to minimise the effect of any drift that may occur.

### **Results to Date .**

At present the stimulator software consists of a framework that is able to track the wearer of the pressure sensing equipment through a complete gait cycle and effect control of the stance phase alone in response to movements made by the user. The fully operational hardware consists of a two channel stimulator system, the channels being used to produce toe lift and push off respectively, in foot drop patients.

### **Further Investigation .**

- The development of software to effect correct stimulation throughout the complete gait cycle.
- Research into the longevity of, and possible improvements upon, the neoprene used in the pressure pad construction. One possible avenue of investigation involves the use of a closed cell, aerated silicon rubber material.
- Research into the uses and effects of the variable rise and fall rate of the voltage pulses applied to the patient. One possibility in this area involves the use of a reduced fall rate and gating system to improve the measurement of inter pulse EMGs.

---

## REFERENCES

---

# REFERENCES.

- [1] Turton A. J, Fraser C. M, A Test to Measure the Recovery of Voluntary Movement Control Following Stroke. *Int. Rehabil. Med*, Vol. 8, pp 74 - 77, 1986.
- [2] Cozean C.D, Pease W.S, Hubbell S.L, Biofeedback and Functional Electric Stimulation in Stroke Rehabilitation. *Arch. Phys. Med. Rehabil*, Vol. 69, pp 401 - 405, 1988.
- [3] Allen C.M.C, Predicting Recovery After Acute Stroke. *British Journal of Hospital Medicine*, pp 428 - 434, 1984.
- [4] Duncan P.W, Goldstein L.B, Horner R.D, Landsman P.B, Samsa G.P, Matchar D.B, Similar Motor Recovery of Upper and Lower Extremities After Stroke. *Stroke*, Vol. 25, No 6, pp 1181 - 1187, 1994.
- [5] Wing A.M, Kirker S, Jenner J.R, Altered Bi-lateral Muscle Synergies After Stroke. *Behavioural and Brain Sciences*, Vol. 19, No. 1, pp 92, 1996.
- [6] Gilad G.M, Gorio A, Kreutzberg G.W (Ed), *Processes of Recovery from Neural Trauma*. Springer-Verlag, Berlin, 1986. ISBN 3-540-15781-6.
- [7] Olney S.J, Colbourne G.R, Martin C.S, Joint Angle Feedback and Biomechanical Gait Analysis in Stroke Patients: A Case Report. *Phys. Ther*, Vol. 69, pp 863 - 870, 1989.
- [8] Olney S.J, Monga T.N, Costigan P.A. Mechanical Energy of Walking of Stroke Patients. *Arch. Phys. Med. Rehabil*, Vol. 67, pp 92 - 98, 1986.
- [9] Chin P.L, Physical Techniques in Stroke Rehabilitation, *Journal of the Royal College of Physicians of London*, Vol. 16, No. 3, pp 165 - 169, 1982.
- [10] Stillings D, The Piscean Origin of Medical Electricity, *Medical Instrumentation*, Vol. 7, Part 2, pp 163 - 164, 1973.
- [11] Rogoff J.B. B. Franklin on Electrotherapy. *N. G. J. M.* Vol. 280, No. 12, p 673, 1969.
- [12] Stillings D, Electrical Stimulation for Drop Foot, 1772. *Medical Instrumentation*, Vol. 9, Part 6, pp 276 - 277, 1975.
- [13] Kralj A, Vodovnik L, Functional Electrical Stimulation of the Extremities: part 1. *Journal of Medical Engineering and Technology*, pp12 - 15, 1977.

## **REFERENCES**

---

- [14] Functional Electrotherapy : Stimulation of the Peroneal Nerve Synchronized with the Swing Phase of the Gait of Hemiplegic Patients. Arch. Phys. Med. Rehabil, pp 101 - 105, 1961.
- [15] MacLean I.C, Pease W.S, Ma D.M, Cassvan A, Johnson E.W, Electrodiagnosis. 2. Peripheral Evoked Potentials. Arch. Phys. Med. Rehabil, Vol. 68, p s-13, 1987.
- [16] Trontelj J, Stalberg E, Responses to Electrical Stimulation of Denervated Human Muscle Fibres Recorded With Single Fibre EMG, Journal of Neurology, Neurosurgery, and Psychiatry, Vol. 46, pp 305 - 309, 1983.
- [17] Malezic M, Kljajic M, Acimovic-Janezic R, Gros N, Krajnik J, Stanic U. Therapeutic Effects of Multisite Electric Stimulation of Gait in Motor-disabled Patients. Arch. Phys. Med. Rehabil, Vol. 68, pp 553 - 559, 1987.
- [18] Carnstam B, Larsson L.E, Prevec T.S, Improvement of Gait Following Functional Electrical Stimulation:1 Investigations on Changes in Voluntary Strength and Proprioceptive Reflexes. Scand. J. Rehabil. Med, Vol. 9, pp 7 - 13, 1977.
- [19] Takebe K, Kukulka C.G, Narayan M.G, Basmajian J.V, Biofeedback Treatment of Foot-Drop After Stroke Compared With Standard Rehabilitation Technique (Part 2) : Effects on Nerve Conduction Velocity and Spasticity. Arch. Phys. Med. Rehabil, Vol. 57, pp 9 - 11, 1976.
- [20] Delitto A, Snyder-Mackler L, Two Theories of Muscle Strength Augmentation Using Percutaneous Electrical Stimulation. Physical Therapy, Vol. 70, No. 3, pp 158 - 164, 1990.
- [21] Balogun J.A, Electrical Stimulation for Strengthening. Physical Therapy, Vol. 65, No. 9, pp 1394 - 1396, 1985.
- [22] Waters R.L, The Enigma of "Carry-Over". Int. Rehabil. Med, Vol. 6, No. 1, pp 9 - 12, 1984.
- [23] Takebe K, Basmajian J.V, Gait Analysis in Stroke Patients to Assess Treatments of Foot-Drop. Arch. Phys. Med. Rehabil, Vol. 57, pp 305 - 310. 1976.
- [24] Marinacci A.A, Horande M, Electromyogram in Neuromuscular Re-education. Bull. Los Angeles Neurol. Soc, Vol. 25, pp 57 - 71, 1960.

## **REFERENCES**

---

- [25] Flom R.P, Quast J.E, Boller J.D, Berner M, Goldberg J, Biofeedback Training to Overcome Post-Stroke Foot-Drop. *Geriatrics*, pp 47 - 51, 1976.
- [26] Finger S, Amli C.R. Brain Damage and Neuroplasticity: Mechanisms of Recovery or Development? *Brain Res. Rev*, Vol. 10, pp 177 - 186, 1985.
- [27] Scherzer A.L, Tscharnuter F. *Early Diagnosis and Therapy in Cerebral Palsy*. New York: Dekker, 1982.
- [28] Bach-y-Rita P. Brain Plasticity as a Basis of the Development of Rehabilitation Procedures for Hemiplegia. *Scand. J. Rehabil. Med*, Vol. 1, No. 13, pp 73 - 83, 1981.
- [29] Carr J.H, Shepherd R.B. *A Motor Re-learning Program for Stroke*. 2nd ed. Rockville, Md: Aspen, 1987.
- [30] Richards C.L, Malouin F, Wood-Dauphinee S, Williams J.I, Bouchard J.P, Brunet D. Task-Specific Physical Therapy for Optimization of Gait Recovery in Acute Stroke Patients. *Arch. Phys. Med. Rehabil*, Vol. 74, pp 612 - 619, 1993.
- [31] Brandell B.R. Development of a Universal Control Unit for Functional Electrical Stimulation. *American Journal of Physical Medicine*, Vol. 61, No. 6, pp 279 - 301, 1982.
- [32] Malezic M, Hesse S, Schewe H, Mauritz K.H, Restoration of Standing, Weight-Shift and Gait by Multichannel Electrical Stimulation in Hemiparetic Patients. *International Journal of Rehabilitation Research*, Vol. 17, pp 169 -179, 1994.
- [33] Malezic M, Hesse S, Restoration of Gait by Functional Electrical Stimulation in Paraplegic Patients: a modified programme of treatment. *Paraplegia*, Vol. 33, pp 126 - 131, 1995.
- [34] Lath R, Rajshekhar V, Unilateral Foot Drop. *Postgrad. Med. J*, pp 573 - 574, 1996.
- [35] Eskandry H, Hamzei A, Yasamy M.T, Foot Drop Following Brain Lesion. *Surg. Neurol*, Vol. 43, pp 89 - 90, 1995.
- [36] Sackley C.M, Lincoln N.B, *Physiotherapy Treatment for Stroke Patients : A Survey of Current Practice*. *Physiotherapy Theory and Practice*, Vol. 12, pp 87 - 96, 1996.
- [37] Malouin F, Potvin M, Prevost J, Richards C.L, Wood-Dauphinee S. Use of an Intensive Task-Orientated Gait Training Program in a Series of Patients with Acute Cerebrovascular Accidents. *Physical Therapy*, Vol. 72, No. 11, pp 781 - 789, 1992.



## **REFERENCES**

---

- [38] Basmajian J.V, Kukulka C.G, Narayan M.G, Takebe K, Biofeedback Treatment of Foot-Drop After Stroke Compared with Standard Rehabilitation Technique: Effects on Voluntary Control and Strength. Arch. Phys. Med. Rehabil, Vol. 56, pp 231 - 236, 1975.
- [39] Dickstein R, Nissan M, Pillar T, Scheer D, Foot-Ground Pressure Pattern of Standing Hemiplegic Patients. Physical Therapy, Vol. 64, No. 1, pp 19 - 23. 1984.
- [40] Brudny J, Korein J, Levidow L, Sensory Feedback Therapy as a Modality of Treatment in Central Nervous System Disorders of Voluntary Movement. Neurology, Vol. 24, pp 925 - 932, 1974.
- [41] Burnside I.G, Tobias H.S, Bursill D, Electromyographic Feedback in the Remobilization of Stroke Patients: A Controlled Trial. Arch. Phys. Med. Rehabil, Vol. 63, pp 217 - 222, 1982.
- [42] Jeong B.Y, Contour Representation of Sway Area in Posturography and its Application. Arch. Phys. Med. Rehabil, Vol. 75, pp 951 - 956. 1994.
- [43] Collen F.M, The Measurement of Standing Balance After Stroke. Physiotherapy Theory and Practice Vol. 11, pp 109 - 118. 1995.
- [44] Hill K, Vandervoort A, Kramer J, Reproducibility of Performance on a Test of Postural Responses in Healthy Elderly Females. Physiotherapy Canada, Vol. 42, pp 61 - 67. 1990.
- [45] Winter D.A, Human Balance and Posture Control During Standing and Walking. Gait and Posture. Vol. 3, pp 193 - 214, 1995.
- [46] Bobath B, Adult Hemiplegia: Evaluation and Treatment, 2nd Edition. Heinemann, London. 1978.
- [47] Sackley C.M, Baguley B.I, Visual Feedback After Stroke with the Balance Performance Monitor : Two Single Case Studies. Clinical Rehabilitation, Vol. 7, pp 189 - 195, 1993.
- [48] Sackley C.M, The Relationships Between Weight Bearing Asymmetry After Stroke, Motor Function and Activities of Daily Living. Physiother. Theory Pract, Vol. 6, pp 179 -185, 1990.

## **REFERENCES**

---

- [49] Shumway-Cook A, Anson D, Haller S, Postural Sway Biofeedback : Its Effect on Re-establishing Stance Stability in Hemiplegic Patients. *Arch. Phys. Med. Rehabil*, Vol. 69, pp 395 - 400, 1988.
- [50] De Weert W, Crossley S.M, Lincoln N.B, Harrison M.A, Restoration of Balance in Stroke Patients : A Single Case Design Study. *Clinical Rehabilitation*, Vol. 3, pp 139 - 147. 1989.
- [51] Nakamura R, Handa T, Watanabe S, Morohashi I, Walking Cycle After Stroke. *Tohoku J. exp. Med*, Vol. 154, pp 241 - 244. 1988.
- [52] Wade D.T, Wood V.A, Heller A, Maggs J, Langton Hewer R, Walking After Stroke, *Scand. J. Rehab. Med*, Vol. 19, pp 25 - 30. 1987.
- [53] Geurts A.C.H, Mulder T.W, Attention Demands in Balance Recovery Following Lower Limb Amputation. *Journal of Motor Behaviour*. Vol. 26, No. 2, pp 162 - 170. 1994.
- [54] Dickstein R, Dvir Z, Jehousua E.B, Rois M, Pillar T, Automatic and Voluntary Lateral Weight Shifts in Rehabilitation of Hemiparetic Patients. *Clinical Rehabilitation*, Vol. 8, pp 91 - 99. 1994.
- [55] Wing A.M, Allison S, Jenner J.R, Retaining and Retraining Balance After Stroke. *Bailliere's Clinical Neurology* Vol. 2, No. 1, pp 87 - 120. 1993.
- [56] Peterka R.J, Benolken M.S, Role of Somatosensory and Vestibular Cues in Attenuating Visually Induced Human Postural Sway. *Exp. Brain Res*, Vol. 105, pp 101 - 110. 1995.
- [57] Peterka R.J, Black F.O, Age-related Changes in Human Posture Control : Sensory Organization Tests. *Journal of Vestibular Research*. Vol. 1, pp 73 - 85. 1990.
- [58] Robbins S, Waked E, McClaran J, Proprioception and Stability : Foot Position Awareness as a Function of Age and Footwear. *Age and Ageing*, Vol. 24, pp 67 - 72. 1995.
- [59] Teasdale N, Bard C, Dadouchi F, Fleury M, Larue J, Stelmach G.E, Posture and Elderly Persons : Evidence for Deficits in the Central Integrative Mechanisms. *Tutorials in Motor Behaviour II*, pp 917 - 931, Elsevier Science Publishers B.V. 1992.
- [60] Horak F.B, Diener H.C, Nashner L.M, Influence of Central Set on Human Postural Responses. *Journal of Neurophysiology*, Vol. 62, No. 4. pp 841 - 853. 1989.

## **REFERENCES**

---

- [61] Diener H.C, Dichgans J, Long Loop Reflexes and Posture. Disorders of Posture and Gait. pp 41 - 49, Elsevier Science Publishers B.V. 1986.
- [62] Hoehnerman S, Dickstein R, Pillar T, Platform Training and Postural Stability in Hemiplegia. Arch. Phys. Med. Rehabil, Vol. 65, pp 588 - 592. 1984.
- [63] Ho D.H.W, Perris R, Bash R, Hodges A.G Balance Aid Tutor For Stroke Patients and Paraplegics. Final year report, University of Bath, 1993.
- [64] Wing A.M, Clapp S, Burgess-Limerick R, Standing Stability in the Frontal Plane Determined by Lateral Forces Applied to the Hip. Gait and Posture, Vol. 3, pp 38 - 42. 1995.
- [65] Day B.L, Steiger M.J, Thompson P.D, Marsden C.D, Effect of Vision and Stance Width on Human Body Motion When Standing : Implications for Afferent Control of Lateral Sway. Journal of Physiology, Vol. 469, pp 479 - 499. 1993.
- [66] Schmidt R.A, Motor Learning Principles for Physical Therapy. Contemporary Management of Motor Control Problems (Ed. Lister M.), Foundation for Physical Therapy, Alexandria V.A. pp 49 - 63. 1991.
- [67] Winstein C.J, Knowledge of Results and Motor Learning - Implications for Physical Therapy. Physical Therapy, Vol. 71, pp 140 - 149. 1991.
- [68] Sohlberg M.M, Mateer C.A, Introduction to Cognitive Rehabilitation : Theory and Practice. The Guilford Press, 1989.
- [69] Franken H.M, Veltink P.H, Baardman G, Redmeyer R.A, Boom H.B.K, Cycle-to-Cycle Control of Swing Phase of Paraplegic Gait Induced by Surface Electrical Stimulation. Med. & Biol. Eng. & Comput. Vol. 33, pp 440 - 451. 1995.
- [70] Andrews B.J, Barnett R.W, Phillips G.F, Kirkwood C.A, Rule-based Control of a Hybrid FES Orthosis Assisting Paraplegic Locomotion. Automedica, Vol. 11, pp 177 - 195. 1989.
- [71] Marsolais E.B, Kobetic R, Functional Electrical Stimulation for Walking in Paraplegia. Journal of Bone and Joint Surgery. Vol. 69-A, pp 728 - 733. 1987.
- [72] Albert A, Andre J.M, State of the Art of Functional Electrical Stimulation in France. Int. Rehabil. Med. Vol. 6, pp 13 - 18, 1984.

## REFERENCES

---

- [73] Takebe K, Kukulka C, Narayan M.G, Milner M, Basmajian J.V, Peroneal Nerve Stimulator in Rehabilitation of Hemiplegic Patients. Arch. Phys. Med. Rehabil. Vol. 56, pp 237 - 240. 1975.
- [74] Trnkoczy A, Variability of Electrically Evoked Muscle Contractions With Special Regard to Closed-Loop Controlled Orthosis. Ann. Biomed. Eng. Vol. 2, pp 226 - 238. 1974.
- [75] Boom H.B.K, Mulder A.J, Veltink P.H, Fatigue During Finite State Control During Neuromuscular Stimulation. Prog. Brain Res. Vol. 97, pp 409 - 418. 1993.
- [76] Allison T, Goff W.R, Brey J.H, An Isolated Constant-Current Stimulator For Use With Man. J. Appl. Physiol. Vol. 22 (3), pp 612 - 613. 1967.
- [77] Ozgirgin N, Bolukbasi N, Beyazova M, Orkun S, Kinematic Gait Analysis in Hemiplegic Patients. Scand. J. Rehab. Med. Vol. 25, pp 51 - 55. 1993.
- [78] Olney S.J, Griffin M.P, McBride I.D, Temporal, Kinematic and Kinetic Variables Related to Gait Speed in Subjects With Hemiplegia : A Regression Approach. Physical Therapy. Vol. 74. No. 9, pp 872 - 885. 1994.
- [79] Perry J, The Mechanics of Walking in Hemiplegia. Clinical Orthopaedics and Related Research. No. 63. pp 23 - 31. 1969.
- [80] Meadows P.M, McNeal D.R, A Four Channel IBM PC / AT Compatible Biphasic Pulse Generator For Nerve Stimulation. IEEE Transactions on Biomedical Engineering , Vol 36, - A Guide to Use, Odstock Hospital, Salisbury.
- [81] Grieve D.W, Monitoring Gait. British Journal of Hospital Medicine. pp 198 - 203. September 1980.
- [82] Baumann J.U, Hanggi A, A Method of Gait Analysis For Daily Orthopaedic Practice. Journal of Medical Engineering and Technology. pp 86 - 91. March 1977.
- [83] Bajd T, Kralj A, Simple Kinematic Gait Measurements. Journal of Biomedical Engineering. Vol. 2, pp 129 - 132. 1980.
- [84] Simkin A, Stokes I.A.F, Characterisation of the Dynamic Vertical Force Distribution Under The Foot. Med. & Biol. Eng. & Comput. Vol. 20, pp 12 - 18. 1982.
- [85] Mann R.A, Hagy J.L, White V, Liddell D, The Initiation of Gait. The Journal of Bone and Joint Surgery. Vol. 61-A, No. 2, pp 232 - 239. 1979.

## **REFERENCES**

---

- [86] Hill K.D, Goldie P.A, Baker P.A, Greenwood K.M, Retest Reliability of the Temporal and Distance Characteristics of Hemiplegic Gait Using a Footswitch System. *Arch. Phys. Med. Rehabil.* Vol. 75, pp 577 - 583. 1994.
- [87] Wing A.M, The Uncertain Motor System : Perspectives on the Variability of Movement. *Attention and Performance XIV Synergies in Experimental Psychology, Artificial Intelligence and Cognitive Neuroscience.* (Ed. Meyer D.E, Kornblum S), The MIT Press, pp 708 - 744. 1992.
- [88] Miyazaki S, Iwakura H, Foot-Force Measuring Device for Clinical Assessment of Pathological Gait. *Med. & Biol. Eng. & Comput.* Vol. 16, pp 429 - 436. 1978.
- [89] The Odstock 2 Channel Stimulator - A Guide To Use, Odstock Hospital, Salisbury.
- [90] Granat M.H, Maxwell D.J, Ferguson A.C.B, Lees K.R, Barbenel J.C, Peroneal Stimulator : Evaluation for the Correction of Spastic Drop Foot in Hemiplegia. *Arch. Phys. Med. Rehabil.* Vol. 77, pp 19 - 24. 1996.
- [91] Waters R.L, McNeal D.R, Faloon W, Clifford B, Functional Electrical Stimulation of the Peroneal Nerve for Hemiplegia. *The Journal of Bone and Joint Surgery*, Vol. 67-A, No. 5, pp 792 - 793. 1985.
- [92] Jackson K.M, Denyer H.T, A Battery Powered Constant Current Stimulator. *Journal of Biomedical Engineering*, Vol. 5, pp 165 - 166. April 1983.
- [93] Patterson R.P, Lockwood J.S, Dykstra D.D, A Functional Electric Stimulation System Using an Electrode Garment. *Arch. Phys. Med. Rehabil*, Vol. 71, pp 340 - 342. 1990.
- [94] Kljajic M, Malezic M, Asimovic R, Vavken E, Stanic U, Pangrsic B, Rozman J, Gait Evaluation in Hemiparetic Patients Using Subcutaneous Peroneal Electrical Stimulation. *Scand. J. Rehab. Med*, Vol. 24, pp 121 - 126. 1992.
- [95] Strojnik P, Acimovic R, Vavken E, Simic V, Stanic U, Treatment of Drop Foot Using An Implantable Peroneal Underknee Stimulator. *Scand. J. Rehab. Med*, Vol 19, pp 37-43, 1987.
- [96] Yergler W.G, McNeal D.R, Perry J, Muscle Response to Internal Stimulation of the Peroneal Nerve in Hemiplegic Patients. *Clinical Orthopaedics and Related Research*. No. 86, pp 164 - 167. 1972.

## **REFERENCES**

---

- [97] Moseley A, Wales A, Herbert R, Schurr K, Moore S, Observation and Analysis of Hemiplegic Gait : Stance Phase. *Australian Journal of Physiotherapy*, Vol. 39. No. 4, pp 259 - 267. 1993.
- [98] Saunders J.B, Inman V.T, Eberhart H.D, The Major Determinants in Normal and Pathological Gait. *Journal of Bone and Joint Surgery*, Vol. 35-A, pp 543 - 559. 1953.
- [99] Olney S.J, Griffin M.P, Monga T.N, McBride I.D, Work and Power in Gait of Stroke Patients. *Arch. Phys. Med. Rehabil*, Vol. 72, pp 309 - 314. 1991.
- [100] Winter D.A, Energy Generation and Absorption at the Ankle and Knee During Fast, Natural and Slow Cadences. *Clin. Orthop. Rel. Res*, Vol. 175, pp 147 - 154. 1983.
- [101] Fields R.W, Electromyographically Triggered Electric Muscle Stimulation for Chronic Hemiplegia. *Arch. Phys. Med. Rehabil*, Vol 68, 1987.
- [102] Smith L.E, Restoration of Volitional Limb Movement of Hemiplegics Following Patterned Functional Electrical Stimulation. *Perceptual and Motor Skills*, 71, pp 851-856, 1990.
- [103] Bray J.T, Cragg P.A, MacKnight A.D.C, Mills R.G, Taylor D.W, *Lecture Notes on Human Physiology*. Blackwell Scientific Publishers, 1986. ISBN 0-6302-00773-7.
- [104] Friedman P.J, Gait Recovery After Hemiplegic Stroke. *Int. Disabil. Studies*, Vol. 12, pp 119 - 122. 1991.
- [105] Sturm W, Willmes K, Efficacy of a Reaction Training on Various Attentional and Cognitive Functions in Stroke Patients. *Neuropsychological Rehabilitation*, Vol. 1, No. 4, pp 259 - 280. 1991.
- [106] Valencic V, Vodovnik L, Stefancic M, Jelnikar T Improved Motor Response Due to Chronic Electrical Stimulation of Denervated Tibialis Anterior Muscle in Humans. *Muscle and Nerve*, Vol. 9, pp 612 - 617, 1986.
- [107] Izzo K.L, Aravabhumi S, *Cerebrovascular Accidents*. *Clinics in Podiatric Medicine and Surgery*, Vol. 6, No 4, pp 745 - 758, 1989.
- [108] Musa I.M, Recent Findings on the Neural Control of Locomotion : Implications for the Rehabilitation of Gait, *International Perspectives in Physical Therapy - 2. Stroke* (Ed. Banks M.A), Churchill Livingstone, pp 79 - 98. 1986.

## **REFERENCES**

---

- [109] Handa Y, Handa T, Ichie M, Murakami H, Hoshimiya, Ishikawa S, Ohkubo K, Functional Electrical Stimulation Systems for Restoration of Motor Function of Paralysed Muscles - Versatile Systems and a Portable System. *Frontiers of Medical and Biological Engineering*, Vol. 4, No. 4, pp 241 - 255. 1992.
- [110] Winstein C.J, Gardner E.R, McNeal D.R, Barto P.S, Nicholson D.E, Standing Balance Training : Effect on Balance and Locomotion in Hemiparetic Adults. *Arch. Phys. Med. Rehabil*, Vol. 70, pp 755 - 762. 1989.
- [111] Turnbull G.I, Charteris J, Wall J.C, Deficiencies in Standing Weight Shifts by Ambulant Hemiplegic Subjects. *Arch. Phys. Med. Rehabil*, Vol. 77, pp 356 - 362. 1996.
- [112] Dettman M.A, Linder M.T, Sepic S.B, Relationships Among Walking Performance, Postural Stability, and Functional Assessments of the Hemiplegic Patient. *Am. J. Phys. Med*, Vol. 66, pp 77- 90. 1987.
- [113] Hamrin E, Eklund G, Hillgren A.K, Borges O, Hall J, Hellstrom O, Muscle Strength and Balance in Post-Stroke Patients. *Ups. J. Med. Sci*, Vol. 87, pp 11 - 26. 1982.
- [114] Rosse C, Hollinshead's Textbook of Anatomy, 5th Edition. Lippincott-Raven Publishers, Philadelphia. 1997. ISBN 0-397-51256-2.
- [115] April E.W, Anatomy. Harwal Publishing Company, Pennsylvania. 1984. ISBN 0-471-09624-5.
- [116] Green J.H, Silver P.H.S, An Introduction to Human Anatomy. Oxford University Press, 1981.
- [117] Warwick R, Williams P.L (Eds), Gray's Anatomy, 35th Edition. Longman. 1973.
- [118] Moffat D.B, Lecture Notes on Anatomy. Blackwell Scientific Publications, 1987. ISBN 0-632-01772-4.
- [119] Snell R.S, Clinical Anatomy for Medical Students, 5th Edition. Little, Brown and Company (Inc.), 1992. ISBN 0-316-80135-6.
- [120] Sonntag V.K.H, Foot Drop and the Peroneal Nerve. *N. Engl. J. Med*, Vol. 295, No. 11. pp 625. 1976.
- [121] Grant J.C.B, Grant's Atlas of Anatomy, 7th Edition, (Anderson J.E. Ed.). Williams and Wilkins, Maryland. 1983. ISBN 0-683-00211-2.

## **REFERENCES**

---

- [122] Burke R.E, Levine D.N, Zajac F.E, Tsairis P, Engel W.K, Mammalian Motor Units : Physiological - Histochemical Correlation in Three Types in Cat Gastrocnemius. Science, Vol. 174. pp 709 - 712. 1971.
- [123] Close R, Properties of Motor Units in Fast and Slow Skeletal Muscle of Rat. J. Physiol. (Lond.), Vol. 193. pp 45 - 55. 1967.
- [124] Ganong W.F, Review of Medical Physiology, 18th Edition. Appleton and Lange. 1997. ISBN 0-8385-8443-8.
- [125] Peachey L.D, Adrian R.H, Geiger S.R, The Handbook of Physiology, Section 10 - Skeletal Muscle. The American Physiological Society. 1983. ISBN 0-683-06805-9.
- [126] Campbell E.J.M, Dickenson C.J, Slater J.D.H, Edwards C.R.W, Sikora E.K, Clinical Physiology, 5th Edition. Blackwell Scientific Publications. 1984. ISBN 0-632-00912-8.
- [127] Schauf C, Moffett D, Stacia M, Human Physiology. Times Mirror / Mosby College Publishing. 1990. ISBN 0-8016-4321-X.
- [128] Buller A.J, Eccles J.C, Eccles R.M, Differentiation of Fast and Slow Muscles in Cat Hind Limb. J. Physiol. (Lond.), Vol. 150. pp 417 - 439. 1960.
- [129] Buller A.J, Eccles J.C, Eccles R.M, Interactions Between Motor Neurones and Muscles in Respect of Characteristic Speeds of their Responses. J. Physiol. (Lond.), Vol. 150. pp 417 - 439. 1960.
- [130] Herbison G.J, Jaweed M.M, Ditunno J.F, Muscle Fiber Types. Arch. Phys. Med. Rehabil, Vol. 63. pp 227 - 230. 1982.
- [131] Hang J, Fleming J.B, Wells M.L, Adair T.H, Miniaturized Electrical Stimulator With Controllable Duty Cycles. Am. J. Physiol, Vol. 268. H1373-H1378. 1995.
- [132] Eisenberg B.R, Salmons S, Stereological Analysis of Sequential Ultrastructural Changes in Adaptive Response of Fast Muscle to Chronic Stimulation. Muscle and Nerve, Vol. 3. p 277. 1980.
- [133] Amphlett G.W, Perry S.V, Syska H, Brown M.D, Vrbova G, Cross Innervation and Regulatory Protein System of Rabbit Soleus Muscle. Nature, Vol. 257. pp 602 - 604. 1975.
- [134] Rhoades R.A, Pflanzler R.G, Human Physiology. Saunders College Publishing, 1989.
- [135] Keynes R.D, Aidley D.J, Nerve and Muscle. Cambridge University Press, 1991.



## **REFERENCES**

---

- [136] Huxley A.F, Muscle Structure and Theory of Contraction. Prog. Biophys. Biophys. Chem, Vol. 7. pp 255 - 318. 1957.
- [137] Massion J, Paillard J, Schultz W, Wiesendanger M (Eds.), Neural Coding of Motor Performance. Springer - Verlag, Berlin. 1983. ISBN 0-387-12140-4.
- [138] Seeley R.R, Stephens T.D, Tate D.A, Essentials of Anatomy and Physiology 2nd Ed. Mosby, 1996.
- [139] Keele C.A, Neil E, Joels N, Samson Wright's Applied Physiology, 13th Edition, Oxford Medical Publications, University Press. 1982. ISBN 0-19-263211-6.
- [140] Simons A.J.R, Measurement of Rise Time of Averaged Muscle Action Potential in Normal Subjects and Patients with Myopathy. Journal of Neurology, Neurosurgery, and Psychiatry, Vol. 43. pp 56 - 62. 1980.
- [141] Schalow G, Zach G.A, Nerve Compound Action Potentials Analysed With the Simultaneously Measured Single Fibre Action Potentials in Humans. Electromyographr. Clin. Neurophysiol, Vol. 34, No. 8. pp 451 - 465. 1994.
- [142] Loof Y, Model for Decomposition of the Motor Unit Action Potential - 1 The Algorithm. Med. & Biol. Eng. & Comput, Vol. 24. pp 506 - 512. 1986.
- [143] Bolton C.F, Sawa G.M, Carter K, The Effects of Temperature on Human Compound Action Potentials. Journal of Neurology, Neurosurgery, and Psychiatry, Vol. 44. pp 407 - 413. 1981.
- [144] Lamb J.F, Ingram C.G, Johnston T.A, Pitman R.M, Essentials of Physiology, 3rd Edition. Blackwells. 1991.
- [145] Greyer R, Windhorst U, Comprehensive Human Physiology, Volume 1. Springer. 1996. ISBN 3-540-58109-X.
- [146] Erioka R.M, Stuart D.G, Neurobiology of Muscle Fatigue. J. Appl. Physiology, Vol. 72. pp 1631 - 1648. 1992.
- [147] Baldwin K.M, Klinkerfuss G.H, Terjung R.L, Mole P.A, Holloszy J.O, Respiratory Capacity of White, Red, and Intermediate Muscle : Adaptive Response to Exercise. Am. J. Physiol, Vol. 222. pp 373 - 378. 1972.

## **REFERENCES**

---

- [148] Yan Z, Salmons S, Dang Y.L, Hamilton M,T, Booth F.W, Increased Contractile Activity Decreases RNA-protein Interaction in the 3'-UTR of Cytochrome *c* mRNA. The American Physiological Society. C1157 - C1166. 1996.
- [149] Lindstrom L, Kadefors R, Petersen I, An Electromyographic Index for Localised Muscle Fatigue. *J. Appl. Physiol*, Vol. 43, No. 4. pp 750 - 754. 1977.
- [150] Cobb S, Forbes A, Electromyographic Studies of Muscular Fatigue in Man. *Am. J. Physiol*, Vol. 65. pp 234 - 251. 1923.
- [151] De Vries H.A, EMG Fatigue Curves in Postural Muscles. A Possible Etiology for Idiopathic Low Back Pain. *Am. J. Phys. Med*, Vol. 17. pp 175 - 181. 1968.
- [152] Kadefors R, Kaiser E, Petersen I, Dynamic Spectrum Analysis of Myo-potentials with Special Reference to Muscle Fatigue. *Electromyog. Clin. Neurophysiol*, Vol. 8. pp 39 - 74. 1968.
- [153] Kaiser E, Petersen I, Frequency Analysis of Action Potentials During Tenanic Contraction. *Electroencephalog. Clin. Neurophysiol*, Vol. 14. pp 955. 1962.
- [154] Inbar G.F, Allin J, Paiss O, Kranz H, Monitoring Surface EMG Spectral Changes by the Zero Crossing Rate. *Med. & Biol. Eng. & Comput*, Vol. 24. pp 10 - 18.1986.
- [155] Lippold O.C.J, Redfearn J.W.T, Vuco J, The Rhythmical Activity of Groups of Motor Units in the Voluntary Contraction of Muscle. *J. Physiol. (Lond.)*, Vol. 137. pp 473 - 487. 1957.
- [156] Lloyd A.J, Surface Electromyography During Sustained Isometric Contractions. *J. Appl. Physiol*, Vol. 30. pp 713 - 719. 1971.
- [157] Stulen F.B, De Luca C.J, Muscle Fatigue Monitor : A Non-invasive Device for Observing Localized Muscle Fatigue. *IEEE Trans. BME-29*. pp 760 - 768. 1982.
- [158] Shearn R.C, Design and Development of a Muscle Fatigue Monitor. Final Year Report, University of Bath, 1988.
- [159] Sime A.C, On Line Monitoring of Muscular Fatigue Using the Surface Myoelectric Signal. Final Year Report, University of Bath, 1987.
- [160] Carr C, Myoelectric Signal Recorder for Use as a Muscle Fatigue Monitor and as a Feedback Parameter for a Closed Loop Control Scheme of Ambulatory Muscle Prostheses. Final Year Report, University of Bath. 1987.

## **REFERENCES**

---

- [161] Weiss G, Sur la possibilite de rendre comparables entre eux les appareils servant a l'excitation electrique. Arch. Ital. Biol, Vol. 35. pp 413 - 446. 1901.
- [162] Brown B.H, Smallwood R.H, Medical Physics and Physiological Measurement. Blackwell Scientific Publications. 1981. ISBN 0-632-00704-4.
- [163] Bostock H, The Strength - Duration Relationship for Excitation of Myelinated Nerve : Computed Dependence on Membrane Parameters. J. Physiol, Vol. 341. pp 59 - 74. 1983.
- [164] Ray C.D, Medical Engineering. Yearbook Medical Publishers Inc. 1974. ISBN 0-8151-7113-7.
- [165] Mogyoros I, Kiernan M.C, Burke D, Strength - Duration Properties of Human Peripheral Nerve. Brain, Vol. 119. pp 439 - 447. 1996.
- [166] Lapicque L, Recherches quantitatives sur l'excitation electrique des nerfs traitee comme une polarisation. J. Physiol. (Paris), Vol. 9. pp 622 - 635. 1907.
- [167] Wyke B, Neurological Mechanisms in Spasticity : A Brief Review of Some Current Concepts. Physiotherapy, Vol. 62, No. 10. pp 316 - 319. 1976.
- [168] Lance J.W, Disordered Motor Control. Spasticity, (Feldman R.G, Young R.R, Koella W.P Eds). Yearbook Medical Publishers, Chicago. pp 485 - 494. 1980.
- [169] Thilmann A.F, Fellows S.J, Garms E, Pathological Stretch Reflexes on the "Good" Side of Hemiparetic Patients. Journal of Neurology, Neurosurgery, and Psychiatry, Vol. 53. pp 208 - 214. 1990.
- [170] Ragnarsson K.T, Functional Electrical Stimulation and Suppression of Spasticity Following Spinal Cord Injury. Bull. N.Y. Acad. Med, Vol. 68, No. 2. pp 351 - 364. 1990.
- [171] Hudgson P, Clinical Features of Spastic States. Physiotherapy, Vol. 62, No. 10. pp 323 - 325. 1976.
- [172] Corcos D.M, Gottlieb G.L, Penn R.D, Myklebust B, Agarwal G.C, Movement Deficits Caused by Hyperexcitable Stretch Reflexes in Spastic Humans. Brain, Vol. 109. pp 1043 - 1058. 1986.
- [173] Dietz V, Berger W, Interlimb Coordination of Posture in Patients with Spastic Paresis. Brain, Vol. 107. pp 965 - 978. 1984.

## **REFERENCES**

---

- [174] Vodovnik L, Bowman B.R, Winchester P, Effect of Electrical Stimulation on Spasticity in Hemiparetic Patients. *Int. Rehabil. Med*, Vol. 6. pp 153 - 156. 1984.
- [175] O'Dwyer N.J, Ada L, Neilson P.D, Spasticity and Muscle Contracture Following Stroke. *Brain*, Vol. 119. pp 1737 - 1749. 1996.
- [176] Dietz V, Quintern J, Berger W, Electrophysiological Studies of Gait in Spasticity and Rigidity : Evidence That Altered Mechanical Properties of Muscle Contribute to Hypertonia. *Brain*, Vol. 104. pp 431 - 449. 1981.
- [177] Alfieri V, Electrical Treatment of Spasticity. *Scand. J. Rehab. Med*, Vol. 14. pp 177 - 182. 1982.
- [178] Carnstam B, Larsson L.E, Electrical Stimulation in Patients with Spasticity. *EEG and Clin. Neurophys. Society Proceedings*, Vol. 38. pp 214. 1975.
- [179] Cerny K, A Clinical Method of Quantitative Gait Analysis. *Physical Therapy*, Vol. 63, No. 7. pp 1125 - 1126. 1983.
- [180] Tibarewala D.N, Mukherjee P, Chakrabarty S, Ganguli S, A Digital Gait Recording Technique. *Journal of Medical Engineering and Technology*, Vol. 3, No. 3. pp 138 - 139. 1979.
- [181] Kauer J.M.G, Wichers M.J, Wijkmans D.W, Treadmill Made of Conducting Rubber in Gait Analysis. *Med. & Biol. Eng. & Comput*, Vol. 23. pp 93 - 94. 1985.
- [182] Wall J.C, Turnbull G.I, Gait Asymmetries in Residual Hemiplegia. *Arch. Phys. Med. Rehabil*, Vol. 67. pp 550 - 553. 1986.
- [183] Mizrahi J, Susak Z, Heller L, Najenson T, Objective Expression of Gait Improvement of Hemiplegics During Rehabilitation by Time - Distance Parameters of the Stride. *Med. & Biol. Eng. & Comput*, Vol. 20. pp 628 - 634. 1982.
- [184] Kirtley C, Whittle M.W, Jefferson R.J, Influence of Walking Speed on Gait Parameters. *J. Biomed. Eng*, Vol. 7. pp 282 - 288. 1985.
- [185] Intiso D, Santilli V, Grasso M.G, Rossi R, Caruso I, Rehabilitation of Walking with Electromyographic Biofeedback in Foot-Drop After Stroke. *Stroke*, Vol. 25. No. 6. pp 1189 - 1192. 1994.
- [186] Harris G.F, Wertsch J.J, Procedures for Gait Analysis. *Arch. Phys. Med. Rehabil*, Vol. 75. pp 216 - 225. 1994.

## REFERENCES

---

- [187] Colborne G.R, Olney S.J, Griffin M.P, Feedback of Ankle Joint Angle and Soleus Electromyography in the Rehabilitation of Hemiplegic Gait. Arch. Phys. Med. Rehabil, Vol. 74. pp 1100 - 1106. 1993.
- [188] Morris J.R.W, Accelerometry in Gait Analysis. Brit. J. Surg, Vol. 59, No. 11. pp 8. 1972.
- [189] Ziporyn T, Improved Technology Steps in to Gait Analysis. (Medical News) J.A.M.A. Vol. 251, No. 5. pp 566 - 567. 1984.
- [190] Kamayama O, Ogawa R, Okamoto T, Kumamoto M, Electric Discharge Patterns of Ankle Muscles During the Normal Gait Cycle. Arch. Phys. Med. Rehabil, Vol. 71. pp 969 - 974. 1990.
- [191] Murray M.P, Kory R.C, Clarkson B.H, Walking Patterns in Healthy Old Men. Journal of Gerontology, Vol. 24. pp 169 - 178. 1969.
- [192] Fisher C.M, Gait Disorders (letter). Neurology, Vol. 44. p 779. 1994.
- [193] Brandstater M.E, De Bruin H, Gowland C, Clark B.M, Hemiplegic Gait : Analysis of Temporal Variables. Arch. Phys. Med. Rehabil, Vol. 64. pp 583 - 587. 1983.
- [194] Lehmann J.F, Condon S.M, Price R, De Lateur B.J, Gait Abnormalities in Hemiplegia : Their Correction by Ankle - Foot Orthoses. Arch. Phys. Med. Rehabil, Vol. 68. pp 763 - 771. 1987.
- [195] Wall J.C, Ashburn A, Assessment of Gait Disability in Hemiplegics. Scand. J. Rehabil. Med, Vol. 11. pp 95 - 103. 1979.
- [196] Wing A.M, Barton J, Turton A, Howick I, Regulation of Lateral Position of Body Centre of Mass in Standing Balance. Physiotherapy Theory and Practice, Vol. 8. pp 131 - 135. 1992.
- [197] Blaszczyk J.W, Hansen P.D, Lowe D.L, Postural Sway and Perception of the Upright Stance Stability Borders. Perception, Vol. 22. pp 1333 - 1341. 1993.
- [198] Collins J.J, De Luca C.J, Random Walking During Quiet Standing. Physical Review Letters, Vol. 73, No. 5. pp 764 - 767. 1994.
- [199] Collins J.J, De Luca C.J, Open - Loop and Closed - Loop Control of Posture : A Random - Walk Analysis of Center - of - Pressure Trajectories. Exp. Brain Res, Vol. 95. pp 308 - 318. 1993.

---

## REFERENCES

---

- [200] Yamada N, Chaotic Swaying of the Upright Posture. *Human Movement Science*, Vol. 14. pp 711 - 726. 1995.
- [201] Lord M, Smith D.M, Foot Loading in Amputee Stance. *Prosthetics and Orthotics International*, Vol. 8. pp 159 - 164. 1984.
- [202] Rosenblum M, Firsov G, Kuuz R, Pompe B, Human Postural Control - Force Plate Experiments and Modelling. *Nonlinear Analysis of Physiological Data* (Kantz H, Kurths J, Mayer-Kress G Eds), Springer. 1996.
- [203] Wing A.M, Goodrich S, Virji-Babul N, Jenner J.R, Clapp S, Balance Evaluation in Hemiparetic Stroke Patients Using Lateral Forces Applied to the Hip. *Arch. Phys. Med. Rehabil*, Vol. 74. pp 292 - 299. 1993.
- [204] Diener H.C, Horak F.B, Nashner L.M, Influence of Stimulus Parameters on Human Postural Responses. *Journal of Neurophysiology*, Vol. 59, No. 6. pp 1888 - 1905. 1988.
- [205] Moore S.P, Rushmer P.S, Windus S.L, Nashner L.M, Human Automatic Postural Responses : Responses to Horizontal Perturbations of Stance in Multiple Directions. *Exp. Brain Res*, Vol. 73. pp 648 - 658. 1988.
- [206] Hamalainen H, Kekoni J, Effect of Unilateral Sensory Impairment of the Sole of the Foot on Postural Control in Man : Implications for the Role of Mehanoreception in Postural Control. *Human Movement Science*, Vol. 11. pp 549 - 561. 1992.
- [207] Lord S.R, Ward J.A, Age - Associated Differences in Sensori - Motor Function and Balance in Community Dwelling Women. *Age and Ageing*, Vol. 23. pp 452 - 460. 1994.
- [208] Lord S.R, Ward J.A, Williams P, Anstey K.J, Physiological Factors Associated with Falls in Older Community Dwelling Women. *J. A. G. S*, Vol. 42. pp 1110 - 1117. 1994.
- [209] Lord S.R, Predictors of Nursing Home Placement and Mortality of Residents in Intermediate Care. *Age and Ageing*, Vol. 23. pp 499 - 504. 1994.
- [210] Lord S.R, Clark R.D, Webster I.W, Physiological Factors Associated with Falls in an Elderly Population. *J. A. G. S*, Vol. 39. pp 1194 - 1200. 1991.

## **REFERENCES**

---

- [211] Lord S.R, Clark R.D, Webster I.W, Postural Stability and Associated Physiological Factors in a Population of Aged Persons. *Journal of Gerontology*, Vol. 46, No. 3. pp M69 - M76. 1991.
- [212] Soechting J.F, Berthoz A, Dynamic Role of Vision in the Control of Posture in Man. *Exp. Brain Res*, Vol. 36. pp 551 - 561. 1979.
- [213] Lee D.N, Lishman J.R, Visual Proprioceptive Control of Stance. *J. Human Move. Stud*, Vol. 1. pp 87 - 95. 1975.
- [214] Nashner L, Berthoz A, Visual Contribution to Rapid Motor Responses During Postural Control. *Brain Research*, Vol. 150. pp 403 - 407. 1978.
- [215] Kerr B, Condon S.M, McDonald L.A, Cognitive Spatial Processing and the Regulation of Posture. *Journal of Experimental Psychology : Human Perception and Performance*, Vol. 11, No. 5. pp 617 - 622. 1985.
- [216] Woollacott M.H, Shumway-Cook A, Nashner L, Postural Reflexes and Ageing. *The Aging Motor System* (Mortimer J.A, Pirozzolo F.J, Maletta G.J Eds), Praeger, New York. pp 98 - 119. 1982.
- [217] Jeka J.J, Lackner J.R, Fingertip Contact Influences Human Postural Control. *Exp. Brain Res*. Vol. 100. pp 495 - 502. 1994.
- [218] Jeka J.J, Lackner J.R, The Role of Haptic Cues from Rough and Slippery Surfaces in Human Postural Control. *Exp. Brain Res*, Vol. 103. pp 267 - 276. 1995.
- [219] Jeka J.J, Easton R.D, Bentzen B.L, Lackner J.R, Haptic Cues for Orientation and Postural Control in Sighted and Blind Individuals. *Perception and Psychophysics*, Vol. 58, No. 3. pp 409 - 423. 1996.
- [220] Peterka R.J, Black F.O, Age - Related Changes in Human Posture Control : Motor Coordination Tests. *Journal of Vestibular Research*, Vol. 1. pp 87 - 96. 1990.
- [221] Arcan M, Brull M.A, Fundamental Characteristic of Human Body and Foot : Foot - Ground Pressure Pattern. *J. Biomech*, Vol. 9. pp 453 - 457. 1976.
- [222] Roland N.J, Smith C.A, Miller I.W, Jones A.S, Lesser T.H, A Simple Technique to Measure Body Sway in Normal Subjects and Patients with Dizziness. *The Journal of Laryngology and Otology*, Vol. 109. pp 189 - 192. 1995.

## **REFERENCES**

---

- [223] Dornan J, Fernie G, Holliday P, Visual Input : Its Importance in the Control of Postural Sway. *Arch. Phys. Med. Rehabil*, Vol. 59. pp 586 - 591. 1978.
- [224] Meldrum D, Finn A.M, An Investigation of Balance Function in Elderly Subjects Who Have and Have Not Fallen. *Physiotherapy*, Vol. 79, No. 12. pp 839 - 842. 1993.
- [225] McClenaghan B.A, Williams H, Dickerson J, Thombs L, Spectral Signature of Forces to Discriminate Perturbations in Standing Posture. *Clin. Biomech*, Vol. 9, No. 1. pp 21 - 27. 1994.
- [226] Maylor E.A, Wing A.M, Age Differences in Postural Stability Are Increased by Additional Cognitive Demands. *Journal of Gerontology*, Vol. 51B, No. 3. pp 143 - 154. 1996.
- [227] Katsarkas A, Smith H, Galiana H, Postural Instability on One Foot in Patients with Loss of Unilateral Peripheral Vestibular Function. *Journal of Vestibular Research*, Vol. 4, No. 2. pp 153 - 160. 1994.
- [228] MacPherson J.M, Horak F.B, Dunbar D.C, Dow R.S, Stance Dependence of Automatic Postural Adjustments in Humans. *Exp. Brain Res*, Vol. 78. pp 557 - 566. 1989.
- [229] Chodera J, Lord M, Pedobarographic Foot - Pressure Measurements and Their Applications. *Proceedings of a Seminar on Rehabilitation of the Disabled*, (Kenedi R, Paul J, Hughes J, Eds), Macmillan, London. pp 173 - 181. 1979.
- [230] McFadyen G.M, Stoner D.L, Polyurethane Foam Wheelchair Cushions : Retention of Supportive Properties. *Arch. Phys. Med. Rehabil*, Vol. 61. pp 234 - 237. 1980.
- [231] Campbell G, Newell E, McLure M, Compression Testing of Foamed Plastics and Rubbers for Use as Orthotic Shoe Insoles. *Prosthetics and Orthotics International*, Vol. 6. pp 48 - 52. 1982.
- [232] Brown A.M, Percy M.J, The Effect of Water Content on the Stiffness of Seating Foams. *Prosthetics and Orthotics International*, Vol. 10. pp 149 - 152. 1986.
- [233] Halleck W.L, Automatic Dual - Channel Stimulator Control Unit. *J. Appl. Physiol*, Vol. 22, No. 3. pp 593 - 594. 1967.
- [234] Hertzler E.C, Kaminski R.J, Compact Stimulator Using Integrated Circuits and Battery Power. *J. Appl. Physiol*, Vol. 24, No. 2. pp 249 - 251. 1968.



## **REFERENCES**

---

- [235] Waters R.L, McNeal D, Perry J, Experimental Correction of Foot Drop by Electrical Stimulation of the Peroneal Nerve. *Journal of Joint and Bone Surgery*, Vol. 57-A, No. 8. pp 1047 - 1054. 1975.
- [236] Goovaerts H.G, Koning G, Schneider H, A Programmable Stimulator for Physiological Applications. *Med. & Biol. Eng.* pp 112 - 118. January 1975.
- [237] Brandell B.R. The Study and Correction of Human Gait by Electrical Stimulation. *The American Surgeon*, Vol. 52, No. 5, 1986.
- [238] Rushton D.N, Functional Electrical Stimulation. *Physiol. Meas*, Vol. 18, No. 4. pp 241 - 275. 1997.
- [239] Bogataj U, Gros N, Malezic M, Kelih B, Kljajic M, Acimovic R, Restoration of Gait During Two to Three Weeks of Therapy with Multichannel Electrical Stimulation, *Physical Therapy*. Vol. 69, No. 5. pp 319 - 327. 1989.
- [240] Backman E, Methods for Measurement of Muscle Function. *Scand. J. Rehab. Med*, Suppl. 20. 1988.
- [241] Hoshimiya N, Naito A, Yajima M, Handa Y, A Multichannel FES System for the Restoration of Motor Functions in High Spinal Cord Injury Patients : A Respiration - Controlled System for Multijoint Upper Extremity. *IEEE Transactions on Biomedical Engineering*, Vol. 36, No. 7. pp 754 - 760.1989.
- [242] Van Griethuysen C.M, Paul J.P, Andrews B.J, Nicol A.C, Biomechanics of Functional Electrical Stimulation, *Prosthetics and Orthotics International*. Vol. 6. pp 152 - 156. 1982.
- [243] Smith L.E. Restoration of Volitional Limb Movement of Hemiplegics Following Patterned Functional Electrical Stimulation. *Perceptual and Motor Skills*, 71, pp 851-856, 1990.
- [244] Gracinin F, Functional Electrical Stimulation in External Control of Motor Activity and Movements of Paralyzed Extremities. *Int. Rehabil. Med*, Vol. 6. pp 25 - 30. 1984.
- [245] Malezic M, Bogataj U, Gros N, Decman I, Vrtacnik P, Kljajic M, Acimovic-Janezic R, Application of a Programmable Dual Channel Adaptive Electrical Stimulation System for the Control and Analysis of Gait. *Journal of Rehabilitation Research and Development*, Vol. 29, No. 4. pp 41 - 53. 1992.

## **REFERENCES**

---

- [246] Kralj A, Acimovic R, Stanic U, Enhancement of Hemiplegic Patient Rehabilitation by Means of Functional Electrical Stimulation. *Prosthetics and Orthotics International*, 17, pp 107 - 114, 1993.
- [247] Davis R, Eckhouse R, Patrick J.F, Delehanty A , Computer Controlled 22 - Channel Stimulator for Limb Movement. *Acta Neurochirurgica, Suppl.* 39, pp 117 - 120, 1987.
- [248] Akazawa K, Makikawa M, Kawamura J, Aoki H, Functional Neuromuscular Stimulation System Using an Implantable Hydroxyapatite Connector and a Microprocessor Based Portable Stimulator, *IEEE Transactions on Biomedical Engineering*, Vol. 36, No. 7. pp 746 - 752. 1989.
- [249] Meadows P.M, McNeal D.R, A Four Channel IBM PC/AT Compatible Biphasic Pulse Generator for Nerve Stimulation. *IEEE Transactions on Biomedical Engineering*, Vol. 36, No. 7. pp 802 - 804. 1989.
- [250] Graupe D, Krdylewski H, Artificial Neural Network Control of FES in Paraplegics for Patient Responsive Ambulation. *IEEE Transactions on Biomedical Engineering*, Vol. 42, No. 7. pp 699 - 707. 1995.
- [251] Carroll S.G, Triolo R.J, Chizeck H.J, Kobetic R, Marsolais E.B, Tetanic Responses of Electrically Stimulated Paralyzed Muscle at Varying Interpulse Intervals. *IEEE Transactions on Biomedical Engineering*, Vol. 36, No. 7. pp 644 - 652. 1989.
- [252] Durfee W.K, MacLean K.E, Methods for Estimating Isometric Recruitment Curves of Electrically Stimulated Muscle. *IEEE Transactions on Biomedical Engineering*, Vol. 36, No. 7. pp 654 - 667. 1989.
- [253] Borges G, Ferguson K, Kobetic R, Development and Operation of Portable and Laboratory Electrical Stimulation Systems for Walking in Paraplegic Subjects. *IEEE Transactions on Biomedical Engineering*, Vol. 36, No. 7. pp 798 - 805. 1989.
- [254] Herbert M.A, Bobechko W.P, Scoliosis Treatment in Children Using a Programmable, Totally Implantable Muscle Stimulator (ESI). *IEEE Transactions on Biomedical Engineering*, Vol. 36, No. 7. pp 801 - 802. 1989.
- [255] Agnew W.F, McCreery D.B, Yuen T.G.H, Bullara L.A, Histologic and Physiologic Evaluation of Electrically Stimulated Peripheral Nerve : Consideration for the Selection of Parameters. *Annals of Biomedical Engineering*, Vol. 17. pp 39-60, 1989.

## **REFERENCES**

---

- [256] Koller R, Girsch W, Liegl C, Gruber H, Holle J, Losert U, Mayr W, Thoma H, Long Term Results of Nervous Tissue Alterations Caused by Epineural Electrode Application: An Experimental Study in Rat Sciatic Nerve. *Pacing Clin. Electrophysiol.* Vol. 15. pp 108 - 115. 1992.
- [257] Rohlicek V, A Device for Polarity Alternation of Pulses for Biological Stimulation. *Med. Electron. Biol. Eng.* Vol. 2. pp 439 - 441. 1964.
- [258] Spencer H.J, An Automatic, Optically Isolated, Biphasic Constant Current Stimulator Adapter for Artefact Suppression. *Electroencephalography and Clinical Neurophysiology*, Vol. 51. pp 215 - 217. 1981.
- [259] Denslow J.S, Double Discharges in Human Motor Units. *J. Neurophysiol*, Vol. 11. pp 209 - 215. 1948.
- [260] Bawa P, Calancie B, Repetitive Doublets in Human Flexor Carpi Radialis Muscle. *J. Physiol*, Vol. 339. pp 123 - 132. 1983.
- [261] Partanen V.S.J, Double Discharges in Neuromuscular Diseases. *J. Neurol. Sci*, Vol. 36. pp 377 - 382. 1978.
- [262] Roth G, Double Discharges of Distal Origin. *J. Neurol. Sci*, Vol. 47. pp 35 - 48. 1980.
- [263] Sandercock T.G, Heckman C.J, Doublet Potentiation During Eccentric and Concentric Contractions of Cat Soleus Muscle. *J. Appl. Physiol*, Vol. 82, No. 4. pp 1219 - 1228. 1997.
- [264] Eken T, Gundersen K, Electrical Stimulation Resembling Normal Motor - Unit Activity : Effects on Denervated Fast and Slow Rat Muscles. *J. Physiol*, Vol. 402. pp 651 - 669. 1988.
- [265] Karu Z.Z, Durfee W.K, Barzilai A.M, Reducing Muscle Fatigue in FES Applications by Stimulating with N-let Pulse Trains. *IEEE Transactions on Biomedical Engineering*, Vol. 42, No. 8. pp 809 - 817. 1995.
- [266] Binder-MacLeod S.A, Barker C.B, Use of a Catchlike Property of Human Skeletal Muscle to Reduce Fatigue. *Muscle and Nerve*, Vol. 14. pp 850 - 857. 1991.
- [267] Garland S.J, Garner S.H, McComas A.J, Relationship Between Numbers and Frequencies of Stimuli in Human Muscle Fatigue. *J. Appl. Physiol*, Vol. 65. pp 89 - 93. 1988.

## REFERENCES

---

- [268] Wilson D.M, Larimer J.L, The Catch Properties of Ordinary Muscle. Proc. Natl. Acad. Sci. (USA), Vol. 61. pp 909 - 916. 1968.
- [269] De N. Donaldson N, Donaldson P.E.K, When are Actively Balanced Biphasic ('Lilly') Stimulating Pulses Necessary in a Neurological Prosthesis? I Historical Background; Pt Resting Potential; *Q* Studies. Med. & Biol. Eng. & Comput, Vol. 24. pp 41 - 49. 1986.
- [270] McCreery D.B, Agnew W.F, Yuen T.G.H, Bullara L.A, Damage in Peripheral Nerve from Continuous Electrical Stimulation : Comparison of Two Stimulus Waveforms. Med. & Biol. Eng. & Comput, Vol. 30. pp 109 - 114. 1992.
- [271] Nilsson J, Ravits J, Hallett M, Stimulus Artifact Compensation Using Biphasic Stimulation. Muscle and Nerve, Vol. 11. pp 597 - 602. 1988.
- [272] Stephens W.G.S, The Current - Voltage Relationship in Human Skin. Med. Electron. Biol. Engng, Vol, 1. pp 389 - 399. 1963.
- [273] Mizrahi J, Braun Z, Najenson T, Graupe D, Quantitative Weightbearing and Gait Evaluation of Paraplegics Using Functional Electrical Stimulation. Med. & Biol. Eng. & Comput, Vol. 23. pp 101 - 107. 1985.
- [274] Whitlock T.L. Muscle Physiology Instrumentation, PhD thesis. University of Bath, 1990.
- [275] Webber D.J. An Investigation into Electrical Stimulator Designs, PhD thesis. University of Bath, 1990.
- [276] Alon G, Kantor G, Ho H.S, Effects of Electrode Size on Basic Excitatory Responses and on Selected Stimulus Parameters. J. Orthop. Sports Phys. Ther, Vol. 20, No. 1. pp 29 - 35. 1994.
- [277] Weinberg D.I, Grounding for Electrical Safety. Med. Electron. Biol. Eng, Vol. 2. pp 435 - 437. 1964.
- [278] Kirkwood C.A, Andrews B.J, Mowforth P, Automatic Detection of Gait Events : A Case Study Using Inductive Learning Techniques. Journal of Biomedical Engineering, Vol. 11, pp 511 - 516. 1989.
- [279] Kljajic M, Krajnik J, The Use of Ground Reaction Measuring Shoes in Gait Evaluation. Clin. Phys. Physiol. Meas, Vol. 8. pp 133 - 142. 1987.

## **REFERENCES**

---

- [280] Smith S, Magnetic Components Design and Application. Van Nostrand Reinhold Company Inc. 1985. ISBN 0-442-20397-7.
- [281] SEI Magnetics Data Book, SEI. 1980.
- [282] McLyman Col. W.T, Transformer and Inductor Design Handbook. Marcel Dekker Inc. 1st Edition. 1978. ISBN 0-8247-6801-9.
- [283] McPherson W.L, Reference Data for Radio Engineers. Standard Telephone and Cables Ltd. 1959.
- [284] Paul J.P, Gait Analysis. Annals of the Rheumatic Diseases, Vol. 48. pp 179 - 181. 1989.
- [285] Lord M, Foot Pressure Measurement : A Review of Methodology. J. Biomed. Eng, Vol. 3. pp 91 - 99. 1981.
- [286] Elftman H.O, A Cinematic Study of the Distribution of Pressure in the Human Foot. Anat. Record, Vol. 59. pp 481 - 490. 1934.
- [287] Amar J, Trottoir Dynamographique, Compt. Rend. Acad. d: Sc 1, Vol. 163. pp 130 - 132. 1916.
- [288] Saunders J.B, The Major Determinants in Normal and Pathological Gait. Journal of Bone and Joint Surgery, Vol. 35-A. pp 543 - 558. 1953.
- [289] Jacobs N.A, Skorecki J, Charnley J, Analysis of the Vertical Component of Force in Normal and Pathological Gait. J. Biomech, Vol. 5. pp 11 - 34. 1972.
- [290] Morton D.J, Structural Factors in Static Disorders of the Foot. Am. J. Surg, Vol. 19. pp 315 - 326. 1930.
- [291] Morton D.J, The Human Foot. New York, Columbia University Press. 1935.
- [292] Harris R.I, Beath T, Army Foot Survey. An Investigation of Foot Ailments in Canadian Soldiers. Nat. Res. Council Canada N.R.C. No. 1547. 1947.
- [293] Barnett C.H, A Plastic Pedograph. The Lancet, Vol 2. pp 273. 1954.
- [294] Hertzberg H.T.E, Some Contributions of Applied Physical Anthropology to Human Engineering. Ann. N.Y. Acad. Sci, Vol. 63, No. 4. 1955.
- [295] Chodera J, Pedobarograph - Apparatus for Visual Display of Pressures Between Contacting Surfaces of Irregular Shape. C.Z.S. Patent No. 104 514 30d. 1960.

## **REFERENCES**

---

- [296] Leduc A, Reynolds I, Liegeois E, Levray P.H, Lievens P, Load Sharing Within the Forefoot. Disability - Proceedings of a Seminar on Rehabilitation of the Disabled in Relation to Clinical and Biomechanical Aspects, Costs and Effectiveness. (Kenedi R, Paul J.P, Hughes J. Ed.), Macmillan. pp 182 - 184. 1979. ISBN 0-03-327091-6.
- [297] Cavanagh P.R, Michiyoshi A.E, A Technique for the Display of Pressure Distributions Beneath the Foot. *J. Biomech*, Vol. 13. pp 69 - 75. 1980.
- [298] Scranton P.E, McMaster J.H, Momentary Distribution of Forces Under the Foot. *J. Biomech*, Vol. 9. pp 45 - 58. 1976.
- [299] Simkin A, Stokes I.A.F, Characterisation of the Dynamic Vertical Force Distribution Under the Foot. *Med. & Biol. Eng. & Comput*, Vol. 20, No.1. pp 12 - 18. 1982.
- [300] LoVerde A, Macellari V, Torre M, Gait Analysis Through a Mat-like Device. Proc. 1st Eur. Conf. on Biomedical Engineering (February 1991), Commission of the European Communities (Faust U. Ed.), Vol. 126. pp 214 - 215. 1991.
- [301] Gerber H, A System for Measuring Dynamic Pressure Distribution Under the Human Foot. *J. Biomech*, Vol. 15. pp 225 - 227. 1982.
- [302] Nicol K, Hennig E.M, Measurement of Pressure Distribution by Means of a Flexible Large - Surface Mat. *Biomechanics VI-A*, University Park Press, Baltimore. pp 374 - 380. 1978.
- [303] Cunningham D.M, Brown G.W, Two Devices for Measuring the Forces Acting on the Human Body During Walking. *Exp. Stress Anal*, Vol. 9. pp 75 - 90. 1951.
- [304] Macellari V, Giacomozzi C, Multistep Pressure Platform as a Stand - Alone System for Gait Assessment. *Med. & Biol. Eng. & Comput*, Vol. 34. pp 299 - 304. 1996.
- [305] Stott J.R.R, Soames R.W, A Method for Recording the Instantaneous Pressure Distribution Under the Feet During Walking. *J. Anat*, Vol. 132. pp 472 - 473. 1981.
- [306] Frost R.B, Cass C.A, A Load Cell and Sole Assembly for Dynamic Pointwise Vertical Force Measurement in Walking. *Eng. in Med*, Vol. 10. pp 45 - 50. 1981.
- [307] Pollard J.P, Le Quesne L.P, Tappin J.W, Forces Under the Foot. *J. Biomed. Eng*, Vol. 5. pp 37 - 40. January 1983.
- [308] Hargreaves P, Scales J.T, Clinical Assessment of Gait Using Load Measuring Footwear. *Acta. Orthop. Scand*, Vol. 46. pp 877 - 895. 1975.

## **REFERENCES**

---

- [309] Durie N.D, Shearman L, A Simplified Limb - Load Monitor. *Physiotherapy Canada*, Vol. 31, No. 1. pp 28 - 31. 1979.
- [310] Bauman J.H, Brand P.W, Measurement of Pressure Between Foot and Shoe. *The Lancet*, Vol 1, pp 629 - 632. 1963.
- [311] Hennacy R.A, Gunther B.S.M.E, A Piezoelectric Crystal Method for Measuring Static and Dynamic Pressure Distribution in the Feet. *J. Am. Podiatry Ass*, Vol. 65. pp 444 - 449. 1975.
- [312] Schwartz R.P, Heath A.L, The Definition of Human Locomotion on the Basis of Measurement. *Journal of Bone and Joint Surgery*, Vol. 29, No. 1. pp 203 - 214. 1947.
- [313] Kernozek T.W, La Mott E.E, Dancisak M.J, Reliability of an In - Shoe Pressure Measurement System During Treadmill Walking. *Foot & Ankle Int*, Vol. 17, No. 4. pp 204 - 209. 1996.
- [314] Vines G, Measuring the Weight on Your Feet. *New Scientist*, Issue 1460, p 24. 1985.
- [315] Popovic R.S, Hall Effect Devices: Magnetic Sensors and Characterization of Semiconductors. Adam Hilger. 1991. ISBN 0-75-030096-5.
- [316] Garcia A.C, Dura J.V, Ramiro J, Hoyos J.V, Vera P, Dynamic Study of Insole Materials Simulating Real Loads. *Foot & Ankle Int*, Vol. 15, No. 6. pp 311 - 323. 1994.
- [317] Godfrey C.M, Lawson G.A, Stewart W.A, A Method for Determination of Pedal Pressure Changes During Weight Bearing : Preliminary Observations in Normal and Arthritic Feet. *Arthritis Rheum*. Vol. 10, No. 2. pp 135 - 140. 1967.
- [318] Granat M.H, Maxwell D.M, Bosch C.J, Ferguson A.C.B, Lees K.R, Barbenel J.C, A Body - Worn Gait Analysis System for Evaluating Hemiplegic Gait. *Med. Eng. Physics*, Vol. 17. pp 390 - 394. 1995.
- [319] Prescott J, *Applied Elasticity*. Dover Publications Inc, 1924 (reissued 1961).
- [320] Warnock F.V, *Strength of Materials*, 8th Edition. Sir Isaac Pitman and Sons Ltd, 1957.
- [321] Warnock F.V, Benham P.P, *Mechanics of Solids and Strength of Materials*, Sir Isaac Pitman and Sons Ltd., 1965.
- [322] R.M. Tennent (Ed) *Science Data Book*, 10th impression. Oliver & Boyd. 1986. ISBN 0-05-002487-6.

## **REFERENCES**

---

- [323] Dummer G.W.A, Blackband W.T, Wires and R.F. Cables. Sir Isaac Pitman and Sons Ltd, 1961.



## **BIBLIOGRAPHY**

---

# **BIBLIOGRAPHY**

The reader is directed to the following texts in support of this thesis:-

- 1) Kernighan B.W, Ritchie D.M, The C Programming Language, 2nd Ed. Prentice Hall, 1988. ISBN 0-13-110362-8.
- 2) Schildt H.C Turbo C/C++ The Complete Reference, 2nd Ed. Osborne McGraw Hill, 1990. ISBN 0-07-881535-5.
- 3) Lenk J.D, Simplified Design of Switching Power Supplies. Butterworth Heinemann, 1995. ISBN 0-75-069507-2.
- 4) Mohan, Undeland, Robbins, Power Electronic Converters, Application and Design. John Wiley and sons Inc, 1989. ISBN 0-471-50537.
- 5) Chryssis. G, High Frequency Switching Power Supplies. McGraw Hill, 1984. ISBN 0-07-010949-4.
- 6) Snelling E.C, Giles A.D, Ferrites for Inductors and Transformers. Research Studies Press Ltd, 1983. ISBN 0-86380-003-3.
- 7) Flanagan W.M, Handbook of Transformer Applications. McGraw Hill Inc, 1986. ISBN 0-07-021290-2.
- 8) Phillips, Single Chip 8-bit Microcontrollers Data Book. Phillips, 1988.
- 9) Woerdeman M.W, Standard Atlas of Human Anatomy, 3rd Ed. Butterworth and Co. 1955.
- 10) Gosling J.A, Harris P.F, Humpherson J.R, Whitmore I, Willan P.L.T Atlas of Human Anatomy. Gower Medical Publishing, 1985. ISBN 0-443-02913-X.
- 11) Kiss F, Szentagothai J, Atlas of Human Anatomy, 17th Ed. Pergamon Press Ltd, 1964.
- 12) Woodburne R.T, Essentials of Human Anatomy, 6th Ed. Oxford University Press, 1978. ISBN 0-19-502257-2.
- 13) Huddleston J.V, Introduction to Engineering Mechanics. Addison Wesley Publishing Co. Inc. 1961.
- 14) Douglas R.A, Introduction to Solid Mechanics, Sir Isaac Pitman and Sons Ltd, 1963.
- 15) Grassie J.C, Applied Mechanics for Engineers, Longmans, Green and Co. Ltd, 1963.